Elucidation of the role of NOA1 and myosins in host response to infection by SACMV

Imanu Msifu Mwaba

A dissertation submitted to the Faculty of Science, University of the Witwatersrand, in fulfilment of the requirements for the degree of Doctor of Philosophy in Science at the School of Molecular and Cell Biology.

Johannesburg 2017

Declaration

I, Imanu Immaculée Mwaba (0302068a), am a student registered for the degree of Doctor of Philosophy in the academic year 2017

I hereby declare the following:

- I am aware that plagiarism (the use of someone else's work without their permission and/or without acknowledging the original source) is wrong.
- I confirm that the work submitted for assessment for the above degree is my own unaided work except where explicitly indicated otherwise and acknowledged.
- I have not submitted this work before for any other degree or examination at this or any other University.
- The information used in the Thesis Report HAS NOT been obtained by me while employed by, or working under the aegis of, any person or organisation other than the University.
- I have followed the required conventions in referencing the thoughts and ideas of others.
- I understand that the University of the Witwatersrand may take disciplinary action against me if there is a belief that this is not my own unaided work or that I have failed to acknowledge the source of the ideas or words in my writing.

Signature___ ____ 5th June 2017

Research Output

IMI Mwaba and M.E.C. Rey (2013). Elucidation of the role of NOA1 in host response to infection by South African Cassava Mosaic Virus. 7th International Geminivirus Symposium & 5th International ssDNA Comparative Virology Workshop, 1 -10 November 2013, Qizhen Hotel" in Zhejiang University, Zijingang Campus, Hangzhou, China.

IMI Mwaba and M.E.C. Rey (2013). Elucidation of the role of NOA1 in host response to infection by South African Cassava Mosaic Virus. The South African Society for Microbiology (SASM), 24-27 November 2013. Forever Resorts Warmbaths, Bela-Bela, South Africa.

Abstract

Different host genes playing a role in replication, transcription and movement of geminiviruses have been identified, allowing a better understanding of host response during infection. The cytoskeletal protein myosin has been shown to associate with RNA viruses movement protein and mediate its movement, however no geminivirus association with myosin has been established. *Arabidopsis thaliana* nitric oxide associated protein 1 (AtNOA1), once thought to be an enzyme involved in a nitric oxide (NO) production, has been reported to be differentially regulated in response to biotic and abiotic stress. In this study we sought to identify the role that myosins and NOA1 play in the development of disease by south african cassava mosaic virus (SACMV). Using a bioinformatics approach, 24 myosin transcripts were identified in *Nicotiana benthamiana*, and phylogeny analysis revealed that seven were class VIII myosins and 17 class XI. Five myosins silencing constructs M15.1 (transcript Niben101Scf11288g00015.1), MYOSIN XI-F (M11.F), MYOSIN XI-K (M11.K), MYOSIN XI-2 (M11.2) and MYOSIN VIII.B were selected for silencing using a virus induced gene silencing (VIGS) approach with SACMV and TRV-VIGS vectors. At 14 days post inoculation (dpi), both SACMV and TRV-VIGS vectors successfully silenced myosins with SACMV-VIGS silencing all five and TRV-VIGS silencing all but M11. F. At 28 dpi, SACMV-VIGS induced silencing of myosin of only two myosins and TRV-VIGS three. TRV-VIGS was found to be more efficient at silencing as the suppression of myosin induced by TRV-VIGS was stronger than that of SACMV-VIGS. To assess the effect of myosin silencing on SACMV infectivity in a separate experiment, 7 dpi of silencing, *N. benthamiana* plants were challenged with SACMV and reduction of myosin expression was assessed as well as viral accumulation. TRV-VIGS did not induce any silencing of myosin at 14 dpi, and at 28 dpi, the expression of M11.K and M11.F were silenced. SACMV-VIGS induced silencing of M11.F at both 14 and 28 dpi. In TRV-VIGS silenced M11.K, viral load at 28 dpi was not lower than the control, however the fold increase in viral load at 28 dpi compared to 14 dpi was 3-fold (*p* value 0.03) for M11.K silenced TRV-VIGS plants and 86-fold for the control 6-fold for the M11.K suggesting that silencing of M11.K decreases the spread of SACMV. In TRV-VIGS silenced M11.K, viral load at 28 dpi was lower than the control (9-fold *p* value 0.03) and the increase in viral load at 28 dpi compared to 14 dpi was insignificant, suggesting that spreading of SACMV was also hampered. The reduction in myosin M11.F expression induced

by SACMV-VIGS resulted in an increase in viral load compared to the control. We hypothesise that the increase in viral load observed in M11.F silenced plants induced by SACMV-VIGS is due to the perceived resistance of SACMV-VIGS control (SACMV-challenged no silencing construct) to SACMV-challenge, and therefore results from the SACMV-VIGS study were inconclusive. From the TRV-VIGS study however, we have identified two candidate myosins in *N. benthamiana* myosin XI-K and myosin XI-F as potential interactor of SACMV during infectivity. Further research into their role in the development of SACMV disease is warranted.

Nitric oxide associated 1 (NOA1) in plants is a cyclic GTPase involved in protein translation in the chloroplast and has been indirectly linked to nitric oxide (NO) accumulation. To understand the role played by NOA1 in response to (SACMV) infection, a bioinformatics approach was used to identify NOA1 homologues in cassava T200. Using the cassava genome data on Phytozome, a putative NOA1 namely cassava 4.1_007735m, was identified. Based on its protein sequence, cassava4.1_007735m shared a 69.6% similarity to Arabidopsis NOA1 (AtNOA1). The expression of cassava4.1_007735.m (*MeNOA1*) and *N. benthamiana* NOA1 (*NbNOA1*) and the accumulation of NO in leaf samples was compared between SACMV-infected and non-infected at early infection stage (14 dpi for *N. benthamiana* and 28 dpi for cassava T200) and full systemic stage (28 dpi for *N. benthamiana* and 56 dpi for cassava T200). Real-time PCR was used to measure SACMV viral load which increased significantly by 2-fold (*p* value 0.05) from 14 to 28 dpi for *N. benthamiana* and 8-fold from 28 to 56 dpi in cassava T200 (*p* value 0.04) as chlorosis and symptom severity concomitantly progressed. At 14 and 28 dpi, *NbNOA1* expression was significantly lower than mock inoculated plants (2-fold lower at 14 dpi, *p* value 0.01 and 4-fold lower at 28, (*p* value 0.00) and the abundance of NO in infected *N. benthamiana* leaf tissue was 10% lower at 14 dpi and 40% lower at 28 dpi when compared to mock inoculated. In cassava T200, *MeNOA1* expression was unchanged at 28 dpi and NO levels were decreased by 40% and at 56 dpi, *MeNOA1* expression was 4-fold lower and NO accumulation was 37 % higher than that of mock inoculated leaf tissue. At 28 dpi for *N. benthamiana* and 56 for cassava T200, the decrease in *NOA1* expression was accompanied by chloroplast dysfunction, evident from the significant reduction in chlorophylls a and b and carotenoids in SACMV-infected leaf samples. Furthermore, the expression of

chloroplast translation factors (chloroplast RNA binding, chloroplast elongation factor G, translation initiation factor 3-2, plastid-specific ribosomal protein 6 and) were found to be repressed in infected *N. benthamiana* and infected cassava T200 relative to mock inoculated plants. GC-MS analysis showed a decrease in fumarate and an increase in glucose in SACMV-infected *N. benthamiana* in comparison to mock samples suggesting a decrease in carbon stores. Collectively, these results provide evidence that in response to SACMV infection in *N. benthamiana*, decrease in photopigment and carbon stores, accompanied by an increase in glucose and decrease in fumarate, lead to a decline in *NbNOA1* and NO levels. This is manifested by suppressed translation factors, and disruption of the chloroplast, resulting in chlorotic disease symptoms. In cassava T200 however, the link could not be established as the level of glucose was not significantly decreased and fumaric acid was not detected and although the concomitant decrease in the expression of *MeNOA1* and chloroplast translation factors indicate dysfunction of the chloroplast, the link between *MeNOA1* expression, carbon store, NO and chloroplast activity could not be established.

Acknowledgements

- I am extremely grateful to my supervisor Prof Chrissie Rey, for valuable advice and guidance throughout this project. The story of this young scientist will never be written without you at the beginning of it. Thank you.

- Special thanks go to the members of the "souls" of 2nd floor biology building, particularly to members of the Cassava Biotechnology Program for the friendships and laughs. As well as for your valuable help and input in getting this project to its completion.

- I would like to acknowledge my family, papa, maman and "my boys". Papa and maman, I took the long road just to be daddy's girl and I hope I made you both proud. And to my boys, I am eternally grateful, having you boys there made this road easier to bear. Thank you.

- To my husband, I would probably not have attempted this PhD if you hadn't made me. Thank you for your encouragements, this is to you and the kids.

- I acknowledge financial support from the National Research Foundation

- Finally and most importantly, I thank God for seeing me through this degree. It has not been easy, thank you for teaching me to be STILL!

Dedication

To Patrick, Malia and Enzi. Mille mercis

Table of contents

List of Tables

List of Figures

Abbreviations

(c)GTPase	(cyclic) Guanosine-5'-triphosphate hydrolase
aa	Amino acid
AbMV	Abutilon mosaic virus
Avr	Avirulence gene product
BDMV	Bean dwarf mosaic virus
bp	Base pair
BPG2	Brassinazole insensitive pale green 2
BYV	Bean yellow virus
CalCuV	Cabbage leaf curl virus
CDS	Coding sequence
cGTPase	Cyclic GTPASE
Chl	Chlorophyll
COP	Coat protein I (vesicle)
CP	Coat protein
CR	Common region
DAMPS	Damage associated molecular patterns
DCL	Dicer-like
dpi	Days post inoculation
dsDNA	Double stranded DNA
dsRNA	Double stranded RNA
EFG	Elongation factor G
EF-Tu	Elongation factor Tu
eNOS	Endothelial NOS
ER	Endoplasmic reticulum
ETC	Electron transport chain
ETI	Effector triggered immunity
FAD	Flavin adenine dinucleotide
FMN	Flavin mononucleotide
GABA	γ-aminobutyric acid
GAPDH	Glyceraldehyde-3-phosphate dehydrogenase
GFLV	Grapevine fanleaf virus
GOI	Gene of interest
GTP/GDP	Guanosine triphosphate/Guanosine diphosphate
GTPase	GTP hydrolase
HAMP	Herbivore associated molecular pattern
HR	Hypersensitive response
HSP	Heat shock protein
iNOS	Inducible NOS
MAPK	Mitogen-activated protein kinase
MCS	Multiple cloning site
MP	Movement protein
MYMV	Mungbean yellow mosaic virus
NADPH	Nicotinamide adenine dinucleotide phosphate
NES	Nuclear export signal
NLS	Nuclear localization signal
nNOS	Neuronal NOS
NO	Nitric oxide
NOA1	Nitric oxide associated 1

NOS	Nitric oxide synthase
NR	Nitrate reductase
NSP	Nuclear shuttle protein
nt	Nucleotides
$ONOO^-$	Peroxynitrite
PAMP	Pathogens associated molecules pattern
PDS	Phytoene desaturase
PR	Pathogenesis related
PR1	Pathogenesis related 1
PRR	PAMP recognition receptor
PTGS	Post transcriptional gene silencing
PTI	PAMP triggered immunity
PVX	Potato virus x
qPCR	Real-time PCR
R	Resistance gene product
RaLCV	Radish leaf curl virus
RCR	Rolling circle replication
RDR	Recombinant dependant replication
REn	Replication enhancer protein
Rep	Replication associated protein
RISC	RNA-induced silencing complex
RLK	Receptor-like kinases
RLP	Receptor-like proteins
RNS	Reactive nitrogen species
ROS	Reactive oxygen species
RRF	Ribosomal recycling factor
RRM	Chloroplast RNA binding
RT-PCR	Reverse transcriptase PCR
SA	Salicylic acid
SACMV	South african cassava mosaic virus
SAR	Systemic acquired resistance
siRNA	Small interfering RNA
SqLCV	Squash leaf curl virus
ssDNA	Single stranded DNA
SSS	Symptom severity score
SYTA	Synaptogamins
TCA	The citric acid cycle
TCV	Turnip crinkle virus
TGB	Triple gene block
TMV	Tobacco mosaic virus
TNA	Total nucleic acid
TRV	Tobacco rattle virus
TuM	Turnip mosaic virus
TYLCV	Tomato yellow leaf curl virus
TYMV	Turnip yellow mosaic
UBQ10	Ubiquitin 10
vDNA	Viral DNA
VIGS	Virus induced gene silencing

Chapter 1. Literature review

1.1 Cassava geminiviruses

Geminiviruses are insect transmitted, circular single stranded DNA (ssDNA) viruses, with genomes encapsidated in 2 (twinned) icosahedral particles. There are 9 genera under the *Geminiviridae* family, *Begomovirus*, *Becurtovirus, Capulavirus, Curtovirus*, *Eragrovirus, Grablovirus, Mastrevirus, Topocuvirus*, and *Turncurtovirus* that infect a wide range of plants (Varsani et al. 2017). Cassava (*Manihot esculenta* Crantz) is a tropical crop, mostly grown in sub-Saharan Africa as a cash crop by small farmers. Globally, cassava is gaining importance as an animal feedstock, a cheaper alternative to starch substrates and a potential source for bioethanol production (Nuwamanya et al. 2012). The production of cassava is severely threatened by cassava mosaic diseases (CMDs) which in Africa account for major losses in cassava production, up to 82% (Graziosi et al. 2016). The loss of revenue caused by CMD has been estimated to vary between 1.9 and 2.7 billion US dollar (Scholthof et al. 2011).

Cassava mosaic geminiviruses (CMGs), the causative agents of CMD and are single-stranded bipartite DNA viruses, belonging to the genus *Begomovirus*, transmitted to dicotyledonous plants in a circulative persistent manner by the whitefly species, *Bemisia tabaci* Gennadius (Brown et al. 1995; Harrison 2002; Fondong 2013). Characteristics of CMGs infection in cassava include severe stunting, chlorosis, leaf area reduction, leaf curling and blistering (Legg and Thresh 2000) (figure 1-1).

To date, nine species and various variants of begomoviruses causing CMD have been reported namely south african cassava mosaic virus (SACMV), east african cassava mosaic virus (EACMV), east african cassava mosaic kenya virus (EACMKV), east african cassava mosaic malawi virus (EACMMV), east african cassava mosaic zanzibar virus (EACMZV), cassava mosaic madagascar virus (CMMGV), african cassava mosaic virus (ACMV), indian cassava mosaic virus (ICMV) and sri lankan mosaic virus (SLCMV) (Brown et al. 2015). south african cassava mosaic virus (SACMV) was first isolated in South Africa (Berry and Rey 2001) but its incidence has since been reported in various others Southern African countries (Briddon et al. 2004; Harimalala et al. 2012).

Figure 1-1: SACMV infected cassava T200 in the laboratory

Symptoms of SACMV infection include leaf are reduction, leaf curling, blistering and chlorosis.

Begomoviruses are mainly bipartite (with some monopartite) circular ssDNA viruses; encapsidated in two twinned (geminate) icosahedral capsids and in each capsid is enclosed a genomic component, either DNA-A or DNA-B (figure 1-2). The two genomic components of bipartite begomoviruses, DNA-A and DNA-B, have sizes ranging between 2.7-2.8 kb and share a common region (CR) of about 200 bp with a similar sequence (Bisaro 2006) that contains the origin of replication, a conserved TAATATT/AC sequence and other regulatory sequences (Lazarowitz et al. 1992). DNA-A generally encodes for six proteins, two on the virion (sense) strand and four on the complimentary (antisense) strand. On the virion or sense strand, DNA-A encodes for the coat protein (CP; AV1) and the precoat protein (AV2). AC1-4 are found on the complimentary strand and code for a replication associated protein (Rep/AC1), transcription activator protein (TrAP/AC2), replication enhancer protein (REn/AC3), and the symptom enhancer and suppressor of RNA silencing, AC4 (Fondong 2013). Recently, AC5 was identified on the complimentary strand and characterised as an RNA silencing suppressor in mungbean yellow mosaic india virus (MYMIV) (Li et al. 2015). The DNA-B component of geminiviruses encodes the 2 movement protein genes, the nuclear shuttle protein (NSP/BC1) on the complimentary sense responsible for transporting newly formed ssDNA viral particles from the nucleus to the cytoplasm through nuclear pores

and the movement protein (MP/BV1) in the virion sense which aides in transporting viral particles to neighbouring cells (Gafni and Epel 2002).

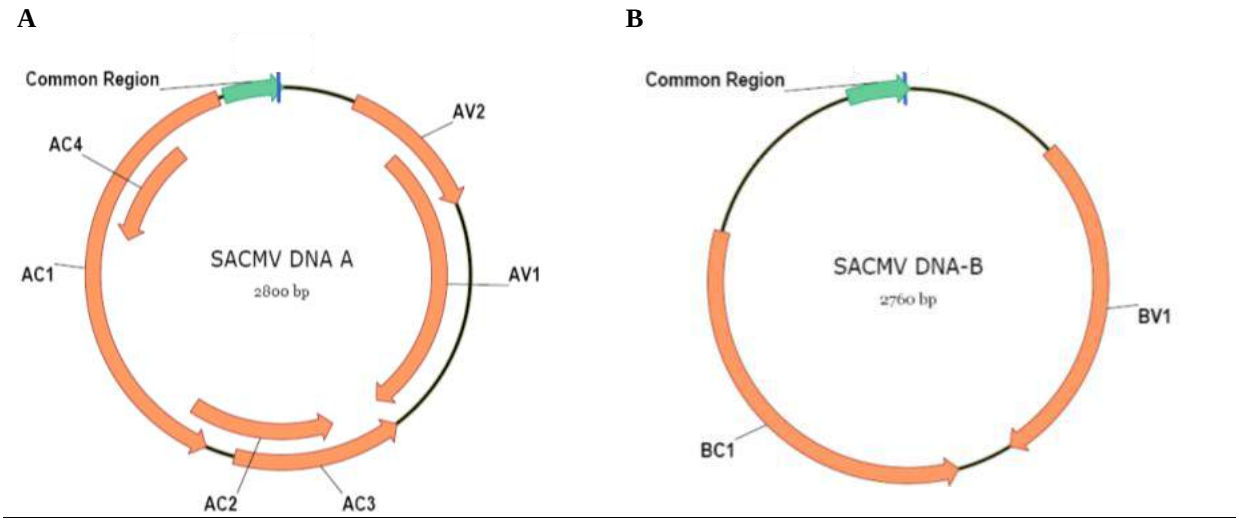

Figure 1-2: Genomic organization of SACMV

[**A**] DNA A component of SACMV is 2800 bp long. Two genes are encoded for in the sense strand, AV2 or precoat and AV1 or coat protein. In the antisense strand, four genes are encoded for, AC1 or Rep protein, AC2 or TrAP, AC3 or REn and AC4. [**B**] DNA-B component of SACMV is 2760 bp long, showing in the sense strand, the NSP BV1 and in the antisense strand, the MP. The common region as indicated is found in the intergenic region, shared by both DNA-A and DNA-B components, and contains different regulatory factors. Please refer to text for gene descriptions.

1.2 Replication and transcription of geminiviral genes

Genes found on the complimentary strand AC1-4 are needed for early infection processes such as DNA replication and transcription (Yang et al. 2016). Because geminiviruses do not encode all the genes required for replication and transcription they recruit the host machinery for these purposes (Hanley-Bowdoin et al. 2013). Geminivirus replication occurs in the nucleus via a combination of two mechanisms, rolling circle replication (RCR) (Nagar et al. 1995; Jeske et al. 2001) and recombinant dependent replication (RDR) (Jeske et al. 2001) and is dependent on the Rep protein.

Rep is mainly responsible for replication and it interacts with proteins involved in the cell cycle such as the Retinoblastoma-related protein, in order to reinitiate DNA replication in dormant cells, and through this process, viral DNA (vDNA) is replicated (Hanley-Bowdoin et al. 2013). Rep has also been shown to interact with other geminiviral proteins such as the REn and this interaction is believed to promote association with host factors as well as to

enhance ATPase activity of Rep promoting the replication of the geminiviral genome (Hanley-Bowdoin et al. 2013; Yang et al. 2016). Replication of geminiviral genomes yield a double stranded DNA (dsDNA) intermediate from which viral genes are transcribed (Shivaprasad et al. 2005). Within the common region of geminiviruses are two bidirectional promoters that allow for the transcription of genes on the sense and the complimentary strand. The AC2/TrAP protein has been shown to interact with transcription factors such as PEAPOD2 (Lacatus and Sunter 2009) and JDK (Lozano-Durán et al. 2011) to promote the transcription of "late" geminiviral genes such as the CP and the NSP. The REn interacts with NAC transcription factors and although it isn't clear how this benefits viral genes transcription, this interaction promotes the accumulation of viral ssDNA (Selth et al. 2005).

It has been suggested that the bidirectionality of geminivirus transcription results in 3' transcript overlap that, as a result of complementary base pairing, yields double stranded RNA (dsRNA) (Voinnet 2001; Sharma and Ikegami 2008). The presence of dsRNA triggers the onset of RNA silencing mechanism by the host, to suppress the expression of geminiviral genes. The dsRNA arising from viral replication and transcription are recognised by DICER-LIKE (DCL) protein and cleaved into small RNA fragments of 21-24 nt in length which serve as templates, leading the RNA-induced silencing complex (RISC) to degrade viral RNAs (Pallas and Garcia 2011). The TrAP/AC2 and AC4 are suppressors of RNA silencing, (reviewed in Sharma and Misra 2011) and are believed to work in synergy to provide an efficient RNA silencing suppression (Nawaz-ul-rehman and Fauquet 2009) perhaps together with the recently characterised RNA silencing suppressor AC5 (Li et al. 2015) and the precoat protein, AV2 whose role in bipartite begomovirus is unclear at this point, but has been found to have RNA silencing suppressing activity in monopartite begomoviruses (Zrachya et al. 2007; Sharma and Ikegami 2010).

1.3 Movement of geminiviruses

Once the viral genome is successfully replicated and viral proteins are translated, the virus needs to infect neighbouring cells to establish a successful infection, for which an efficient transport system is required. The CP, the MP and the NSP of bipartite begomoviruses are responsible for movement. The CP is multi-functional. It is involved in virus-vector specificity and transmission (Roberts et al. 1984), viral encapsidation (Harrison 2002), targeting the

virus into the nucleus and out to the cell membrane (Unseld et al. 2001) and accumulation of ssDNA particles in the cytoplasm (Qin et al. 1998). In monopartite begomoviruses, CP serves a nuclear shuttling role (Gafni and Epel 2002) and with either V2 or C4 are responsible for movement (Rojas et al. 2001; Rojas et al. 2016).

Cassava mosaic viruses are generally viewed as non-phloem limited begomoviruses, with the exception of ICMV (Rothenstein et al. 2007). Non-phloem-limited begomoviruses such as SACMV are dispensable of the CP for cell-to-cell movement which is rather mediated through a partnership between the NSP and the MP, with the CP required for plant-vector transmission (Pooma et al. 1996; Kelkar et al. 2016). The NSP of begomoviruses is responsible for transporting infecting viral complexes into the nucleus and newly formed ssDNA vDNA from the nucleus to the cytoplasm, through nuclear pores. Upon initial infection, ssDNA is released from the virion capsid and with the help of NSP, enters the nucleus, where replication and transcription occurs. The NSP has, like the CP of monopartite begomoviruses, 2 nuclear localisation signals (NLS) at its N-terminus, which mediate import of vDNA into the nucleus (Sanderfoot et al. 1996), however the host factors that the NSP interacts with to aid in nuclear import haven't been identified.

Nuclear import is mediated by importins alpha and beta, and although no NSP has yet been shown to interact with importins, the CP of the monopartite tomato yellow leaf curl virus (TYLCV) and the bipartite mung bean yellow mosaic virus (MYMV) have been shown to interact with importin alpha (Kunik et al. 1999; Guerra-Peraza et al. 2005). Importin alpha was also identified to be differentially expressed in tomato infected with tomato yellow leaf curl Sardinia virus (TYLCSV) infection (Lozano-Durán et al. 2011; Chandran et al. 2012). Once in the nucleus, vDNA is replicated into dsDNA forms used for templates for RCA-mediated replication and transcription, and some vDNA is packaged into DNA-protein complexes consisting of ssDNA, some dsDNA, NSP and host cofactors (Zhou et al. 2011; Gorovits et al. 2013). The NSP of cabbage leaf curl virus (CaLCuV) infecting Arabidopsis has been shown to inhibit the nuclear acetyltransferase and the nuclear shuttle protein interactor (AtNSI) (McGarry et al. 2003; Carvalho and Lazarowitz 2004; Carvalho et al. 2006; Lozano-Durán et al. 2011). Inhibition of AtNSI leads to the inhibition of histone 3 acetylation, and this is believed to promote the integration of histones H3 in the vDNA-protein complex, leading to the formation of minichromosomes (Zhou et al. 2011) that are exported from the nucleus

through nuclear pores (Gafni and Epel 2002; Hehnle et al. 2004). The export of NSP-vDNA complex from the nucleus into the cytoplasm is mediated by a leucine-rich nuclear export signal (NES), located at the C-terminus of NSP, which interacts with the host's NSP interacting GTPase (NIG) (Carvalho et al. 2008a; Carvalho et al. 2008b). Comparatively to nuclear export of geminiviruses, little is known about intracellular and intercellular mechanisms of geminiviral movement.

The NSP and MP collaborate to allow a successful cell to cell movement for begomoviruses and this collaboration has been suggested to occur via 2 different models, namely "relay race" and "double skating" model (Rojas et al. 2005; Frischmuth et al. 2007). In the relay race model, the NSP shuttles viral ssDNA particles from the nucleus to the cytoplasm where the vDNA complexes are released and the MP takes over, transporting the vDNA complexes to the cellular periphery where they move to neighbouring cells through the plasmodesmata. This model has been shown to be true for bean dwarf mosaic virus (BDMV). The MP of BDMV was shown to have affinity for dsDNA particles and it was also shown that it is through a formation of MP-dsDNA complex that BDMV viral particles spread to neighbouring cells (Noueiry et al. 1994; Rojas et al. 1998; Levy and Tzfira 2010).

In the couple skating model, the NSP shuttles the vDNA complexes out of the cytoplasm and associates with the MP and the whole cargo is transported to the cell periphery where MP is released and the NSP-vDNA complex moves to neighbouring cells through the plasmodesmata (Frischmuth et al. 2007). It is believed that abutilon mosaic virus (AbMV) and squash leaf curl virus (SqLCV) use this model for proliferation. When expressed independently, the NSP of AbMV localises around the nucleus, and when expressed concurrently with the MP of AbMV, NSP localises around the nucleus as well as at the cell periphery (Zhang et al. 2001; Frischmuth et al. 2007) and the NSP of SqLCV was shown to have an affinity for both dsDNA and ssDNA but its MP only showed a weak affinity to dsDNA and no affinity to ssDNA (Pascal et al. 1994; Rojas et al. 1998; Hehnle et al. 2004; Levy and Tzfira 2010).

It is not yet known which model of movement cassava mosaic viruses use as their movement proteins have not yet been characterised. Irrespective of the model that cassava mosaic viruses use, they like other geminiviruses require the participation of host factors in

order to reach the cell periphery and infect neighbouring cells. Plant RNA viruses have been used to draw models of plant virus movements, as in contrast to geminiviruses, considerable attention has been focused the movement of RNA viruses. Two different pathways through which macromolecular trafficking occurs in plants have been identified as ways that plant viruses could hijack to their advantage (Harries et al. 2010; Harries and Ding 2011).

Cellular organelles and macromolecules can move along the cytoskeleton, either by binding to a motor protein, myosin, kinesin and dynein, to be carried to various destinations along actin filaments and microtubules, or the cargo could bind directly to actin and microtubules and move along them through the polymerization/depolymerization of the cytoskeleton (Harries et al. 2010). Molecular movement can also be mediated through the endomembrane system. Movement via the endomembrane system utilises vesicles, in which the cargo is enclosed, and transported to its various destinations. Vesicles form by budding off the endomembrane system, enclosing macromolecules, and moving either along the cytoskeleton, or through membrane continuities and continuous fission and fusion of the membrane (Brandizzi et al. 2002; Moreau et al. 2007; Harries et al. 2010). Both transport through the cytoskeleton or the endomembrane highlight a central role by cytoskeletal proteins in the movement of macromolecules throughout the cell.

1.3.1 The cytoskeleton and viral movement

The cytoskeleton consists of three types of filaments, the actin filament, intermediate filament and microtubules. Actin filaments and microtubules are composed of actin and tubulin subunits, respectively, that polymerise and depolymerise, changing the dynamic of the filament. This change in cytoskeleton dynamic is believed to be one of the methods through which viruses move (Harries et al. 2010). The exact mechanism by which the cytoskeleton participate in viral movement is not clear. The plant cytoskeleton is involved in various processes in the cell including cell division, cell expansion, organelles organization and motility (Takemoto and Hardham 2004) and besides a direct involvement in plant virus movement, these different processes suggest that the cytoskeleton could be part of defence or susceptible responses to viral infection.

As mentioned previously, plant virus movement have been modelled using RNA viruses and RNA virus movement suggest a role of both the endomembrane system and the cytoskeleton in viral movement. tobacco mosaic virus (TMV) has been shown to replicate in the endoplasmic reticulum (ER), where it forms viral complexes with their movement protein (P30) as well has host proteins such as the chaperone calreticulin (Chen et al. 2005) or the synaptogamins SYTA (Lewis and Lazarowitz 2010), and can either be transported by vesicles or a protein complex bound to either the actomyosin network or to the microtubule network and move to the cell periphery (Harries et al. 2009; Harries et al. 2010). potato virus x (PVX) movement occurs through the interaction of its CP with the ER's triple gene blocks (TGB) 2 and 3 vesicles, and the viral complex formed moves to the plasmodesmata, along the actin network (Lucas 2006). PVX CP can move bound to TGB2 and 3 along the actin network without the use of vesicles to the cell periphery (Kumar et al. 2014) or it can diffuse as modified virion bound to TGB1 (Rojas et al. 2016).

In terms of the movement of geminiviruses, although a model has not yet been drawn, cellular host proteins have been linked to geminiviral movement proteins. The MP of CalCuV and SqLCV were shown to interact with the synaptogamin SYTA (Lewis and Lazarowitz 2010). SYTA are conserved calcium-and lipids-binding proteins, involved in anchoring the endomembrane system to the plasma membrane. SYTA was found to bind directly to the MP of CaLCuV and SqLV and knocking down of SYTA delayed virus infection, endosome formation, as well as cell to cell viral proliferation by CalCuV MP, suggesting CalCuV uses an endosome-dependant pathway to spread intercellularly (Lewis and Lazarowitz 2010). Silencing of the heat shock cognate 70 kDa protein cpHSC70-1 in *Nicotiana benthamiana* restricted the movement of AbMV and cpHSC70-1 and MP of ABMV were shown to interact using yeast 2 hybrid system (Krenz et al. 2010). The cpHSC70-1 is found associated with stromules which are projection of the plastidial membrane, that are believed to serve as sites of molecules exchange and connection between plastids. Stromules were found to extend during AbMV infection to various organelles and by extending they could potentially carry viral proteins and complexes to different sites in the cell (Krenz et al. 2012; Caplan et al. 2015). Downregulation of coatomer delta subunit (deltaCOP) in *N. benthamiana* prevented the movement of TYLCV. DeltaCOP encodes a component of the vesicle coat

protein I (COPI) which is involved in the retrograde endomembrane transport system, from the Golgi bodies to the endoplasmic reticulum (Lozano-Durán et al. 2011).

Besides chaperones like HSP70, kinases have been shown to aid in diffusion of molecules to the plasma membrane (Harries et al. 2010; Niehl and Heinlein 2011). The MP and NSP of SqLCV and the CP of ACMV have been shown to be targeted by phosphorylation (Kleinow et al. 2008; Hipp et al. 2016) and phosphorylation sites at the C- terminus of MPs are believed to be responsible for modifying the size exclusion limit of the plasmodesmata (Levy and Tzfira 2010). The MP of ACMV can also be targeted by posttranslational modification, however the nature of these modifications is not known (Von Arnim et al. 1993; Kleinow et al. 2008; Kleinow et al. 2009). Posttranslational modifications of geminiviral MPs suggest a possible interaction between MPs and posttranslational modification proteins that could play a role in viral movement.

1.3.1.1 Plant myosin and viral movement

As mentioned previously, the role played by the cytoskeleton or actin filaments is believed to be either by direct interaction with viral proteins, or interactions with host factors bound to viral proteins (Rojas et al. 2016). Given that there are report suggesting the involvement of either the actomyosin or the microtubule network in viral movement (Kawakami et al. 2004; Prokhnevsky et al. 2005; Avisar et al. 2008a; Harries et al. 2009), we sought to establish a link, if any, between the actomyosin network and SACMV movement, by looking at a possible role for myosins in SACMV movement.

Myosin motors belong to a superfamily of motor proteins, conserved throughout Eukarya with 18 classes previously reported (Foth et al. 2006), however a recent next generation sequencing analysis revealed there might be at least 31 classes of myosins in eukaryotes (Sebe-Pedros et al. 2014). In plants, only two of these classes, class VIII and class XI are represented, with seventeen members having been identified in Arabidopsis (figure 1-3) (Reddy and Day 2001; Lee and Liu 2004), 14 members in maize (Wang et al. 2014) and so far, six members characterised in *N. benthamiana* (Avisar et al. 2008b). Myosins generally contain three domains, an ATPase dependent actin binding domain (motor domain), a neck domain with affinity for light chains and Ca^{2+}/calmodulin and a tail of coiled coil domain (Reddy and Day 2001; Sparkes et al. 2008).

Class VIII myosins are found associated with endosomes, the ER, the plasmodesmata and the nascent cells plasma membrane as well as the plasma membrane of plastids (Reichelt et al. 1999; Avisar et al. 2008a; Maule 2008; Haraguchi et al. 2014). They are believed to be involved in trafficking to the plasmodesmata as well as endocytosis in plants (Golomb et al. 2008; Sattarzadeh et al. 2008) and are involved with microtubules in plant cell division (Wu and Bezanilla 2014). Class VIII myosins have a lower processive activity to class XI but with a stronger affinity for actin they are believed to act as a tension sensor and generator (Haraguchi et al. 2014). Plants class VIII myosins have a relatively longer N-terminus and shorter C-terminus when compared to Class XI myosins (figure 1-3). At the N-terminus of class VIII myosins is a PEST motif believed to contain regulatory signals, followed by a motor domain where ATP hydrolysis and actin interaction takes place and leading into the C-terminus are 3 or 4 IQ domains believed to be a binding and regulatory site for calmodulin and a coiled coil domain of various length responsible for dimerization (Yokota and Shimmen 2011).

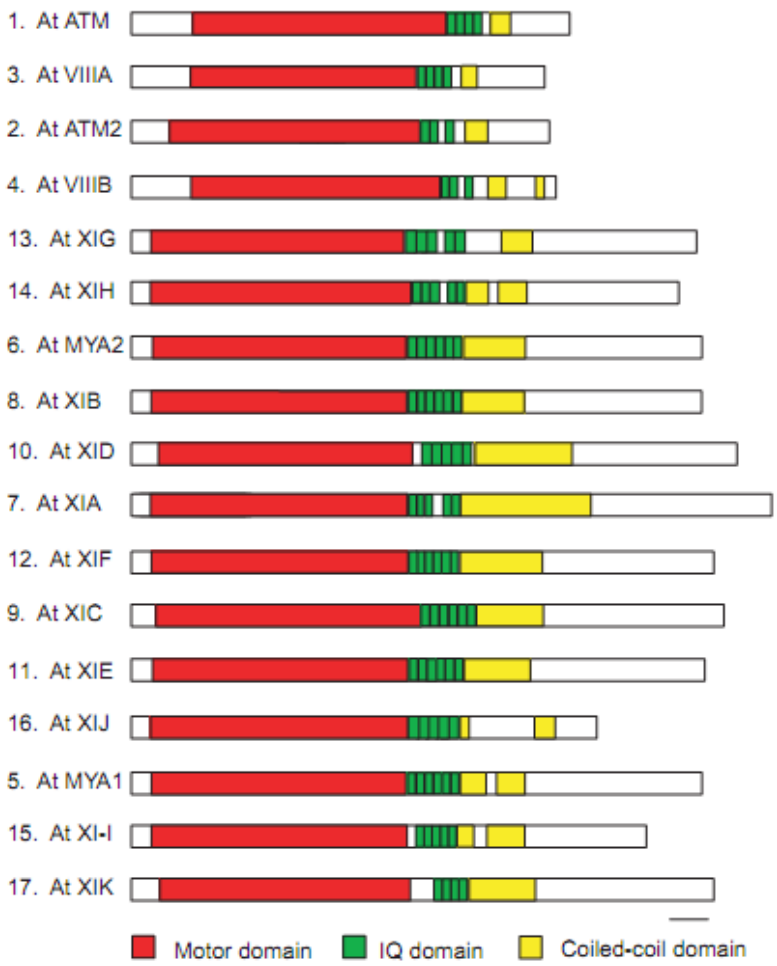

Figure 1-3: Arabidopsis myosin domains, adapted from Reddy and Day 2001.

Class XI myosin are the fastest known motor proteins (Lee and Liu 2004) and are involved in vesicles and organelle fluidity, cytoplasmic streaming, cellular morphogenesis, expansion and elongation, gravitropism, actin integrity and organisation gravitropism (Ojangu et al. 2007; Peremyslov et al. 2008; Prokhnevsky et al. 2008; Sparkes et al. 2008; Avisar et al. 2008b; Peremyslov et al. 2010; Ueda et al. 2010; Yokota and Shimmen 2011; Park and Nebenführ 2013; Tamura et al. 2013a; Ueda et al. 2015; Talts et al. 2016). The architecture of class XI myosin consists of N-terminus SH3 like domain of unknown function, a motor domain followed by 4- 6 IQ domains, coiled coil domains of varying length and lastly a DIL domain, responsible for cargo binding (Sattarzadeh et al. 2008; Reddy et al. 2011; Sattarzadeh et al. 2011; Yokota and Shimmen 2011). Arabidopsis myosin XI-I has a slower processing speed but stronger affinity to actin compared to other myosins XI. Myosin XI-I is

phylogenetically distant from other class XI myosins as its branches out on its own away from other myosins XI on the phylogenetic tree (Peremyslov et al. 2011) and is believed to regulate organelle movement and similarly to myosin VIII, to function as a tension generator (Haraguchi et al. 2016).

Given that plant myosins class VIII and class XI are involved in different plant processes it is unsurprising that their involvement in plant virus movement differs (Avisar et al. 2008a; Peremyslov et al. 2008; Amari et al. 2011; Amari et al. 2014). With regards to plant virus movement, there are reports suggesting the participation of either class VIII or class XI myosins, or both. Disruption of myosins in general using the inhibitor 2,3-butanedione monoxime, affected TMV spread (Kawakami et al. 2004), however disruption of class VIII myosins had no effect on TMV MP localization, but was shown to affect the interaction of the beet yellow virus (BYV) HSP70 homologue (Avisar et al. 2008a). In *N. benthamiana,* VIGS mediated silencing of myosin XI-2, but not of myosin XI-K, myosin VIII-1 and myosin VIII-2, inhibited TMV propagation (Harries et al. 2009). Myosins XI have been shown to play a role in the movement of grapevine fanleaf virus (GFLV) (Amari et al. 2014) and turnip mosaic virus (TuMV) (Agbeci et al. 2013) and both members of myosins class VIII and XI play a role in the movement of viral replication complexes of TMV to the plasmodesmata (Amari et al. 2014).

The evidence of a possible involvement of myosins in geminivirus movement is at this point limited, however there are reports of a possible indirect link. The movement of AbMV was shown to occur with the help of stromules (Krenz et al. 2012) and in turn, their dynamism is reliant on myosin XI and actin (Natesan et al. 2009; Sattarzadeh et al. 2009). In another study, the integrity of microtubules and actin filaments was shown to influence the cellular distribution of TYLCV, in turn impacting on its movement (Moshe et al. 2015). The involvement of SYTA and deltaCOP strongly suggests a central role for the endomembrane system in geminivirus movement and the cytoskeleton could indirectly influence geminivirus movement through its role in maintaining the integrity of the ER and different players of the endomembrane system (Peremyslov et al. 2008; Prokhnevsky et al. 2008; Avisar et al. 2008b; Ueda et al. 2015).

In order to evaluate whether or not, plant myosins play a role in the cytosolic movement of SACMV, we opted for the use of a virus induced gene silencing approach (VIGS) to silence myosins in *N. benthamiana* and assess the effect on SACMV accumulation.

1.3.1.2 Virus induced gene silencing

RNA silencing is a process used by plants to regulate gene expression and is triggered by the presence of dsRNA. Although the role of RNA silencing in plant is the regulation of endogenous gene expression, dsRNA that arises from the transcription viral RNA can trigger the RNA silencing machinery leading to suppression of transcription of virus genes and hence RNA silencing has been described as adaptive immunity (Waterhouse et al. 2001). With regards to geminivirus gene transcription, the abundant and bidirectional transcription of its circular genome as well as secondary structures formed by viral RNA can give rise to dsRNA intermediate targeted by the host RNA silencing machinery, resulting in viral RNA degradation (Bieri et al. 2002; Aregger et al. 2012). Plants viruses encode silencing suppressors to evade the host's RNA silencing machinery, shielding their genome from being targeted (Sharma and Ikegami 2008; Csorba et al. 2015).

The ability of the host to target viral RNA has been adapted in laboratories to trick the plant into silencing endogenous genes or transgenes, by inserting a fragment of the target sequence in the antisense orientation into the genome of a virus and as the host RNA machinery attempts to silence viral RNAs, the target gene is inherently silenced (Robertson 2004; Senthil-Kumar and Mysore 2011b; Lange et al. 2013). The use of a virus as a vector to silence plant genes dubbed virus induced gene silencing or VIGS, has been extensively used as a tool for functional genomics. VIGS is preferred over other functional genomic tools as the process from selecting the gene of interest to observing the silenced phenotypes is less laborious and quicker to achieve compared to other functional genomics tools (Robertson 2004; Senthil-Kumar and Mysore 2014).

Tobacco rattle virus (TRV) is a bipartite positive sense RNA virus that has been preferentially used as a VIGS vector as it has a wide host range and it can spread to every organ in the plant while causing minimal symptoms (Ruiz et al. 1998; Ratcliff et al. 2001; Senthil-Kumar and Mysore 2014). TRV was modified for VIGS study by replacing the 2 non-structural proteins found on TRV2 by a multiple cloning site, allowing for the insertion of the target

sequence fragment (Ratcliff et al. 2001; Liu et al. 2002a; Liu et al. 2002b). Besides TRV, other RNA viruses commonly used as VIGS vectors include PVX (Ruiz et al. 1998) and TMV (Kumagai et al. 1995).

VIGS vectors have also been designed on plant DNA viruses. Plant DNA VIGS is believed to provide a more stable silencing as their genome is not RNA based and therefore cannot be targeted by the plant's RNA silencing mechanism (Robertson 2004). Different plant geminiviruses have been designed for VIGS (Kjemtrup et al. 1998; Peele et al. 2001; Gosselé et al. 2002; Turnage et al. 2002; Muangsan et al. 2004; Tao and Zhou 2004; Golenberg et al. 2009; Huang et al. 2009; Ju et al. 2016) and cassava geminiviruses have been used as VIGS vector to successfully silence the *su* gene in *N. benthamiana* and cassava (figure 1-4)(Fofana et al. 2004; Mwaba 2010) and phytoene desaturase gene in cassava (Beyene et al. 2017).

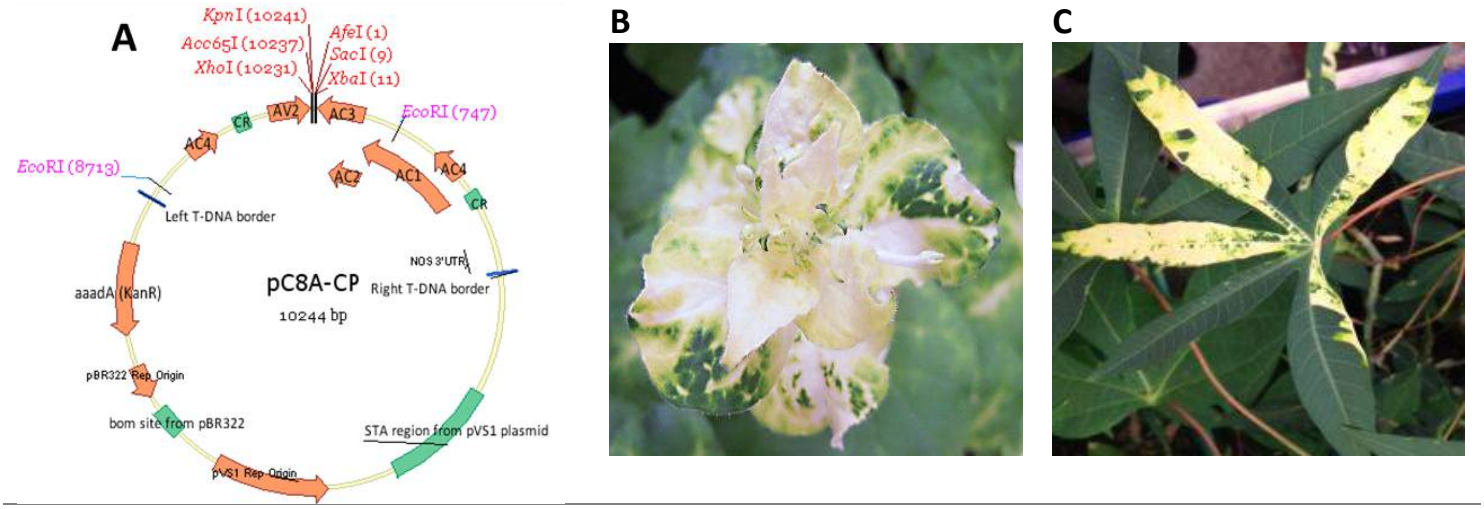

Figure 1-4: SACMV VIGS vector and su silencing in *N. benthamiana* and cassava T200

[**A**] SACMV-A VIGS, 568 bp at the 3' end of AV1 was replaced with an MCS containing different restriction sites for XhoI, Acc65I, KpnI, AfeI, SacI and XbaI. The multiple cloning site was inserted without disrupting the ORF of AV2 and AC3. [**B**] Silencing of the *Su*-gene (*Chl* I) a subunit of magnesium chelatase, an enzyme involved in chlorophyll production. *Su* silencing using SACMV silencing construct at 35 dpi. [**C**] *Su* silenced cassava T200 at 35 dpi.

The development of a SACMV VIGS vector system was prompted by the lack of available vectors that infect cassava, leading functional studies on cassava geminivirus responsive genes being carried out in model host such as Arabidopsis and *N. benthamiana.* The SACMV VIGS vector was constructed by replacing 568 bp portion of the coat protein with a multiple cloning site (Mwaba 2010), without disrupting AV2 and AC3 open reading frames, flanking

AV1 in wild type SACMV (figure 1-4a) and the SACMV-VIGS vector has been successfully used to silence *su* in *N. benthamiana* and cassava.

While VIGS is a power tool for functional genomics studies, it has several limitations that need to be considered when designing a VIGS study. Because VIGS silencing is based on sequence similarity, the insert sequence used for the VIGS construct will induce silencing of any genes that has some degree of similarity with it. While this can be an advantage for heterologous silencing like is the case for silencing of *su* where the *Su*-gene from *Nicotiana tabacum* has been used to silence *su* in *N. benthamiana* and in cassava (Fofana et al. 2004; Mwaba 2010), this can pose a problem when attempting to target a gene that shares sequence similarity with other genes, like members of a gene family, or different genes having similar domains. To avoid off-target silencing by VIGS, there are tools developed like the VIGS tool from Solgenomics network (SGN) which identifies potential off-targets (Fernandez-Pozo et al. 2015). Off-target silencing can also be caused by transitive silencing, where the VIGS construct results in amplification of RNA silencing signals. Although so far, transitive silencing has only been shown for VIGS targeting a transgene (Robertson 2004; Petersen and Albrechtsen 2005; Jones et al. 2006).

Silencing induced by VIGS doesn't results in a complete inactivation of the gene expression, and therefore some residual expression of the target is to be expected. This is an issue when the silenced tissues can't be identified visually, unlike silencing of *su* (figure 1-4) and phytoene desaturase (PDS) which have both been used as visual markers of silencing when designing VIGS constructs. Although the incomplete inactivation has been said to be an advantage for VIGS studies of genes whose mutation are lethal for the plants, it can affect the perceived overall efficiency of silencing by VIGS (Robertson 2004; Senthil-Kumar and Mysore 2011a; Lange et al. 2013). Residual gene expression of the target gene can also be translated to enough protein to carry out its function without affecting the phenotype or the processes that the protein participates in (Velasquez et al. 2009).

The efficiency of silencing can also be affected by the silencing construct sequence, its length, its orientation, the position of the gene target in the genome as well at the inoculation method chosen for vector delivery (Senthil-Kumar and Mysore 2011b). Sequences of length smaller than 100 and larger than 400 nucleotides have been shown to

have a reduced silencing efficiency (Liu and Page 2008; Senthil-Kumar and Mysore 2014) and the recommended insert size for TRV-VIGS vector is estimated at 250 – 300 nucleotides (Senthil-Kumar and Mysore 2011a).

The VIGS vector chosen for the study can also influence silencing as a vector with a strong suppressor of RNA silencing can impact on the ability of a vector to induce silencing. In a study where VIGS was based on a geminiviral vector, it was shown that mutation of the silencing suppressor AC2 promoted the efficiency of VIGS (Pandey et al. 2009). The efficiency of silencing is also affected when silencing of the gene of interest has the potential to affect the spread of the vector itself (Liu and Page 2008). The 'virus effect" by the chosen VIGS vector can't be ignored as although modified, treatment of plants with a VIGS vector elicits an attenuated response in the host, which can influence the results of a VIGS study (Oláh et al. 2016). When VIGS silencing is coupled with inoculation of another virus, like is the case during plant – pathogen studies mediated by VIGS, the possible synergistic, antagonistic and additive effect of VIGS vector on the virus being investigated cannot be ignored and to circumvent the virus effect, the use of appropriate controls is required (Robertson 2004; Morilla et al. 2006; Czosnek et al. 2013; Senthil-Kumar and Mysore 2014).

1.4 SACMV and host interactions: beyond the cytoskeleton, the case of the cyclic GTPase *Nitric Oxide Associated 1*

In addition to host genes involved in movement, there are other virus-induced complex host stress responses which directly or indirectly influence the movement and replication of geminiviruses. Different families of guanosine triphosphatase (GTPase) have been found to participate in molecules trafficking in plants. The Rab protein family is a family of small GTPases, involved in mediating the specificity between the target membranes and trafficking vesicles (Rutherford and Moore 2002), as well as regulating the interaction between the vesicle proteins v-SNAREs and t-SNAREs (Nebenführ 2002; Rutherford and Moore 2002).

The exact mechanism by which Rabs participate in plant virus movement has not yet been elucidated however it is speculated that plant MP could bind a Rab directing itself to the

plasmodesmata (Oparka 2004). Our interest in small GTPase stems from the recent identification of a novel family of GTPase, namely cyclic GTPase (cGTPase) that has been linked to the indirect production of nitric oxide (NO) in plant cells (Gas et al. 2009; Leitner et al. 2009). NO mediates signalling events during plant-pathogen interactions, and many genes have been identified in transcriptome studies to be targeted by NO either directly or indirectly (Polverari et al. 2003; Parani et al. 2004). Among the NO downstream effectors are cytoskeletal proteins which are involved in processes regulated by NO (reviewed in Yemets et al. 2011). In Arabidopsis, the formation of papillae in response to pathogen attack is regulated by NO and by the rearrangement of the cytoskeleton (Prats et al. 2005). Rearrangement of the cytoskeleton was also shown to regulate the site of reactive oxygen species (ROS) production and probably NO and it is conceivable that NO could play a role in the rearrangement of plant cytoskeletal components in response to virus infection.

Despite being ubiquitously present in plants, the major source of NO production has not yet been deciphered. The cGTPase nitric oxide associated 1 (NOA1), a protein once thought to be a nitric oxide (NO) producer, localises in the chloroplast and its function indirectly contributes to the overall NO availability in plant cells but itself isn't a NO producing protein (Moreau et al. 2008; Sudhamsu et al. 2008). NOA1 is a member of the cGTPase family YlqF/YawG family with nucleic acids and protein binding abilities (Moreau et al. 2008; Sudhamsu et al. 2008) and the expression of NOA1 is differentially regulated in response to different biotic and abiotic stimuli (Zeier et al. 2004; Kato et al. 2007; Zhao et al. 2007; Wünsche et al. 2011; Mandal et al. 2012).

Guanosine triphosphate (GTP) and guanosine diphosphate (GDP) are involved in various processes in a cell, however the function of cGTPase in plants and mammals has not yet been clarified. In the second part of the research, we sought to highlights the involvement if any, of the cGTPase NOA1 in SACMV pathogenesis in *N. benthamiana* and cassava, and elucidate the link between NO accumulation and expression of NOA1 in SACMV-infected *N. benthamiana* and cassava.

1.4.1 Nitric oxide associated protein 1 (NOA1), NO and plant disease

Nitric oxide (NO) is a free radical, signalling molecule that participates in many processes in a cell. It is highly reactive; it has a singlet electron and can be found in a cell in different

forms, nitrosonium cation (NO^+), nitroxyl anion (NO^-) and nitric oxide radical ($NO^{\cdot}$; Arasimowicz-Jelonek and Floryszak-wieczorek 2007; Leitner et al. 2009; Wojtaszek 2000) and gives rise to various NO derived molecules.

Because of its highly reactive nature, NO tends to readily react with different targets in a cell. The targets that have been mostly studied in relation to their association with NO are ROS. As their name suggest ROS are also highly reactive molecules, consisting of the superoxide anion ($0_2^{\cdot-}$) and hydrogen peroxide (H_20_2). These ROS are consistently being produced and used up in a cell by various processes and when the amount of produced ROS exceed that which is being used up, a cell is said to be under oxidative stress (Neill et al. 2002). In the presence of ROS, NO readily reacts with them and give rise to more reactive molecules termed reactive nitrogen species (RNS; Leitner et al. 2009). RNS include peroxynitrite ($ONOO^-$) derived through interaction with ROS, *S*-nitrosothiols derived through interactions with thiols, mononitrosyl-iron and dinitrosyl-iron complexes derived through interactions with haeme and iron-sulphur centre of proteins, metal-nitrosyl derived through the interaction with transition metals and higher oxide of nitrogen derived through spontaneous oxidation (Neill et al. 2008; Leitner et al. 2009). These RNS together with the different forms of NO present in a cell, provide different possibilities through which NO affects the cellular environment, like contributing to disease resistance (Mur et al. 2006; Hong et al. 2008; Leitner et al. 2009; Bellin et al. 2013; Jeandroz et al. 2013; Sun and Li 2013; Agurla et al. 2014; Trapet et al. 2015). Beside biotic stress responses, NO is also involved in abiotic stress responses, various growth and developmental processes, and it participates in different metabolic reactions in organelles such as the chloroplast, the mitochondrion and the peroxisome as well as in the cytosol (del Río et al. 2004; Qiao and Fan 2008; Igamberdiev et al. 2014; Misra et al. 2014; Sanz et al. 2015).

1.4.1.1 NO and biotic stress

Plant survival is persistently threatened by pests and pathogens, whose mode of attack and the pathways they each elicit may differ from one to the other, however there is a crosstalk existing between them. To mount an effective response against an invading pathogen, plants need to be able to identify the threat. Pathogens bear distinctive conserved patterns recognised by the plants known as herbivores- and microbes- associated molecular patterns (HAMPs/MAMPs) and damage associated molecular patterns (DAMPs). Examples of these

patterns include lipopolysaccharides, peptidoglycan and flagellin of bacteria, fungal cell wall carbohydrates, compounds present in oral secretion of insects as well as compounds released by the plants in response to wounding (Erb et al. 2012; Newman et al. 2013; Savatin et al. 2014). The presence of MAMPs, HAMPs and DAMPs are sensed by plant cells transmembrane pattern recognition receptors (PRRs) (Jones and Dangl 2006) which are either receptor-like kinases (RLKs) or receptor-like proteins (RLPs) (Newman et al. 2013). Upon perceptions of these molecular patterns, the plant responds by initiating pattern triggered immunity (PTI) and as a counter defence response and some pathogens have evolved means to suppress PTI by expressing effector proteins. In retaliation, plants express resistance gene (*R*-gene) products, which can recognise effector proteins, in a response known as effector triggered immunity (ETI) (Jones and Dangl 2006; Cui et al. 2015). Unlike PRRs which recognise a broad class of pathogen signature, *R*-genes belong to the nucleotide binding and leucine rich repeats (NB-LRR) family and recognise specific pathogen effectors known as avirulence (avr) protein (Jones and Dangl 2006; Gururani et al. 2012). *R*-gene products can recognise and bind directly to avr proteins but can at times, recognise plant proteins modified by the presence of an avr protein (Gururani et al. 2012).

While bacterial and fungal MAMPs have been widely studied, only recently have dsRNAs associated with viral infection been recognised as viral PAMPs (Niehl et al. 2016) and some plant-virus infections have been shown to trigger PTI responses (Nicaise 2014; Onaga and Wydra 2016). A model for PTI responses to viruses suggests that the host recognises naked viral PAMPs and virus-encoded proteins act as effectors that are targeted by *R*-genes, triggering an antiviral ETI response (Mandadi and Scholthof 2013; Nicaise 2014). There is evidence that geminiviruses can elicit antiviral ETI responses in the host, through the interaction between the NSP and the RLK, NSP interacting kinase (NIK) 1-3 (Fontes et al. 2004; Mariano et al. 2004; Carvalho et al. 2008c). Geminiviral MP and NSP have been identified as targets of plant defence response (Garrido-Ramirez et al. 2000; Hussain et al. 2005; Zhou et al. 2007) and evidence suggests that the expression of *R*-genes and *R*-genes like are modulated upon infection with SACMV in cassava (Allie et al. 2014; Louis and Rey 2015).

As a result of a successful PTI and ETI lies a cascade of signalling pathways that changes the status quo in plant cells leading to defence responses. The Hypersensitive response (HR) is

one such response that results in increases in the production ROS as well as in the expression or pathogenesis-related (PR) genes (Mur et al. 2008; Zurbriggen et al. 2010). The oxidative damage and activation of PR genes that occur during the HR leads to the onset of programmed cell death, causing necrosis in infected cells, in order to contain the pathogen and prevent its propagation to adjacent cells. The onset of HR in infected cells can in some cases lead to systemic acquired resistance (SAR) and in other cases, SAR can be induced independently of a HR. During SAR, the phytohormone salicylic acid (SA), produced in infected cells, move to non-infected cells, to induce the expression of resistance genes and prevent the spread of the pathogen (Fu and Dong 2013; Janda and Ruelland 2014). Downstream of the onset of both the HR and SAR lies a signalling cascade leading to the activation defence responsive genes with NO at the center of the signalling crosstalk (Romero-Puertas and Delledonne 2004).

1.4.1.1.1 NO AND PLANT VIRUSES

The link between NO and biotic stress responses was highlighted when it was found that the oxidative burst, i.e. production of $0_2^{\cdot-}$ and H_2O_2 that precedes the HR, required the action of NO (Delledonne et al. 1998) and application of NO scavengers and inhibitors of NO synthesis in Arabidopsis suppresses the HR, resulting in loss of resistance to *Pseudomonas synringae* (Delledonne et al. 1998; Zeier et al. 2004). The interaction between NO and the H_2O_2 is believed to be central to cell death during the HR. Exogenously applied NO causes DNA fragmentation during HR and the ensuing NO-mediated death is inhibited by caspase inhibitors in plants (Clarke et al. 2000). Features of programmed cell death such as loss in mitochondrial membrane potential and release of cytochrome C, known in animals to initiate apoptosis, are initiated by NO in plants (Mur et al. 2006; Locato et al. 2016). Beside its involvement in the HR, NO has been linked to other pathogen responses. A burst in NO production was recorded in response to different MAMPs in Arabidopsis (Zeidler et al. 2004; Sun et al. 2012; Sun and Li 2013), in tobacco (Foissner et al. 2000), in tomato (Laxalt et al. 2007), in barley (Prats et al. 2005), in response to wounding-associated DAMPs (Rasul et al. 2012; Jeandroz et al. 2013) and that of HAMPs (Wu and Baldwin 2009).

With relation to responses to plant virus, infection of resistant but not susceptible tobacco with TMV resulted in enhanced NO production (Durner et al. 1998) and treatment with NO donors in tobacco triggered expression of the defence genes (Durner et al. 1998; Song and

Goodman 2001) and has been shown to prevent the spread of TMV and PVX (Li et al. 2014). In susceptible tomato, TMV infections results in NO production which leads to the production of alternative oxidase and the induction of mitochondrial alternative electron transport resulting in the induction of basal defence (Fu et al. 2010) and in Arabidopsis, a NO burst was required for the activation of SA and alternative oxidase, upstream of defence genes induction (Jian et al. 2015). The role of the alternative electron transport in plant defence responses is not known, however alternative oxidase is believed to shield the plant cell from ROS damage as well as protect the photosystem (Fu et al. 2010; Jian et al. 2015; Jian et al. 2016). In *Hibiscus cannabinus*, infection with the geminivirus mesta yellow vein mosaic virus (MYVMV) resulted in an increase in NO production, as well as an increase in NO mediated post translational modifications (Sarkar et al. 2010).

1.4.1.1.2 MODE OF NO ACTION IN PLANT CELLS

Being a ubiquitous molecule, the mode of action of NO is not confined to a specific pathway. Application of NO donors is known to cause differential gene expression of NO responsive genes which include heat shock proteins, antioxidants, genes involved in iron homeostasis, defence-related genes and mitogen-activated protein kinases (Durner et al. 1998; Huang et al. 2002; Polverari et al. 2003; Parani et al. 2004; Grün et al. 2006; Palmieri et al. 2008; Mata-pérez et al. 2016).

The exact mechanism by which NO induces changes in gene expression is not known, but evidence suggests it occurs indirectly via posttranslational modification of transcription factors (Grün et al. 2006), leading to changes in accumulation of signalling molecules and phytohormones, further amplifying the responses to NO. Two main NO mediated posttranslational modifications namely nitration of tyrosine residues and *S*-nitrosylation of cysteine residues can result in gain or loss of function of the targeted protein. These modifications can sometimes cooperate to modulate the activity of proteins as is the case for the antioxidant Peroxiredoxin II E, which is activated by tyrosine nitration and inactivated by *S*-nitrosylation (Romero-Puertas et al. 2007).

S-nitrosylation is the most studied posttranslational modification mediated by NO in plants. S-nitrosylation is modification of thiol groups in cysteine residues, and has been linked to gene regulation, phytohormonal signalling and cell death (Leitner et al. 2009). An example

of gene regulation by *S*-nitrosylation is the *S*-nitrosylation of the nonexpressor of pathogenesis-related proteins1 (NPR1), a transcription coactivator that regulates the accumulation of phytohormones SA and jasmonic acid (Mur et al. 2013). NPR1 when nitrosylated is inactive in its oligomeric form and located in the cytoplasm. Denitrosylation by thioredoxin results in the monomerisation of NPR1 and its translocation in the nucleus (Tada et al. 2008; Sun et al. 2012; Bellin et al. 2013; Mur et al. 2013; Kovacs et al. 2015), leading to the expression of SA-induced genes (Song and Goodman 2001; Zottini et al. 2007; Vlot et al. 2009; Mur et al. 2013; Janda and Ruelland 2014). Downstream to NPR1 activation, NO is once again required as *S*-nitrosylation of TGA1 transcription factors has been shown to enhance their promoter binding activity (Mur et al. 2013). The *S*-nitrosylation of methionine adenosyltransferase, a key enzyme in the production of ethylene and polyamine is inhibited by *S*-nitrosylation (Lindermayr 2006; Bellin et al. 2013; Mur et al. 2013). NO has also been linked to pathogen induced programmed cell death in plants during HR, and this is believed to occur through the regulation of genes involved in programmed cell death by *S*-nitrosylation, with caspases and glyceraldehyde-3-phosphate dehydrogenase (GAPDH) having been confirmed as *S*-nitrosylation targets (Wang et al. 2013; Locato et al. 2016).

Tyrosine nitration mediated by NO can alter protein function as well as conformation. Detection of proteins targeted by nitration in plants have revealed that proteins involved in photosynthesis, ATP synthesis, the Calvin cycle, glycolysis, and nitrogen metabolism are regulated by tyrosine nitration (Cecconi et al. 2009; Chaki et al. 2009; Lozano-Juste et al. 2011). The list of proteins modified by protein nitration is still being populated due to the challenges observed during detection of protein tyrosine nitration under physiological conditions (Lozano-Juste et al. 2011).

1.4.1.2 Nitric oxide synthases

The main source of NO production in mammals is through the enzymatic conversion of L-arginine to L-citrulline with NO being released (figure 1-5). This enzymatic reaction is mediated by three different nitric oxide synthases (NOS), neuronal NOS (nNOS), endothelial NOS (eNOS) and inducible NOS (iNOS) found in different cells and tissues and the localization at the tissue level is transcriptionally regulated (Alderton et al. 2001; Stuehr 2004). The 3 mammalians NOS and their splicing variants are encoded for by three different genes that share approximately 50% homology (Alderton et al. 2001). These three NOS are

regulated by different mechanisms: iNOS is produced mainly in response to pathogen infection, nNOS and eNOS are constitutively expressed and they were first identified in neuronal and endothelial cells respectively (Alderton et al. 2001). Mammalian NOS active form are homodimers, associated with calmodulin homodimers and requiring (6R)-5,6,7,8-tetrahydrobiopterin (BH_4), flavin adenine dinucleotide (FAD), flavin mononucleotide (FMN) and iron protoporphyrin IX (haem) as co-factors (Alderton et al. 2001). They have at the N-terminus a cellular localization signal, a zinc binding domain and an oxygenase domain with binding sites for haem, BH_4 and L-arginine. At the C-terminus they have a reductase domain with binding sites for nicotinamide adenine dinucleotide phosphate (NADPH), FAD and FMN and between both terminus, a calmodulin binding region (Alderton et al. 2001; Fröhlich and Durner 2011).

$$2\mathrm{L-arginine} + 3\mathrm{NADPH^+} + 2\mathrm{O_2} \rightarrow 2\mathrm{L-citrulline} + 3\mathrm{NADP} + 4\mathrm{H_2O} + 2\mathrm{NO}$$

Figure 1-5: Production of NO from L-arginine.

A NOS has recently been identified from the algae *Ostreococcus tauri* and has a 40-50% similarity to mammalian NOS (Qiao et al. 2009). On a regulatory level, it is closely similar to iNOS as it can be active without the presence or surge in Ca^{2+}. Structurally OtNOS bears similarities to mammalian NOS. It has at the N-terminus, a zinc binding motif as well as L-arginine and haem binding sites, followed by a calmodulin binding region. At the C-terminus it has reductase domain with binding sites for FAD, FMN and NADPH (Foresi et al. 2010; Correa-aragunde et al. 2013).

No plant NOS has yet been identified, however the conversion of L-arginine to L-citrulline depicted in figure 1-5 has been measured in plants peroxisomes (Corpas et al. 2009; Corpas and Barroso 2014). Evidence of L-arginine dependent NO production is furthered by the fact that in Arabidopsis, an increase in NO production occurs in knockout lines of the enzymes *arginase* (*atargh)* and *no overproducer1* (*atnox1*) (Crawford and Guo 2005; Leitner et al. 2009). Loss of function of AtARGH results in an accumulation of L-arginine (Flores et al. 2008) and Atnox1 encodes a chloroplast phosphoenolpyruvate/phosphate translocator and when silenced, results in an increase in L-arginine accumulation, however the exact

mechanism through which L-arginine is related to Atnox1 is unknown (Crawford and Guo 2005).

1.4.1.3 NOA1 and the NO link

Arabidopsis nitric oxide associated protein 1 (AtNOA1) formerly called Arabidopsis nitric oxide synthase 1 (AtNOS1) was predicted a plant NOS even though it bears neither sequence similarity, nor similar co-factor requirements to mammalian NOS (Guo et al. 2003). Since its initial discovery in Arabidopsis, homologues to AtNOA1 have been identified in different plants (Kato et al. 2007; Qiao et al. 2009; Yang et al. 2011; Kwan et al. 2015) as well as in mammals (Zemojtel et al. 2007; Parihar et al. 2008; Kolanczyk et al. 2011). It is now known that AtNOA1 is not a plant NOS but a member of the conserved circularly permutated GTPase (cGTPase) (Moreau et al. 2008; Sudhamsu et al. 2008; Moreau et al. 2010).

Based on their structural features, the GTPase superclass of protein can be divided in two classes, translation factor class (TRAFAC) and signal recognition particle MinD and BioD (SIMIBI; Britton 2009; Leipe et al. 2002). NOA1 is a circularly permutated GTPase (cGTPase) which falls under the TRAFAC class. Members of the TRAFAC class have been shown to bear sequence similarity to bacterial ancestral homologues, implicated in ribosomal assembly (Britton 2009; Suwastika et al. 2014). cGTPase proteins are found in both prokaryotes and eukaryotic organisms. They are known as permutated because the order of GTP binding domains in these proteins does not conform to the order of G1-G2-G3-G4-G5 of canonical GTPases. In cGTPase, the order of GTP binding domains is permutated to the order G4-G5-G1-G2-G3 (Moreau et al. 2008; Sudhamsu et al. 2008; Britton 2009; Anand et al. 2010).

cGTPases were first identified in bacteria and since similar conserved sequences have been isolated in plants and animals. Bacterial cGTPases are mostly involved in ribosomal assembly (Britton 2009). Unlike most G-proteins, cGTPases do have additional domains believed to participate in ribosomal RNA binding (Britton 2009). They also have a substitution in their catalytic domains where a conserved catalytic glutamic acid is substituted by a hydrophobic amino acid hence cGTPase are sometimes called HAS-GTPase for hydrophobic amino acids substituted GTPase (Britton 2009; Anand et al. 2010). This substitution results in HAS-GTPase having a different hydrolysis mechanism to other GTPase (Anand et al. 2010).

Null-mutations in bacterial cGTPase are mostly non-lethal however do result in impaired growth and a reduction of 70S ribosomes in bacteria, most probably due to an impairment in the small (30S) and larger (50S) subunit assembly (Himeno et al. 2004; Campbell et al. 2005; Matsuo et al. 2006; Britton 2009). *NOA*1 is homologous to YqeH from *Bacillus subtilis,* a cGTPase protein associated with ribosomes and involved in ribosome assembly (Flores-Pérez et al. 2008; Moreau et al. 2008; Sudhamsu et al. 2008; Gas et al. 2009). YqeH knock-out *B. subtilis* mutants are lethal, however a decrease in its expression leads to an increase in chromosomal DNA in *B. subtilis* (Morimoto et al. 2002; Sudhamsu et al. 2008). A decrease in YqeH expression also results in a decrease in 16srRNA, a component of the small bacterial ribosomal subunit, 30S (Uicker et al. 2007) as well as a decreased in assembled 70S ribosomes (Uicker et al. 2007; Britton 2009). GTP/GDP are needed for various processes in a cell, hence GTPases are associated with many different processes. cGTPase have been only recently discovered in eukaryotes and only a glimpse of their functions has been revealed. Plant NOA1 is a nuclear encoded, chloroplast protein and has been linked to translation in the chloroplast. It has nucleic acids and protein binding abilities, and lacks binding sites for L-arginine or for any NOS associated co-factors (Flores et al. 2008; Moreau et al. 2008; Gas et al. 2009).

Brassinazole insensitive pale green 2 (BPG2) is a homologue of NOA1 and another member of the YqeH family that has been characterised in plants (Komatsu et al. 2010). The expression of BPG2 is regulated by light, and akin to NOA1, BPG2 is involved in chloroplast assembly, with its loss of function resulting in impaired photosynthesis and accumulation of chloroplast proteins (Kim et al. 2012). NOA1 and BPG2 were together shown to be involved in the assembly of thylakoid protein complexes (Qi et al. 2016). Besides YqeH cGTPases, members of other cGTPases classes (*YjeQ/YloQ, Era, YlqF/RbgA/YawG, YhbZ/ObgE, YsxC/YihA* and *YhpC*) with bacterial ancestral homologues have been identified in plants (Ingram et al. 1998; Im et al. 2011; Suwastika et al. 2014; Chen et al. 2016).

1.4.1.4 NOA1 and plant disease responses

Exactly how NOA1/cGTPase homologues participate in disease responses is speculative. Expression of AtNOA1 and its plant homologues has been shown to be differentially regulated in response to disease (Kato et al. 2007; Wünsche et al. 2011; Mandal et al. 2012; Kwan et al. 2015) and downregulation of NOA1 activity has been shown to render the plant

more susceptible to invading pathogens (Zeidler et al. 2004; Zeier et al. 2004; Kato et al. 2007; Qiao et al. 2009).

The expression of AtNOA1 was found to be modulated by lipopolysaccharide and *atnoa1* mutants were shown to be highly susceptible to *Pseudomonas syringae* pv. *tomato* DC3000 (Zeidler et al. 2004). In *N. benthamiana,* silencing of *NbNOA1*, a *AtNOA1* homolog, using VIGS, resulted in an increase in susceptibility to *Colletotrichum lagenarium*, and a decrease in expression of PR1 gene, a marker of defence response, when these plants were challenged with *Colletotrichum lagenarium* (Kato et al. 2007).

It is possible that NOA1 participation in disease response could be through its association with chloroplasts (Reinero and Beachy 1989; Bhat et al. 2012; Liu et al. 2014). Many pathogen defence responses have been shown to be light dependent. The HRT mediated HR response to turnip crinkle virus (TCV) infection in Arabidopsis and SA production and initiation of HR responses in response to TMV infection in *N* gene tobacco are light dependent (Chandra-Shekara et al. 2006), the Arabidopsis mutant *constitutive shade-avoidance* with an impaired light perception mechanism has a reduced resistance to the avirulent *P. aeruginosa* (Faigon-Soverna et al. 2006) and in soybean, various pathogen defence response genes were differentially expressed (Yoon et al. 2016). Chloroplasts are main sites of defence molecules production such as ROS, SA and jasmonic acid (Rodio et al. 2007; Padmanabhan and Dinesh-Kumar 2010; Palukaitis et al. 2013; Caplan et al. 2015; Serrano et al. 2016) and different chloroplasts proteins are targeted by pathogen effectors during infection (reviewed in Bobik and Burch-Smith 2015). The expression of many genes associated with chloroplast function and photosynthesis are differentially expressed in ACMV infected cassava (Liu et al. 2014).

Chloroplasts can also be directly targeted during plant virus infection (de Torres Zabala et al. 2015) as the geminiviral encoded betasatellite βC1 and MP of AbMV are targeted to the chloroplast (Krenz et al. 2010; Bhattacharyya et al. 2015) and turnip yellow mosaic virus (TYMV), turnip mosaic virus (TuMV) and AbMV have been shown to replicate within the chloroplast (Gröning et al. 1987; Bhattacharyya and Chakraborty 2017).

AtNOA1 participation in disease response could also stem from its association with ribosome assembly. *YqeH*, the *NOA*1 homolog in *B. subtilis*, is involved in ribosome assembly

and since *YqeH* can rescue phenotypes produced by *atnoa1* null mutation, the activity of YqeH is said to mirror that of *AtNOA*1 (Sudhamsu et al. 2008). It has been shown that down-regulation in YqeH promotes chromosomal replication in *B. subtilis* (Sudhamsu et al. 2008) highlighting a role in both ribosomal assembly and possibly cell cycle regulation. As geminiviruses modify the dormant state of a cell in favour of replication, there could be a link between geminiviruses and AtNOA1, which warrants further investigation.

Another player in the involvement of AtNOA1 in plant disease response could be NO accumulation as although AtNOA1 cannot directly produce NO, *atnoa1* mutants show a lower NO production (Guo et al. 2003; Zeidler et al. 2004; Guo and Crawford 2005; Bright et al. 2006; Zhao et al. 2007; Chen et al. 2010). The decrease in accumulation of NO in *atnoa1* has been shown to be as a result of its inability to fix carbon in the form of sucrose, resulting in a decrease in fumaric acid stores, resulting in a decrease in overall L-arginine accumulation (Van Ree et al. 2011). A decrease in L-arginine can contribute to the overall NO accumulation, from the conversion of L-arginine to L-citrulline (figure 1-5).

1.4.1.5 Other sources of NO production in plants

The production of NO in plant has been linked to the reduction of nitrite and this reduction can be enzymatically-mediated and not. The mostly studied enzymatic source of NO from nitrite is the cytosolic nitrate reductase (NR). In Arabidopsis, 2 NR have been identified, NIA1 and NIA2 which account for 10% and 90% NR activity respectively (Zhao et al. 2009). The main activity of NR in a cell is a NADPH-dependent reduction of nitrate to nitrite. However in a low pH hypoxic environment, NR has been shown to be able to produce NO, when nitrate concentrations are lower than that of nitrite and this reaction is also dependent on NADPH (figure 1-6; Gupta et al. 2011; Zhao et al. 2009), and uses molybdenum as a cofactor (Silaghi-Dumitrescu et al. 2012). When measured in vitro, NO producing activity of NR only represents 1% of its nitrate reductase activity (Rockel et al. 2002; Planchet and Kaiser 2006). Because NO production by NR is dependent on the availability of nitrite compared to that of nitrate, the production of NO by NR is believed to be an indirect result of an accumulation of nitrite in a cell (Bellin et al. 2013). The production of NO by NR has been shown in response to abiotic stresses (Dean and Harper 1988; Desikan et al. 2002; Bright et al. 2006; Sang et al. 2008; Besson-Bard et al. 2009; Kolbert et al. 2010) and biotic stresses (Modolo et al. 2006; Oliveira et al. 2010; Perchepied et al. 2010).

$$NAD(P)H + 3H_3O^+ + 2NO_2^- \rightarrow NAD^+ + 2NO + 5H_2O$$

Figure 1-6: Nitrate reductase mediated production of NO from nitrite.

In plants roots, a succinic acid dependent NR can be found bound to the plasma membrane of apoplasts. The plasma membrane bound NR (PM-NR) has been found associated with a root specific nitrite to NO oxidoreductase (NI-NOR) (Stöhr and Ullrich 2002). This enzyme is believed to convert the nitrite produced by PM-NR to NO. There exist distinct differences between the production of NO from NI-NOR to that of cytosolic NR. Production of NO by Ni-NOR can occur during normal oxygen concentration, at a more neutral pH than that of NR, cytochrome c instead of NADPH acts as an electron donor and NI-NOR activity does not depend on higher nitrite to nitrate concentration (Stöhr and Ullrich 2002). The ability of NI-NOR to produce NO has a complex relationship with nitrate concentration of the cell as well as the surrounding soil. It is believed that the NO oxide produced by Ni-NOR in roots facilitates the colonization of roots by mycorrhizae and mycorrhiza symbiosis can be affected by nitrate accumulation (Moche et al. 2010; Calcagno et al. 2012).

In plant mitochondria, nitrite reductase activity has been noted during oxygen deprivation. For NO to be produced by plant mitochondria, nitrite has to be abundantly available, and conditions that favour an increase in nitrite concentration in the cell such as hypoxia needs to be met for the mitochondria to produce NO from nitrite reduction. Production of NO from nitrite in the mitochondrion is believed to be mediated by haem-containing members of the electron transport chain (Gupta et al. 2011a; Gupta et al. 2011b; Igamberdiev et al. 2014). The reduction of nitrite during oxygen deprivation may serve as two purposes, on one end the production of NO and on the other end, mitochondria use nitrite as an electron acceptor for ATP production, when oxygen is not available (Gupta et al. 2011a; Igamberdiev et al. 2014). Leaves and roots mitochondria have been reported to produce NO at different rates (Planchet and Kaiser 2006), and this can be explained by the anoxic nature of roots when compared to photosynthetic leaves (Igamberdiev et al. 2014). Chloroplasts have also been shown as a potential source for NO production even though, no enzymes involved NO production have yet been identified and locate to chloroplast (Jasid et al. 2006; Tewari et al. 2013; Misra et al. 2014).

Beside NR related NO production, other molybdenum dependent enzymes have been identified, with the ability to reduce nitrite to NO, hence being a potential alternative source of NO production in plants. Xanthine oxidoreductase, aldehyde oxidase, sulfite oxide and mitochondrial amidoxime reducing component 1 (mARC1) NO producing capacity has been shown either in-vitro or in mammalian cells to produce NO from nitrite (Yesbergenova et al. 2005; Maia and Moura 2011).

Production of NO can also occur via non-enzymatic means. In vitro, a reaction between L-arginine and H_2O_2 can generate NO (Nagase et al. 1997; Gotte et al. 2002; del Río et al. 2004). In an acidic environment, NO can be spontaneously produced in plants from a reduction of nitrite (Wojtaszek 2000) and in the chloroplast and the apoplastic space, by a reduction of ascorbic acid (Stöhr and Ullrich 2002). In the presence of light, NO can be produced from nitrite by carotenoids (Wojtaszek 2000; Stöhr and Ullrich 2002). Nitrification and denitrification reactions can result in the production of NO as a by-product of the nitrogen fixation cycle (Wojtaszek 2000; Stöhr et al. 2001; del Río et al. 2004).

1.5 Rationale for the study

Cassava is a woody shrub, belonging to the family of *Euphorbiaceae,* that originated from South America, and was introduced by European settlers in West Africa in the 16th century and later in 18th century to South-Eastern Asia (Fauquet and Fargette 1990). Its production has since then spread inland in both continents. Cassava easily grows in areas of low rainfall and poor soil fertility, hence requiring minimal financial input for cultivation, resulting in cassava being a cheap crop to grow and an affordable staple food to resource-poor populations.

In sub-Saharan Africa, cassava is cultivated by small farmers mainly for the consumption of its leaves, roots and derived products such as *fufu,* chips and bread. Globally, cassava is gaining importance in different industries, as an animal feedstock and as a cheaper alternative to starch substrates. Cassava is also an ideal candidate for bioethanol production due to the high starch content of its roots (Okigbo 1980). Because of the potential of cassava plants, as well as the devastating effect of geminivirus infection, research being carried out in different laboratories across the world aims to confer resistance to susceptible cassava cultivars, either through traditional breeding methods or using the transgenic approach. Traditional breeding involves identifying resistance traits from wild resistant cultivars and integrating them into susceptible lines. This approach faces various obstacles, including the inability to insert a single desired treat into newly bred plants, as well as the risk of losing the desired traits from the said cultivar (Vanderschuren et al. 2007; Bull et al. 2011).

Improving resistance using the transgenic approach requires firstly the development of a successful transformation method which has been developed for cassava (Bull et al. 2011). Secondly, a deep knowledge and understanding of the mechanism of cassava mosaic virus-host interactions leading to infection, which is the broad umbrella under which our research falls. Identification of gene(s) that function in virus-host interactions will provide new insights on how to reduce the impact of this disease, both through GM, and use of endogenous gene manipulation.

1.6 General objectives and aims

1.6.1 AIM A: Investigation of possible genes involved in SACMV movement

Different host genes playing a role in replication and transcription have been identified but genes involved in geminivirus movement have not been as extensively covered. While some research has been performed on nuclear export of geminiviruses (McGarry et al. 2003; Mariano et al. 2004; Carvalho et al. 2008a; Carvalho et al. 2008b; Carvalho et al. 2008c), little is known about intracellular and intercellular movement mechanisms. Plant virus movement is believed to occur either via the cytoskeleton or the endomembrane system, and whilst interactions between component of the endomembrane system and geminiviruses movement proteins have been established (Lewis and Lazarowitz 2010; Lozano-Durán et al. 2011), the possible involvement of the cytoskeleton in geminivirus movement is sketchy. As a contribution to the field of viral movement with regard to cassava mosaic viruses, we aim to investigate the role that the cytoskeleton plays in response to SACMV infection by looking at myosin (actin filaments motor proteins).

We hypothesise that as myosin are motor proteins of actin filaments and this actomyosin network is one of the main pathway by which macromolecular trafficking occurs in a cell, disruption of the actomyosin network via silencing of myosin using a VIGS approach will eventually impede myosin/actin mediated viral movement. The hypothesis on which we based this research is that myosin could bind directly to the geminiviral cargo, SACMV in this case, and transports it along the actin tracks.

As highlighted previously, most of the studies associated with plant viral movement has been based on RNA viruses. In terms of myosin, we seek to identify myosins in *N. benthamiana* and to determine which myosin members of both class VIII and XI do play a role in SACMV infection. This study will be useful in future evaluate approaches in using the VIGS vector system for geminiviral studies in cassava.

1.6.2 AIM B: Determination of a potential role for NOA1 in SACMV pathogenicity in N. benthamiana and cassava

In a separate study to that of myosin, we look at NOA1, a protein once thought to be a NO producer, which has been identified to be differentially regulated in response to biotic and abiotic stress. We would like to evaluate if *NOA1* plays a role in SACMV pathogenicity and to attempt to create a model linking cGTPases to virus susceptibility. As AtNOA1 homologue has been identified in *N. benthamiana* (*NbNOA1*), we seek to identify a AtNOA1 homologue in cassava (*Manihot esculenta; MeNOA1*) and assess the roles that *NbNOA1* and *MeNOA1* plays in response to SACMV pathogenicity in the model. Given that NOA1 are now known to be chloroplast translation factors, this research aims to shed some light on questions regarding the involvement of the chloroplast and NOA1 in plant disease response to SACMV, in the susceptible model host *N. benthamiana* and the susceptible natural host cassava T200. The hypothesis is that given that NOA1 is involved in translation in the chloroplast, dysregulation in its expression will have an impact on the functioning of the chloroplast, contributing to the development of SACMV disease.

Chapter 2. Comparative study of myosin class XI and VIII knockdown by VIRUS INDUCED GENE SILENCING (VIGS)

2.1 Introduction

South african cassava mosaic virus (SACMV) is a bipartite begomovirus (Berrie et al. 2001), endemic to southern Africa and is one of seven species infecting cassava (*Manihot esculenta* Crantz) on the sub-Saharan African continent (Brown et al. 2015). Its genome comprises of two components, a 2.8 kb DNA-A and 2.7 kb DNA-B that encodes for six and two genes respectively. DNA-A encodes for in the sense orientation, coat protein (CP; AV1) and the pre-coat protein (pre-CP; AV2) and in the antisense orientation, replication protein (REP; AC1), transcriptional activator (TrAP; AC2), replication enhancer protein (REn; AC3) and a pathogenesis determinant (AC4). DNA-B encodes for the movement protein (MP; BV1) in the sense orientation and the nuclear shuttle protein (NSP; BC1) in the antisense orientation. These genes products work in synergy to establish a successful infection permitting the infecting geminivirus to reprogram the plant cell cycle, transcription and translation processes and inhibits pathogen defence processes such as endogenous gene silencing.

For a successful infection to be established, a virus needs to be able to replicate and transcribe its genome, move to neighbouring cells and eventually systemically throughout the plants vascular system. Movement of plant viruses has been described as an example of convergent evolution as viruses of different genera and families have been shown to employ similar pathways to move, perhaps due to their need to adapt to a similar cellular environment (Rojas et al. 2016). Cassava mosaic viruses are generally viewed as non-phloem limited begomoviruses, with the exception of indian cassava mosaic virus (Rothenstein et al. 2007). Non-phloem-limited begomoviruses such as SACMV are dispensable of the CP for cell to cell movement which is rather mediated through a partnership between the NSP and the MP, with the CP required for plant-vector transmission. Once in the nucleus, the single stranded DNA (ssDNA) of SACMV is replicated into double stranded (dsDNA) used for

transcription, and the viral DNA (vDNA) is packaged into DNA-protein complexes consisting of ssDNA, some dsDNA, NSP and host cofactors (Hanley-Bowdoin et al. 2013). The NSP of cabbage leaf curl virus (CaLCuV) in Arabidopsis (Carvalho et al. 2006) was shown to inhibit a nuclear acetyltransferase and nuclear shuttle protein interactor (AtNSI), leading to the inhibition of histone 3 acetylation, and this is believed to promote the integration of histones H3 in the vDNA-protein complex, leading to the formation of minichromosomes (Zhou et al. 2011) that are exported from the nucleus through nuclear pores (Gafni and Epel 2002; Hehnle et al. 2004). The export of NSP-vDNA complex from the nucleus into the cytoplasm is mediated by a leucine rich nuclear export signal (NES), located at the C-terminus of NSP, which interacts with the host's NSP interacting GTPase (NIG) (Carvalho et al. 2008a; Carvalho et al. 2008b).

In the cytoplasm, the NSP binds to the MP and together facilitate the movement of viral molecules through the cytoplasm. The NSP and MP are believed to interact with various cytoplasmic host factors in order to reach the plasma membrane, where the MP modifies the structure of plasmodesmata, increasing the size exclusion limit allowing for viral particles to move to adjacent cells (Gafni and Epel 2002). Comparatively little is known about cytoplasmic movement or movement protein (BC1) of geminiviruses compared to plant RNA viruses and in comparison, to (BV1)/NSP-mediated nuclear transport. The host factors involved in plant virus trafficking are either members of the Golgi apparatus such as the vesicle coat protein coatomer delta subunit (delta COP) (Lozano-Durán et al. 2011) and the synaptogamins A (SYTA) (Lewis and Lazarowitz 2010) which have both been linked to geminiviral responses or members of the cytoskeleton, where few reports of involvement in geminivirus movement are reported. For the interest of this research, we are focusing on myosins.

Myosin motors are associated with actin filaments and conserved throughout Eukarya with 18 classes having been identified (Foth et al. 2006). They generally contain three domains, an ATPase dependent actin binding domain (motor domain), a neck domain with affinity for light chains and Ca^{2+}/calmodulin and a tail of coiled coil domain (Reddy and Day 2001; Sparkes et al. 2008). Two classes of myosins are found in plants, class VIII and class XI and in Arabidopsis, seventeen members have been identified (13 class XI and 4 class VIII), with some represented by more than one splicing variant (Reddy and Day 2001; Lee and Liu

2004) and in *Nicotiana benthamiana,* six members have been reported in the literature (Avisar et al. 2008b).

Class XI myosin are believed to be involved in vesicles and organelle fluidity, cytoplasmic streaming, cellular morphogenesis, expansion and elongation, gravitropism and actin integrity and organisation (Ojangu et al. 2007; Peremyslov et al. 2008; Prokhnevsky et al. 2008; Sparkes et al. 2008; Avisar et al. 2008b; Peremyslov et al. 2010; Ueda et al. 2010; Yokota and Shimmen 2011; Park and Nebenführ 2013; Tamura et al. 2013a). Class VIII myosins are found associated with endosomes, the ER, the plasmodesmata and the nascent cells plasma membrane and the plasma membrane of plastids (Reichelt et al. 1999; Avisar et al. 2008a; Maule 2008; Haraguchi et al. 2014). They are believed to be involved in trafficking to the PD and endocytosis in plants (Golomb et al. 2008; Sattarzadeh et al. 2008) and are involved with microtubules in plant cell division (Wu and Bezanilla 2014).

With regards to plant viruses, there are reports suggesting the participation of either class VIII or class XI myosins or both in movement. Myosins XI have been shown to play a role in the movement of grapevine fanleaf virus (GFLV) (Amari et al. 2014) and turnip mosaic virus (TuMV) (Agbeci et al. 2013) and both members of myosins class VIII and XI play a role in the movement of viral replication complexes of TMV to the plasmodesmata (Amari et al. 2014). A HSP70 homolog which is a component of the of the closterovirus beet yellow virus (BYV) virion, traffics along the actin filaments using members of Arabidopsis myosin VIII (Avisar et al. 2008a). The involvement of myosin in plant virus movement can also be through a partnership with the endomembrane system, as shown in the case of the viral replication complex of potato virus x (PVX) which interacts with the vesicles associated triple gene block (TGB) proteins 2 and 3, and together move along the endoplasmic reticulum (ER) using the actomyosin network (Kumar et al. 2014).

The evidence of a possible involvement of myosins in geminivirus movement is at this point limited, however there are reports of a possible indirect link. The movement of abutilon mosaic virus (AbMV) was shown to occur with the help of stromules (Krenz et al. 2012) and in turn, their dynamism is reliant on myosin XI and actin (Natesan et al. 2009; Sattarzadeh et al. 2009). In another study, the integrity of microtubules and actin filaments were shown to

influence the cellular distribution of tomato yellow leaf curl virus (TYLCV), in turn impacting on its movement (Moshe et al. 2015).

To establish a possible link between myosins and SACMV infectivity/movement, the objective of this study was to target several *N. benthamiana* myosins using virus induced gene silencing (VIGS) vectors derived from tobacco rattle virus (TRV) (Liu et al. 2002b) and SACMV (Mwaba 2010). Knockdown of myosins, involved in putative movement of viruses, was hypothesised to slow down SACMV movement leading to slower symptom development and virus load, and reduced pathogenicity. Additionally, results from the two different VIGS vectors were compared, one being a VIGS vector based on the same virus as the one under investigation i.e. SACMV and the other being a VIGS vector used frequently in VIGS studies, namely one based on tobacco rattle virus which is unrelated to the virus under investigation. Results from this study will be useful in future evaluate approaches in using the VIGS vector system for geminiviral studies in cassava. since besides african cassava mosaic virus (ACMV; Fofana et al. 2004) and SACMV-Based VIGS vectors (Mwaba 2010), no other VIGS vector has been designed from viruses that can infect cassava (table 2-1).

Table 2-1: The viruses of cassava

Virus name	Genus/Family	Reference
Cassava virus X	*Alphaflexiviridae/Potexvirus*	(Lennon et al. 1986)
Cassava common mosaic virus	*Alphaflexiviridae/Potexvirus*	(Costa 1940)
Cassava Colombian symptomless virus	*Alphaflexiviridae/Potexvirus*	(Lennon et al. 1986)
Cassava new alphaflexivirus	*Alphaflexiviridae/Potexvirus*	(Carvajal-Yepes et al. 2014)
Cassava carribean mosaic virus	*Alphaflexiviridae/Potexvirus*	(Lennon et al. 1986)
Cassava Ivorian bacilliform virus	*Anulavirus/Bromoviridae*	(Scott et al. 2014)
Cassava mosaic geminivirus	*Begomovirus/Geminiviridae*	(Brown et al. 2015)
Cassava vein mosaic virus	*Caulimoviridae/Cavemovirus*	(Costa 1940)
Cassava brown streak virus	*Ipomovirus/Potyviridae*	(Winter et al. 2010)
Cassava polero-like virus	*Luteoviridae/Polerovirus*	(Carvajal-Yepes et al. 2014)
Cassava green mottle virus	*Nepovirus/Comoviridae*	(Lennon et al. 1987)
Cassava Q virus	*Ourmiavirus*	(Calvert and Thresh 2002)
Cassava frogskin associated virus	*Reoviridae/Oryzavirus*	(Calvert et al. 2008)
Cassava symptomless virus	*Rhabdoviridae/Nucleorhabdovirus*	(Kitajima and Costa 1979)
Cassava American latent virus	*Secoviridae/Nepovirus*	(Walter et al. 1989)
Cassava torrado-like virus	*Secoviridae/Torradovirus*	(Carvajal-Yepes et al. 2014)

2.2 Experimental Procedure

2.2.1 Bioinformatics searches

The sequences of six *N. benthamiana* myosins previously identified (Sattarzadeh et al. 2009) were used to search Sol Genomics Network (http://solgenomics.net) for putative homologous sequences in *N. benthamiana* "genome v1.01 predicted cDNA" using the Basic Local Alignment Search Tool (BLAST; https://solgenomics.net/tools/blast/). The obtained nucleotides sequences were aligned using the online tool ClustalOMEGA (http://www.ebi.ac.uk/Tools/msa/clustalo/) to compute a percentage identity table.

Table 2-2: Characterised myosins from *A. thaliana* and *N. benthamiana* used for phylogenetic analysis

Specie (Class)	Gene name	Accession
***A. thaliana* (class VIII)**	AtM-1	AT3G19960
	AtM-2	AT5G54280
	AtVIII-A	AT1G50360
	AtVIII-B	AT4G27370
***A. thaliana* (class XI)**	AtXI-A	AT1G04600
	AtXI-B	AT1G04160
	AtXI-C	AT1G08730
	AtXI-D	AT2G33240
	AtXI-E	AT1G54560
	AtXI-F	AT2G31900
	AtXI-G	AT2G20290
	AtXI-H	AT4G28710
	AtXI-I	AT4G33200
	AtXI-J	AT3G58160
	AtXI-K	AT5G20490
	AtXI-MYA1	AT1G17580
	AtXI-MYA2	AT5G43900
***N. benthamiana* (class VIII)**	NbVIII-2	DQ875139.1
	NbVIII-1	DQ875138.1
	NbVIII-B	DQ875140.1
***N. benthamiana* (class XI)**	NbXI-F	DQ875136.1
	NbXI-K	DQ875137.1
	NbXI-2	DQ875135.1

The presumptive homologs nucleotides sequences were translated and the amino acids (aa) sequences aligned using the MUSCLE tool in MEGA 7 (Tamura et al. 2013b) alongside the aa sequences of the six previously characterised myosins from *N. benthamiana* and 17 Arabidopsis myosins sequences (table 2-2). Using the data obtained from the multiple alignment, a phylogenetic tree was generated in MEGA 7 (Tamura et al. 2013b) using maximum likelihood analysis and a bootstra*p* value of 100. The phylogenetic tree was built to separate the putative homologs in the two known plant myosin classes. Protein domains and motifs were predicted using the PFAM database found under the MOTIF web portal (http://www.genome.jp/tools/motif/).

2.2.2 Construct design

To select regions for antisense VIGS constructs design, the SGN VIGS Tool from Sol genomics (SGN; Bombarely et al. 2011) (http://vigs.solgenomics.net/) was used, and sequence length of circa 300 nucleotides selected (Senthil-Kumar and Mysore 2014). Five reference sequences were selected on which the VIGS constructs would be designed (table 2-3).

To isolate the selected myosin silencing fragments, 2 step RT-PCR was carried out on 1 µg of *N. benthamiana* RNA. RNA was extracted from about 100 mg of leaf tissue using Tri reagent (Sigma-Aldrich; St Louis, USA) per the manufacturer's recommendation and resuspended in nuclease-free H_2O containing 1 U/µl of Ribolock RNAse inhibitor (Thermo Fisher Scientific; Waltham, USA). Concentrations of extracted RNA were determined using the NanoDrop™ 1000 spectrophotometer (Thermo Fisher Scientific; Waltham, USA) and RNA integrity was assessed by electrophoresis on 1.0% agarose gel. The extracted RNA was treated with DNAse I (Thermo Fisher Scientific; Waltham, USA) per manufacturer's recommendation before proceeding to first strand DNA synthesis. First strand cDNA synthesis was performed using random hexamers and RevertAid First Strand cDNA Synthesis Kit (Thermo Fisher Scientific; Waltham, USA), per manufacturers' recommendation. The produced cDNA (2 µl) was used in the second step PCR using Dreamtaq™ DNA polymerase (Thermo Fisher Scientific; Waltham, USA) and PCR was carried out for 35 cycles, per the manufacturer's recommendations, with an annealing temperature 58ºC. The PCR reaction components

were used as recommended by the manufacturer and the forward and reverse primer sets, M15.1, M8.B, M11.F, M11.2 and M11.K (table 2-4).

Table 2-3: Names and sequences of antisense constructs used in the study

Name of construct	Reference myosin sequence	Construct region (bp-bp)	Sequence
M15.1	Niben101Scf11288g00015.1	232-531	TTGCAGAATTTGGCTGCAAGATATCATCTCAATGAAATCTATACTTATACTGGAAG TATTCTCATCGCCATCAATCCATTCCAAAGGCTACCCCATCTATACGATCGCCACA TGATGGAACAATACAAGGGAGCCCCGCTTGGCGAACTAAGTCCTCATGTCTTTGCT ATTGCTGATGCCGCTTACAGGCAAATGATCAATGAAGGTAAAAGCAATTCTATATT GGTCAGTGGTGAAAGTGGGGCTGGTAAGACTGAAACTACTAAAATGCTTATGCAAT ACCTTGCTTATTTGGGTGGC
M8.B	NbVIII-B (DQ875140.1)	1343-1597	TGATTGGATGCAGAGTAAATGACCTCATGCTAGCTTTATCAACACGCCAAATACAA GTCGGCAAGGATAAGGTTGCCAAGAGTTTAACTATGGAGCAGGCAACTGATAGAAG AGATACATTGGCGAAGTTCATCTATGCAAACTTGTTTGACTGGATAGTTGATCAAA TGAACAGAAAGCTTGCAATGGGTAAAGAACAGAAGGGTAGATCCATAAATATTCTG GATATTTATGGTTTTGAATCATTTAAGAGAA
M11.F	NbXI-F (DQ875136.1)	2101-2400	TGTGATAGGATGGGCTTAAAGGGTTATCAGATTGGGAAAACCAAAGTTTTTCTCAG AGCCGGGCAGATGGCTGAATTAGATGCCAGAAGAACTGAAGTTCTAGCTCATGCTG CAAAGCGCATTCAGAGGCAAATTCGAACACATCTTACGCGGAAGGAGTTCATAGCC CTAAGGAGAGCTACAATTCATTTCCAGAAACTTTGGAGAGCAAAACTTGCCAGAGT GCTGTATGAACAAATGAAAAGGGAAGCTGCTTCAATCCGCATACAGAAACACGTGC GTTCTCATTCAGCAAGAAAA
M11.2	NbXI-2 (DQ875135.1)	3631-3930	ACATCTCTATTTGGGAGAATGACAATGGGATTTCGTTCGTCGCCTTCTGCAGTGAA TCTTGCTGCAGCTGCAGCTGCATTGGTAGTACGCCAAGTTGAAGCAAAATACCCTG CTCTGCTTTTCAAGCAGCAACTTACAGCATATGTTGAAAAGATTTATGGAATTATT AGGGATAACTTGAAGAAGGAGTTGGGATCACTCCTTTCCTTATGCATCCAGGCACC AAGGACTTCCAAAGGAAGTTTGAGAAGTGGGCGATCCTTTGGCAAAGACTCTTCTA CAAATCACTGGCAGCGGATT
M11.K	NbXI-K (DQ875137.1)	3544-3843	TACTGGTTATGCAATACGTCCACATTATTGATGCTGCTTCAACAAACACTTAAAGC TAGCGGGGCTGCTAGTTTGACTCCGCAGAGGCGGAGAACCAGTTCAGCTTCTTTGT TTGGGAGGATGTCCCAAGGCTTACGAGGTTCTCCCCAGAGTGCTGGACTTTCAGTT CTCAATGGGCGTATGCTTGGGAGATTGGATGACTTACGTCATGTTGAGGCCAAATA TCCTGCACTGCTGTTCAAGCAGCAGCTCACTGCCTTTTTGGAGAAAATATACGGAA TGATAAGAGACAATCTGAAG

Table 2-4: Sequences and features of primers used for this study.

	Target	Primer name	Forward primer sequence (5'3')	Reverse primer sequence (5'3')	Amplicon length (bp)
Real time PCR	SACMV-A	AV1	CAGGCTTTGGTGAGGAGATT	AGCGTAGCATACACTGGATTAG	146
	SACMV-B	BV1	GTCACCGGTATCGCGTTATT	GGATATTTCCCTCCACTTAGTCTTC	109
	Myosin 8.B	qM8.B	CTCAGATCCTGTGGTGTTCTTG	GAAGCCATACCTGCTAGTGAAT	96
	Myosin 11-F	qM11.F	GAGAAGAAACCTGGAGGCATTA	GGGCTTTGTATGTCTGGTACA	106
	Myosin 15.1	qM15.1	GTGTCACAGATTAACGGACAGA	CAGCAGGAGCATCTTCATCTT	106
	Myosin 11-K	qM11.K	GGAGTGTTGCTCGTTCAGTAA	CCCATGCTGAGCCTACATATTC	104
	Myosin 11-2	qM11.2	CCAATCATGTGCCTCCATTTC	CTTCTCAGCAGAAGGCTGTTA	94
Construct design	M8.B	M8.B	TGATTGGATGCAGAGTAAAT	TTCTCTTAAATGATTCAAAACC	255
	M11.F	M11.F	TGTGATAGGATGGGCTTAAA	TTTTCTTGCTGAATGAGAACGCAC	300
	M15.1	M15.1	TTGCAGAATTTGGCTGCAAG	GCCACCCAAATAAGCAAGGTATT	300
	M11.K	M11.K	TACTGGTTATGCAATACGTC	CTTCAGATTGTCTCTTATCATTCCG	300
	M11.2	M11.2	ACATCTCTATTTGGGAGAAT	AATCCGCTGCCAGTGATTTGTAG	300
Screening	TRV2	TRV2	CGGACGAGTGGACTTAGATTCTGTG	CTCGAGACGCGTGAGCTCGG	260
	SACMV-A	SAA/	GCGTGTCAACATGTGGGATCCATT	ACCACAACATCAGGAAGGCATTGG	667

The PCR products were purified using GeneJET gel extraction kit (Thermo Fisher Scientific; Waltham, USA). The purified PCR products were blunted using T4 DNA polymerase (Thermo Fisher Scientific; Waltham, USA) and then ligated using Rapid DNA ligation kit (Thermo Fisher Scientific; Waltham, USA) in a 1: 10 ratio (vector : insert) in TRV-VIGS vector (pTRV2; pYL156) and SACMV-VIGS vector (pC8A-CP) that were respectively linearised using the blunt cutters Fast digest^{TM} SmaI and Eco47III (Thermo Fisher Scientific; Waltham, USA) yielding fragments that are 9663 and 10244 bp long respectively (figure 2-1).

The ligation products were transformed into chemically competent DH5α cells, and colony PCR was used to confirm for successful recombination, using as forward primers SAA/F and TRV2F and as reverse primer, the forward primer of each myosin VIGS fragment sequences (myosin insert). The colony PCR was set up to screen for colonies with myosin inserts in the antisense orientation (figure 2-2). Positive colonies were cultured overnight in SOB medium containing 100 mg/l kanamycin, plasmid was extracted using GeneJET plasmid Miniprep kit (Thermo Fisher Scientific; Waltham, USA). A restriction digest procedure using the enzymes EcoRI for SACMV-VIGS and ScaI for TRV-VIGS was used to further confirm the presumptive VIGS vector recombinants. EcoRI cuts SACMV-VIGS vector twice, yielding 2 fragments of

sizes 7966 bp and 2278 bp when not recombined and for TRV-VIGS vector ScaI cuts three times, yielding three fragments of sizes 599 bp, 1096 bp and 7968 bp when not recombined (figure 2-1). The fragment sizes expected from recombined VIGS vectors (referred to as VIGS constructs) are 7966 bp and 2578 bp (2533 bp for VIGS construct M8.B) for SACMV-VIGS and for TRV-VIGS, fragment sizes of 599 bp, 7968 bp and 1396 bp (1351 bp for VIGS construct myosin 8.B). VIGS vectors that were positive for successful recombination of the VIGS constructs in the antisense orientation were transformed into chemically competent *Agrobacterium tumefaciens* strain C58C1. VIGS constructs for each gene of interest (GOI) will be referred to as SACMV::GOI and TRV::GOI.

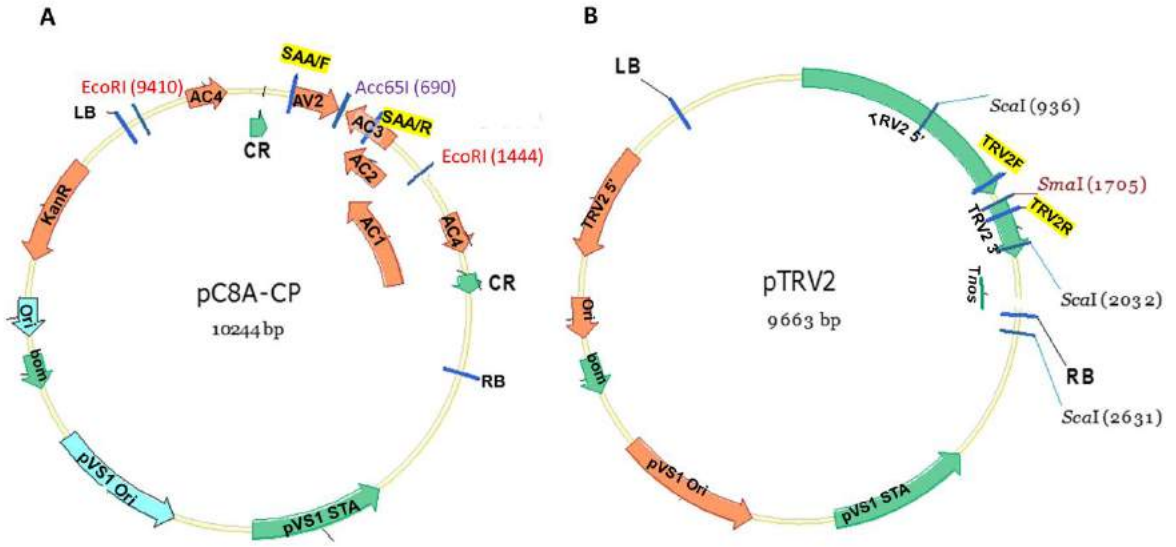

Figure 2-1: Plasmid maps of vectors SACMV-VIGS vector (pC8A-CP) and TRV-VIGS vector (pTRV2)

The size of each VIGS vector is indicated in the middle of the map. The restriction enzymes used for the cloning strategy in [**A**] SACMV-VIGS vector were the blunt cutter Acc651 (Eco47III) which linearises SACMV-VIGS vector at position 690 bp. Shown on the map are the restriction sites of EcoRI which digests SACMV-VIGS vector twice, at position 1444 bp and 9410 bp. [**B**] Restriction enzymes used for TRV-VIGS vector cloning strategy were the blunt cutter SmaI which linearises the TRV-VIGS vector by cutting at position 1705 bp and ScaI, which cuts TRV-VIGS vector thrice, at positions 936, 2032 and 2631 bp. Shown on both maps are the vector specific primers SAA/F and SAA/R for SACMV-VIGS and TRV2F and TRV2R for TRV-VIGS vector.

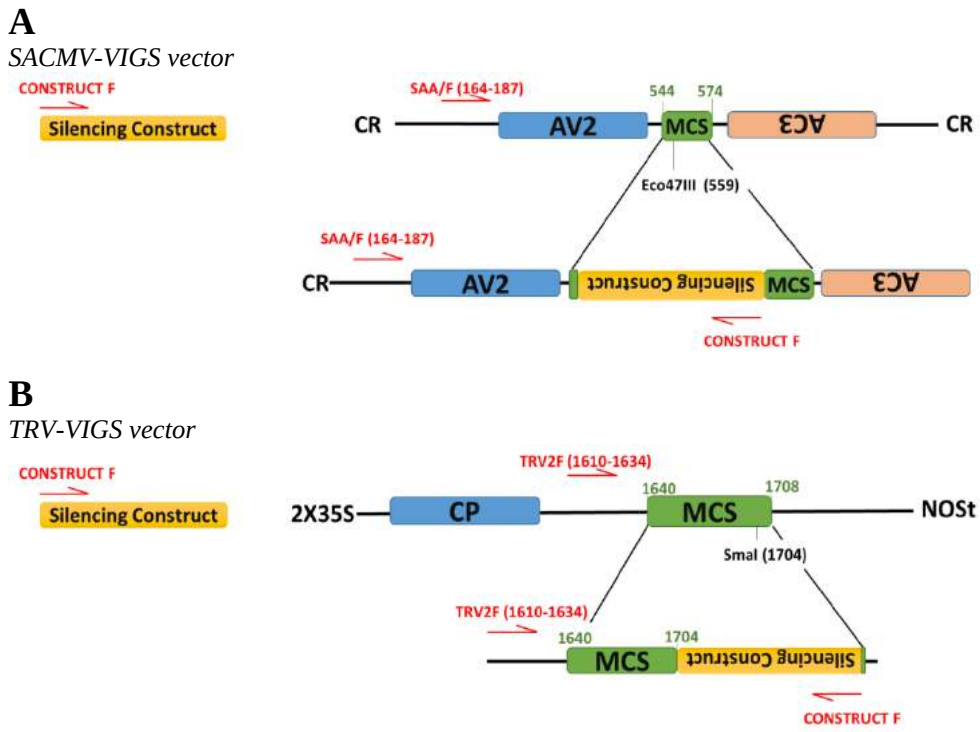

Figure 2-2: Screening strategy for testing for successful recombination in creating the VIGS constructs.

Vector specific primers SAA/F for SACMV-VIGS vector [**A**] and TRV2F for TRV-VIGS vector [**B**] are shown in red with their start and end sites in brackets. Construct F in red indicate the forward primer of each myosin VIGS fragment sequence (insert). Numbers in green show the start and end site of the MCS. To confirm for positive recombination of VIGS constructs in the antisense orientation, PCR was run with vector specific forward primers and the forward primer of the insert. The PCR products size expected were approximately 695 bp for SACMV-VIGS vector recombinant (or 650 bp for *SACMV::8.B*) and 368 bp (or 323 bp for *TRV::8.B*). CR, common region; AV2, pre-coat protein; AC3, replication enhancer; CP, coat protein; 2X35S, duplicated CaMV 35S promoter; NOSt, nopaline synthase terminator.

2.2.3 Myosin silencing experiment vectors

Unless indicated otherwise, reagents used for this section were purchased from Sigma Aldrich. All VIGS vectors and VIGS constructs used in this study are depicted in table 2-5. TRV vectors used were pYL192 (pTRV1) and pYL156 (pTRV2) or a SACMV- A derived vector (Mwaba, 2012). For the myosin silencing, three weeks after seedling emergence, the source leaves of plantlets at the 4-leaves stage were agroinfiltrated with Agrobacterium C58C1

cultures containing VIGS vectors only (non-silenced controls) or one of five VIGS constructs (myosin-silenced plants) (table 2-5).

Table 2-5: Different VIGS and silencing vectors used in treatments (plants and corresponding controls) for myosin knockouts in *N. benthamiana*.

	SACMV	**TRV**
Myosin silencing experiment (NO SACMV challenge)		
VIGS vector control	SACMV-VIGS vector & SACMV-B (SACMV-VIGS vector)*	TRV-VIGS vector & TRV1 (TRV-VIGS vector)*
VIGS construct	SACMV-VIGS construct myosin 15.1 & SACMV-B (SACMV::M15.1)*	TRV-VIGS construct myosin 15.1 & TRV1 (TRV::M15.1)*
	SACMV-VIGS construct myosin 8.B & SACMV-B (SACMV::M8.B)*	TRV-VIGS construct myosin 8.B & TRV1 (TRV::M8.B)*
	SACMV-VIGS construct myosin 11-F & SACMV-B (SACMV::M11.F)*	TRV-VIGS construct myosin 11-F & TRV1 (TRV::M11.F)*
	SACMV-VIGS construct myosin 11-K & SACMV-B (SACMV::M11.K)*	TRV-VIGS construct myosin 11-K & TRV1 (TRV::M11.K)*
	SACMV-VIGS construct myosin 11-2 & SACMV (SACMV::M11.2)*	TRV-VIGS construct myosin 11-2 & TRV1 (TRV::M11.2)*
SACMV-challenge experiment		
SACMV-challenged/VIGS vector	SACMV-VIGS vector + SACMV-A & B challenge 7 days later	TRV-VIGS vector + SACMV-A & B challenge 7 days later
SACMV-challenged/VIGS construct	(SACMV-challenged/SACMV::M15.1)*	(SACMV-challenged/TRV::M15.1)*
	(SACMV-challenged/SACMV::M8.B)*	(SACMV-challenged/TRV::M8.B)*
	(SACMV-challenged/SACMV::M11.F)*	(SACMV-challenged/TRV::M11.F)*
	(SACMV-challenged/SACMV::M11.2)*	(SACMV-challenged/TRV::M11.2)*
	(SACMV-challenged/SACMV::M11.K)*	(SACMV-challenged/TRV::M11.K)*
Mock inoculation control	Empty Agrobacterium C58C1 (mock)*	
SACMV-A & B infection of non-treated plants	untreated plants challenged with SACMV DNA-A & B (SACMV challenged/NO VIGS)*	

*** Written in bracket are the names referred to in the text**

All VIGS vectors and VIGS constructs were co-inoculated with either SACMV DNA-B or TRV1 required for replication and movement of SACMV and TRV2 vectors, respectively. The silencing experiment was repeated 3 independent times (3 experimental replicates). Each experimental replicate comprised of 13 groups of plants each comprising of 18 plants. The first 2 groups were agroinfiltrated with each VIGS vector, SACMV-VIGS vector and SACMV-B and TRV-VIGS vector and TRV1 (vector control). Ten of the remaining groups were agroinfiltrated with the five VIGS constructs (table 2-5).

Agroinfiltration proceeded as follow. Agrobacterium C58C1 cultures (VIGS vector and VIGS constructs) were used to inoculate YEP media containing 100 mg/l kanamycin and 50 mg/l rifampicin and grown overnight at 28°C. The following day, 50 ml of fresh YEP media supplemented with 10 mM morpholino ethane sulfonic acid (MES), 20 µM acetosyringone, 100 mg/l kanamycin and 50 mg/l rifampicin was inoculated with the overnight culture and allowed to grow overnight. The cells were collected by centrifugation and the pellet resuspended in infiltration media (10 mM $MgCl_2$, 10 mM MES, and 200 µM acetosyringone) to an OD_{600} of 0.4-0.6. The cultures were incubated for 3 h at room temperature before proceeding with agroinfiltration. Mock inoculation controls were agroinfiltrated with empty Agrobacterium C58C1, cultured as specified for the VIGS vectors and VIGS construct, with the exception that YEP media for empty Agrobacterium C58C1 contained only 50 mg/l of rifampicin and no kanamycin.

2.2.4 SACMV challenge post initiation of silencing

SACMV-challenge of myosin-silenced or non-silenced control (VIGS vector) plants was performed 7 days post silencing. Nine plants within each of the 13 groups detailed in section 2.2.3 were challenged with infectious clones of SACMV-A and B.

Nine plants from the group inoculated with SACMV and TRV-VIGS vector and challenged with SACMV-A and B 7 days later would be referred to *"SACMV-challenged/(SACMV or TRV) VIGS vector"* and the nine not infected with SACMV-A and B would be referred to as "*VIGS vector "*. From of the 10 groups inoculated with the VIGS constructs, those not challenged with SACMV-A and B would be referred to as "*(SACMV or TRV)::GOI"*, and those challenged with SACMV-A and B would be referred to as "*SACMV-challenged/(SACMV or TRV)::GOI*". From the mock inoculated group, the nine infected with the virus would be referred to as

"*SACMV challenged/NO VIGS"* and the nine uninoculated would be referred to as *"mock"* (see table 2-5). As a general term SACMV-VIGS or TRV/VIGS refers to the SACMV or VIGS study respectively.

Agroinfiltration for SACMV-challenge proceeded as follow. Agrobacterium C58C1 colonies of SACMV-A and -B were used to inoculate YEP media containing 100 mg/l kanamycin and 50 mg/l rifampicin and grown overnight at 28°C. The following day, 50 ml of fresh YEP media supplemented with 10 mM MES, 20 µM acetosyringone, 100 mg/l kanamycin and 50 mg/l rifampicin was inoculated with the overnight culture and allowed to grow overnight. The following day, the cells were collected by centrifugation and the pellet resuspended in infiltration media (10 mM $MgCl_2$, 10 mM MES, and 200 µM acetosyringone) to an OD_{600} of 0.4-0.6. The cultures were incubated for 3 h at room temperature before proceeding with agroinfiltration. The newly formed source leaves, one position above the leaves agroinfiltrated in section 2.2.3, were agroinfiltrated with the infectious clones cultures (figure 2-3). At 14 and 28 dpi post SACMV challenge, the leaves just below the apex were harvested for nucleic acid extraction, silencing measurements and viral load determination. Symptom severity score (SSS) and plant height were measured at 14 and 28 dpi.

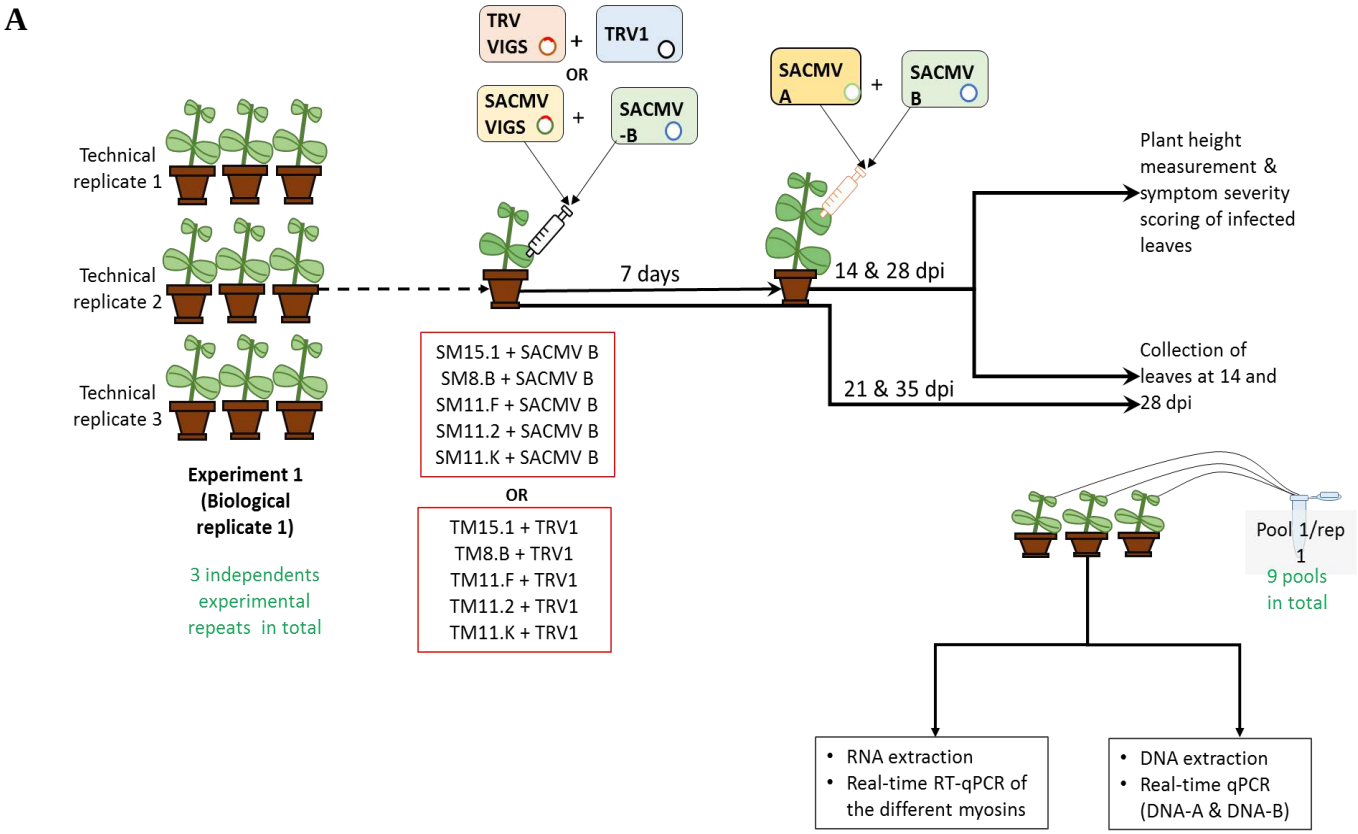

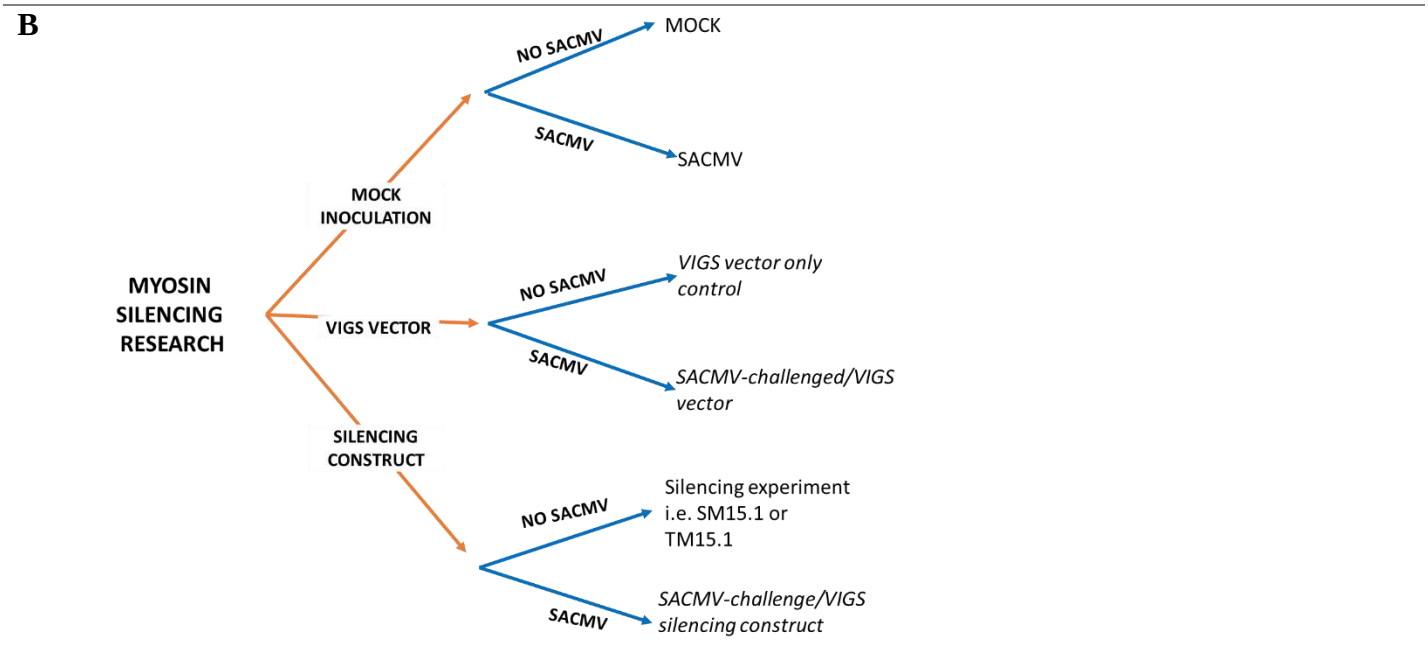

Figure 2-3: Research experimental outline.

[**A**] Inoculation for the silencing experiment was done using the combination of the SACMV and TRV VIGS constructs shown in the two red boxes and 18 plants were used for each. 18 plants were mock inoculated with Agrobacterium C58C1. 7 days after the initial inoculation, 9 of the 18 plants were challenged with SACMV-A and B and leaves were harvested at 14 and 28 dpi after SACMV challenge, as indicated. 9 plants were left unchallenged. The experiments were carried out at 3 independent times, and each experiment consisted of 3 pools as indicated. [**B**] Breakdown of experimental treatments and controls used in the research. Orange arrows represent the initial silencing inoculation and blue arrow the virus inoculation, 7 days later. SM denotes SACMV VIGS constructs and TM denotes TRV VIGS constructs.

2.2.5 Nucleic acid extraction and viral load determination

DNA from infected and mock-inoculated tissues were extracted from three biological replicates, each comprising of 3 technical replicates (figure 2-3) using a modified Cetyl trimethylammonium bromide (CTAB) method (Doyle and Doyle 1987; Porebski et al. 1997). For total DNA extraction, about 100 mg of leaf tissue was ground in the presence of liquid nitrogen and to the powdered tissue was added 500 µl of extraction buffer (2% w/v CTAB, 2% w/v PVP, 20 mM EDTA, 1.4 M NaCl, 100 mM Tris-HCl pH 8.0 and 0.1% v/v β-mercaptoethanol) and incubated at 65°C for 60 minutes. After incubation 500 µl of chloroform : isoamyl alcohol (24:1) was added and the plants were centrifuged at 12,000 *g* for 10 min, and the aqueous phase was extracted to a new microfuge tube, to which an equal volume of isopropanol was added to precipitate DNA. The plants were centrifuged as described above. The tubes were decanted and the precipitated pellet was washed in 1 ml ice cold 70% ethanol (v/v) and centrifuged for 5 min at 12,000 *g*. DNA pellets were air dried and resuspended in TE buffer containing 200 µg/ml of RNAse A. The extracted DNA was quantified using the NanoDrop™ 1000 spectrophotometer (Thermo Fisher Scientific; Waltham, USA).

All real-time (qPCR) assays were performed using Maxima SYBR Green (Thermo Fisher Scientific; Waltham, USA) and the LightCycler® LC480 (Roche; Basel, Switzerland). No template controls were included in each run. Viral load determination was carried out using absolute qPCR using primer AV1 primer set for SACMV-A quantification, BV1 primer set for SACMV-B quantification and glyceraldehyde 3-phosphate dehydrogenase (GAPDH) set as an internal control. For a sequence of primers used, see (table 2-4). For each quantification reaction, the DNA sample was diluted to a final concentration of 20 ng/µl. One µl of extracted DNA was run in triplicate. To 5 µl of Maxima SYBR green master mix was added, either AV1, BV1 or GAPDH forward and reverse primer to a final concentration of 0.3 µM for each primer and nuclease free water to a total volume of 10 µl. Real-time PCR was run for 35 cycles. Initial denaturation and enzyme activation was carried out at 95°C for 10 min, denaturation at 95°C, 15 sec, annealing at 60°C for 30 s and elongation at 72°C for 30 s. The crossing points for DNA-A and B amplification were subtracted from crossing point of GAPDH to calculate the ΔCt values to quantify DNA-A and B relative to the internal control.

2.2.6 Quantification of myosin silencing

RNA was extracted from about 100 mg of leaf tissue using Tri reagent (Sigma-Aldrich; St Louis, USA) per the manufacturer's recommendation and resuspended in nuclease-free H_2O containing 1 U/µl of Ribolock RNAse inhibitor (Thermo Fisher Scientific; Waltham, USA). Concentrations of extracted RNA plants were determined using the NanoDrop™ 1000 spectrophotometer (Thermo Fisher Scientific; Waltham, USA) and RNA integrity was assessed by electrophoresis on 1.0% agarose gel. The extracted RNA was treated with DNAse I (Thermo Fisher Scientific; Waltham, USA) per manufacturer's recommendation before proceeding to first strand DNA synthesis.

First strand DNA synthesis was carried out using random hexamers and RevertAid First Strand cDNA Synthesis Kit (Thermo Fisher Scientific; Waltham, USA), per manufacturers' recommendation. The synthesised cDNA was diluted 1 in 10 and 1 µl of diluted cDNA was added to 5 µl of Maxima SYBR green master mix. Specific primers were added to a final concentration of 0.3 µM for each primer, and nuclease free water to a total volume of 10 µl. Real-time PCR was run for 35 cycles. Initial denaturation and enzyme activation was carried out at 95°C for 10 min, denaturation at 95°C, 15 sec, annealing at 60°C for 30 s and elongation at 72°C for 30 s. GAPDH primer set was used for normalization as endogenous control (Allie and Rey 2013; Allie et al. 2014). For relative expression calculations ΔΔCt method was applied.

2.2.7 Statistical analysis

Results are presented as median ± standard error of the mean (SEM). Student's t-tests were performed on values obtained from myosin expression, viral load, DNA-A/DNA-B ratio, SSS and plant height. Viral load, DNA-A/DNA-B ratio, SSS and plant height from either SACMV-challenged/TRV VIGS-silenced myosin or SACMV-challenged/SACMV VIGS-silenced myosin were compared to SACMV-challenged/No VIGS by one-way ANOVA. Two-way ANOVA analyses were used to assess viral load, DNA-A/DNA-B ratio, SSS and plant height values obtained from SACMV-challenged/TRV VIGS-silenced myosin and SACMV-challenged/SACMV VIGS-silenced myosin.

Pearson's correlation test was performed in Microsoft Excel, to determine a correlation between viral load and DNA-A/DNA-B ratio, viral load to SSS, viral load to plant height and plant height to SSS. Statistical inferences from Pearson's r values were made by calculating the probability for the Student t-distribution in excel using the formula

$$= \boldsymbol{TDIST}\left(\left(\boldsymbol{r} \times \frac{\sqrt{\boldsymbol{df}}}{\mathbf{1} - \boldsymbol{r^2}}\right), \boldsymbol{n}, \mathbf{1}\right)$$

where
r is the Pearson's r value
df is the degree of freedom
n is the number of observations

For each statistical consideration, $p \leq 0.05$ was taken to indicate a significant difference.

2.3 Results

2.3.1 Structural, functional and phylogenetic analyses of 24 myosins encoded by N. benthamiana

According to the cytoskeletal and motor protein base (CyMoBase; http://www.cymobase.org), a total of 23 proteins have been recorded for *N. benthamiana*, including the six previously published and characterised (Avisar et al. 2008a; Sattarzadeh et al. 2009), and the 17 others predicted in version v0.4.2 of *N. benthamiana* genome in Solgenomics. The sequences of the uncharacterised myosins genes found at CyMoBase are partial with questions regarding some of the introns and exons found. For this reason, we used the sequences of six myosins previously identified for *N. benthamiana* and searched the predicted cDNA genome and found 24 different genes on different scaffolds (table 2-7). Searching through the genome without restricting to predicted cDNAs revealed that transcripts Niben101Scf04193g02006.1 and Niben101Scf04193g02004.1 are located on the same the same scaffold, adjacent to one another (figure 2-4) with predicted protein sequence of 437 and 156 aa respectively. Since Niben101Scf04193g02006.1 and Niben101Scf04193g02004.1 are located adjacent to each other, they could be part of the same gene, inaccurately separated during gene prediction and consequently neither of these transcripts were included in the subsequent analysis.

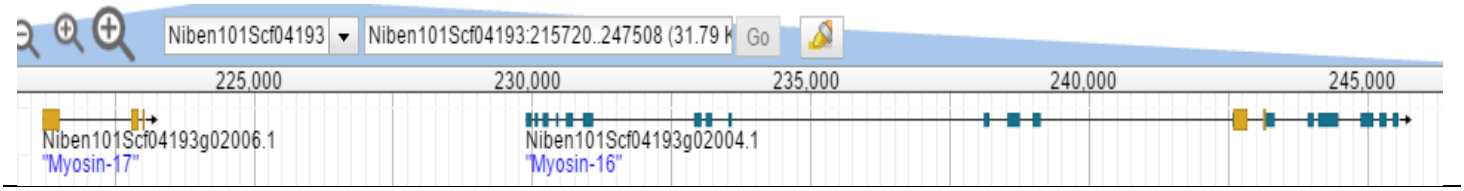

Figure 2-4: Scaffold positioning of putative myosin homologues Niben101Scf04193g02006.1 and Niben101Scf04193g02004.1 in the JBROWSE module of Solgenomics.

Phylogenetic analysis was used to define the different identified myosin sequences according to two plant myosin classes. The 24 putative *N. benthamiana* myosins were grouped in the two classes of myosin known to occur in plant, with seven class VIII myosins and 17 class XI (figure 2-5). In Arabidopsis, class VIII myosins can be further divided in subtypes A and B with two members found under each subtype, and class XI myosins have been divided under eight subtypes (Mühlhausen and Kollmar 2013).

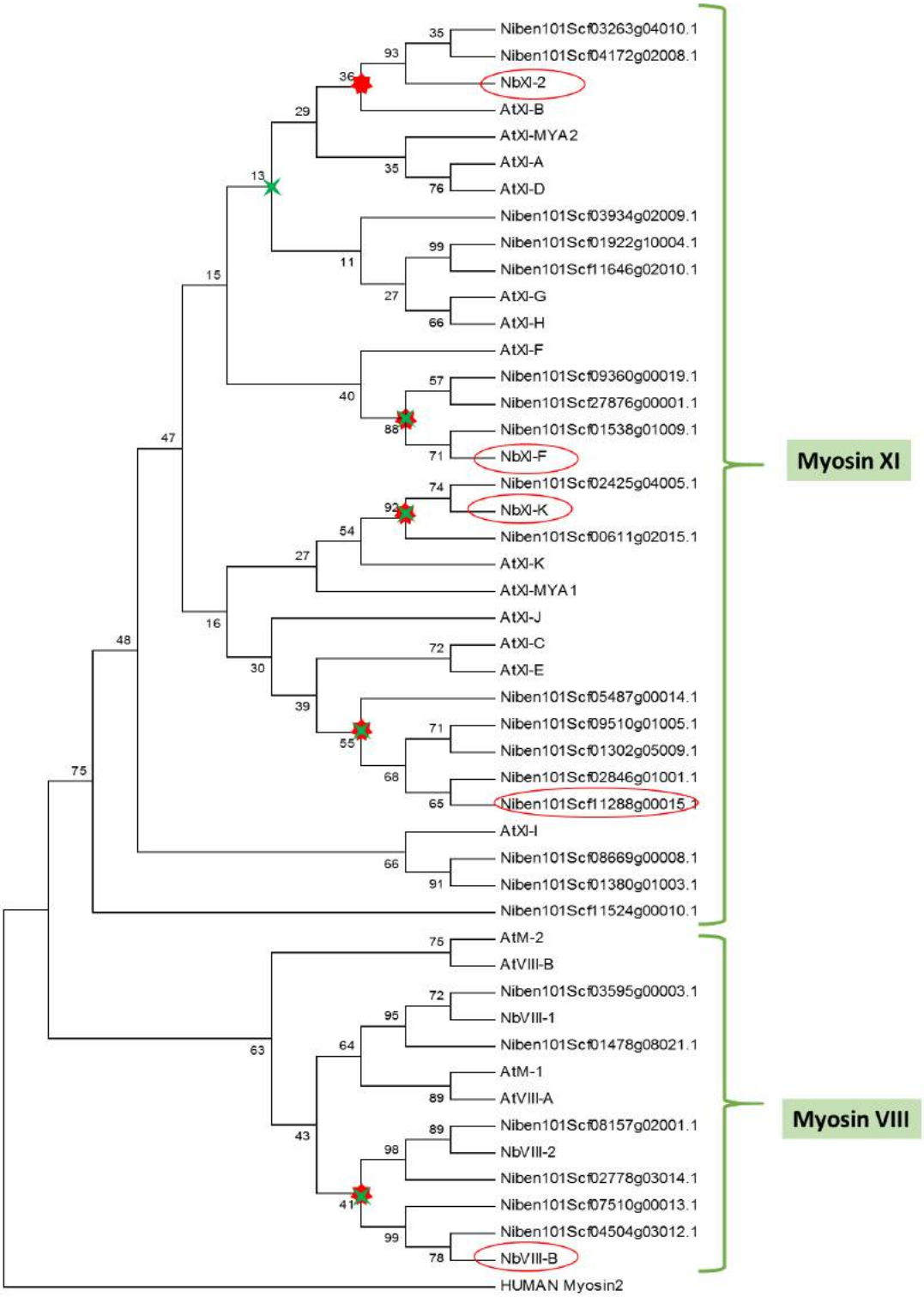

Figure 2-5: Molecular phylogenetic analysis of nucleotide similarities between putative myosins in *N. benthamiana*.

The evolutionary history was inferred by using the Maximum Likelihood method based on the JTT matrix-based model (Jones et al. 1992). The bootstrap consensus tree inferred from 1000 replicates is taken to represent the evolutionary history of the taxa analysed (Felsenstein 1985). Branches corresponding to partitions reproduced in less than 50% bootstrap replicates are collapsed. The percentage of replicate trees in which the associated taxa clustered together in the bootstrap test (1000 replicates) are shown next to the branches (Felsenstein 1985). Initial tree[s] for the heuristic search were obtained automatically by applying Neighbour-Join and BioNJ algorithms to a matrix of pairwise distances estimated using a JTT model, and then selecting the topology with superior log likelihood value. The analysis involved 48 aa sequences. There were a total of 2441 positions in the final dataset. Evolutionary analyses were

conducted in MEGA7 (Kumar et al. 2016). The sequence of human Myosin 2 (Q9UKX2) was used to root the tree. Brackets on the side indicate the two different classes of plant myosins and the branches that fall within each class. Circled in red are the sequences on which the VIGS constructs were designed. The red diamond indicates the branches where potential off-targets are found, based on the result from the SGN VIGS tool. The cross in green indicates branches under which sequences that bore similarities to the VIGS construct sequence are found.

Phylogenetic analysis identified four possible members for subtype A and 3 for subtype B, and for class XI myosins, based on the phylogenetic analyses, it was difficult to associate Arabidopsis myosins to their *N. benthamiana* homologues as they did not always group together (figure 2-5). In Arabidopsis, myosin XI-I has been found to have a slower velocity to other myosin XI-I and is believed to have a different function to other myosins (Haraguchi et al. 2016). Myosin XI-I forms a separate branch from other class XI myosins (Peremyslov et al. 2011; Haraguchi et al. 2016). In this study, two presumptive homologues of AtXI-I were found in *N. benthamiana* and they also segregated from the other class XI myosins (figure 2-5).

The nucleotides sequences of the 24 putative *N. benthamiana* myosins were aligned using ClustalOMEGA (www.ebi.ac.uk/Tools/msa/clustalo/). It revealed high percentage nucleotide sequence similarity between myosins of each class (table 2-6) with myosins class VIII appearing to be closely related compared to myosins class XI as pairwise comparison revealed percentage similarity between members of this group to range between 54 to 98% whilst the similarity between members of myosins Class XI ranges from 36-98% (figure 2-5).

Table 2-6: Nucleotide sequence percentage identity matrix of putative myosin homologues in *N. benthamiana* [a].

	1	2	3	4	5	6	7	8	9	10	11	12	13	14	15	16	17	18	19	20	21	22	23	24
1. Niben101Scf27876g00001.1	100	ND	92	60	61	61	61	33	45	50	34	39	49	50	49	50	45	49	50	51	52	ND	50	49
2. Niben101Scf03595g00003.1		100	98	54	61	56	62	39	39	43	42	43	43	43	42	40	36	43	42	43	43	41	43	42
3. Niben101Scf01478g08021.1			100	57	60	58	63	37	42	47	43	43	48	48	47	45	41	47	47	48	48	36	47	47
4. Niben101Scf04504g03012.1				100	93	76	78	36	39	46	44	42	44	45	44	42	41	44	44	46	46	32	43	44
5. Niben101Scf07510g00013.1					100	77	78	33	42	49	51	45	49	48	49	48	43	48	48	49	49	ND	50	49
6. Niben101Scf08157g02001.1						100	96	37	41	48	44	43	46	46	45	43	42	45	46	47	47	46	46	46
7. Niben101Scf02778g03014.1							100	38	42	49	50	48	48	49	49	49	43	49	49	50	51	ND	49	49
8. Niben101Scf08669g00008.1								100	78	44	43	46	46	46	46	45	36	48	48	48	47	54	48	42
9. Niben101Scf01380g01003.1									100	48	40	48	52	52	53	49	51	55	55	53	54	53	52	52
10. Niben101Scf01922g10004.1										100	95	59	66	65	59	55	54	59	59	60	61	42	58	62
11. Niben101Scf11646g02010.1											100	57	58	57	52	49	51	53	52	53	53	42	53	56
12. Niben101Scf05487g00014.1												100	79	79	58	57	48	61	61	59	59	58	59	57
13. Niben101Scf03934g02009.1													100	98	62	61	54	64	65	64	65	60	64	63
14. Niben101Scf03263g04010.1														100	63	60	53	64	64	64	65	61	64	64
15. Niben101Scf04172g02008.1															100	96	56	63	63	62	63	53	61	62
16. Niben101Scf09360g00019.1																100	57	61	61	60	61	53	60	62
17. Niben101Scf01538g01009.1																	100	69	69	60	59	ND	60	58
18. Niben101Scf02846g01001.1																		100	98	70	70	72	74	70
19. Niben101Scf11288g00015.1																			100	70	70	73	74	70
20. Niben101Scf00611g02015.1																				100	98	68	70	66
21. Niben101Scf02425g04005.1																					100	68	69	65
22. Niben101Scf11524g00010.1																						100	93	ND
23. Niben101Scf09510g01005.1																							100	92
24. Niben101Scf01302g05009.1																								100

[a]Class VIII myosins members are highlighted in green whilst class XI are highlighted in orange

The aa sequence length of the predicted *N. benthamiana* myosins ranges from 443 to 1622 aa (table 2-7). According to data available at The Arabidopsis Information Resource (TAIR), Arabidopsis myosins aa sequence length ranges between 1134 (AtVIII-A; AT1G50360) to 1770 (AtXI-D; AT2G33240). Arabidopsis myosins VIII are generally smaller to that of class XI with sizes ranging from 1134 to 1220 aa. The size range of class XI is between 1465 aa to 1770 aa, except for AtXI-J, which is 1242 aa long.

Table 2-7: Identities and sequence of *N. benthamiana* myosins

ID	Genomic (bp)	CDS (bp)	Translated protein (aa)
Niben101Scf08157g02001.1	19699	3465	1155
Niben101Scf01478g08021.1	30891	3717	1239
Niben101Scf04504g03012.1	36645	3036	1012
Niben101Scf07510g00013.1	11997	2247	749
Niben101Scf03595g00003.1	9279	1617	539
Niben101Scf27876g00001.1	9953	1530	510
Niben101Scf02778g03014.1	11949	1428	476
Niben101Scf11524g00010.1	2496	1329	443
Niben101Scf05487g00014.1	11373	2448	816
Niben101Scf01302g05009.1	11729	2205	735
Niben101Scf02846g01001.1	16298	1530	510
Niben101Scf01380g01003.1	41498	3222	1074
Niben101Scf03934g02009.1	27873	3543	1181
Niben101Scf01538g01009.1	12877	3522	1174
Niben101Scf08669g00008.1	33901	3180	1060
Niben101Scf11646g02010.1	29031	4101	1367
Niben101Scf09360g00019.1	12371	4539	1513
Niben101Scf04172g02008.1	23600	4410	1470
Niben101Scf01922g10004.1	33769	4866	1622
Niben101Scf02425g04005.1	25303	4635	1545
Niben101Scf03263g04010.1	22185	4347	1449
Niben101Scf09510g01005.1	15857	3837	1279
Niben101Scf11288g00015.1	23556	4236	1412
Niben101Scf00611g02015.1	24825	4761	1587

Sequences obtained from SGN reveals *N. benthamiana* myosins of sequence lengths that falls well outside the 1134-1770 aa range in Arabidopsis myosins (table 2-7). The aa

sequence of four members of class VIII myosins (Niben101Scf07510g00013.1, Niben101Scf03595g00003.1, Niben101Scf27876g00001.1, Niben101Scf02778g03014.1) and four of class XI (Niben101Scf11524g00010.1, Niben101Scf05487g00014.1, Niben101Scf01302g05009.1, Niben101Scf02846g01001.1) of each class were found to be smaller than 1000 aa long (table 2-7). Class VIII myosin range from 476 to 1239 aa whilst class XI range from 443 to 1622 aa.

Using the putative myosin protein sequences, we predicted the domain architecture in Pfam. The architecture of *N. benthamiana* myosins revealed that most of the proteins of less than 1000 aa, have truncated domains or lack feature canonical of plant myosins (figure 2-6), suggesting possible errors during the introns/exons boundary prediction. Shorter myosin-like proteins have been identified in different plants like *headless derivative of myosin* in Arabidopsis and maize and they are both about 680 aa, missing the N-terminus, a motor/head and IQ domains (Peremyslov et al. 2011; Wang et al. 2014). According to its sequence data from Solgenomics, Myosin Niben101Scf11524g00010 was the shortest myosin XI identified, and its predicted structure revealed that it is missing the N-terminus, the head, the IQ and the coiled coil domain (figure 2-6; table 2-7) it is shorter than the headless derivative from maize and Arabidopsis.

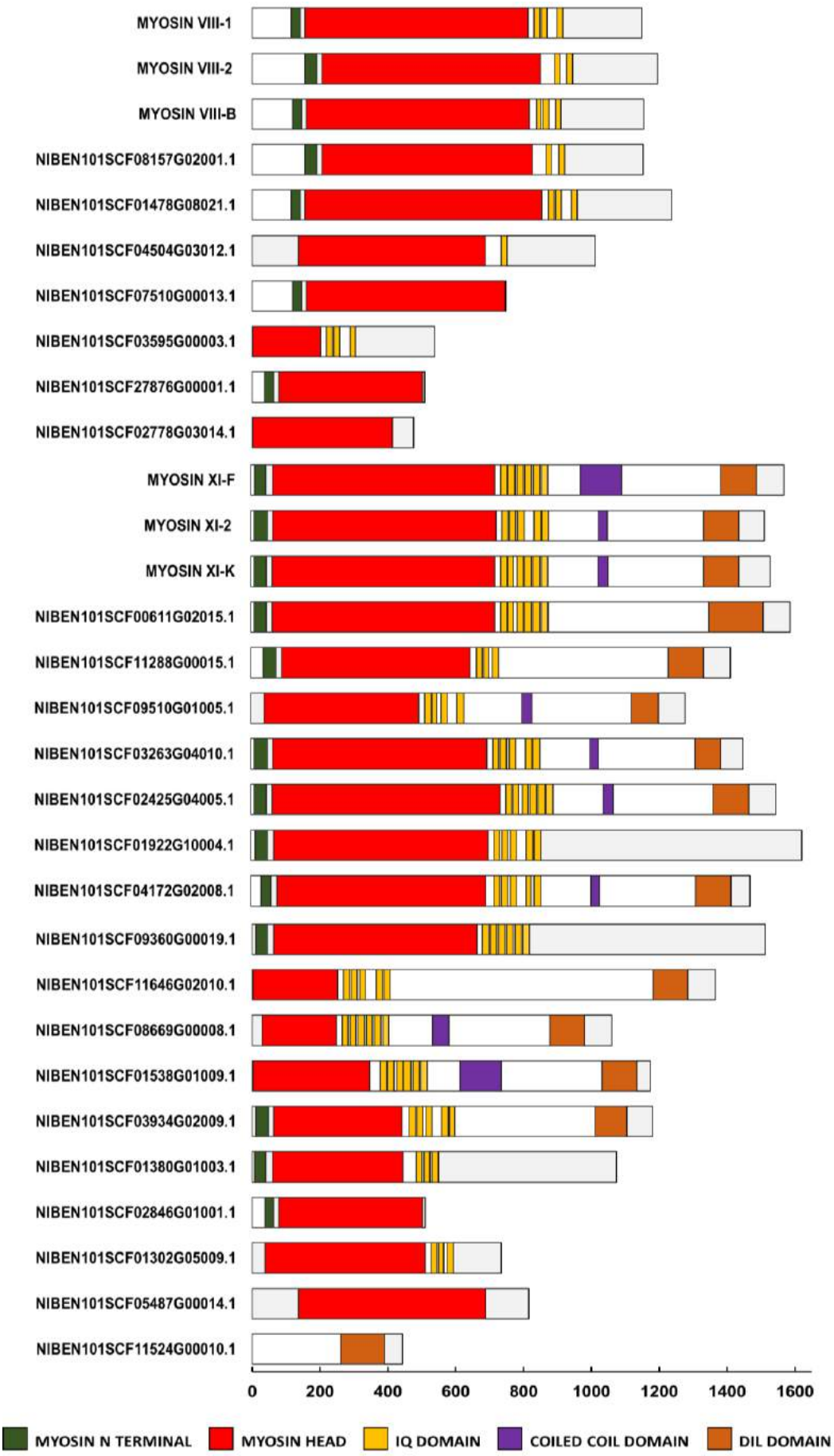

Figure 2-6: Myosin architecture.

The aa and nucleotides sequence lengths are presented in table 2-7. Plant myosins of class VIII and XI domains architecture comprises of an N-terminal SH3-like domain, followed by the myosin head or motor domain, 1 to 6 IQ motifs and a coiled-coil region of varying length. At the C-terminus of class XI myosins is a DILUTE or DIL domain.

2.3.2 Construction of SACMV and TRV-silencing vectors targeting N. benthamiana myosins

To minimise potential off-targets of myosin silencing, the SGN VIGS (http://vigs.solgenomics.net/) was used to identify regions for VIGS constructs design. Due to the percentage similarity between the different myosin members in *N. benthamiana* (table 2-6) no sequence of length that falls between the recommended 200 - 400 nucleotides (Senthil-Kumar and Mysore 2014) for silencing of single myosin members could be found. Based on the results of the phylogenetic analysis (figure 2-5), five major internal nodes were identified, and reference sequences selected (table 2-3) and used in SGN VIGS tool, to select possible silencing regions (figure 2-7). Of all the five silencing regions selected, a stretch of 190 nucleotides of myosin 11-2 shared a 95 % (181/190) nucleotide similarity with a phospholipase C 2 transcript (Niben101scf04093g00004.1; figure 2-8). The selected myosin VIGS fragment sequences were aligned against the *N. benthamiana* genome in SGN, to identify potential off targets based on sequence similarity, not predicted by the SGN VIGS tool (figure 2-8).

A

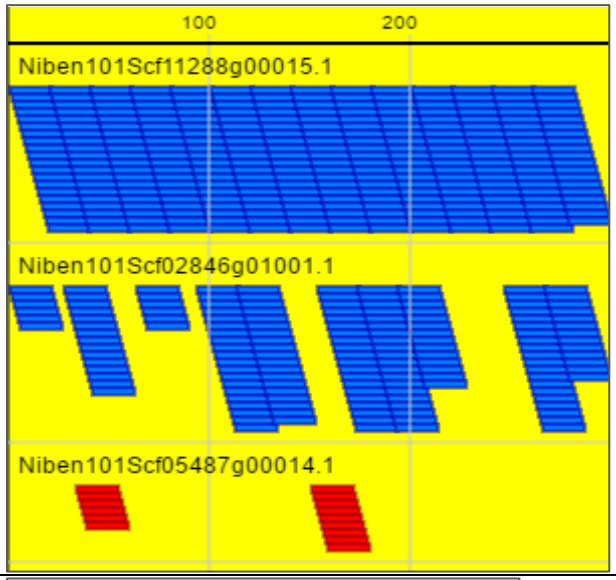
100
200
Niben101Scf11288g00015.1
Niben101Scf02846g01001.1
Niben101Scf05487g00014.1

B

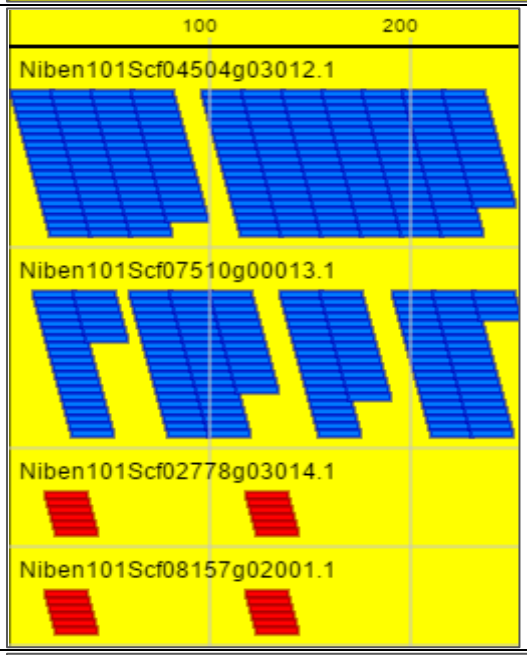
100
200
Niben101Scf04504g03012.1
Niben101Scf07510g00013.1
Niben101Scf02778g03014.1
Niben101Scf08157g02001.1

C

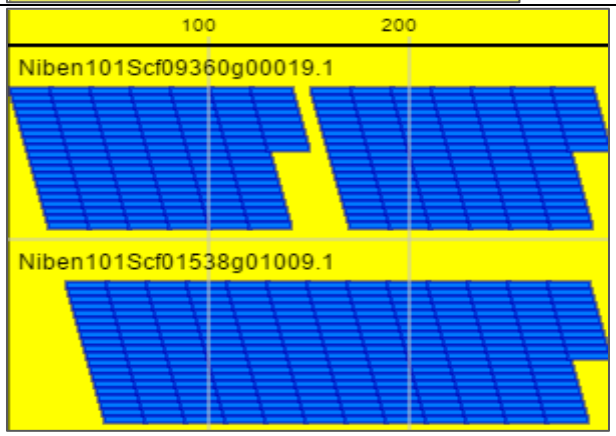
100
200
Niben101Scf09360g00019.1
Niben101Scf01538g01009.1

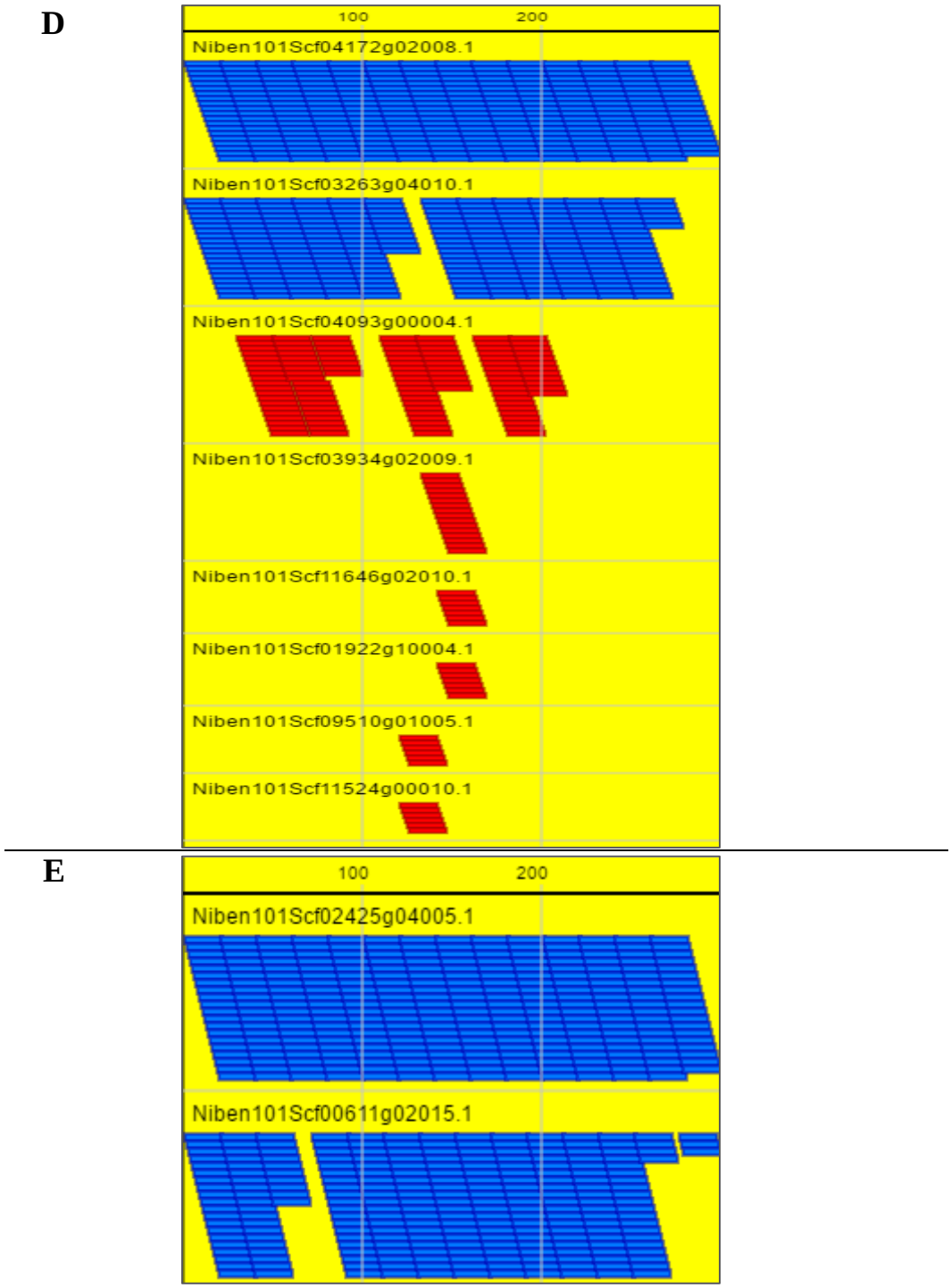

Figure 2-7: Expanded graphical representation of siRNA produced by each myosin fragment sequence as predicted by VIGS tool SGN.

Each row represents a target. The search was limited to identify two targets, shown in blue that had the highest similarity to the search sequence. Potential predicted "off target" are shown in red. The score graph that comes at the bottom indicates the best region, based on the alignment that would give the least off-targets and the worst region which has the most off-targets was cropped out. The numbers on top represent the length of the sequence, drawn to scale. Constructs were designed for **A.** M15.1, **B.** M8.B, **C.** M11.F, **D.** M11.2, **E.** M11.K.

A

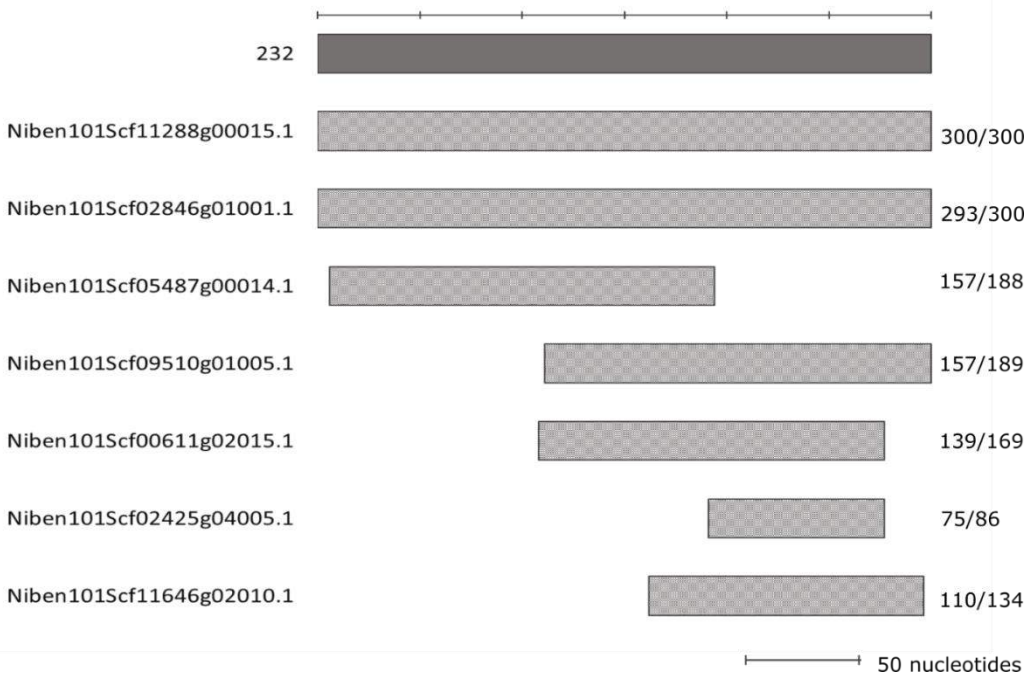
232
Niben101Scf11288g00015.1
300/300
Niben101Scf02846g01001.1
293/300
Niben101Scf05487g00014.1
157/188
Niben101Scf09510g01005.1
157/189
Niben101Scf00611g02015.1
139/169
Niben101Scf02425g04005.1
75/86
Niben101Scf11646g02010.1
110/134
50 nucleotides

B

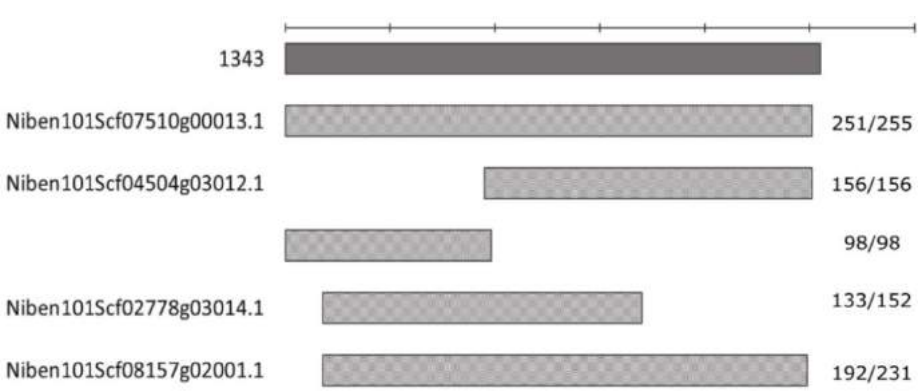
1343
Niben101Scf07510g00013.1
251/255
Niben101Scf04504g03012.1
156/156
98/98
Niben101Scf02778g03014.1
133/152
Niben101Scf08157g02001.1
192/231

C

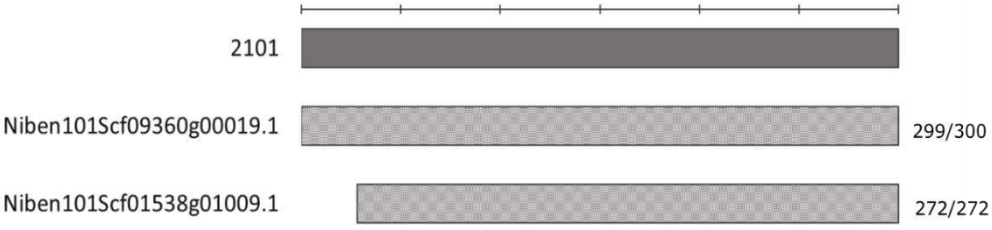
2101
Niben101Scf09360g00019.1
299/300
Niben101Scf01538g01009.1
272/272

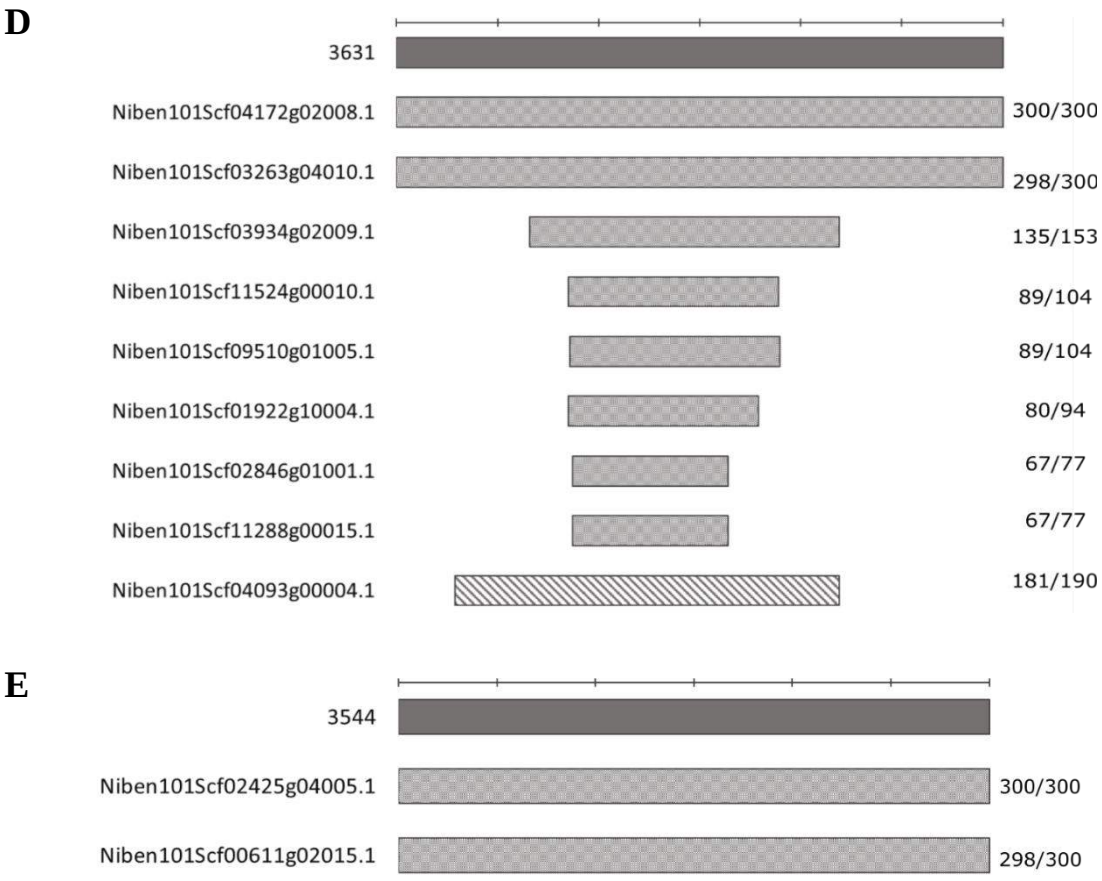

Figure 2-8: Percentage nt sequence similarities between myosin VIGS fragment sequences and *N. benthamiana* myosin CDS.

To highlight the similarity between each myosin VIGS fragment sequence [**A**] M15.1, [**B**] M8.B, [**C**] M11.F, [**D**] M 11.2, [**E**] M 11.K, and *N. benthamiana* coding sequences, the myosin VIGS fragment sequences were aligned against the *N. benthamiana* genome in SGN. The VIGS construct sequence is shaded in grey and the sequences that they are similar to are found below. The numbers on the right are the identities scores. Bar on top of the figures represent 50 nucleotides.

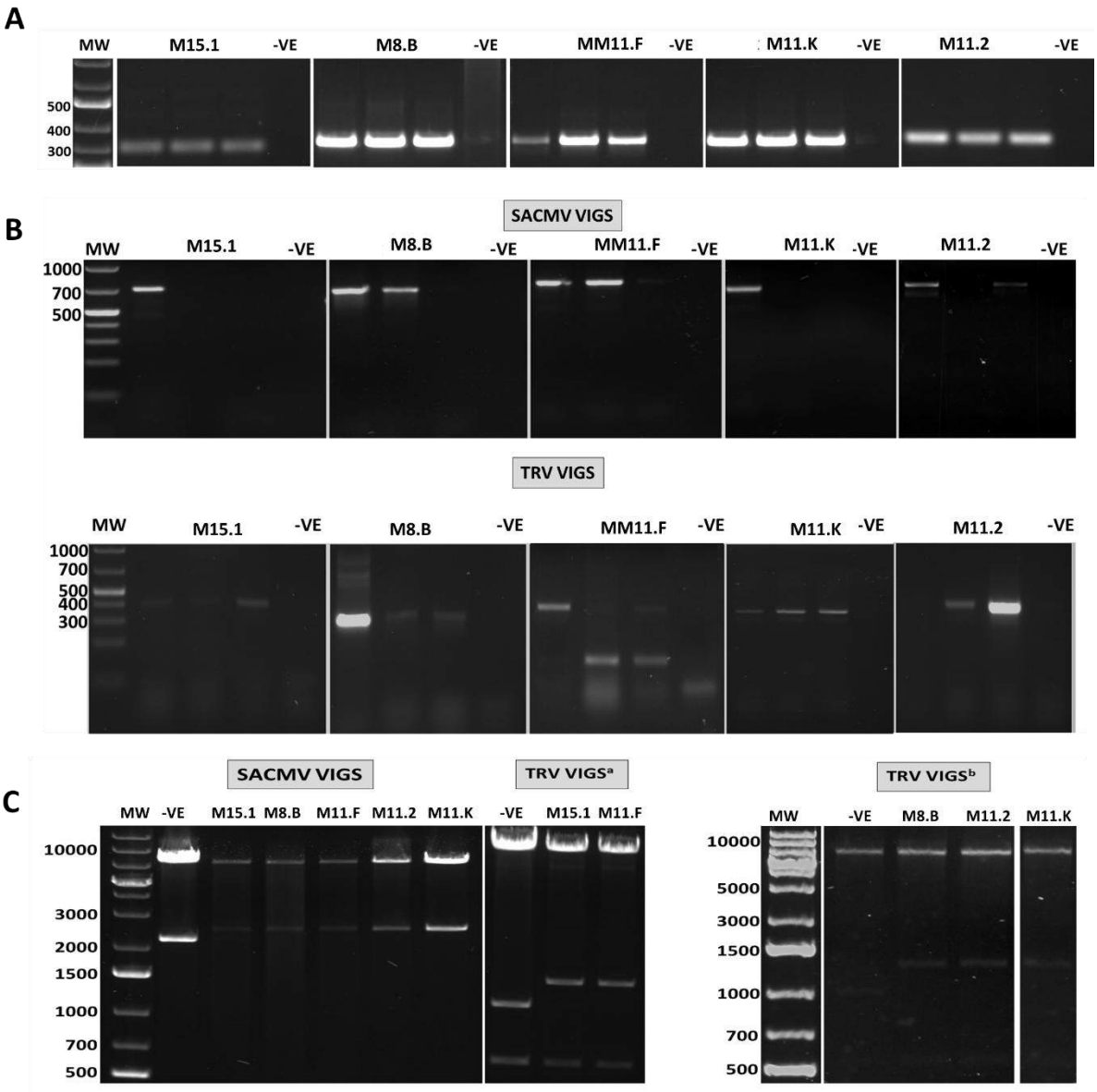

Figure 2-9: Cloning approach for construction of myosin silencing VIGS vectors.

[**A**] The VIGS fragment sequences were amplified using a RT-PCR approach with the primers specified in the text. All the selected myosin VIGS fragment sequences beside M8.B were 300 bp long with M8.B being 255 bp long. [**B**] The recombined VIGS constructs were screened by PCR, using the forward primer of vector backbone and the forward primer of the insert fragment as detailed in figure 2-2. The PCR products size expected were 695 bp for SACMV::myosin (or 650 bp for SACMV::M8.B) and 368 bp (or 323 bp for TRV::M8.B). [**C**] Positive recombinants were also screened by restriction digest using the restriction enzymes ScaI for TRV::myosin and TRV VIGS vector and EcoRI for SACMV-VIGS vector and SACMV::myosin. The expected size of fragments resulting from EcoRI digest of SACMV-VIGS vector (labelled -VE) were 2278 and 7966 bp and for SACMV::myosin, 2578 bp (2533 bp for SACMV::M8.B) and 7966 bp and for VIGS constructs. The expected size of fragments from ScaI digest of TRV-VIGS vector (labelled -VE) were 7968 bp, 599 bp and 1096 bp and for TRV::myosin, 7968 bp, 599 bp and 1396 bp (1351 bp for TRV::M8.B).

A PCR based approach was used to isolate the myosin VIGS fragments from *N. benthamiana* cDNA (figure 2-9a). The PCR fragment obtained were cloned into the silencing vectors TRV-VIGS vector (Ratcliff et al. 2001) and SACMV-VIGS vector (Mwaba 2010). To confirm for the antisense orientation, the recombined VIGS constructs were screened by PCR as detailed in figure 2-2, using the vector backbone forward primer and the forward primer of the PCR insert fragment (figure 2-9b) and the positive recombinant were further screened using restriction digest with ScaI and EcoRI (figure 2-1) for TRV and SACMV construct respectively (figure 2-9c).

2.3.3 SACMV and TRV-VIGS constructs produce efficient silencing of myosins in N. benthamiana not challenged with SACMV

The TRV and SACMV-VIGS constructs (table 2-5) were used to silence myosins in *N. benthamiana*. Seven days post initiation of myosin silencing, the plants were agroinfiltrated with SACMV-DNA-A and B infectious clones. To test for the ability of the VIGS constructs to induce significant silencing of myosin, expression of myosin was detected using relative RT-qPCR, against expression in vector-only inoculated plants (table 2-5). Silencing was measured at 14 and 28 days post the initiation of SACMV infection, which corresponds to 21 and 35 days post silencing initiation (*p* value appendix A1.2.1, A1.3.1 and A1.3.2).

The detected myosin expression in plants inoculated with VIGS constructs revealed that SACMV::myosin produced significant silencing at 14 dpi, in all five tested VIGS constructs. Expression of myosin M15.1 was reduced by 4-fold, expression of M8.B, M11.F and M11.K were reduced by 2-fold, and expression of M11.2 was reduced by 3-fold lower. At 28 dpi, expression of M11.2 and M11.K were significantly silenced plants inoculated with the respective SACMV VIGS constructs, with a 1.5-fold decrease for M11.2 and 2-fold for M11.K. No significant silencing was measured for M15.1, M8.B and M11.F at 28 dpi (figure 2-10a).

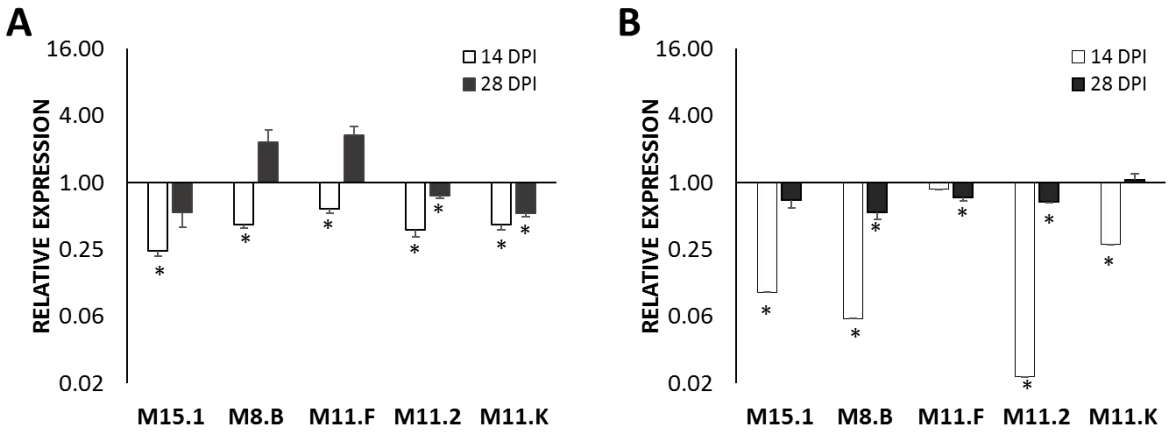

Figure 2-10: Relative expression of myosins at 14 and 28 days post inoculation (dpi) in plants inoculated with VIGS myosin constructs.

Expression of myosin genes was measured using relative RT-qPCR in plants inoculated with SACMV-VIGS constructs (SACMV::myosin) [**A**] and TRV-VIGS constructs (TRV::myosin) [**B**]. Expression of myosin in silenced plants is reported relative to vector-only plant. GAPDH was used as a reference. Values represent the median of three independent replicates each with 3 plants per treatment and bars indicate SEM. T-test was used for statistical analysis p value ≤ 0.05 and the asterisks denote significant changes.

For TRV-VIGS constructs, at 14 dpi significant silencing was produced by four of the five TRV::myosin, with no reduction in M11.F expression detected in plants inoculated with TRV::M11.F. Expression of myosin M15.1 was 8-fold lower, M8.B, 27-fold lower, M11.2, 15-fold and M11.K 5-fold lower. At 28 dpi, plants inoculated with TRV::M8.B, TRV::M11.F and TRV::M11.2 induced significant silencing, reducing expression of the myosin targets by 2-fold in TRV::M8.B plants and 1.5-fold in both TRV::M11.F plants and TRV::M11.2 plants. The silencing observed at 14 dpi in plants inoculated with TRV::M15.1 and TRV::M11.K wasn't observed at 28 dpi, hence only two of the four VIGS constructs that induced significant silencing at 14 dpi, resulted in significant silencing at 28 dpi (figure 2-10b).

SACMV::myosin successfully induced silencing at 14 and 28 dpi for in SACMV::M11.2 and SACMV::M11.K and TRV::myosin successfully induced silencing at both time points in TRV::M8.B and TRV::M11.2. A 1-way ANOVA study revealed that myosin silencing induced at 14 dpi was

stronger than myosin silencing induced at 28 dpi for both vectors (SACMV::VIGS approximately 2-fold *p* value = 0.03 and approximately 10-fold for TRV::VIGS, *p* value = 0.00).

Comparing the degree of myosin silencing between the two types of vector, a 1-way ANOVA study revealed that when reduction of myosin expression was successfully achieved by SACMV::VIGS-construct and TRV::VIGS-construct, TRV-VIGS constructs induced a stronger suppression (2-fold) in myosin expression than SACMV-VIGS constructs (*p* value = 0.01).

The expression of myosin in vector-only plants relative to mock was quantified using RT-qPCR, to assess for the "vector effect" on myosin expression. Whilst no change was observed in myosin expression in plants inoculated with TRV-VIGS vector (figure 2-11b), M11.F was downregulated 5-fold (*p* value 0.00) in SACMV-VIGS vector plants, relative to mock (figure 2-11a) at 28 dpi. At 14 dpi, no change in myosin expression was detected in SACMV-VIGS vector inoculated plants.

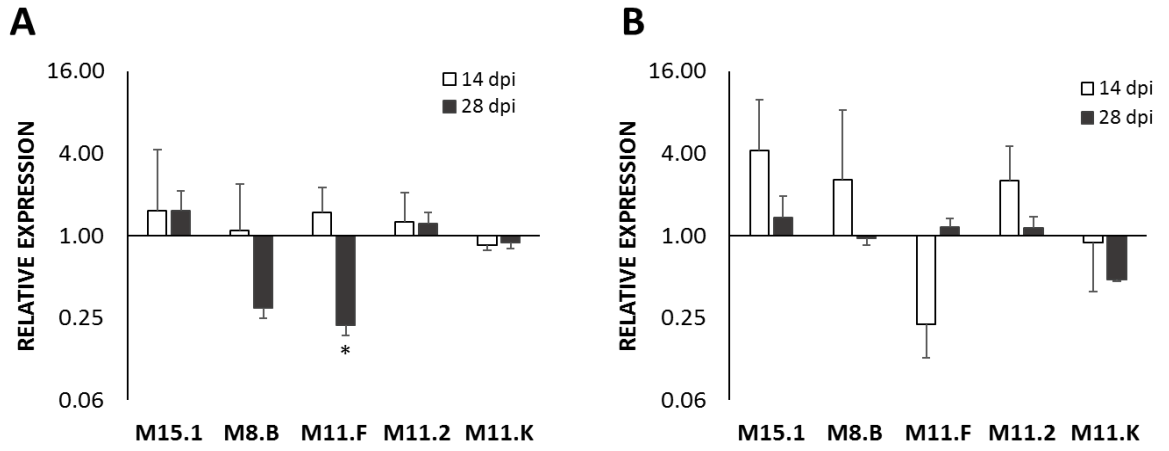

Figure 2-11: Expression of myosins at 14 and 28 days post inoculation (dpi) in SACMV and TRV-VIGS vector inoculated plants, relative to mock.

Expression of myosin was measured using relative RT-qPCR, to assess for the "vector effect" caused by inoculation of SACMV [**A**] and TRV-VIGS vector only [**B**] in *N. benthamiana*, relative to mock. GAPDH was used as a reference. Values represent the median of three independent replicates each with 3 plants per treatment and bars indicate SEM. T-test was used for statistical analysis *p* value ≤ 0.05 and the asterisks denote significant changes.

2.3.4 SACMV challenge of myosin silenced plants affects the silencing efficiency of the VIGS vector

Seven days after the initiation of myosin silencing, plants were challenged with SACMV-A and B infectious clones (*p* value in appendix A1.2.2-0). The reduction in myosin expression was measured in SACMV-challenged/SACMV::myosin and SACMV-challenged/TRV::myosin plants, relative to expression to vector-only plants. In SACMV-challenged/SACMV::myosin at 14 dpi, expression of M11.F and M11.K was reduced by 2-fold and the expression of M11.2 was reduced by 3-fold. At 28 dpi, expression of M11.K was reduced by 2-fold in SACMV-challenged/SACMV::M11.K and the expression of M11.F was increased 4-fold in SACMV-challenged/SACMV::M11.F plants (figure 2-12a). In SACMV-challenged/TRV::myosin experiments, at 14 dpi, significant silencing was only measured for M15.1 (10-fold). At 28 dpi, in SACMV-challenged/TRV::myosin, the expression of M15.1, M11.F and M11.K was reduced 3-fold, 2-fold and 3-fold respectively relative to the TRV-VIGS vector, the expression of M8.B remained unchanged and the expression of M11.2 was increased by 2-fold (figure 2-12b).

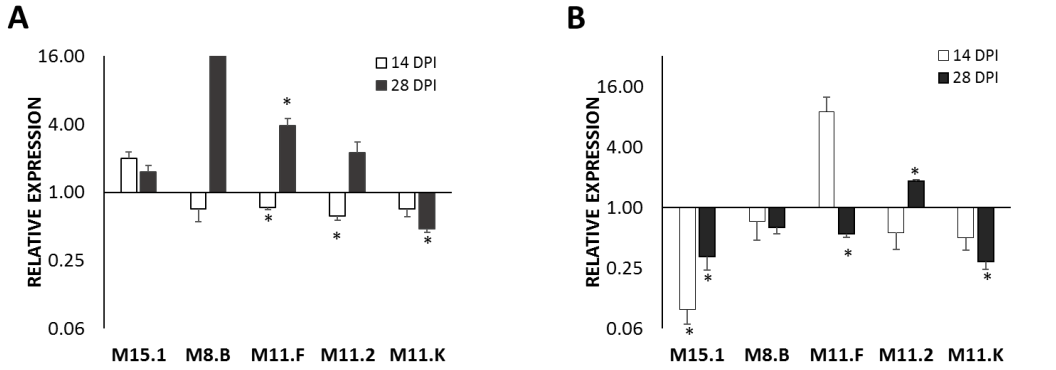

Figure 2-12: Expression of myosin genes measured in SACMV-challenged/VIGS::myosin, relative to vector-only

Expression of myosin was measured using relative qPCR in SACMV-challenged/VIGS::myosin plants is reported relative to vector-only plants in SACMV-challenged/SACMV::myosin [**A**] and SACMV-challenged/TRV::myosin [**B**] plants. GAPDH was used as a reference. Values represent the median of three independent replicates each with 3 plants per treatment and bars indicate SEM. T-test was used for statistical analysis *p* value ≤ 0.05 and the asterisks denote significant changes.

We sought to compare whether the expression of myosin in SACMV-challenged/VIGS::myosin plants differed when reported relative to myosin expression in vector only plants to when reported relative to myosin expression in SACMV-challenged/VIGS vector. At 14 dpi and 28 dpi, expression of M11.F was downregulated in SACMV-challenged/SACMV::M11.F plants relative to SACMV-challenged/SACMV::myosin. Expression of M15.1, M8.B and M11.K remained unchanged at both time points whilst expression of M11.2 remained unchanged at 14 dpi and was upregulated by 5-fold at 28 dpi (figure 2-13a).

The decrease in myosin expression in SACMV-challenged/SACMV::M11.F at 14 dpi and 28 dpi were compared and there was no significant difference and silencing induced by SACMV-challenged/SACMV::M11.F at 14 dpi was not significantly different to silencing in SACMV::M11F (no SACMV-challenge) at 14 dpi.

In SACMV-challenged/TRV::myosin, expression of myosin M11.F and M11.K was downregulated at 28 dpi in SACMV-challenged/TRV::M11.F and SACMV-challenged/TRV::M11.K respectively relative to SACMV-challenged/TRV::myosin. At 14 dpi there was no difference in expression of myosins in any of the SACMV-challenged/TRV::myosin and at 28 dpi there was no differential expression for M15.1, M8.B and M11 (figure 2-13b). Common to both SACMV-challenged/SACMV::myosin and SACMV-challenged/TRV::myosin plants, was the downregulation of M11.F at 28 dpi (figure 2-13).

The reduction of myosin expression in SACMV-challenged/TRV::M11.F at 28 dpi was 2-fold higher (p value = 0.05) compared to TRV::M11.F (no silencing) at 28 dpi and silencing detected in SACMV-challenged/TRV::M11.F at 28 dpi was not different to silencing detected in SACMV-challenged/SACMV::M11.F at 28 dpi.

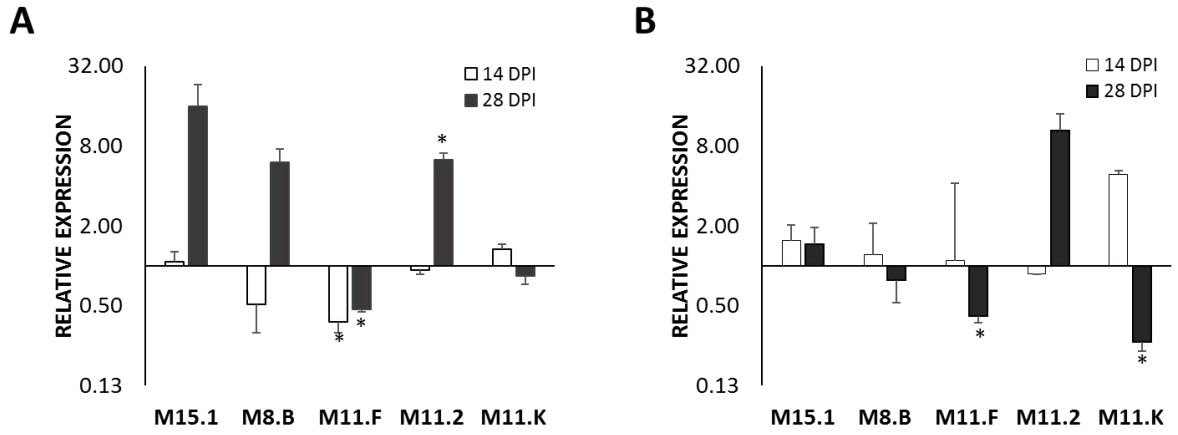

Figure 2-13: Expression of myosin genes measured in "*SACMV-challenged/VIGS::myosin*", relative to SACMV-challenged/VIGS vector

Expression of myosin genes was measured using relative RT-qPCR in "SACMV-challenged/VIGS::myosin plants" plants. Expression of myosin in SACMV-challenged/VIGS::myosin plants is reported relative to SACMV-challenged/VIGS vector. [**A**] SACMV-challenged/SACMV::myosin plants, [**B**] SACMV-challenged/TRV::myosin plants. GAPDH was used as a reference. Values represent the median of three independent replicates each with 3 plants per treatment and bars indicate SEM. T-test was used for statistical analysis p value ≤ 0.05 and the asterisks denotes significant changes

Given the different pattern of myosin expression obtained in and Figure 2-13, the expression of myosin in SACMV-challenged/VIGS vector was measured relative to myosin expression in vector-only plants. At 14 dpi, expression of myosin in SACMV-challenged/SACMV-vector was 1.5-fold lower for myosins M11.2 and 2-fold higher for M11.F. No differential expression was noted for myosins M15.1, M8.B and M11.K. At 28 dpi, M11.K was downregulated by 2-fold and expression of M11.F increased by 8-fold and the expression of M15.1, M8.B and M11.2 remained unchanged (figure 2-14a). Expression of myosin M15.1, M11.2 and M11.K was upregulated by 3-fold in SACMV-challenged/TRV-vector at 14 dpi, and expression of M11.2 was upregulated 2-fold (figure 2-14b). At 28 dpi, the expression of M11.2 was downregulated 2-fold, and the expression of M8.B, M11.F, M11.K and M15.1 remained unchanged.

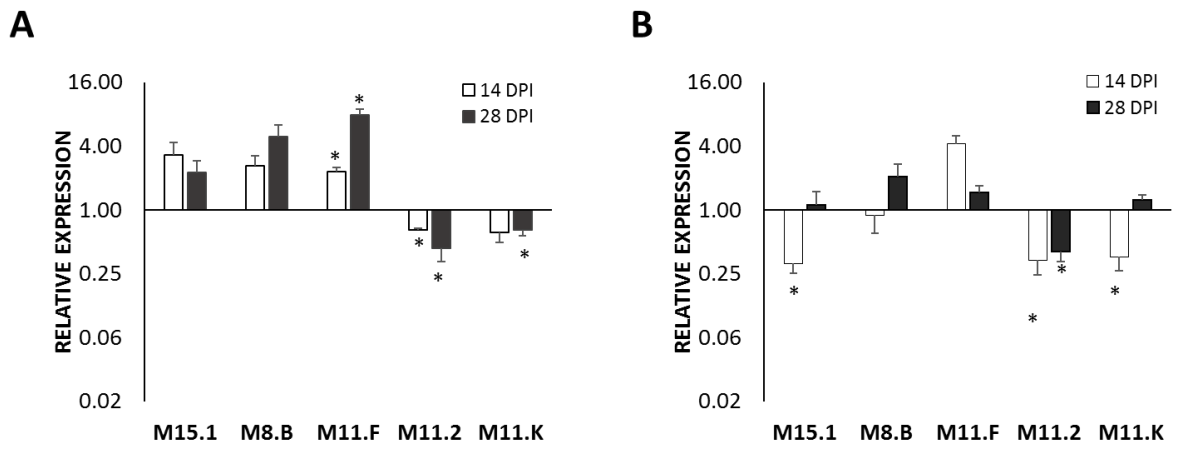

Figure 2-14: Relative expression of myosin genes measured in SACMV-challenged/VIGS vector relative to vector only

Expression of myosin genes was measured using relative RT-qPCR in *SACMV-challenged* plants previously inoculated with VIGS vector, relative to vector-only plants. [**A**] SACMV-challenged/SACMV VIGS vector [**B**] SACMV-challenged/TRV VIGS vector. GAPDH was used as a reference. Values represent the median of three independent replicates each with 3 plants per treatment and bars indicate SEM. T-test was used for statistical analysis p value ≤ 0.05 and the asterisks denote significant changes.

2.3.5 Myosin expression in SACMV-challenged/NO-VIGS N. benthamiana, non-treated

The expression of the five myosins was measured in SACMV-challenged/NO-VIGS to assess expression of myosins induced by SACMV infection without VIGS vectors or constructs present. At 14 dpi, expression of all the five myosins were not statistically different in SACMV-challenged/NO-VIGS plants with comparison to mock inoculated plants and at 28 dpi, expression of M11.F myosins was upregulated 2-fold (p value = 0.02) whilst no significant change was observed for the other four myosins (figure 2-15a; appendix A1.2.5).

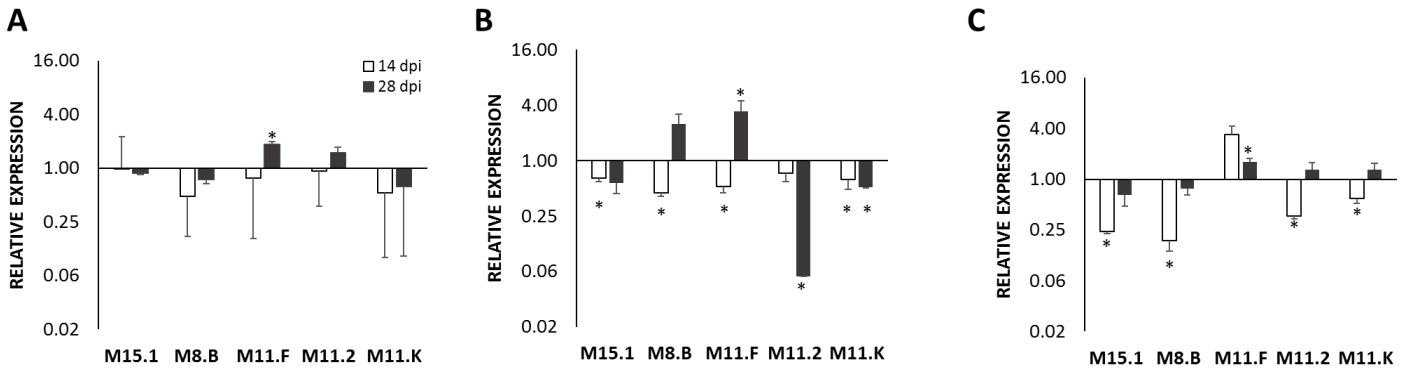

Figure 2-15: Relative expression of myosin in SACMV-challenged/NO-VIGS

Expression of myosin genes was measured using relative RT-qPCR in "*SACMV infected"* plants and is reported relative to [**A**] Mock, [**B**] SACMV-VIGS vector and [**C**] TRV-VIGS vector. GAPDH was used as a reference. Values represent the median of three independent replicates each with 3 plants per treatment and bars indicate SEM. T-test was used for statistical analysis p value ≤ 0.05 and the asterisks denotes significant changes

Because the expression of SACMV-challenged/VIGS vector was reported relative to the expression in vector only, for comparative purposes, the expression of myosin in SACMV-challenged/NO-VIGS was detected relative to expression of myosin in SACMV and TRV-VIGS vector-only (figure 2-15b, c; appendix A1.2.6). Relative to SACMV-VIGS vector, at 14 dpi expression of M11.2 and M11.K myosin was not significantly altered whilst expression of M15.1 myosin was 1.5-fold less, M8.B and M11.F myosins 2-fold less and expression. At 28 dpi, expression of myosin was 20-fold lower for M11.2 and 2-fold for M11.K whilst expression of M15.1, M8.B and M11.F remained unchanged (figure 2-15b).

Relative to TRV-VIGS vector at 14 dpi, expression of myosin in SACMV-challenged/NO-VIGS was not significantly altered for M11.F myosin whilst expression of M15.1 myosin was 4-fold lower, M8.B 5-fold lower and M11.2 myosins 3-fold less and expression of M11.K myosins 2-fold less. At 28 dpi, expression of M11.F was upregulated 1.5-fold (figure 2-15c) whilst expression of other myosins remained unchanged.

2.3.6 SACMV viral load in SACMV-challenged plants

To measure the impact of downregulation of the five selected myosins on viral accumulation, viral load was measured at 14 and 28 days in SACMV-challenged plants (table 2-5). Viral load is

reported as the value of SACMV-A molecules relative to the internal control, GAPDH. Unless stated otherwise, the comparison of viral load was done relative SACMV-challenged/SACMV-VIGS vector and SACMV-challenged/TRV-VIGS vector (figure 2-13; appendix 0).

At 14 dpi, viral load in SACMV-challenged/SACMV-VIGS vector and control experiment, the expression of myosin was successfully silenced at both 14 and 28 dpi for SACMV-challenged/SACMV::M11.F plants at both 14 and 28 dpi (figure 2-13a). At 14 dpi, viral load in SACMV-challenged/SACMV::M11.F plants was 13-fold higher than SACMV-challenged/SACMV-VIGS vector and at 28 dpi, viral load in SACMV-challenged/SACMV::M11.F plants was 3-fold higher.

Expression of myosins in the other SACMV-challenged/SACMV::myosin plants was not suppressed (figure 2-13a) however viral load at 14 dpi was higher for SACMV-challenged/SACMV::M15.1 plants (48-fold) and viral load in SACMV-challenged/SACMV::M8.B, SACMV-challenged/SACMV::M11.2 plants and SACMV-challenged/SACMV::M11.K plants was not statistically different (figure 2-16a). At 28 dpi, SACMV-A accumulation in SACMV-challenged/SACMV::myosin plants was 6-fold higher for SACMV-challenged/SACMV::M15.1, 3-fold higher for SACMV-challenged/SACMV::M11.K, 5-fold higher for SACMV-challenged/SACMV::M11.2 plants and 5-fold lower for SACMV-challenged/SACMV::M8.B plants (figure 2-16a).

In SACMV-challenged/TRV::myosin, there was no significant silencing detected for the five myosins at 14 dpi (figure 2-13b) and viral was not statistically different SACMV-challenged/TRV::myosin plants when compared to SACMV-challenged/TRV-VIGS vector (figure 2-16b). At 28 dpi, the expression of myosin was successfully suppressed for myosin M11.F and M11.2 in SACMV-challenged/TRV::M11.F plants and SACMV-challenged/TRV::M11.K plants (figure 2-13b) and viral load was 15-fold lower in SACMV-challenged/TRV::M11.F plants and not significantly different in SACMV-challenged/TRV::M11.K. Viral load was 6-fold lower in SACMV-challenged/TRV::M11.2 plants and not significantly different for SACMV-challenged/TRV::15.1 and SACMV-challenged/TRV::M8.B plants (figure 2-16b).

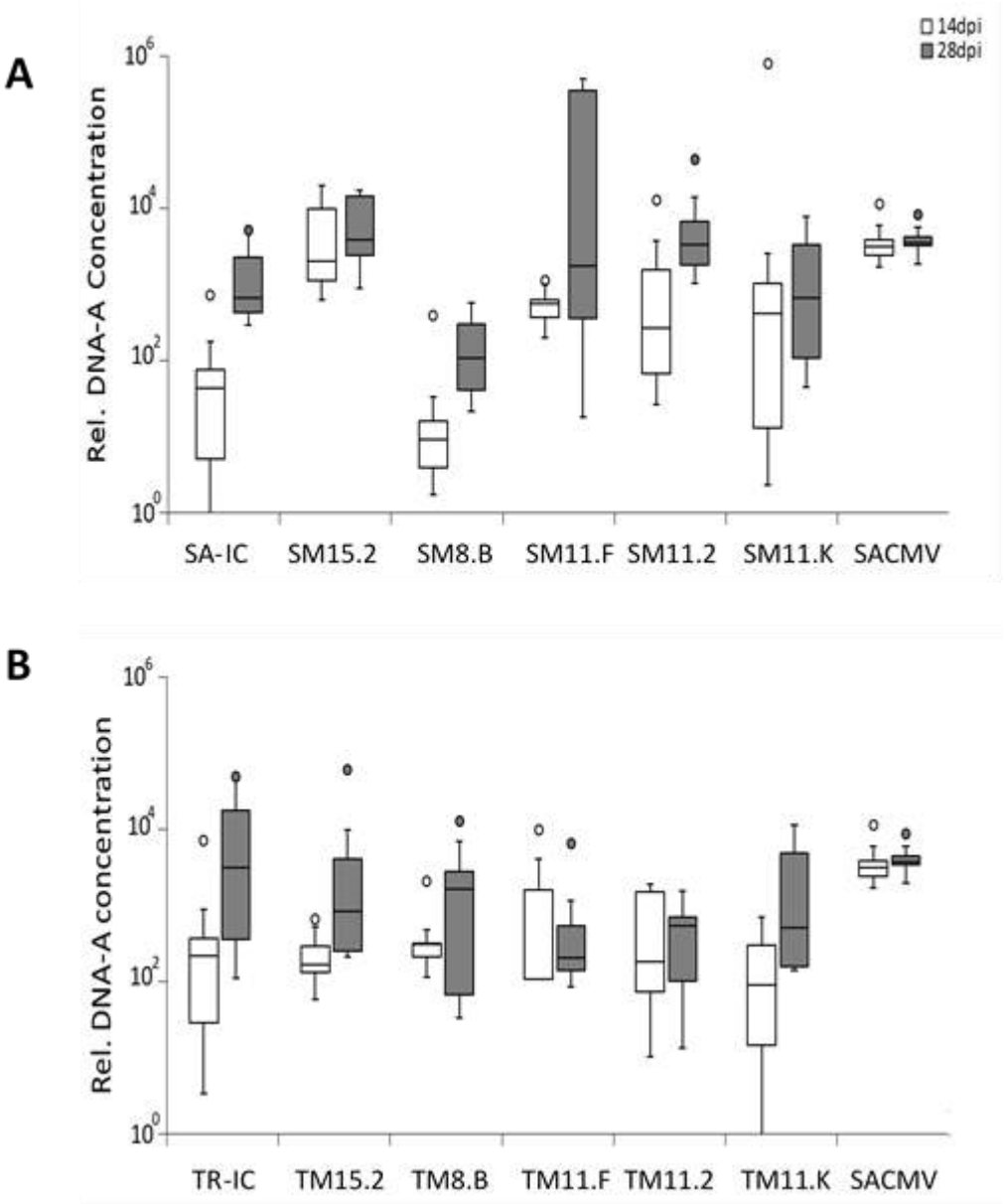

Figure 2-16: SACMV-A viral accumulation at 14 and 28 days post inoculation (dpi).

Relative viral accumulation was measured using (qPCR) to compare the accumulation of DNA-A component from SACMV-challenged *N. benthamiana* that were pre-inoculated with SACMV-VIGS vector (SA-IC) and SACMV::myosin (SM) [**A**] and TRV-VIGS vector (TR-IC) and TRV::myosin (TM) [**B**]. Viral accumulation is reported by measuring DNA-A relative to GAPDH internal control at 14 and 28 dpi for *N. benthamiana.* The ends of the whisker are set at 1.5*IQR above the third quartile and 1.5*IQR below the first quartile. The midline represents the median value of three independent replicates

Comparing the viral accumulation in SACMV-challenged/SACMV::myosin plants to SACMV-challenged/TRV::myosin plants, a 2-way ANOVA revealed that at both time points, there were no statistical differences between the viral load accumulated (appendix A1.3.3). At 28 dpi, however, there was statistical difference in viral load between the VIGS constructs used (*p* value 0.01), thus viral load was compared in plants silenced by the VIGS constructs, targeting the same myosin. There was no significant difference between SACMV-challenged/SACMV or TRV-VIGS vectors only, at both 14 and 28 dpi (appendix A1.2.8). At 14 dpi, the viral load in SACMV-challenged/SACMV::M15.1 plants was 12-fold higher in comparison to SACMV-challenged/TRV::M15.1 plants and the viral load of SACMV-challenged/SACMV::M8.B plants was 33-fold lower than SACMV-challenged/TRV::M8.B. At 28 dpi viral load in SACMV-challenged/SACMV::M8.B plants was 14-fold lower to SACMV-challenged/SACMV::M8.B plants, and the viral load of SACMV-challenged/SACMV::M11.F plants and SACMV-challenged/SACMV::M11.2 plants was higher than viral load of SACMV-challenged/TRV::M11.F plants (9-fold) and SACMV-challenged/TRV::M11.2 plants (6-fold) respectively.

Viral load at 28 dpi was compared to viral load at 14 dpi, to measure the fold increase over the two time points. There was a significant increase of SACMV-A accumulation in SACMV-challenged/SACMV::myosin (16-fold), SACMV-challenged/SACMV::M8.B plants (13-fold), SACMV-challenged/SACMV::M11.F plants (3-fold), SACMV-challenged/TRV::myosin (86-fold) and SACMV-challenged/TRV::M11.K plants (6-fold). No significant increase was observed for the other plants (appendix A1.2.9).

2.3.7 DNA-A/DNA-B ratio of SACMV-challenged plants

The ratio of SACMV DNA-A/DNA-B was measured to assess the extent at which the myosin VIGS constructs would affect the accumulation of SACMV-B relative to SACMV-A (figure 2-17). DNA-A/DNA-B ratio from SACMV-challenged/VIGS::myosin plants was compared to SACMV-challenged/VIGS vector. In plants inoculated with SACMV-challenged/SACMV::myosin, at 14 dpi the ratio of DNA-A/DNA-B ratio was 36 % lower for SACMV-challenged/SACMV::M11.2 plants compared to SACMV-challenged/SACMV::myosin and no difference was observed for the other SACMV-challenged/VIGS::myosin plants (figure 2-17). At 28 dpi, no significant differences were

noted. In plants inoculated with TRV-VIGS construct, there was no statistically significant differences noted at 14 dpi but at 28 dpi, the DNA-A/DNA-B ratio in all SACMV-challenged/TRV::myosin plants was 13 – 29 % lower than the control (figure 2-17; appendix A1.2.10).

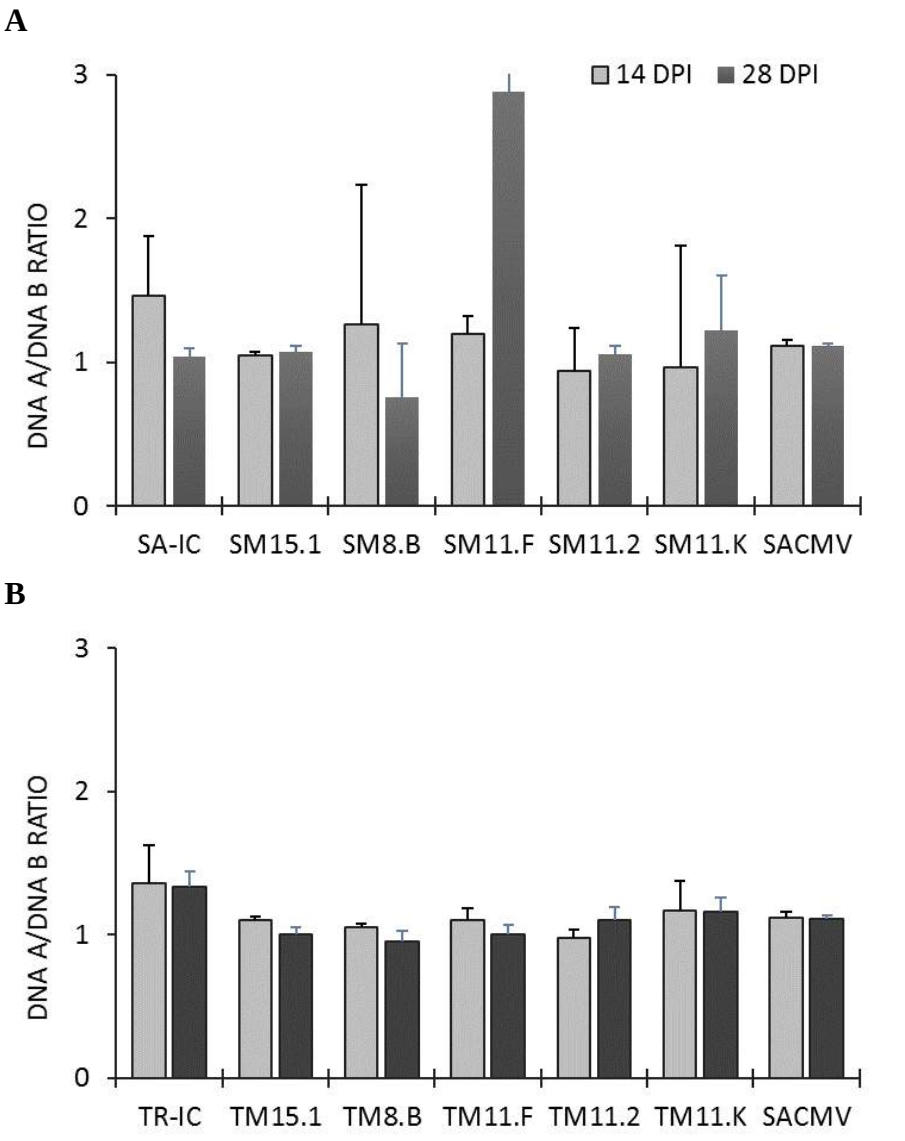

Figure 2-17: DNA-A/DNA-B ratios were measured at 14 and 28 days post inoculation (dpi) in *N. benthamiana* infected with SACMV-VIGS construct [**A**] **and TRV-VIGS constructs** [**B**]

The levels of DNA-A to DNA-B were measured by qPCR from SACMV-challenged/SACMV-VIGS vector (SA-IC) and SACMV-challenged/SACMV::myosin (SM) [**A**] and SACMV-challenged/TRV-VIGS vector (TR-IC) and SACMV-challenged/TRV::myosin (TM) [**B**]. DNA-A and B were related the levels of GAPDH as internal control. Values represent the median of three independent replicates each with 3 plants per treatment and bars indicate SEM.

2.3.8 Leaf symptoms and plant height evaluation of SACMV-challenged plants

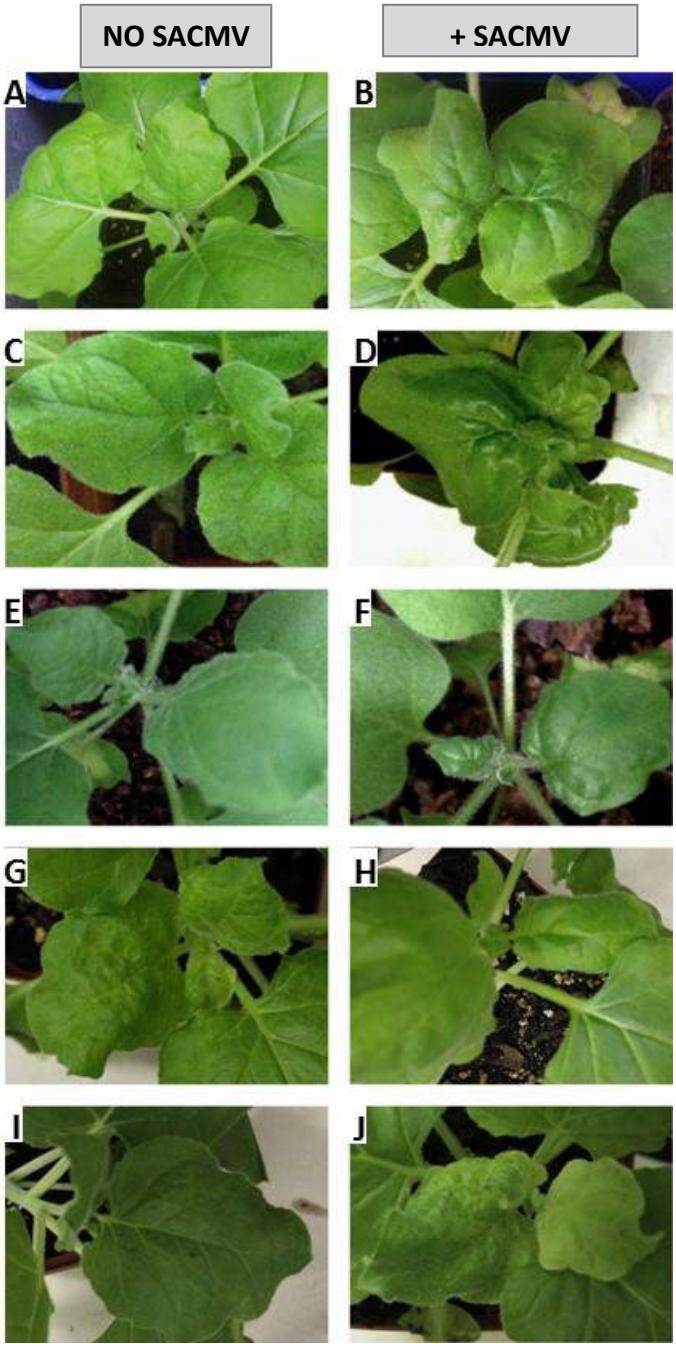

Figure 2-18: Symptoms on *N. benthamiana* leaves inoculated with SACMV-VIGS constructs at 14 dpi in SACMV-challenged and SACMV unchallenged plants

[**A**], [**B**] SACMV-VIGS vector; [**C**], [**D**] SACMV::M15.1 plants; [**E**], [**F**] SACMV::M8.B plants; [**G**], [**H**] SACMV::M11.F plants; [**I**], [**J**] SACMV::M11.2 plants

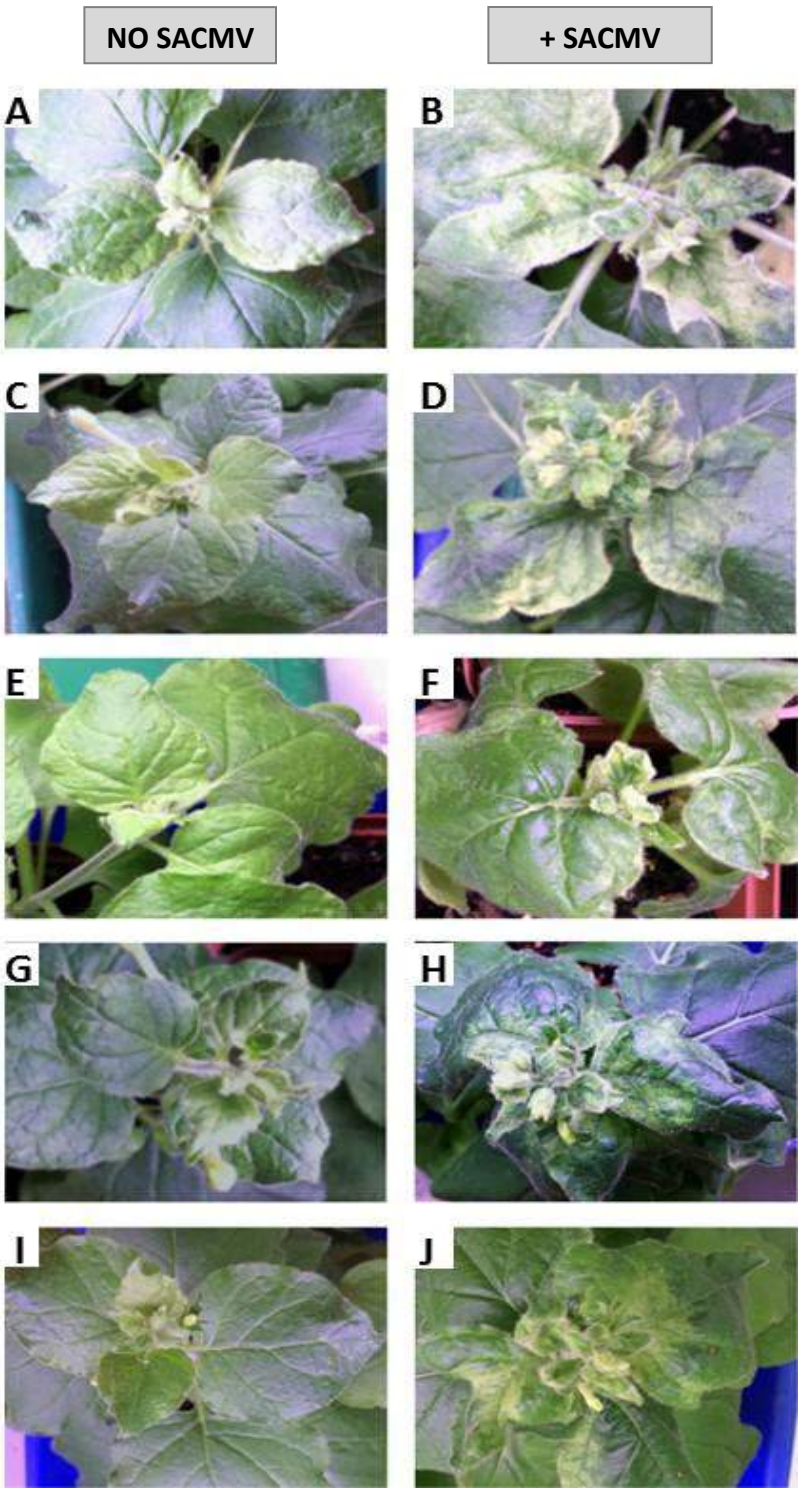

Figure 2-19: Symptoms on *N. benthamiana* leaves inoculated with SACMV-VIGS constructs at 28 dpi in SACMV-challenged and SACMV unchallenged plants

[**A**], [**B**] SACMV-VIGS vector; [**C**], [**D**] SACMV::M15.1 plants; [**E**], [**F**] SACMV::M8.B plants; [**G**], [**H**] SACMV::M11.F plants; [**I**], [**J**] SACMV::M11.2 plants.

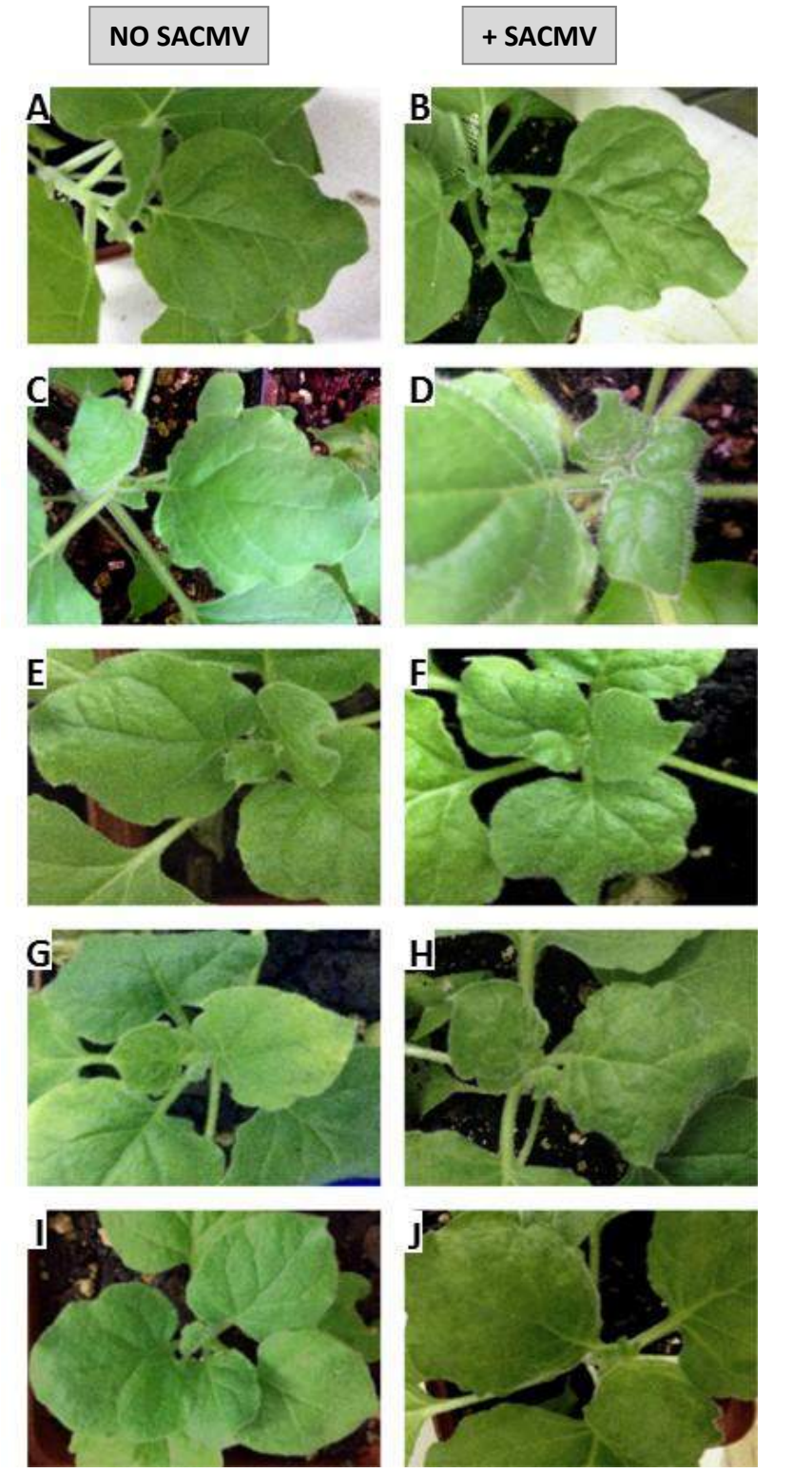

Figure 2-20: Symptoms on *N. benthamiana* leaves inoculated with TRV-VIGS constructs at 14 dpi in SACMV-challenged and SACMV unchallenged plants

[**A**], [**B**] TRV-VIGS vector; [**C**], [**D**] TRV::M15.1 plants; [**E**], [**F**] TRV::M8.B plants; [**G**], [**H**] TRV::M11.F plants; [**I**], [**J**] TRV::M11.2 plants.

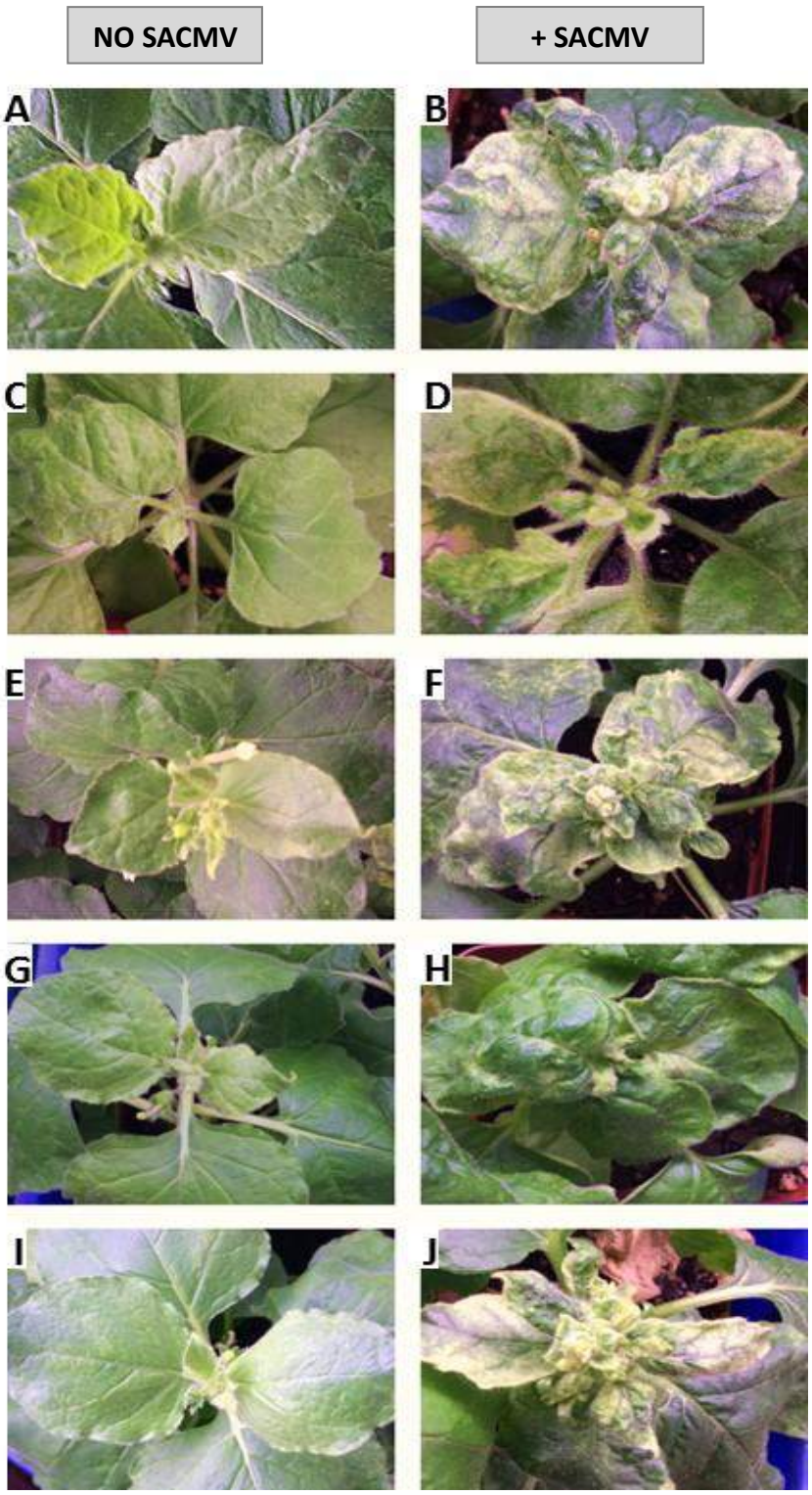

Figure 2-21: Symptoms on *N. benthamiana* leaves inoculated with TRV-VIGS constructs at 28 dpi in SACMV-challenged and SACMV unchallenged plants

[**A**], [**B**] TRV-VIGS vector; [**C**], [**D**] TRV::M15.1 plants; [**E**], [**F**] TRV::M8.B plants; [**G**], [**H**] TRV::M11.F plants; [**I**], [**J**] TRV::M11.2 plants.

Typical geminiviral symptom such as curling, blistering and leaf area reduction was observed with varying degree in all infected plants (figure 2-18-figure 2-21). Plants were scored according to the 0 to 5 scale, with 0 indicating no symptoms and 5 severe leaf reduction (Allie and Rey 2013). Plant agroinfiltrated with VIGS constructs showed minimal to no symptoms. SACMV::M15.1 plants agroinfiltrated plants had a score of 2 with the rest of the plants scoring 1 or less and the SSS were not reported.

The SSS for SACMV-challenged/SACMV-VIGS plants revealed that at 14 dpi, SACMV-challenged/SACMV::M15.1 plants had a higher SSS (score 3) and SACMV-challenged/SACMV::M11.F plants infected plants had lower SSS (score 1.5) then the SACMV-challenged/SACMV-VIGS vector (score 2). The SSS of SACMV-challenged/SACMV::M8.B, SACMV-challenged/SACMV::M11.2 plants and SACMV-challenged/SACMV::M11.K plants weren't significantly different to SACMV-challenged/SACMV-VIGS vector. At 28 dpi, SACMV-challenged/SACMV::M8.B plants and SACMV-challenged/SACMV::M11.K plants had a lower SSS (score 3 for both vs score 5 for the control) whilst the SSS revealed no difference for SACMV-challenged/SACMV::M15.1, SACMV-challenged/SACMV::M11.F plants and SACMV-challenged/SACMV::M11.2 plants relative to SACMV-challenged/SACMV-VIGS vector (figure 2-22a; appendix A1.2.11).

In SACMV-challenged/TRV-VIGS plants, at 14 dpi, SSS in SACMV-challenged/TRV::M15.1, SACMV-challenged/TRV::M8.B plants and SACMV-challenged/TRV::M11.F plants were higher (score 3) than in of SACMV-challenged/TRV-VIGS vector (score 2). No difference was observed in SSS for SACMV-challenged/TRV::M11.2 and SACMV-challenged/TRV::M11.K plants compared to SACMV-challenged/TRV-VIGS vector. At 28 dpi, no difference in SSS was observed between SACMV-challenged/TRV VIGS-silenced myosin constructs and SACMV-challenged/TRV-VIGS vector (figure 2-22b; appendix A1.2.11).

To assess for the worsening of symptoms, often likened to an increase in infection, the SSS between the 2 time points were compared and for SACMV-challenged/SACMV VIGS-silenced myosin plants, there was a significant increase in symptoms from 14 dpi to 28 dpi for all the plants except for SACMV-challenged/SACMV::M11.K, where the increase in symptom was not significant (figure 2-22a). Comparing the scores between 14 and 28 dpi

for SACMV-challenge TRV-VIGS myosin silencing plants, there was a significant increase in symptoms from 14 dpi to 28 dpi, across all plants (figure 2-22b; appendix A1.2.12).

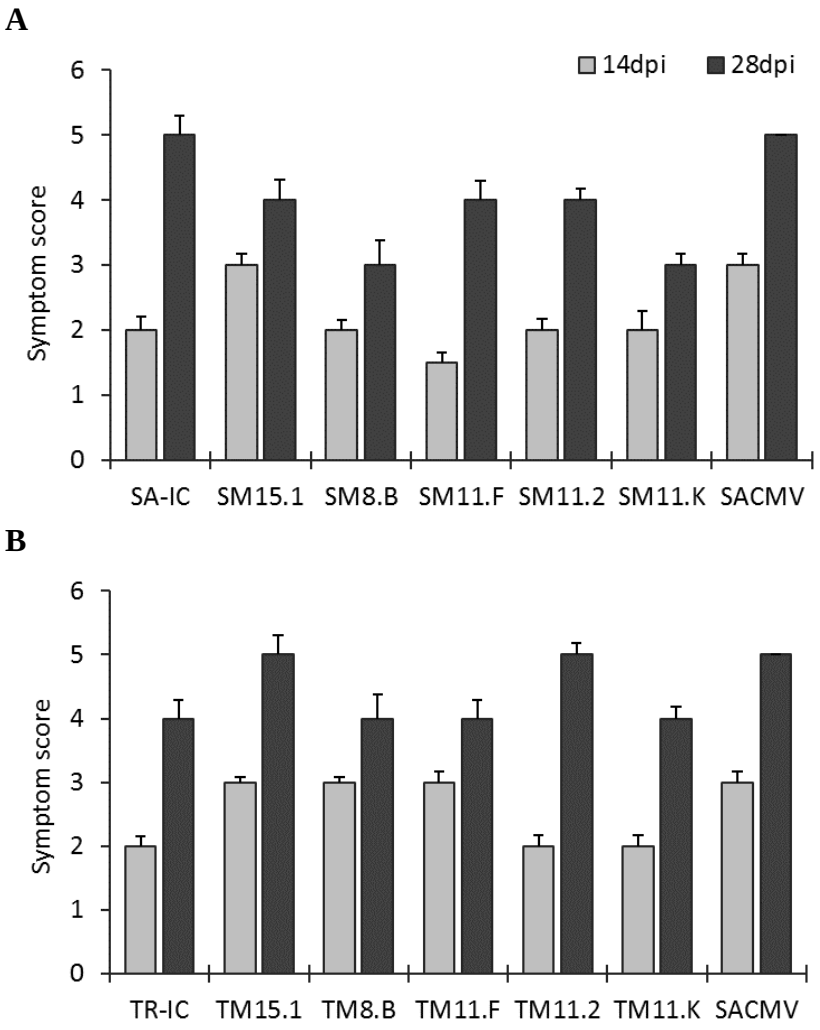

Figure 2-22: SSS measured at 14 and 28 days post inoculation (dpi) in *N. benthamiana* infected with SACMV-VIGS construct [**A**] **and TRV-VIGS constructs** [**B**]

Symptomatic leaves of infected plants were scored at 14 and 28 dpi according to the 0 to 5 SSS, with 0 being the least symptomatic or uninfected and 5 being the most infected. [**A**] SACMV-challenged/SACMV::myosin (SM) and SACMV-challenged/SACMV-VIGS (SA-IC) and [**B**] TRV-SACMV-challenged/VIGS::myosin (TM) and SACMV-challenged/TRV-VIGS vector (TR-IC). The median value of three independent plants is plotted and the error bars represent the standard error of the mean.

Comparing the SSS in SACMV-challenged/SACMV::myosin plants to their corresponding SACMV-challenged/TRV::myosin plants, a 2-way ANOVA analysis revealed that on average,

SSS for SACMV-challenged/TRV-VIGS plants were higher compared to SACMV-challenged/SACMV-VIGS plants (2.57 vs 2.32 at 14 dpi and 3.81 *p* value 0.01 vs 4.17 at 28, *p* value 0.03; A1.3.4). A Pearson's correlation analysis revealed at 14 dpi, a significant positive correlation between DNA-A viral load and SSS for SACMV-challenged/SACMV::M8.B (0.64), a negative correlation between viral load and SSS for SACMV-challenged/TRV::M11.F plants (-0.68). At 28 dpi, there was a negative correlation between DNA viral load and SSS for SACMV-challenged/SACMV::M15.1 plants (-0.73) and SACMV-challenged/SACMV::M11.F plants (0.85). There were no significant correlations between and SSS for SACMV-challenged/TRV-VIGS (appendix A1.4.1).

Stunting is a known symptom that occurs with geminivirus infection, and the height of SACMV-challenged plants was measured to assess whether the presence of myosin VIGS constructs affected plant height. The height of SACMV-challenged/SACMV-VIGS vector plants at 14 dpi was not different to SACMV-challenged/SACMV::myosin, except for SACMV-challenged/SACMV::M8.B plants that was on average shorter. By 28 dpi however, plant height of SACMV-challenged/SACMV::M8.B plants was not different to SACMV-challenged/ SACMV-VIGS vector plants, while SACMV-challenged/SACMV::M15.1, SACMV-challenged/SACMV::M11.F, SACMV-challenged/SACMV::M11.2 plants and SACMV-challenged/SACMV::M11.K plants all grew taller (figure 2-23a; appendix A1.2.13). With SACMV-challenged/TRV-VIGS, at 14 dpi SACMV-challenged/TRV::M15.1 plants grew taller than the SACMV-challenged/TRV-VIGS, and at 28 dpi all SACMV-challenged/TRV::myosin grew taller than SACMV-challenged/TRV-VIGS vector plants and there was no statistical different in height between SACMV-challenged/TRV-VIGS vector and the other SACMV-challenged/TRV::myosin (figure 2-23b). At 28 dpi, all SACMV-challenged/TRV::myosin plants grew taller than SACMV-challenged/TRV-VIGS vector (figure 2-23b; appendix A1.2.13).

All the SACMV-challenged plants grew significantly at 28 dpi, from 14 dpi (A1.2.14). A 2-way ANOVA study (appendix A1.3.5) revealed that at 14 and 28 dpi, infected TRV-VIGS plants were shorter than SACMV-VIGS plants (4.50 vs 4.86 at 14 dpi and 9.69 vs 13.56 at 28 dpi. *p* value 0.00). A Pearson's correlation analysis revealed, a negative correlation between DNA-A viral load and height in at 14 dpi for SACMV-challenged/SACMV::M15.1 plants (-0.63), SACMV-challenged/SACMV::M8.B plants (-1) , SACMV-challenged/SACMV::M11.F (-0.83) and SACMV-challenged/SACMV::M11.2 plants (-0.61). At 28 dpi, there was a negative

correlation between SACMV-challenged/SACMV-VIGS vector (-0.79) and SACMV-challenged/TRV::M8.B (-0.60). There was a positive correlation between SACMV-challenged/SACMV::M15.1 (0.83). No correlation was observed for the other samples (appendix A1.4.2).

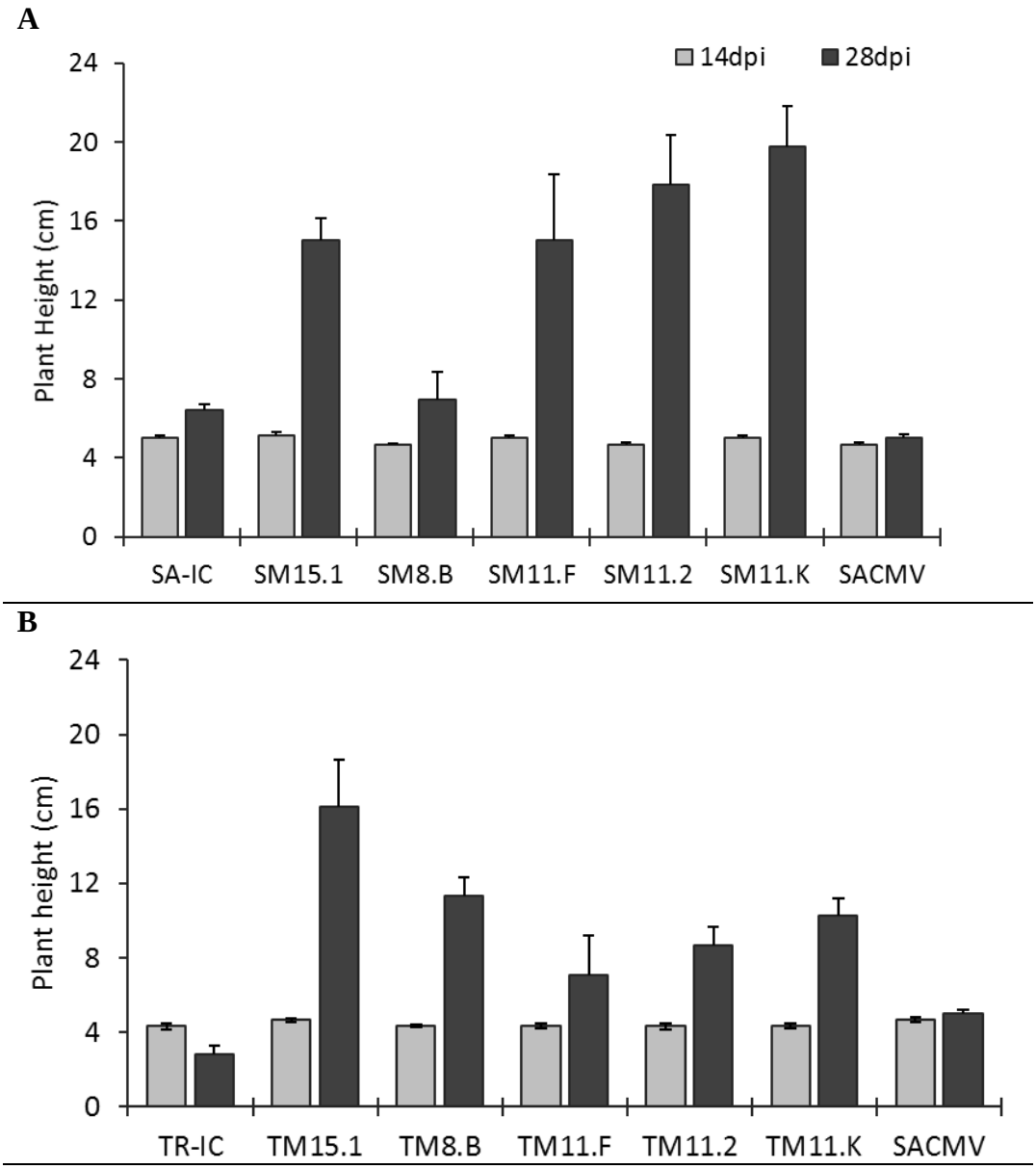

Figure 2-23: Plant height measured at 14 and 28 days post inoculation (dpi) in *N. benthamiana* infected with SACMV

The height of infected plant was measured at 14 and 28 dpi. [**A**] SACMV-challenged/SACMV::myosin (SM) and SACMV-challenged/SACMV-VIGS (SA-IC) and [**B**] TRV-SACMV-challenged/VIGS::myosin (TM) and SACMV-challenged/TRV-VIGS vector (TR-IC). The median values of three independent plants are plotted and the error bars represent the standard error of the mean.

2.3.9 SACMV infection in the absence of myosin silencing vectors compared with SACMV infection in the presence of myosin silencing vectors.

To assess whether the presence of the VIGS vectors during infection affected the proliferation of SACMV, the accumulation of DNA-A molecules of the SACMV-challenged/SACMV-VIGS vector and SACMV-challenged/TRV-VIGS vector plants was compared to that of SACMV-challenged/NO-VIGS plants. At 14 dpi, the accumulation of DNA-A viral molecules was lower in SACMV-challenged/SACMV-VIGS vector and SACMV-challenged/TRV-VIGS vector (about 200-fold lower for both) when compared to SACMV-challenged/NO-VIGS. At 28 dpi the difference between SACMV-challenged/NO-VIGS plants and SACMV-challenged/SACMV-VIGS vector or SACMV-challenged/TRV-VIGS vector decreased, with SACMV-challenged/SACMV-VIGS vector accumulating on average 17 times less SACMV-A molecules, and the difference of SACMV-A accumulated in the presence of TRV at 28 dpi was statistically insignificant (figure 2-16b). Viral load at 28 dpi was not statistically different to viral load at 14 dpi in SACMV-challenged/NO-VIGS, no VIGS vector (1.5-fold higher, *p* value 0.14) whilst for the SACMV-challenged/SACMV-VIGS vector and SACMV-challenged/TRV-VIGS vector, there was a significant increase from 14 dpi to 28 dpi (appendices 0 and A1.2.9).

The DNA-A/DNA-B ratio in SACMV-challenged/NO-VIGS revealed that the ratio between DNA-A/DNA-B was 1.12 at 14 dpi, and 1.11 at 28 dpi. At 14 dpi, this ratio was not different, statistically to DNA-A/DNA-B ratio in SACMV-challenged/SACMV-VIGS vector plants and SACMV-challenged/TRV-VIGS vector. At 28 dpi, there was no difference in ratio between DNA-A/DNA-B in SACMV-challenged/SACMV-VIGS vector whilst in SACMV-challenged/TRV-VIGS vector, the ratio was 17 % lower (figure 2-17; appendix A1.2.10).

The SSS of SACMV-challenged/NO-VIGS plants were higher than SACMV-challenged/TRV-VIGS vector plants at 14 dpi and not for SACMV-challenged/SACMV-VIGS vector. At 28 dpi, SSS in SACMV-challenged/NO-VIGS was significantly higher then SACMV-challenged/SACMV-VIGS vector and SACMV-challenged/TRV-VIGS vector plants. Similarly to the increase in SSS reported for SACMV-challenged/SACMV-VIGS vector and SACMV-challenged/TRV-VIGS vector at 28 dpi, in comparison to 14 dpi, a significant increase in SSS was observed at 28 dpi

in plants SACMV-challenged/NO-VIGS plants, when compared to 14 dpi (figure 2 – 19; appendices A1.2.11-A1.2.12).

At 14 dpi, SACMV-challenged/NO-VIGS plants were significantly taller than SACMV-challenged/TRV-VIGS vector plants, whilst no difference was observed with SACMV-challenged/SACMV-VIGS vector plants. At 28 dpi, SACMV-challenged/SACMV-VIGS vector plants were significantly taller than SACMV-challenged/NO-VIGS plants and there was no statistical difference in SACMV-challenged/TRV-VIGS vector plants height in comparison to SACMV-challenged/NO-VIGS. Comparing the height at 28 dpi to that at 14 dpi, there was a minimal but significant increase in plant height for SACMV-challenged/NO-VIGS (4.67 cm at 14 dpi to 5 cm at 28 dpi) and for SACMV-challenged/SACMV-VIGS vector plants, (5.03 cm at 14 dpi to 6.42 cm at 28 dpi) but not for SACMV-challenged/TRV-VIGS vector plants (figure 2-22; appendices A1.2.13, A1.2.14).

2.4 Discussion

Geminiviruses proliferate by hijacking the cell's replication mechanism to their own advantage to replicate their genomic DNA, transcribe their genes and translate their mRNA into protein (Hanley-Bowdoin et al. 2013). Proliferation would be incomplete without an efficient trafficking system and geminiviruses take advantage of the readily available cellular transport mechanism, to spread from a cell to another. Cytoskeletal proteins are involved in many processes and amongst others, intracellular organization, cell motility and organelles trafficking, and different members of the cytoskeleton have been found associated with plant virus movement (Heinlein 2016). With regards to plant viruses, there are reports suggesting the participation of either class VIII or class XI myosins or both in virus movement. The involvement of myosin in plant virus movement could also be through a partnership with the endomembrane system which interacts with vesicles associated with viral proteins and together move along the endoplasmic reticulum (ER) using the actomyosin network (Kumar et al. 2014). In this study we identified putative myosin homologs from the draft genome of *N. benthamiana* available on the Solgenomics platform. Results from myosin VIGS silencing experiments suggest a role for myosin NbXI-F (M11.F, DQ875136.1) and NbXI-K (M11.K, DQ875137.1) in SACMV infectivity in *N. benthamiana.* Reduction in myosin NbXI-F expression resulted in a decrease in SACMV viral load and although it didn't for the reduction in myosin NbXI-K expression, when viral load at 28 dpi was compared to viral load at 14 dpi, reduction in expression of NbXI-K and NbXI-F resulted in a lower viral increase than non-silenced plants.

2.4.1 Identification of N. benthamiana myosins

One of the main pitfalls of automated gene prediction from genomic and transcriptomics data is the inaccurate intron/exon prediction, which has been previously reported for myosins (Odronitz and Kollmar 2007; Mühlhausen and Kollmar 2013) and this poses a challenge for subsequent analysis like determining phylogenetic relationship between different members of a gene family. Based on the available genomic data from Solgenomics, 26 possible myosin transcripts were identified in *N. benthamiana* and 23 of them are recorded at CyMoBase (http://www.cymobase.org) (Mühlhausen and Kollmar 2013). Two of the 26 presumptive myosins, Niben101Scf04193g02006.1 and Niben101Scf04193g02004,

were excluded as they are found adjoining on the same scaffold (figure 2-4), raising the possibility that they could together encode for a single myosin. Phylogenetic analysis of the remaining 24 transcripts revealed seven class VIII myosins and 17 class XI (figure 2-5).

Myosins are highly conserved and in terms of percentage nucleotide sequence similarity and conservation of plant myosins is reported either relative to their motor domain or relative to their full sequence (Reddy and Day 2001). The high nucleotide sequence similarity observed between some plant myosins is believed to be due to single or multiple gene duplication event (Mühlhausen and Kollmar 2013; Wang et al. 2014). In Arabidopsis, the percentage similarity of full length class VIII myosins ranges from 50-83% and the motor domain 64-92% and the percentage similarity of full length class XI myosins in Arabidopsis ranges from 40-85% and the motor domain ranges from 61-91% (Reddy and Day 2001). In this study, the percentage identity search revealed ten pairs of myosins transcripts, whose nucleotides similarities were higher than 92% (table 2-6). Six of those pairs involved sequences that had less than 1000 aa, and were excluded from being considered "full length" sequence comparisons. The percentage identity of the remaining four pairs, Niben101Scf01922g10004.1 (1622 aa) and Niben101Scf11646g02010.1 (1367 aa), Niben101Scf03934g02009.1 (1181 aa) and Niben101Scf03263g04010 (1449 aa), Niben101Scf04172g02008.1 (1470 aa) and Niben101Scf09360g00019.1 (1513 aa) and Niben101Scf00611g02015.1 (1587 aa) and Niben101Scf02425g04005.1 (1545 aa), were well above 90% and given that their protein sequence length are longer than 1000 amino acids (table 2-7), these pairs could be considered for the full length comparison and the high percentage similarity between them supports the theory of gene duplication.

Gene duplication has been shown to be a reason for the high numbers of myosin members in plants (Wang et al. 2014). Class VIII myosins with smallest number of members, have a smaller range for nucleotides sequence similarity between the two classes as the similarity percentage within the group varies from 54-98 % (table 2-6). Class VIII myosins are further divided into two major subtypes, A and B and in Arabidopsis, each class has two members (Mühlhausen and Kollmar 2013). In *N. benthamiana,* we identified three members for subtype A and four for subtype B (figure 2-5). Within subtype A, there were no similarities observed between transcript Niben101Scf27876g00001.1 and Niben101Scf03595g00003.1, however they each shared a high percentage similarity with Niben101Scf01478g08021

(table 2-6), and based on their domain architecture, Niben101Scf27876g00001.1 appears truncated, containing only parts of the N-terminal domains typical of myosin VIII and Niben101Scf03595g00003.1 appears truncated with only part of the middle to C-terminal domains of myosins VIII (figure 2-6). This raises the possibility that both these transcripts are two truncated parts of a single transcript. If this were true, it would bring down the number of myosin class VIII subtype A to 2, which would be in line with previous reports in *N. benthamiana* bringing the number down of *N. benthamiana* myosin to the reported 23 (Mühlhausen and Kollmar 2013).

Eight myosin subtypes are found under class XI myosins, however in this study it is not clear from the phylogenetic tree which *N. benthamiana* genes are homologous to the available Arabidopsis genes, perhaps due to the truncated transcript sequences and missing domains observed (figure 2-6). As an example, myosin Niben101Scf11524g00010.1 shares no similarity to myosin Niben101Scf01538g01009.1 and according to their domain architecture, they have no domain in common (figure 2-4), however both these myosins share a high nt sequence similarity (92-93%) with Niben101Scf01302g05009 (table 2-6). Due to the possible missing sequences information for these myosins and other presumed truncated myosins (table 2-6), it is difficult to assign homology as well as to class them under the different myosin XI subtypes. Three other types of myosins have been described under class XI; headless derivative of myosin XI-K variant in Arabidopsis (Peremyslov et al. 2011), headless myosin XI-4 variant in maize (Wang et al. 2014) and long-tailed myosin XI-I in plants of the Poales order (Mühlhausen and Kollmar 2013). With the data at our disposal, we were unable to classify *N. benthamiana* myosins class XI under these categories either.

Amongst the plant myosins, At-XII has been identified as phylogenetically distant (Haraguchi et al. 2016), as seen in the phylogenetic tree (figure 2-5) they branch out on their own, away from other class XI myosins. Two sequences, Niben101Scf01380g01003.1 and Niben101Scf08669g00008.1 were identified as putative At-XII in *N. benthamiana*. Based on their sequence length and their predicted domain architecture, these two are shorter than their Arabidopsis homolog, AtXI-I which is about 1520 aa long, whilst Niben101Scf01380g01003.1 and Niben101Scf08669g00008.1 are 1074 and 1008 aa long respectively (table 2-7). The sequence of these two myosins can be said to be truncated, as their predicted domain architecture reveals that they either have a partial motor domain or

are missing established myosin XI domains (figure 2-6). Their similarity to one another being 78% suggests that these two sequences possibly represent two separate genes and therefore there are two At-XII homologues in *N. benthamiana*.

2.4.2 TRV-VIGS induces stronger silencing of myosins

Plant virus studies involving VIGS do not customarily use a VIGS vector derived from the same virus being studied for fear that the potential trait observed following the VIGS vector inoculation could be due to plant responses to the silencing vector. However in the case of many non-model crops, such as cassava, they are not susceptible to any of the known viruses used for VIGS vectors. For geminivirus studies in cassava, a SACMV-VIGS vector has been previously constructed for functional gene studies (Mwaba 2010). The only other cassava virus vector tested is the ACMV VIGS vector (Fofana et al. 2004), and more recently east african cassava mosaic virus (EACMV) (Beyene et al. 2017). A VIGS study was performed to knock out myosins in *N. benthamiana* and to ascertain the effect on SACMV infectivity. Comparisons between two different silencing vectors, namely SACMV and TRV, were performed in order to determine if the silencing vectors would yield different silencing results. Furthermore, TRV or SACMV VIGS silenced plants were challenged with SACMV, and possible effects of the two VIGS vectors on subsequent SACMV pathogenicity/infectivity evaluated.

In plants not challenged with SACMV, inoculation of SACMV-VIGS constructs and TRV-VIGS constructs resulted in minimal to no symptom (figure 2-18 - figure 2-21) however TRV-VIGS constructs induced a stronger reduction in myosin silencing compared to SACMV-VIGS constructs (figure 2-10; appendix A1.3.1). Several factors have been shown to determine the efficiency of a VIGS vector system and because TRV-VIGS system has been extensively used, its protocol has been optimised in terms of the length of the insert, the method of inoculation and the timing at which silencing was measured. Although this experiment was not carried out at the optimum temperature established for TRV-VIGS system which is 18-20◦C, the length of the insert, the method of inoculation and the timing at which silencing was measured (21 dpi post initiation of myosin silencing which is equivalent to 14 dpi in this study) was performed as suggested for TRV-VIGS (Senthil-Kumar and Mysore 2011b; Senthil-Kumar and Mysore 2014) and it is possible that those conditions whilst being optimum for

TRV-VIGS studies, aren't for SACMV-VIGS and the SACMV-VIGS system requires more optimization to improve its silencing efficiency.

Despite TRV-VIGS being more efficient at SACMV-VIGS, in both system, the efficacy and efficiency of both VIGS system was better at 14 dpi than at 28 dpi (figure 2-10). At 14 dpi, both SACMV-VIGS and TRV-VIGS silenced more myosins than at 28 but in both system, silencing was stronger at 14 than at 28 dpi. The reduction in silencing efficiency observed at 28 dpi for TRV VIGS system could be due to the TRV genome being targeted by the host's silencing machinery. DNA viruses have an advantage over RNA viruses for VIGS, because their genome is not a direct target of the host's post-transcriptional gene silencing (PTGS) machinery unlike RNA based virus vectors which can be eliminated from the host (Ruiz et al. 1998; Robertson 2004). Although unlike PVX-VIGS and TMV-VIGS which can be cleared from the host, (Ruiz et al. 1998; Hiriart et al. 2003), there is no record of TRV-VIGS being eliminated, it requires a booster application to be maintained in the plants over time (Senthil-Kumar and Mysore 2014) and it's possible that the decrease in silencing efficiency is due to a decrease in its genome accumulation in the plant. Given that SACMV-VIGS is a DNA virus, the decrease in efficiency of silencing for SACMV-VIGS is probably due to an increase in the VIGS vector "load" which results in an increase in the expression of RNA silencing suppressors encoded by the VIGS vector. An efficient VIGS vector must be able to suppress the host's transcriptional PTGS machinery, enough to allow for its genome to carry on proliferating and at the same time allow for expression of the gene of interest to be suppressed and with time an increase in silencing suppressors activity allows SACMV-VIGS vector to proliferate in the host but negatively impacts its ability to induce silencing.

2.4.3 SACMV challenge of N. benthamiana relieves silencing by SACMV-VIGS and TRV-VIGS constructs

Despite the silencing observed in SACMV-challenged/TRV::M11.K plants at 28 dpi, accumulation of DNA-A was not different to that in SACMV-challenged/TRV-VIGS vector (figure 2-16b). When viral load at 28 dpi was compared to viral load at 14 dpi, the fold increase in SACMV-challenged/TRV::M11.K was lower than SACMV-challenged/TRV-VIGS vector, indicating that reduction in M11.K expression slowed the spread of SACMV without affecting its replication. In *N. benthamiana* NbXI-K has been linked with organelles

movement, vesicle transport and movement of Golgi bodies (Avisar et al. 2008b; Avisar et al. 2012; Peremyslov et al. 2012) and members of the endomembrane system have been linked to movement of geminiviruses (Lewis and Lazarowitz 2010; Lozano-Durán et al. 2011). Besides its role in plants trafficking, NbXI-K has been linked to cell growth and expansion as well as gravitropism (Ojangu et al. 2007; Park and Nebenführ 2013; Ueda et al. 2015; Talts et al. 2016). The decrease in SACMV proliferation observed in plants with a reduced expression of M11.K suggests a role for the endomembrane system in SACMV movement. The decrease in SACMV proliferation over the two time points was however not mirrored with a decrease in viral load. Myosin XI-K is known to have redundant role with other myosins both in its involvement with endomembrane trafficking as well as in its role gravitropism and cell growth and expansion and it would be interesting to look into whether the lack of decrease in viral accumulation was masked by the redundancy in M11.K function by these other myosins.

Challenging *N. benthamiana* with SACMV affected the silencing efficacy and efficiency of each vector as TRV::myosin failed to induce any silencing at 14 dpi and SACMV-VIGS constructs resulted in downregulation of M11.F at 14 dpi. At 28 dpi TRV::myosin reduced the expression of M11.F and M11.K and SACMV::myosin reduced the expression of M11.F. Silencing of M11.F in SACMV::M11.F was not different to silencing SACMV-challenged/ SACMV::M11.F however silencing induced by TRV::M11.F and TRV::M11.K was improved upon the introduction of SACMV.

Although the silencing of M11.F by TRV-silencing construct and SACMV-silencing construct was not affected by the presence of SACMV, this isn't true for the other myosins that failed to be silenced in the presence of SACMV. The reversal of silencing induced by the TRV-VIGS system was unexpected as functional genomic studies that combined the use of TRV-VIGS and geminiviruses infection have shown that co-infection of TRV-VIGS constructs and tomato yellow leaf curl Sardinia virus (TYLCSV) doesn't affect the silencing induced by TRV (Luna et al. 2006; Lozano-Durán et al. 2011; Czosnek et al. 2013). The reversal of silencing by SACMV-VIGS in the presence of SACMV however was expected as co-infection of SACMV VIGS vector with wild type SACMV in our laboratory has previously been reported to reverse downregulation of the magnesium chelatase gene (*su*-gene) induced by SACMV VIGS in *N. benthamiana* (figure 2-24; Mwaba 2010).

Silencing induced by VIGS can be uneven or patchy (Senthil-Kumar and Mysore 2011a), and the resulting RNA pool used for detection of myosin expression by qPCR has a mixture of both silenced and non-silenced tissue, which can affect the efficiency of silencing. Unlike silencing in *su-gene* expression which can be visually evaluated, silencing of myosin doesn't result in visual cues, and it is difficult to know if the lack of silencing detected was due to a complete loss in silencing or an increase in unevenness of myosin suppression.

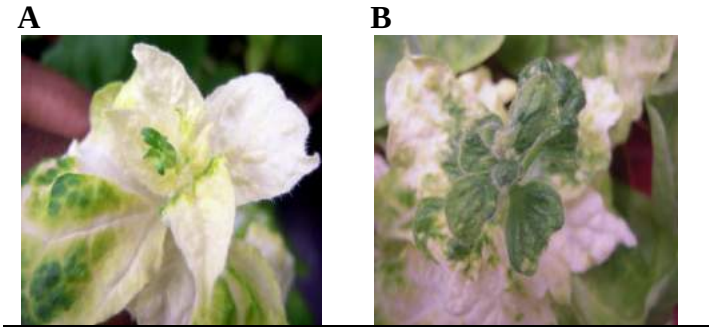

Figure 2-24: Silencing of *su*-gene from *N. benthamiana*
a. SACMV-VIGS construct *su*; **b.** SACMV-A::*su* infected *N. benthamiana* with delayed SACMV inoculation at 7 dpi (Mwaba 2010)

There reversal of silencing by SACMV introduction could be to the effect that the virus on its own, or in partnership with the VIGS construct has on the expression of the gene being investigated. Loss of silencing has been suggested to be due to in-planta partial or full deletion of the insert (Senthil-Kumar and Mysore 2011a; Senthil-Kumar and Mysore 2014) and it is possible that the interaction of SACMV with either TRV-VIGS constructs and SACMV-VIGS constructs resulted in loss of the silencing insert. Furthermore the delayed introduction of SACMV brings with it the expression of SACMV encoded suppressors of RNA silencing such as the Transactivating protein (TrAP or AC2) and AC4 which work in synergy to supress RNA silencing for the benefit of the invading challenger (Nawaz-ul-rehman and Fauquet 2009) but with the consequence of negatively affecting silencing induced by the VIGS vectors. Although SACMV-VIGS vector is derived from SACMV, it accumulates at lower level than wildtype SACMV (Mwaba 2010), therefore the expression of silencing suppressors encoded by SACMV-VIGS vector and constructs is lower as well as its capacity to supress RNA-silencing.

Understanding the mechanism behind the reversal of silencing by SACMV-challenge would further explain whether VIGS silencing of M11.F in the presence of SACMV was preserved due to its involvement in SACMV pathogenicity. The expression of M11.F was upregulated by SACMV-challenge in *N. benthamiana* (figure 2-15) and the expression of the other myosins were not and M11.F is the only myosin that was positively silenced by both SACMV::myosin and TRV::myosin.

2.4.4 2.6.3 Downregulation of NbXI-F and NbX-K and its effect on SACMV pathogenicity

In this study, suppression of M11.F expression by TRV-VIGS at 28 dpi led to a decrease in SACMV-A accumulation however the suppression of M11.F expression by SACMV-VIGS at 14 and 28 dpi did not and resulted in an increased viral accumulation (figure 2-16a). There was no significant increase in viral load at 28 dpi, from viral at 14 dpi and fold change in viral load over the two time points was lower for SACMV-challenged/TRV::M11.F than for SACMV-challenged/TRV-VIGS, suggesting that virus proliferation in SACMV-challenged/TRV::M11.F was impeded. These results together with the fact that expression of M11.F in SACMV-challenged/NO-VIGS was upregulated at 28 dpi provide strong evidence that *NbXI-F* is involved in SACMV responses in *N. benthamiana*.

Myosin NbXI-F have been shown to bind to chloroplasts and stromules and are believed to aid in their cellular movement (Sattarzadeh et al. 2009). Stromules or stroma filled tubules are extension of plastidial membrane allowing an increase in the surface area of plastids. Formation of stromules can be induced by sucrose and glucose, salicylic acid (SA) and reactive oxygen species like hydrogen peroxide (H_20_2) but not nitric oxide (NO) (Schattat and Klösgen 2011; Brunkard et al. 2015; Caplan et al. 2015). During plant defence responses, stromules extend to the nucleus and they have been shown to transport pro-defence proteins and signalling molecules from the chloroplast during defence responses to TMV (Caplan et al. 2015; Ho and Theg 2016). In Arabidopsis, the geminivirus abutilon mosaic virus (AbMV) induces stromules formation, which could provide a way along which viral particles travel through the plasmodesmata to neighbouring cells (Krenz et al. 2012). Inhibition of myosin activity has been shown to interfere with stromules formation (Natesan et al. 2009) and interfering with expression of M11.F using a VIGS approach, could therefore affect the

stability of the stromule network and should SACMV employ stromules as a mean of transport like it has been suggested of AbMV, SACMV movement would be consequently disturbed.

2.4.5 SACMV infectivity in the presence of TRV-VIGS vector and SACMV-VIGS vector

Unlike silencing of M11.F by TRV::M11.F, silencing of M11.F induced by SACMV::M11.F did not result in a decreased viral load at either 14 and 28 dpi. At both time points, viral load in SACMV-challenged/SACMV::M11.F was higher, although the fold increase at 28 dpi was lower for SACMV-challenged/SACMV::M11.F than SACMV-challenged/SACMV:::M11.F.

At 14 dpi, SACMV-challenged/SACMV-VIGS vector and SACMV-challenged/TRV-VIGS both accumulated less virus than SACMV-challenged/NO-VIGS, suggesting that the presence of both SACMV-VIGS vector and TRV-VIGS vector delayed SACMV infection at 14 dpi. By 28 dpi there was no difference between the virus accumulated by SACMV-challenged/TRV-VIGS vector and SACMV-challenged/NO-VIGS. However SACMV-challenged/SACMV-VIGS vector plants accumulated significantly less virus comparatively to SACMV-challenged/NO-VIGS and SACMV-challenged/ SACMV-VIGS vector. Although the presence of both VIGS vectors seemed to have initially an impact on viral accumulation, by 28 dpi, SACMV-challenged/TRV::myosin had “normalised” whilst SACMV-challenged/SACMV-VIGS vector had not. The higher viral load observed in SACMV-challenged/SACMV::M11.F relative to SACMV-challenged/SACMV-VIGS vector plants could be due to the low virus titre accumulated by the latter which masked any potential effects of the reduction of M11.F expression. As mentioned before, VIGS-based plant virus studies use a VIGS vector that is different to the virus under investigation for fear that the resulting phenotype could be as a result of plant responses to two related viruses. Cross protection non RNA-silencing based plant response to infection by two closely related viruses where the weaker variant virus that infects the host first, protects the host from infection by a more virulent challenger (Ziebell and Carr 2010; Zhang and Qu 2016). Given both SACMV-challenged/SACMV-VIGS vector and SACMV-challenged/TRV-VIGS vector and that TRV and SACMV are not related excludes cross protection as the reason for the delayed infection.

We propose a model where upon perception of the invading VIGS vector, the host triggers RNA silencing as counter attack, kept in check by the suppressor of RNA silencing that are expressed by the VIGS vector, AC2 and AC4 (Vanitharani et al. 2004) for SACMV-VIGS vector and protein 29K MP and 16K for TRV-VIGS vector (Deng et al. 2013) allowing for the VIGS vectors to replicate and move. When plants are challenged with SACMV seven days later, the host is in a "primed state" with the RNA silencing on the watch, ready to counter attack any invading pathogen. For TRV-VIGS vector plants, given that there is no sequence similarity with SACMV, the host RNA machinery is activated but not specifically primed for SACMV-A, resulting in a delayed infection that eventually normalises. A delay in TYLCSV infection has been previously observed in a study where TYLCSV was combined with TRV VIGS (Luna et al. 2006; Lozano-Durán et al. 2011). For SACMV-VIGS vector plants, given its similarity to SACMV, the host is primed against the invading virus, resulting in the presumed resistance observed at 14 and 28 dpi. Possibly with the progression of infection, the viral silencing suppressor eventually gains the upper hand over the host' PTGS. The downside to suppression of the host PTGS by the increase in SACMV accumulation is the eventual repression of VIGS.

2.4.6 Behaviour of SACMV in the presence of SACMV-VIGS and TRV-VIGS

According to this model, both TRV-VIGS vector and SACMV-VIGS vector presence initially interfere with the proliferation of SACMV. We sought to investigate the nature of SACMV infectivity in plants inoculated with SACMV-VIGS vector, TRV-VIGS vector and untreated plants.

A comparison over the viral load accumulated revealed that at 28 dpi, plants infected with three out of the five VIGS constructs accumulated higher viral load for TRV-VIGS than SACMV VIGS. this trend is similar to the previous comparison of SACMV-challenged plants infected by the vectors only. These results fit our model as at the early time point 14 dpi, there is no difference in viral load accumulation as viral load accumulation in both TRV-VIGS and SACMV-VIGS is hampered and at 28 dpi, accumulation of SACMV-A in SACMV-VIGS is still lower, but isn't for TRV-VIGS and hence the observed difference.

The DNA-A/DNA-B ratio in the plants inoculated with the different VIGS systems was investigated, to determine how the DNA-A/DNA-B ratio in the plants inoculated with VIGS

vectors and constructs varied from that of SACMV. The relationship between DNA-A and B of CMV has not yet been established, and the meaning of a deviation between this ratio is at this point unknown. The relationship between SACMV-A and B here however shows that with a ratio of 1.11, there is not much different in the accumulation of DNA-A in comparison to DNA-B at both time points, in SACMV-challenged *N. benthamiana*.

A one factor ANOVA analysis revealed that the DNA-A/DNA-B ratio of SACMV-challenged/NO-VIGS plants was not different for SACMV-challenged/SACMV-VIGS plants at 14 and 28 dpi. Whilst there was no difference in DNA-A/DNA-B ratio at 14 dpi for SACMV-challenged/TRV-VIGS plants, there was at 28 dpi. A plausible explanation to the effect that TRV-VIGS vector has on DNA-A/DNA-B ratio comparative to SACMV-challenged/NO-VIGS based on our proposed model, where inoculation of the VIGS vector primes the host RNA-silencing machinery to target SACMV, SACMV A and B would equally be targeted, resulting in no change in DNA-A/DNA-B ratio in SACMV-challenged/SACMV-VIGS vector. With a SACMV-challenged/TRV-VIGS however, the host is not specifically primed against either SACMV A or B and the presence of TRV in the host could have a synergistic effect or an interfering effect of SACMV resulting in the change in DNA-A and B dynamics.

The height of plants and the SSS revealed that SACMV-challenged/TRV-VIGS plants were slightly shorter with an overall higher SSS compared to SACMV-challenged/SACMV-VIGS. Although the difference is minimal in terms of value, the statistical significance supports the hypothesis that the presence of SACMV-VIGS vector in SACMV-challenged plants, affects the plants differently to TRV-VIGS vector in SACMV-challenged plants.

Although stunting is associated with geminiviral infection, across the entire study, plants infected with either SACMV-challenged/TRV::myosin or SACMV-challenged/SACMV::myosin grew taller than SACMV-challenged/TRV-VIGS vector and SACMV-challenged/SACMV-VIGS vectors only. The increase in plants height was observed even in plants were no reduction of the targeted myosin was detected. Because this was also observed in plants where myosin was not silenced, it is possible that the presence of the myosin VIGS constructs somehow affected the growth of the plants, in an unknown mechanism, resulting in plants growing taller than the control. There are reports suggesting that non-targeted effects of VIGS on gene expression in plants, based on the sequence present in the VIGS vector's multiple

cloning site. In tomato, the presence of a fragment of the *β-Glucuronidase* gene which shares no homology to endogenous tomato genes in the multiple cloning site of VIGS, resulted in a different phenotype to plants infected with an TRV- VIGS vector only (Wu et al. 2008) and a recent paper highlighted the effect of TRV-VIGS system on gene expression revealing that TRV-VIGS vector only has "vector effect" that are often overlooked and TRV-VIGS constructs (with a gene of interest) can result in modulating expression of genes not target by the construct (Oláh et al. 2016).

Vector effect in this study revealed that TRV-VIGS vector did not differentially affect the expression of myosins however SACMV-VIGS vector downregulated M11.F (figure 2-11). Surprisingly, the effect of the SACMV-VIGS vector on expression of myosin was different to that of wild type SACMV (figure 2-15) hence the vector effect for a VIGS study should be measured and not assumed based on the knowledge of the effect from its parent virus.

The expression of myosin in SACMV-challenged/NO-VIGS was reported against mock inoculated as well as against each of the vector-only controls and the expression of myosin in SACMV-challenged/VIGS was reported against vector only and SACMV-challenged/VIGS vector to highlight the effect of the controls on the reported silencing. Differential results were obtained depending on the control used to relate the expression of myosins highlighting the effects of the proper choice of controls for a VIGS study.

2.4.7 Off-target silencing by myosin constructs

One of the limitations of silencing using the VIGS approach is the potential off-target silencing induced by VIGS constructs. The mechanism of gene silencing induced by VIGS constructs mirrors that of post transcriptional gene silencing (PTGS), where homology recognition of the target gene RNA by the VIGS construct yields dsRNA detected by dicer-like ribonucleases (DCL), resulting in the formation of 21–24 nucleotide long small interfering RNA (siRNA) which can further induce silencing of genes it shares homology with.

To assess the likelihood of the chosen constructs to produce off-targets silencing, the VIGS tool from SGN was used. The sequence similarities shared by the different myosins in *N. benthamiana* (table 2-6) affected the ability to identify silencing regions that did not share similarities to other myosins. Given that previous studies have shown that due to the

overlapping function shared by different myosins, the knocking down of a single myosin member often does not results in observable phenotypic changes (Prokhnevsky et al. 2008), the ability of the constructs to silence more than a single myosin was seen as an advantage.

Of all the five silencing regions selected, analysis of M11.F and M11.K predicted two potential closely related myosin targets within the same cluster according to the phylogenetic tree (figure 2-5). Analysis of silencing regions M15.1, M8.B and M11.2 revealed that these regions potentially targeted many more myosins within other clades than M11.F and M11.K, and these myosins were not all closely related and in the case of construct M11.2, a non-myosin off-target was predicted (figure 2-8). Often the erratic silencing results obtained from VIGS studies cannot be fully explained and have been attributed mainly to the uneven silencing induced by VIGS constructs (Senthil-Kumar and Mysore 2011). In the case of this research, it cannot be overlooked that the various potential silencing off-targets of constructs M15.1, M8.B and M11.2 could have affected the level of silencing of the different myosins. This could have contributed to masking the potential effect that downregulation of their targets would have had on SACMV infectivity in *N. benthamiana* unlike downregulation using M11.F and M11.K constructs which have only two targets.

The potential off-targets of the VIGS myosin constructs also highlights the need to measure the expression of other myosin genes, and also to conduct experiments silencing myosins in different combinations.

2.5 Conclusion

The results from the study are summarised in appendix A1.1. Silencing of myosins *NbXI-F* and *NbXI-K* affected SACMV pathogenicity differently with silencing of NbXI-F affecting both proliferation and accumulation and NbXI-K affecting proliferation and not accumulation is probably a reflection of their function in the cell. There is stronger evidence for a role for NbXI-K in transport via the endomembrane system, then there is for NbXI-F. Therefore, whilst the results obtained with reduction in *NbXI-K* points toward a decrease in virus movement due to its association with vesicles transport, the reduced expression of *NbXI-F* most probably affects the life cycle of the virus (replication, transcription) rather than its movement through interactions with organelles such as the chloroplast. Whether SACMV

viral molecules/complexes bind directly to myosin NbXI-F and NbXI-K for intracellular movement will need to be elucidated by further research.

On the comparison of the different vectors used for VIGS, TRV-VIGS was more efficient that SACMV-VIGS, resulting in stronger silencing in the absence of SACMV-challenge. When plants were challenged with SACMV however, the efficiency of silencing by each VIGS vector changed for both TRV-VIGS and SACMV-VIGS. A previous study has suggested that challenging with TYLCV delayed VIGS induced by PVX by 10 – 16 days (Luna et al. 2006). Both TRV-VIGS and SACMV-VIGS had an effect of the infectivity of SACMV, however in terms of viral load comparisons, the effect of TRV-VIGS could be said to be minimal compared to SACMV-VIGS suggesting that more will need to be understood on the complexity of VIGS before plant virus studies involving a VIGS vector derived from the same virus as the virus under investigation can be used.

Chapter 3. NOA1 and homologues in host response to SACMV

3.1 Introduction

During infection, plants pattern recognition receptors (PRRs) are often the first receptor to sense the presence of an invading pathogen, by recognising molecular patterns from the pathogen. Recognition of pathogen associated molecular patterns (PAMPs) by plants PRRs triggers the onset of pathogen triggered immunity (PTI) as a defence response. (Jones and Dangl 2006; Newman et al. 2013). Some pathogens can evade this first line of defence by expressing effector proteins, to circumvent the plant's PTI response, and plants encode for resistance gene (R-gene) products, which are able to recognise pathogen's effector proteins, triggering a response known as effector triggered immunity (ETI) (Jones and Dangl 2006; Cui et al. 2015).

Until recently, plant viruses were not known to possess MAMPs *per se* and plant responses to viruses were believed to follow an ETI rather than PTI approach. Various viral *avr* genes have been identified as well as their corresponding host *R*-genes (Soosaar et al. 2005; Mandadi and Scholthof 2013). Although no avr proteins have been directly identified for SACMV, alterations in *R* gene expression have been demonstrated in the natural host cassava (Allie et al. 2014). Other geminivirus proteins have been identified as targets of plant defence response, such as several geminiviral movement proteins (MP) and nuclear shuttle protein (NSP) (Garrido-Ramirez et al. 2000; Hussain et al. 2005; Zhou et al. 2007).

Downstream of a successful PTI and ETI is the activation of a signalling pathways often mediated by reactive oxygen species (ROS) which constitute of a large group of molecules, including the multitasked nitric oxide (NO), that have evolved as signalling hormones in plants (Domingos et al. 2015). Besides being a key player in regulation of different plant developmental processes, NO is involved in plant biotic defence responses (Mur et al. 2006). The hypersensitive response (HR) is one such response that results in increases in the production of ROS as well as in the expression or pathogenesis-related (PR) proteins.

The signalling NO molecule is highly reactive and found in different forms in a cell; the nitrosonium cation (NO^+), the nitroxyl anion (NO^-) and the nitric oxide radical ($NO^{\cdot}$; Arasimowicz-Jelonek and Floryszak-wieczorek 2007; Leitner et al. 2009; Wojtaszek 2000), giving rise to various NO derived molecules. Peroxynitrite ($ONOO^-$) is derived through interaction with ROS, *S*-nitrosothiols through interactions with thiols, mononitrosyl-iron and dinitrosyl-iron complexes through interactions with haeme and iron-sulphur centre of proteins, metal-nitrosyl through the interaction with transition metals and higher oxide of nitrogen through spontaneous oxidation (Neill et al. 2008; Leitner et al. 2009). These different derivatives are termed reactive nitrogen species (RNS) and together with the different forms of NO present in a cell, provide different possibilities through which NO can affect the cellular environment, like contributing to disease resistance (Mur et al. 2006; Hong et al. 2008; Leitner et al. 2009; Bellin et al. 2013; Jeandroz et al. 2013; Sun and Li 2013; Agurla et al. 2014; Trapet et al. 2015).

The link between NO and disease resistance was highlighted when it was found that application of NO scavengers and inhibitors of NO synthesis in Arabidopsis rendered it susceptible to *Pseudomonas syringae* (Delledonne et al. 1998; Zeier et al. 2004). In susceptible tomato, tobacco mosaic virus (TMV) infections results in NO production which leads to the induction of the mitochondrial alternative electron transport resulting in the induction of basal defence (Fu et al. 2010). Infection of resistant but not susceptible tobacco with TMV resulted in enhanced NO production (Durner et al. 1998). Treatment with NO donors in tobacco triggered expression of the defence genes (Durner et al. 1998; Song and Goodman 2001) and has been shown to prevent the spread of TMV and potato virus x (PVX; Li et al. 2014). In *Hibiscus cannabinus*, infection with the geminivirus mesta yellow vein mosaic virus (MYVMV) resulted in an increase in NO production, as well as an increase in tyrosine-nitrated proteins (Sarkar et al. 2010).

In mammals, nitric oxide synthases (NOS) are the main NO producing enzymes. There are three different NOS, neuronal NOS (nNOS), endothelial NOS (eNOS) and inducible NOS (iNOS) encoded for by three different genes that share approximately 50% homology (Alderton et al. 2001; Stuehr 2004). They catalyse the conversion of L-arginine to NO and L-citrulline, requiring (6R)-5,6,7,8-tetrahydrobiopterin (BH_4), flavin adenine dinucleotide (FAD), flavin mononucleotide (FMN) and iron protoporphyrin IX (haem) as co-factors

(Moncada et al. 1989; Mayer and Hemmens 1997; Alderton et al. 2001). Despite being ubiquitously produced in plants, there is no consensus on the central source of NO (Domingos et al. 2015). A NOS has recently been identified from the algae *Ostreococcus tauri* and it bears sequence and structural similarities to mammalian NOS with different co-factor requirements (Foresi et al. 2010; Correa-aragunde et al. 2013).

Arabidopsis nitric oxide associated protein 1 (AtNOA1) formerly dubbed Arabidopsis nitric oxide synthase 1 (AtNOS1) was believed to be a plant NOS even though it bears neither sequence similarity, nor similar co-factor requirements to mammalian NOS (Guo et al. 2003). Since its initial discovery in Arabidopsis, homologues to AtNOA1 have been identified in different plants (Kato et al. 2007; Qiao et al. 2009; Yang et al. 2011; Kwan et al. 2015) as well as in mammals (Zemojtel et al. 2007; Parihar et al. 2008; Kolanczyk et al. 2011). It is now known that AtNOA1 is not a plant NOS but a member of the conserved circularly permutated GTPase (cGTPase) family YlqF/YawG with nucleic acids and protein binding abilities, and lacks binding sites for L-arginine or for any NOS associated co-factors.

Expression of AtNOA1 and its plant homologues has been shown to be differentially regulated in response to disease (Kato et al. 2007; Wünsche et al. 2011; Mandal et al. 2012; Kwan et al. 2015) and downregulation of NOA1 activity renders the plant more susceptible to invading pathogens (Zeidler et al. 2004; Zeier et al. 2004; Kato et al. 2007; Qiao et al. 2009). AtNOA1 participation in disease response could be through its association with chloroplast as there is evidence of chloroplast involvement in disease response (Reinero and Beachy 1989; Bhat et al. 2012; Liu et al. 2014; Bhattacharyya and Chakraborty 2017). Beside its role as the cellular energy generator, the chloroplast is a site of defence molecules production (Rodio et al. 2007; Caplan et al. 2015; Serrano et al. 2016), it can be directly targeted during plant virus infection (de Torres Zabala et al. 2015) and some plant pathogens can localise or replicate within the chloroplast (Gröning et al. 1987; Rodio et al. 2007; Krenz et al. 2010; Zhao et al. 2016). The hallmark of chloroplast involvement in plant disease, particularly in respect to plant viruses can be seen through symptoms like chlorosis, bleaching and mosaic (Liu et al. 2014).

The involvement of AtNOA1 in plant disease response could also be due to the indirect decrease in NO accumulation in plants with impaired AtNOA1 function (Guo et al. 2003;

Zeidler et al. 2004; Guo and Crawford 2005; Bright et al. 2006; Zhao et al. 2007; Chen et al. 2010). The decrease in NO observed in null *atnoa1* mutations was shown to be due to a decrease in carbon fixation in *atnoa1* mutants, leading to a decrease in fixed sucrose and in fumaric acid stores, resulting in an decrease in L-arginine accumulation and indirectly, to a decrease in NO (Van Ree et al. 2011). Although to date no enzyme catalysing the conversion of L-arginine to L-citrulline and NO has been characterised, the conversion of L-arginine to L-citrulline and NO is known to occur in plants (del Río et al. 2004; Corpas et al. 2009).

To this day however the role of AtNOA1 and the indirect accumulation of NO and the chloroplast is not well studied in plant virus infections, and no studies on geminiviruses have been reported. Central to AtNOA1, NO and disease, is the chloroplast, where not only AtNOA1 is localised, but is also a site of NO and fumaric acid production. In this study the aim was to evaluate if AtNOA1 plays a role in SACMV pathogenicity in the susceptible model plant *Nicotiana benthamiana* and susceptible natural host cassava landrace T200. We hypothesise that the NOA1/cGTPase status is important in terms of chloroplast 'health' and plant growth, and that infection with viruses such as SACMV influences this status, leading to physiological perturbations and disease symptoms.

3.2 Experimental procedure

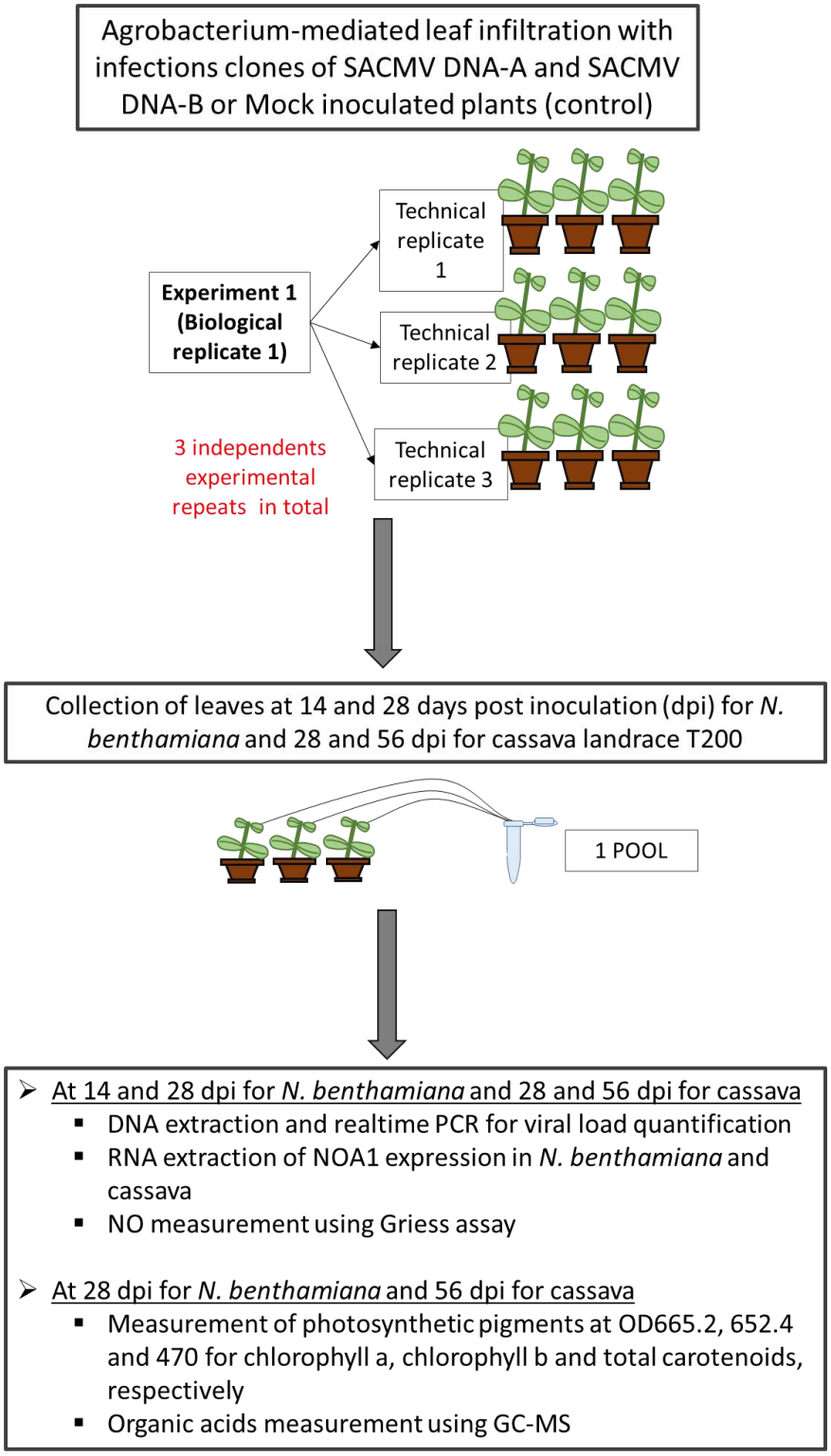

Figure 3-1: Experimental procedure outline.

3.2.1 *Bioinformatics searches of NOA1 homologue in the cassava genome*

The amino acid sequence of AtNOA1 (accession number NP_850666.1) was used to search Phytozome (https://phytozome.jgi.doe.gov/Mesculenta) for homologous sequences in cassava genome (*Manihot esculenta* v4.1), using the TBLASTN tool. The obtained amino acid sequences were aligned using BLASTP tool at the National Center for Biotechnology Information (NCBI; https://blast.ncbi.nlm.nih.gov/Blast.cgi?PAGE=Proteins) against the Arabidopsis protein database to find sequences of characterised proteins that they are mostly similar to.

Clustal omega (https://www.ebi.ac.uk/Tools/msa/clustalo/) was used to align the amino acid sequences of the candidate NOA1 homologues obtained from Phytozome, to previously predicted, putative and characterised NOA1 homologue from different plant species; *A. thaliana* NP850666.1, *N. benthamiana* BAF93184.1, *Ricinus communis* EEF51564.1, *Medicago truncatula* ADK47527.1, *Brassica juncea* ACX61572.1 as well as the Arabidopsis GTP binding protein brassinazole insensitive pale green 2 (AtBPG2) NP191277.4 and AtBPG2-like NP567364.1. Plant cGTPase domains were identified using the NCBI Conserved Domain Search (CD-Search) tool (https://www.ncbi.nlm.nih.gov/Structure/cdd/cdd.shtml).

The prediction software Plant-mPLoc (Chou and Shen 2010) and TargetP1.1 (Emanuelsson et al. 2007) were used to predict the subcellular location of each homologue based on homology. Using Phyre^2 web portal (Kelley et al. 2015), the protein three dimensional structures of cassava4.1_007735m, cassava4.1_002874m , cassava4.1_025372m, AtNOA1 as well as AtBPG2 and ATBPG2-like were modelled. Images were modified using PyMOL (Schrödinger 2015).

3.2.2 *Plant growth and virus inoculation*

Unless indicated otherwise, reagents used for this section were purchased from Sigma Aldrich. *N. benthamiana* plants were grown from seed at 25°C, with a 16 h light, 8 h dark photoperiod under 120 µmoles/m^2/s. For infection, *N. benthamiana* plants were allowed to grow to the 4-6 leaf stage and the source leaves were infiltrated using a needless syringe. *Agrobacterium tumefaciens* strain C58C1 containing head to tail infectious clones of SACMV-A and SACMV-B (Berrie et al. 2001) were used to inoculate YEP media containing 100 mg/l

kanamycin and 50 mg/l rifampicin and grown overnight at 28°C. The following day, 50 ml of fresh YEP media supplemented with 10 mM morpholino ethane sulfonic acid (MES), 20 µM acetosyringone, 100 mg/l kanamycin and 50 mg/l rifampicin was inoculated with the overnight culture and allowed to grow overnight. The cells were collected by centrifugation and the pellet resuspended in infiltration media (10 mM $MgCl_2$, 10 mM MES, and 200 µM acetosyringone) to an OD_{600} of 0.4-0.6. The cultures were incubated for 3 h at room temperature before proceeding with agroinfiltration. The experiment was carried out at 3 independent times, dubbed experimental replicates. For each experimental replicate, 9 plants were inoculated with infectious clones of SACMV-A and SACMV-B (figure 3-1) and 9 plants were mock inoculated with *A. tumefaciens* strain C58C1 harbouring no clones.

Cassava landrace T200 was micropropagated by nodal cuttings on Murashige and Skoog (MS) medium (Murashige and Skoog 1962) supplemented with 20 g/l sucrose, 7.8 g agar at a pH of 5.8. The nodal explants were grown at 25°C, with a 16 h light, 8 h dark photoperiod, 120 µmoles/m^2/s, until the appearance of roots, after which they were acclimatised in a growth chamber set at 28°C, with a 16 h light, 8 h dark photoperiod. At the 4-6 leaf stage, cassava plants were inoculated with *A. tumefaciens* strain AGL1 clones containing infectious SACMV DNA-A and DNA-B clones (Berrie et al. 2001). The infection cultures were grown as described for *N. benthamiana* however the inoculum was corrected to an OD_{600} of 2.0. Cassava plants were inoculated along the stem using a 1 ml syringe fitted with a hypodermic needle. Control plants were inoculated with *A. tumefaciens* strain AGL1 harbouring no clones.

3.2.3 Nucleic acid extraction

DNA and RNA from infected and mock-inoculated tissues were extracted from three experimental replicates, each comprising of 3 pools or biological replicates (figure 3-1). Each pool was made from apical leaves collected from 3 plants.

For *N. benthamiana* DNA was extracted at 14 and 28 dpi and for cassava at 28 and 56 dpi, using a modified Cetyl trimethylammonium bromide (CTAB) method (Doyle and Doyle 1987; Porebski et al. 1997). For total DNA extraction, 100 mg of leaf tissue was ground in the presence of liquid nitrogen and to the powdered tissue was added 500 µl of extraction buffer (2% w/v CTAB, 2% w/v PVP, 20 mM EDTA, 1.4 M NaCl, 100 mM Tris-HCl pH 8.0 and

0.1% v/v β-mercaptoethanol) and incubated at 65°C for 60 min. After incubation 500 µl of chloroform: isoamyl alcohol (24:1) was added and the samples were centrifuged at 12,000 *g* for 10 min, and the aqueous phase was extracted to a new microfuge tube, to which an equal volume of isopropanol was added to precipitate DNA. The samples were centrifuged as described above. The tubes were decanted and the precipitated pellet was washed in 1 ml ice cold 70% ethanol (v/v) and centrifuged for 5 min at 12,000 *g*. DNA pellets were air dried and resuspended in TE buffer containing 200 µg/ml of RNAse A.

RNA was extracted from 100 mg of leaf tissue for both *N. benthamiana* and cassava. *N. benthamiana* RNA was extracted using Tri reagent (Sigma-Aldrich; St Louis, USA) according to the manufacturer's recommendation. For cassava, RNA extraction was carried out using a modified CTAB extraction (Xu et al. 2010). 100 mg of fresh tissue was ground in liquid nitrogen to which was added 600 µl of extraction buffer (2% w/v CTAB, 2% w/v PVP, 25 mM EDTA, 2 M NaCl, 100 mM Tris-HCl pH 8.0 and 2% v/v β-mercaptoethanol) prewarmed to 65°C. The samples were incubated for 15 min at 65°C after which 500 µl of chloroform was added and the samples were mixed centrifuged at 12,000 *g* for 10 min at 4°C. The aqueous phase was removed and 100 µl of 5 M NaCl and 300 µl of chloroform was added, and the samples were centrifuged as before. The aqueous layer was once again collected and transferred into a microfuge tube to which half a volume of isopropanol and high salt solution (0.8 M $Na_3C_6H_5O_7$ + 1.2 M NaCl) was added and the samples were incubated at room temperature for 15 min. After incubation, the samples were centrifuged as before, then the supernatant was discarded and the pellet was washed in 1 ml ice cold 75% ethanol (v/v) and centrifuged for 5 min at 12,000 *g*. RNA pellets were air dried and resuspended in nuclease-free H_2O containing 1 U/µl of Ribolock RNAse inhibitor (Thermo Fisher Scientific; Waltham, USA). Concentrations of extracted *N. benthamiana* and cassava RNA samples were determined using the NanoDrop™ 1000 spectrophotometer (Thermo Fisher Scientific; Waltham, USA) and RNA integrity was assessed by electrophoresis on 1.0% agarose gel. The extracted RNA was treated with DNAse *I* (Thermo Fisher Scientific; Waltham, USA) according to manufacturer's recommendation before proceeding to first strand DNA synthesis.

3.2.4 Viral load determination by absolute quantitative PCR

All real-time PCR (qPCR) assays were performed using Maxima SYBR Green (Thermo Fisher Scientific; Waltham, USA) and the LightCycler® LC480 (Roche; Basel, Switzerland). No template controls were included in each run. Each extracted DNA sample was diluted to a final concentration of 50 ng/µl. One µl of extracted DNA was run in triplicate. To 5 µl of Maxima SYBR green master mix was added, AC1/AC4 RT to a final concentration of 0.3 µM for each primer and nuclease free water to a total volume of 10 µl. Real-time PCR was run for 35 cycles. Initial denaturation and enzyme activation was carried out at 95°C for 10 min, denaturation at 95°C for 15 sec, annealing at 60°C for 30 s and elongation at 72°C for 30 s. For *N. benthamiana* samples, glyceraldehyde 3-phosphate dehydrogenase (GAPDH) was used as an internal control and ubiquitin10 (UBQ10) for cassava. The crossing points obtained were subtracted from crossing point of GAPDH in order to calculate the ΔCt values to quantify DNA-A in relation to the internal control.

3.2.5 Differential expression studies by relative quantitative PCR

First strand DNA synthesis was carried out using random hexamers and RevertAid First Strand cDNA Synthesis Kit (Thermo Fisher Scientific; Waltham, USA), using 1 µg of total RNA. The synthesised cDNA was diluted 1 in 10 and 1 µl of diluted cDNA was added to 5 µl of Maxima SYBR green master mix. Specific primers were added to a final concentration of 0.3 µM for each primer, and nuclease free water to a total volume of 10 µl. Real-time PCR was run for 35 cycles. Initial denaturation and enzyme activation was carried out at 95°C for 10 min, denaturation at 95°C for 15 sec, annealing at 60°C for 30 s and elongation at 72°C for 30 s. GAPDH and UBQ10 were used for normalization as endogenous controls for *N. benthamiana* and cassava respectively (Allie and Rey 2013; Allie et al. 2014). To quantify NOA1 in cassava and *N. benthamiana,* the primers MeNOA77 and qRT-Nb was designed respectively. Scouting through the Arabidopsis information resource (TAIR), we obtained sequences of other proteins involved in chloroplast ribosomal binding/assembly namely, chloroplast RNA binding (RRM; AT2G35410), chloroplast elongation factor G (EFG; AT1G62750), translation elongation factor Tu (EFTu; AT4G20360), translation initiation factor 3-2 (IF3-2; AT2G24060) and plastid-specific ribosomal protein 6 (PSRP6;AT5G17870), Plastid ribosome recycling factor (RRF; AT3G63190). We used these sequences in

Phytozome and The Sol Genomics Network (www.solgenomics.net) to find putative homologues in cassava and *N. benthamiana* respectively and designed primers based on these sequences (table 3-1). For relative expression calculations ΔΔCt method was applied (Schmittgen 2001).

Table 3-1: Sequences and features of primers used in this study.

		Primer name	Forward Primer sequence (5'3')	Reverse primer sequence (5'3')	Amplicon length (bp)
SACMV	DNA-A	AC1/AC4F	GTCTCCGTCCTTGTCCAAATAG	AACGATTCTTCGACCTCATATCC	110
Cassava T200	cassava4.1_007735m	MeNOA	AAGCTGATGGTGTCTCTTCTTC	CCGCAGTGGTTTGTTGTTATG	110
	Ubiquitin10	UBQ10	TGCATCTCGTTCTCCGATTG	GCGAAGATCAGTCGTTGTTGG	136
	chloroplast RNA binding	MePPR	TCCTCTCATCTCCCAATCTACC	TCTGTGGGTGAGAGGAGATAC	104
	Chloroplast elongation factor G	MeEFG	GACTGGAGGAGTGCATGAATAA	CGAATCCACATCGTGGTAAGA	98
	Translation elongation factor Tu	MeETu	CATGGGAAGACCACTCTTACAG	CGGCGTCAATTTCATCGTATTT	91
	Translation initiation factor 3-2	MeIF3-2	CAGCAGCTTTCCCTTCAATC	GAGATGAGAGAGTCGGGTTTAG	126
	Plastid-specific ribosomal protein 6	MePsp	GCCTTAAGACTAGGCCAAGAAA	GGAGTCAAATCAGTCGGAAGAG	97
	Plastid ribosome recycling	MeRRF	GAAGCGGAGAAGTCCTCTATTG	CCTGCCTGTCCTTACAGAATTA	99
N. benthamiana	NbNOA1	qRT-Nb	GCGTTGCAACTTCATATGGTGCCT	TTCCTGTCGGCGGTGTCAATAGAA	88
	GAPDH	GAPDH	ATGGCCTTCAGAGTACCAACTGCT	GCTTGACCTGCTGTCACCAACAAA	189
	chloroplast RNA binding	NbPPR	CCATGGTCTTTGACTGTTCCT	AGCCTCTATTCTTCCCATCTTTG	103
	Chloroplast elongation factor G	NbEFG	GTCCTTGAACGCATGGATTTC	AAGCCTGTCGCCATCTTATC	92
	Translation elongation factor Tu	NbETu	TCCCTATCCCACAAAGACAAAC	CCTTAACAGTCCCTCTCTCTACT	117
	Translation initiation factor 3-2	NbIF3-2	ACACCCACCATTTCCTCTAAAC	GGAGACAGTGGCAGCATAATAG	138
	Plastid-specific ribosomal protein 6	NbPSP	CGTCAAGGCCACAGAAGAA	GGCAGGCAATGGAGGATAAA	110
	Plastid ribosome recycling	NbRRF	GTCGGCTCTGATCTTGGTATG	TGGATAACTCCTTCCTCCTGT	97

3.2.6 NO measurement

NO production was determined using the method described by (Zhou et al. 2005). Whole newly emerging leaves (100 mg) were ground with a mortar and pestle in 1 ml of 50 mM cool acetic acid buffer (pH 3.6, containing 4% zinc diacetate). The homogenate was centrifuged at 10.000 *g* for 15 min at 4°C. The supernatant was reserved, and the pellet washed twice with 0.5 ml of cold acetic acid buffer pellet, and centrifuged. The extracted supernatants were pooled, and 0.05 g of activated charcoal was added to the supernatant. The slurry was vortexed then filtered using 0.2 µM filters. The filtrate was mixed with equal volume of Griess reagent (Sigma-Aldrich; St Louis, USA) and was incubated at room temperature in the dark for 30 min. Absorbance was determined at 540 nm. NO content was calculated by comparison to a standard curve of $NaNO_2$ (FIGURE 3-2).

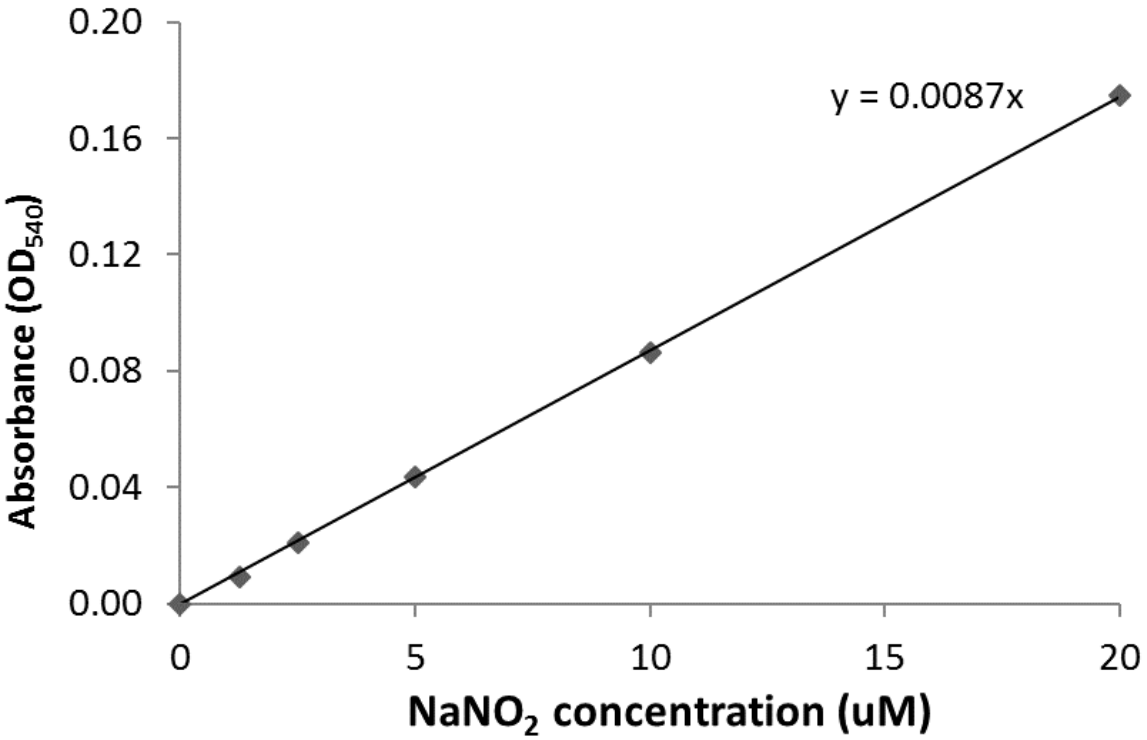

Figure 3-2: $NANO_2$ standard curve.

3.2.7 Chlorophyll and carotenoids measurement

Measurement of photosynthetic pigments (Chlorophylls *a*, *b* and carotenoids) was carried out from leaf extract in pure methanol. Absorbance of the extract was measured at 665.2, 652.4 and 470 nm for chlorophyll a, chlorophyll b and total carotenoids, respectively (Lichtenthaler and Buschmann 2001).

3.2.8 GC-MS Organic sugars extraction

Organic sugars were extracted according to Lisec et al. 2006. In brief, 100 mg of leaves was snap frozen in liquid nitrogen upon harvest, and homogenised using a micropestle into a fine powder. To the homogenised leaves, 1.4 ml of precooled 100% methanol was added, and the mixture was vortex for 10 s. Ribitol was used as an internal standard and 60 µl of a 0.2 mg/ml ribitol solution was added to each aliquot, the samples were vortexed to mix and incubated for 10 min at 70°C in heating block. After incubation, the samples were centrifuged for 10 min at 11.000 *g*, the supernatant was transferred to a glass centrifuge vial, in which was added 750 µl of ice-cold chloroform and 1.5 ml of cold dH_2O (4°C). The samples were vortexed for 10 s and centrifuged for 15 min at 2,200 *g*. A 150 µl aliquot of the upper polar fraction was transferred into a fresh 1.5 ml microfuge tube and dried at room temperature under vacuum. Argon gas was pumped in each microfuge tube and the samples were frozen at -80°C. Prior to derivitazation, the frozen extracted samples were allowed to equilibrate to room temperature in a vacuum concentrator, at room temperature for 30 min. Derivitazation was achieved by adding 40 µl of freshly prepared 20 mg/ml methoxyamine hydrochloride in pyridine, followed by incubation, with shaking at 37°C for 2 hours. To each aliquot was added 70 µl of *N*-methyl-*N*-trimethylsilyltrifluor(*o*)acetamide (MSTFA) containing 20 µl/ml of fatty acid methylesters mix (F.A.M.E mix C8-C24, Sigma Aldrich). The aliquots were incubated at 37°C for 1 h and transferred to glass GC-MS vials. Gas chromatography was performed using an Agilent GC with a DB-35 capillary column using Helium as a carrier gas, with a constant flow set at 2 ml/min. For sample analysis, 1 µl of sample was injected at 230°C, in split mode, with a split ratio of 1:25. The following oven temperature was used, 2 min at 80°C, followed by a 15°C/min ramp to 330°C for 6 min. Mass spectra were recorded with scanning rate of 70-600 *m*/*z,* 20 scans/s. Metabolites were selected by comparing their similarity (>80%) and

retention indexes (+/− 2 s) against compounds stored in the NIST library. Metaboanalyst tool 2.0 (http://www.metaboanalyst.ca/) was used for normalizing the data, as well as for data analysis, using the non-parametric t-test (Xia et al. 2015).

3.2.9 Statistical analysis

Median values obtained throughout the study were compared using the Student's *t*-test with a cut of *p* value of 0.05.

3.3 Results

3.3.1 cassava4.1_007735m encodes a putative AtNOA1 homologue in cassava

To obtain a candidate putative NOA1 gene in cassava, a bioinformatics approach was used, aligning the amino acid sequence of AtNOA1 against the cassava database in Phytozome. Three candidates cGTPases were identified based on their amino acid sequence similarity: cassava4.1_007735m, cassava4.1_002874m and cassava4.1_025372m. According to the latest genome mapping on Phytozome v6.1 (Bredeson et al. 2016), these three candidates cGTPases are located on three different chromosomes (table 3-2). Using subcellular location prediction software cassava4.1_007735m and cassava4.1_002874m were predicted to localise to the chloroplast and cassava4.1_025372m was predicted to localise both to the chloroplast and the cytoplasm (table 3-2).

Table 3-2: Description of putative AtNOA1 protein homologues in cassava.

Genome location	Transcript Name*	Predicted cellular location	CDS Length (nt)	*A. thaliana* homologue	Percentage amino acids similarity (%)
Chromosome 3	cassava4.1_025372m (Manes.03G089300.1)	Chloroplast/ cytoplasm	1743	BPG2-LIKE	64.77
Chromosome 8	cassava4.1_002874m (Manes.08G054900.1)	Chloroplast	2001	BPG2	62.91
Chromosome 2	cassava4.1_007735m (Manes.02G134200.1)	Chloroplast	1704	AtNOA1	69.55

Although all three transcripts are annotated in Phytozome as NOS1 homologues, based on their sequence similarity with putative uncharacterised homologues in other plant species, a multiple alignment of their amino acid sequences revealed that cassava4.1_007735m had the highest percentage amino acid sequence similarity against previously characterised NOA1 (NOS1), 65% from Arabidopsis, 72% from *N. benthamiana*, 73% from *M. truncatula*

and 86.3% with *R. communis,* a close relative of cassava (table 3-3). Amino acid sequences of cassava4.1_002874m and cassava4.1_025372m had low sequence similarity with AtNOA1 as well as plants AtNOA1 homologues, around 30% (table 3-3). Sequences of cassava4.1_002874m and cassava4.1_025372m showed a higher similarity to two other plant cGTPases AtBPG2 (62.91%) and AtBPG2-like (69.55%) respectively (table 3-2; table 3-3). Like AtNOA1, AtBPG2 and AtBPG2-like have conserved domains essential for cGTPase activity and have been classified under the YqeH subfamily (Komatsu et al. 2010; Qi et al. 2016).

Table 3-3: Percentage identity matrix of 3 AtNOA1 putative homologues against characterised NOA1 amino acid sequences from various plant sources.

		1	2	3	4	5	6	7	8	9	10
1.	Cassava4.1_025372m		41.96	24.7	22.42	23.56	22.56	24.18	24.65	42.29	64.77
2.	Cassava4.1_002874m	41.96		25.2	24.4	25.39	24.5	25.45	24.95	62.91	43.36
3.	Cassava4.1_007735m	24.7	25.2		69.55	72.07	70.18	72.84	86.3	24.08	25.84
4.	*A. thaliana*	22.42	24.4	69.55		65.41	92.61	65.31	68.17	23.78	24.79
5.	*N. benthamiana*	23.56	25.39	72.07	65.41		65.03	69.47	72.51	22.54	23.66
6.	*B. juncea*	22.56	24.5	70.18	92.61	65.03		65.99	67.82	23.44	24.95
7.	*M. truncatula*	24.18	25.45	72.84	65.31	69.47	65.99		71.03	24.9	26.87
8.	*R. communis*	24.65	24.95	86.3	68.17	72.51	67.82	71.03		23.83	24.11
9.	AtBPG2	42.29	62.91	24.08	23.78	22.54	23.44	24.9	23.83		42.68
10.	AtBPG2-like	64.77	43.36	25.84	24.79	23.66	24.95	26.87	24.11	42.68	

Domains and motifs were identified using CD-Search online tool, and all three putative cGTPase homologues were found to bear domains belonging to the sub-family YqeH (ID, CD01855) (figure 3-4). They had the G-protein motifs, G1-G5, aligned in the G4, G5, G1, G2 and G3 order, known to occur in cGTPases differently to the G1-G5 order known of canonical GTPases (Moreau et al. 2008; Sudhamsu et al. 2008) and the switches 1 and 2, overlapping G2 and G3. A multiple sequence alignment confirmed the G-proteins motifs and switches, but also revealed at the N-terminus, a zinc finger motif with the residues $CXGCX_nCXRC$ was found in the amino acid sequence of cassava4.1_007735m, cassava4.1_002874m and cassava4.1_025372m as well as the characterised AtNOA1, AtBPG2 and AtBPG2-like. At the C-terminus, The G-protein motifs are followed by a C-terminal domain, which has been shown essential for AtNOA1 function, probably conferring its RNA binding activity.

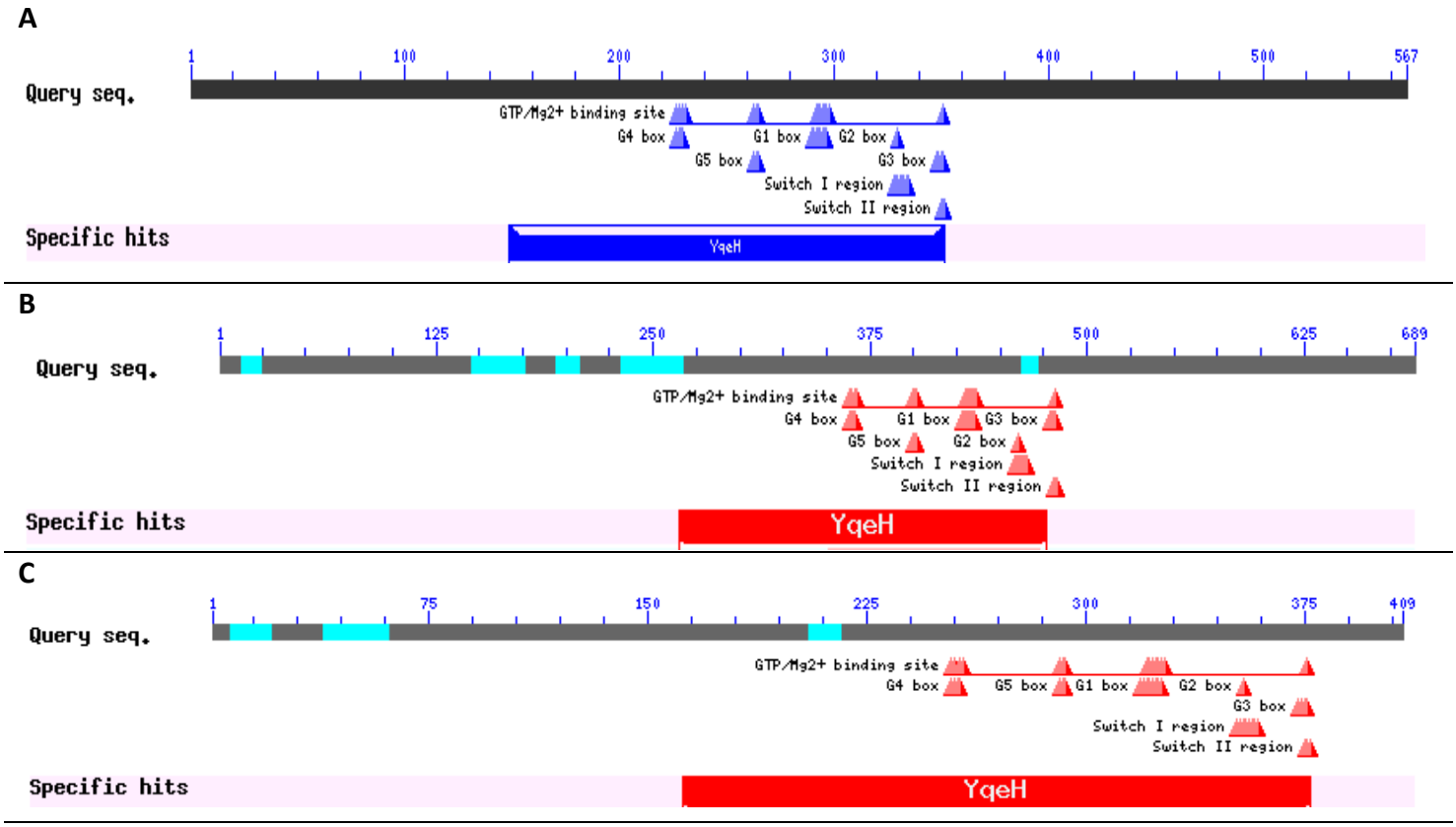

Figure 3-3: Conserved domain search results for putative AtNOA1 homologues in cassava.

Domain architecture of AtNOA1 putative homologues in cassava was predicted using the CD-Search online tool from NCBI. [A] cassava4.1_007735m; [B] cassava4.1_002874m ; [C] cassava4.1_025372m.

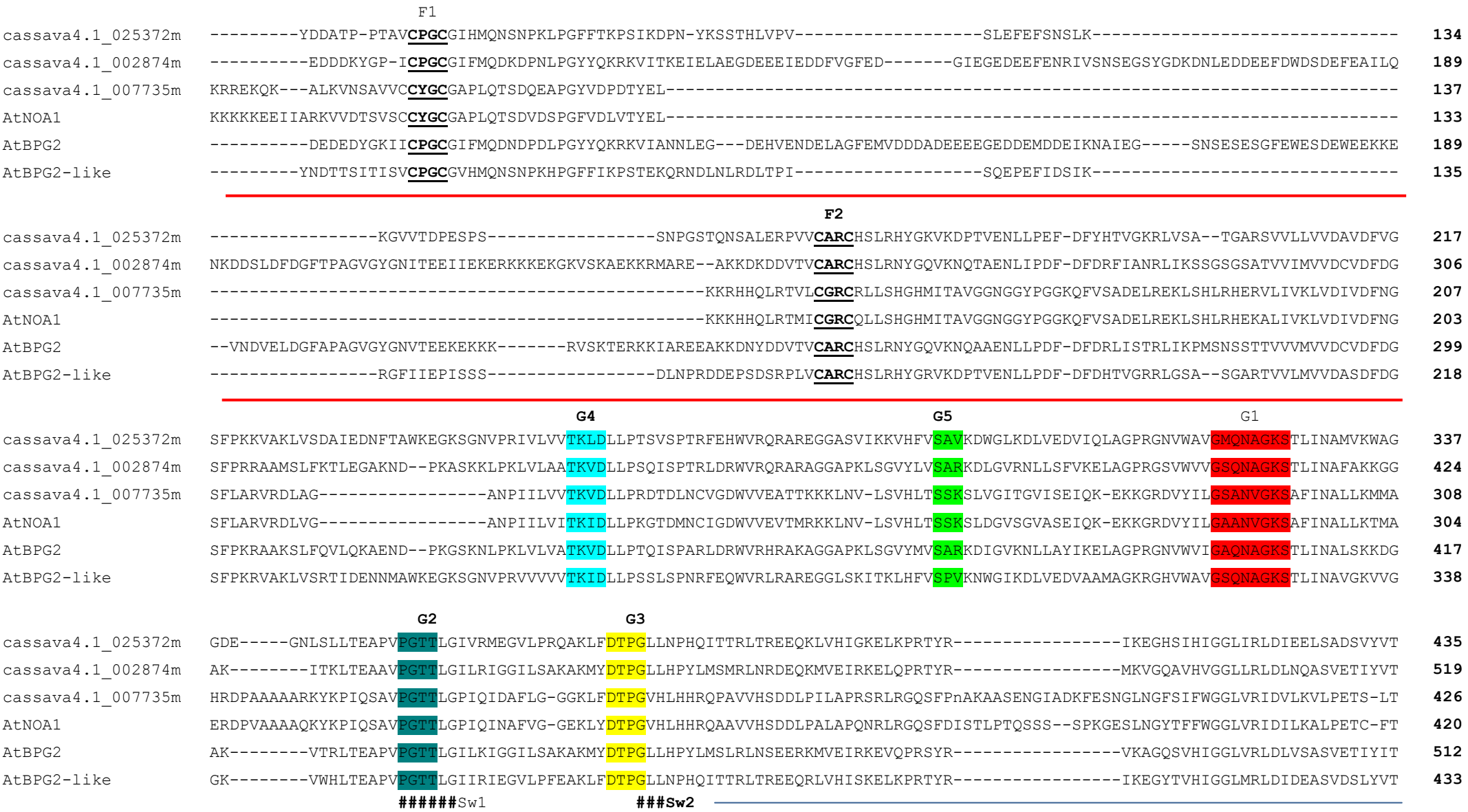

Figure 3-4: Multiple amino acid sequence alignments of AtNOA1 and homologues in cassava, as well as cGTPase family members.

Amino acid sequences of cassava4.1_007735m; cassava4.1_002874m; cassava4.1_025372m, AtNOA1 (NP_850666.1), AtBGP2 (NP191277.4) and AtBGP2-like (NP567364.1) were aligned using ClustalOMEGA. Highlighted regions indicate G-domains in the typical G4-G5-G1-G2-G3, know of cGTPases. The red line denotes the N-terminal domains, known to contain localization signals (not shown); the blue arrow denotes the C-terminal domains, whose function has not yet been well established, but is believed to contain RNA binding

domains (not shown). At the N-terminus, the bold/underlined residues show two putative finger motifs belonging to the treble clef family of zing finger motifs, CXGCXnCXRC shown by the two “fingers” F1 and F2. Overlapping with highlighted G2 and G3 are the switches 1 (sw1) and 2 (sw2), known to change conformation upon GTP binding. Note that the entire sequence of each protein wasn’t shown, the display was limited to the portion of sequences that encompasses the described features.

The C-termini of all three candidates, cassava4.1_002874m, cassava4.1_025372m and cassava4.1_007735m, were studied using in silico three dimensional structural analyses, alongside that of their characterised Arabidopsis homologues. AtBPG2 and AtBPG2-like were found to have a similar fold to the bacterial mRNA-binding protein family, *carbon storage regulator A*-like (*csrA*-like) protein.

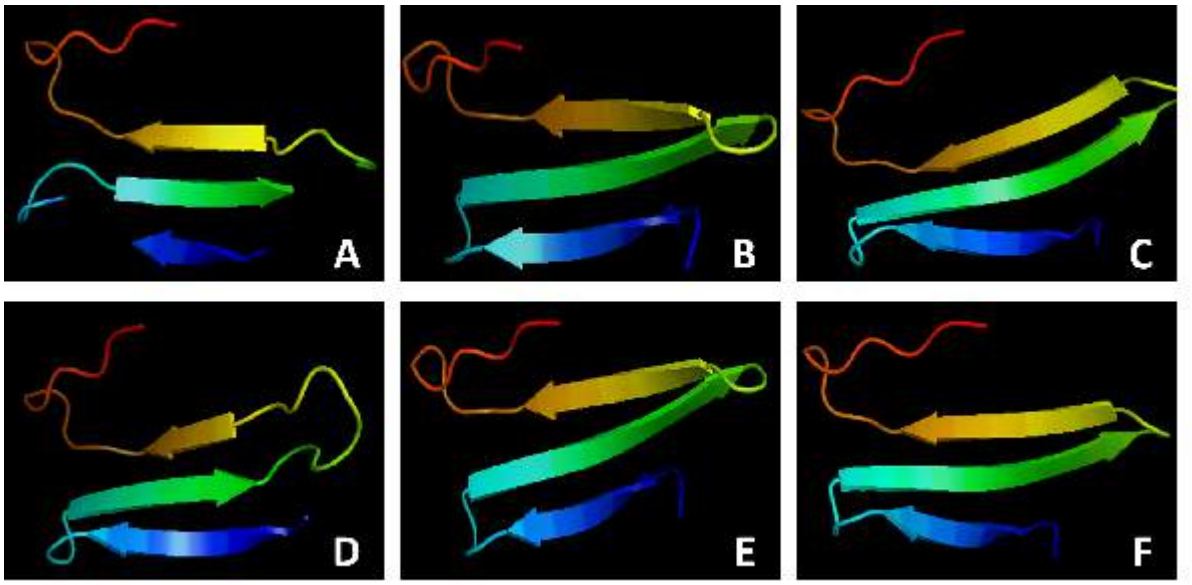

Figure 3-5: Three-dimensional structure prediction.

The three dimensional structures were predicted in Phyre2 (Kelley et al. 2015) based on their similarity against the crystal structure of a putative carbon storage regulator protein (csrA) Pseudomonas aeruginosa. Protein structure was performed using Phyre2 (Kelley et al. 2015) and viewed using PyMOL (Schrödinger 2015). The general predicted structures consisted of three consecutive antiparallel β-strands. For the structures with the highest confidence, the second β-strand was the largest (in green) with the first (in blue) and the last (in yellow) being about 1.5 times smaller. Those were cassava4.1_002874m [B] with 82.3% confidence, 21% identity for aa 493-531; cassava4.1_025372m [C] with 89% confidence and 16% identity for aa 409-448; AtBPG2 [E] with 83.7% confidence and 18% identity for aa residues 486-524 and AtBPG2-like [F] with 85.9% confidence and 18% identity. Three dimensional structures of cassava4.1_007735m [A] and AtNOA1 [B] had the lowest confidence %, with 42% confidence and 22% identity for aa residue 402-437 for cassava4.1_007735m and 41% confidence and AtNOA1, with 41% confidence and 22% identity for aa residues 396-431.

The predicted three dimensional structures of cassava4.1_007735m and its Arabidopsis homologue, resulted in a more disordered structure, with lower confidence number. The three

dimensional structure of the C-terminus of AtNOA1 has previously been likened to Tryptophan RNA-binding attenuator protein (TRAP; Moreau et al. 2008; Sudhamsu et al. 2008), however our structural similarity searches did not yield similar results. The three-dimension structure of a TRAP protein was aligned against the C-termini of cassava4.1_007735m and AtNOA1 and no structural model was obtained. Since both sequence alignments and structural evidence supported cassava4.1_007735m as a legitimate NOA1 homologue in cassava, further study focused on its role in SACMV disease response.

3.3.2 Expression of MeNOA1 (cassava4.1_007735m) and NbNOA1 are downregulated during SACMV infection

Expression of *NOA1* has been linked with responses to different pathogens and its upregulation has been shown to promote resistance to some pathogens (Zeidler et al. 2004; Zeier et al. 2004; Kato et al. 2007; Wünsche et al. 2011; Mandal et al. 2012; Kwan et al. 2015). In order to assess the level of *MeNOA1* transcript abundance during SACMV infection, *N. benthamiana* and cassava landrace T200 plants were infected with SACMV. To confirm for the progression of infection, qPCR was used to quantify viral load at 14 and 28 dpi in *N. benthamiana* and in cassava at 28 and 56 dpi, representing early and late infection in both plant systems respectively. The early time points correspond with the appearance of symptoms in both *N. benthamiana* and cassava T200, whilst the later time points correspond with fully symptomatic plants. In cassava there was an 8-fold significant increase in viral load at 56 dpi, in comparison to 28 dpi (p value = 0.04) and in *N. benthamiana* there was a about 2-fold increase in viral load at 28 dpi, in comparison to 14 dpi (p value = 0.05).

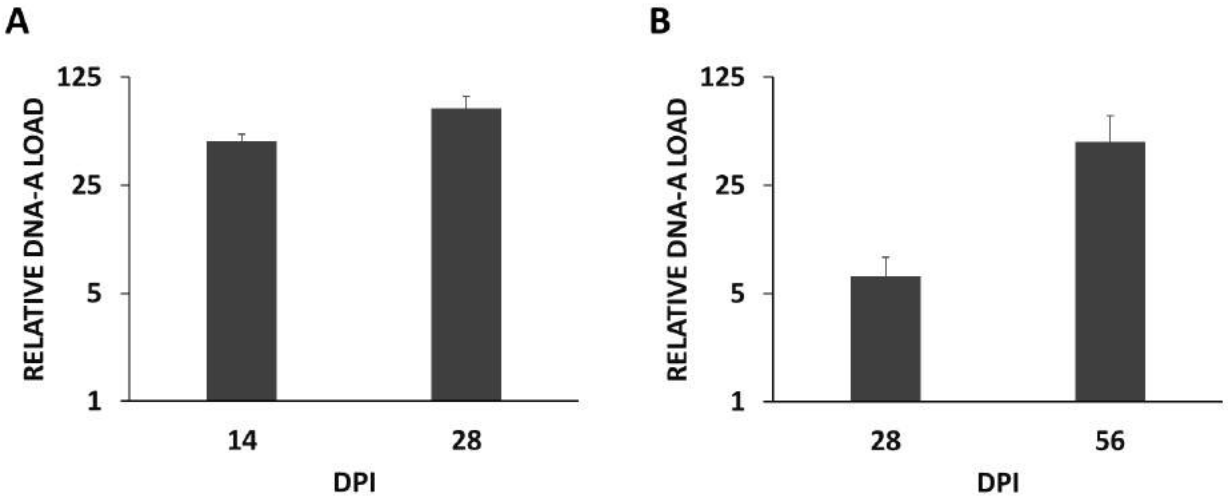

Figure 3-6: SACMV viral accumulation at several days post inoculation (dpi) in *N. benthamiana* [A] and cassava [B].

Viral accumulation was measured using qPCR from SACMV-infected *N. benthamiana* and cassava leaf tissue. Viral accumulation is reported at 14 and 28 dpi for *N. benthamiana* [A] and 28 and 56 dpi for cassava [B]. SACMV virus accumulation measured by quantifying SACMV DNA-A molecules in relation to the internal control GAPDH for *N. benthamiana* and UBQ10 for cassava using relative qPCR. Values represent the median of three independent replicates each with 3 plants per treatment and bars indicate SEM. T-test was used for statistical analysis p value ≤ 0.05.

Progression of infection was also manifested by the aggravation of symptoms between the two-time points (figure 3-7). Symptoms appeared in *N. benthamiana* at around 8 dpi, where mild curling and bubbling on leaves were observed, and by 14 dpi, the bubbling and curling was more obvious. By 28 dpi, the symptoms were more pronounced with severe leaf area reduction, leaf distortion and mosaic (figure 3-7c). In cassava, mild curling could be observed as early as 12 dpi in some plants, and by 28 dpi, mild curling and leaf distortion could be seen in most plants, and by 56 dpi, severe leaf distortion with leaf lobes curling could be observed.

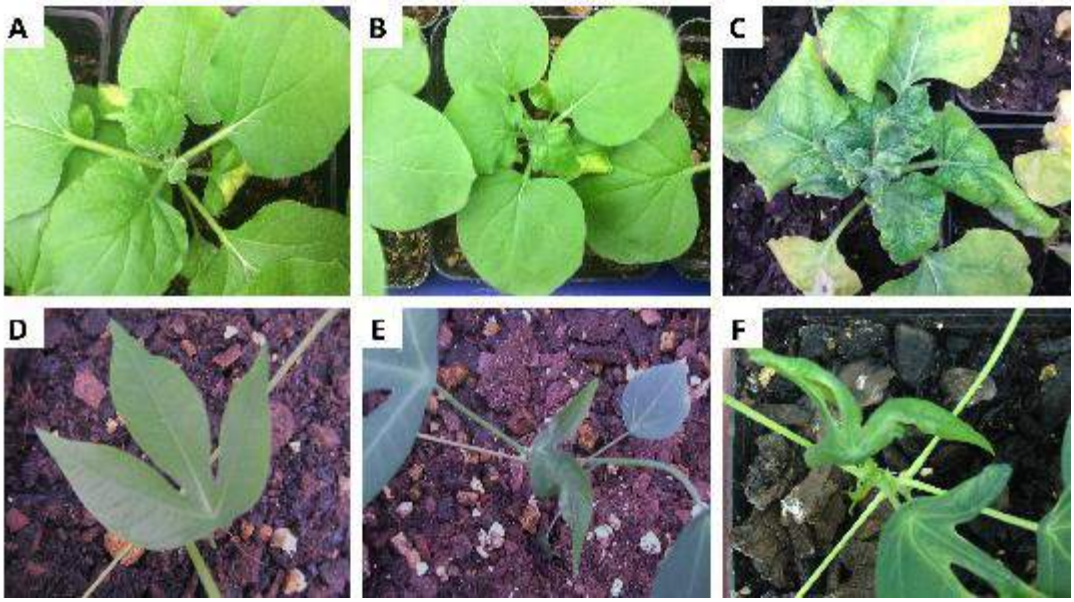

Figure 3-7: SACMV-infected *N. benthamiana* and cassava at 28 and 56 dpi respectively.

At 14 dpi for *N. benthamiana* [B] and 28 dpi for cassava [E], mild curling and some bubbling can be observed. At 28 dpi for *N. benthamiana* [C] and 56 dpi for cassava [F] the symptoms are more pronounced with severe leaf area reduction, leaf distortion, leaf mosaic, and in some cases vein clearing, when compared to mock inoculated plants for *N. benthamiana* [A] and cassava [D].

The expression of NOA1 homologues *NbNOA1* in *N. benthamiana* and cassava4.1_007735m (*MeNOA1*) in cassava was measured alongside viral load quantification. Relative qPCR was carried out to quantify NOA1 expression using GAPDH and UBQ10 as endogenous controls in *N. benthamiana* and cassava respectively. In *N. benthamiana NbNOA1* was downregulated at 14 dpi by 2-fold (*p* value = 0.00), and 28 dpi by 4-fold (*p* value = 0.00). In cassava, the expression of *MeNOA1* was not significantly different at 28 dpi, and at 56 dpi, *MeNOA1* expression was downregulated at 56 dpi by 3-fold (*p* value = 0.00; figure 3-8).

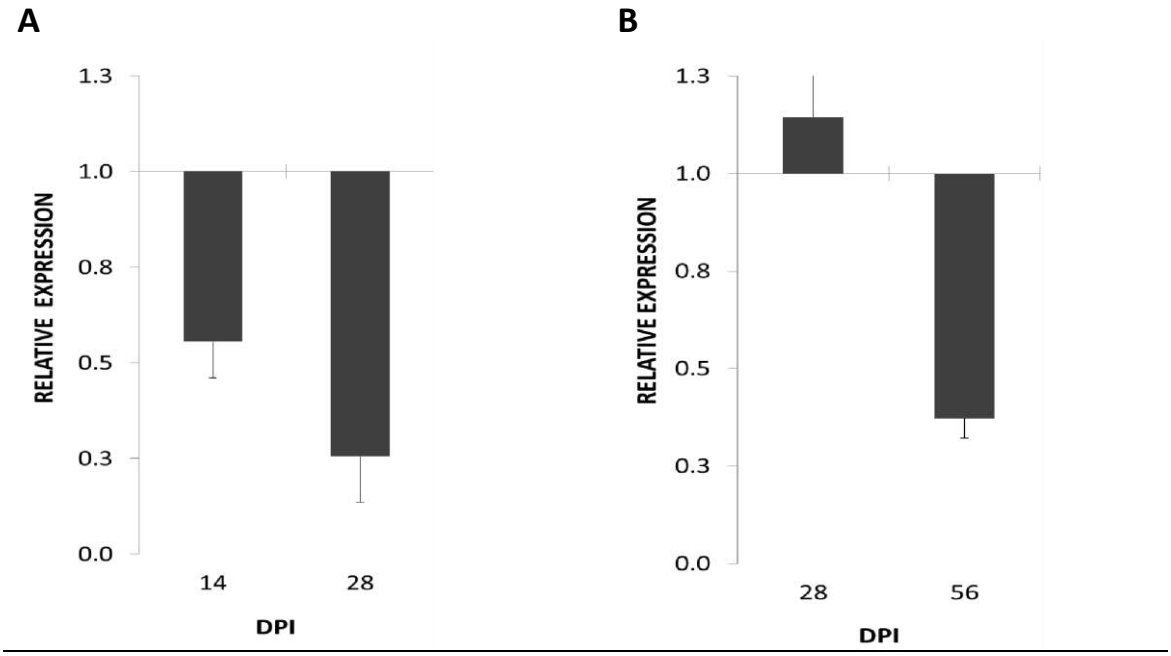

Figure 3-8: Expression of NOA1 homologues in *N. benthamiana* and cassava.

The expression of NOA1 homologues in *N. benthamiana* and cassava was measured using relative qPCR. GAPDH was used as an internal control for *N. benthamiana* [A] and UBQ10 for cassava [B]. In *N. benthamiana* NbNOA1 was downregulated at both 14 and 28 dpi [A]. In cassava, MeNOA1 was only downregulated at 56 dpi whilst its expression remained unchanged at 28 dpi [B]. Values represent the median of three independent replicates and bars indicate SEM. T-test was used for statistical analysis.

3.3.3 Differential expression of NOA1 homologues in cassava and N. benthamiana indicates a disruption in chloroplast protein translation

In order to assess whether the downregulation of *NbNOA1* in *N. benthamiana* and *MeNOA1* in cassava is associated with the concomitant downregulation of chloroplast translation, the relative expression of other nuclear-encoded chloroplast genes, involved in protein translation was measured in mock and SACMV-infected leaf tissue, at the later time points, 28 dpi for *N. benthamiana* as the expression of *NbNOA1* at this time point was measured to be the lowest, and 56 dpi for cassava, as the expression of *MeNOA1* was only down at 56 dpi. In *N. benthamiana* at 28 dpi, the expression of translation factors *NbRRM* and *NbRRF* was downregulated by 3-fold, the expression of *NbEF-G, NbEF-Tu, NbIF3-2* was downregulated 5-fold and the expression of *PSRP6* was down by 10-fold (figure 3-9). In cassava, the expression

measured at 56 dpi showed a statistically significant downregulation of about 1.5-fold for *MeRRM*, 5-fold for *MePSPR-6,* 3-fold for *MeEF-G* and *MeIF3-2*. Although the measured expression values for *MeEF-Tu* and *MeRRF* were lower in infected samples than in mock (0.72 and 0.9 respectively), the decrease was not statistically significant (figure 3-9).

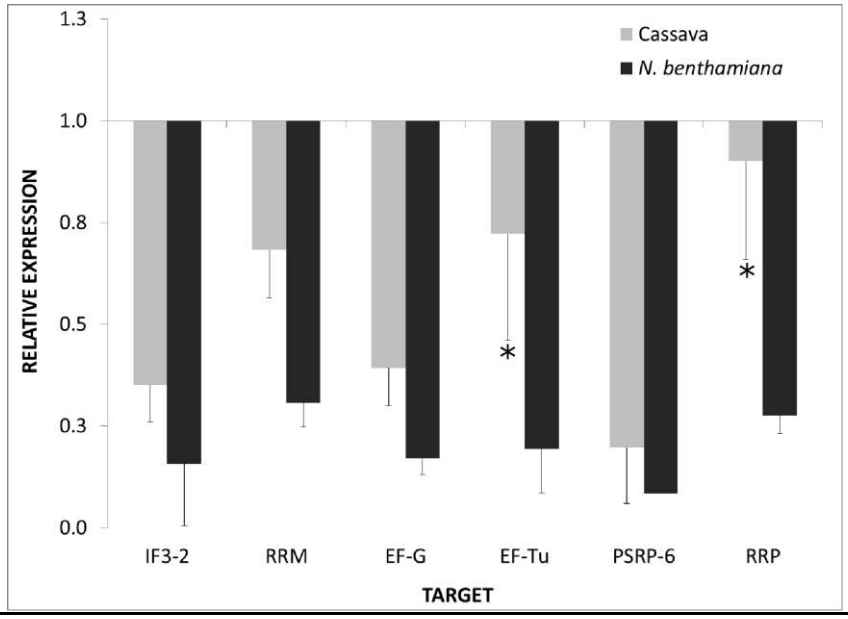

Figure 3-9: Expression of chloroplast translation factors in infected *N. benthamiana* and cassava.

The expression of chloroplast translation factors was measured in in *N. benthamiana* at 28 dpi and cassava at 56 dpi using relative qPCR. GAPDH was used as an internal control for *N. benthamiana* and UBQ10 for cassava. RRM: chloroplast RNA binding; EF-G: chloroplast elongation factor G; EF-Tu: translation elongation factor Tu; IF3-2: translation initiation factor 3-2; PSRP-6: plastid-specific ribosomal protein 6; RRF: Plastid ribosome recycling factor. Sequences were obtained from Phytozome and The Sol Genomics Network for primer design. The stars (*) on error bars for cassava EF-Tu and RRP denotes that downregulation was not statistically significant. Values represent the median of three independent replicates and bars indicate SEM. T-test was used for statistical analysis p value≤ 0.05.

Since differential expression of NOA1 homologues (now identified as chloroplast associated cGTPases) was observed in both cassava and *N. benthamiana*, a comparison of the chlorophyll and carotenoids contents of infected vs mock-inoculated plants was performed in order to determine the “health” status of the chloroplasts. In both plants species, there was a decrease

in abundance of all three pigments investigated. In *N. benthamiana* plants, total chlorophyll contents decreased by 37.5% (*p* value = 0.00), chlorophyll a (chla) by 33.5% (*p* value = 0.00), chlorophyll b (chlb) by 42.4% (*p* value = 0.00) and total carotenoids by 31.8% (*p* value = 0.00; figure 3-10a). In cassava T200, SACMV infection resulted in 44.8% decrease in total chlorophyll (*p* value = 0.02), 45.3% decrease in chla (*p* value = 0.00), 43.4% decrease in chlb (*p* value = 0.00) and 50.4% decrease in carotenoids (*p* value = 0.00; figure 3-10b).

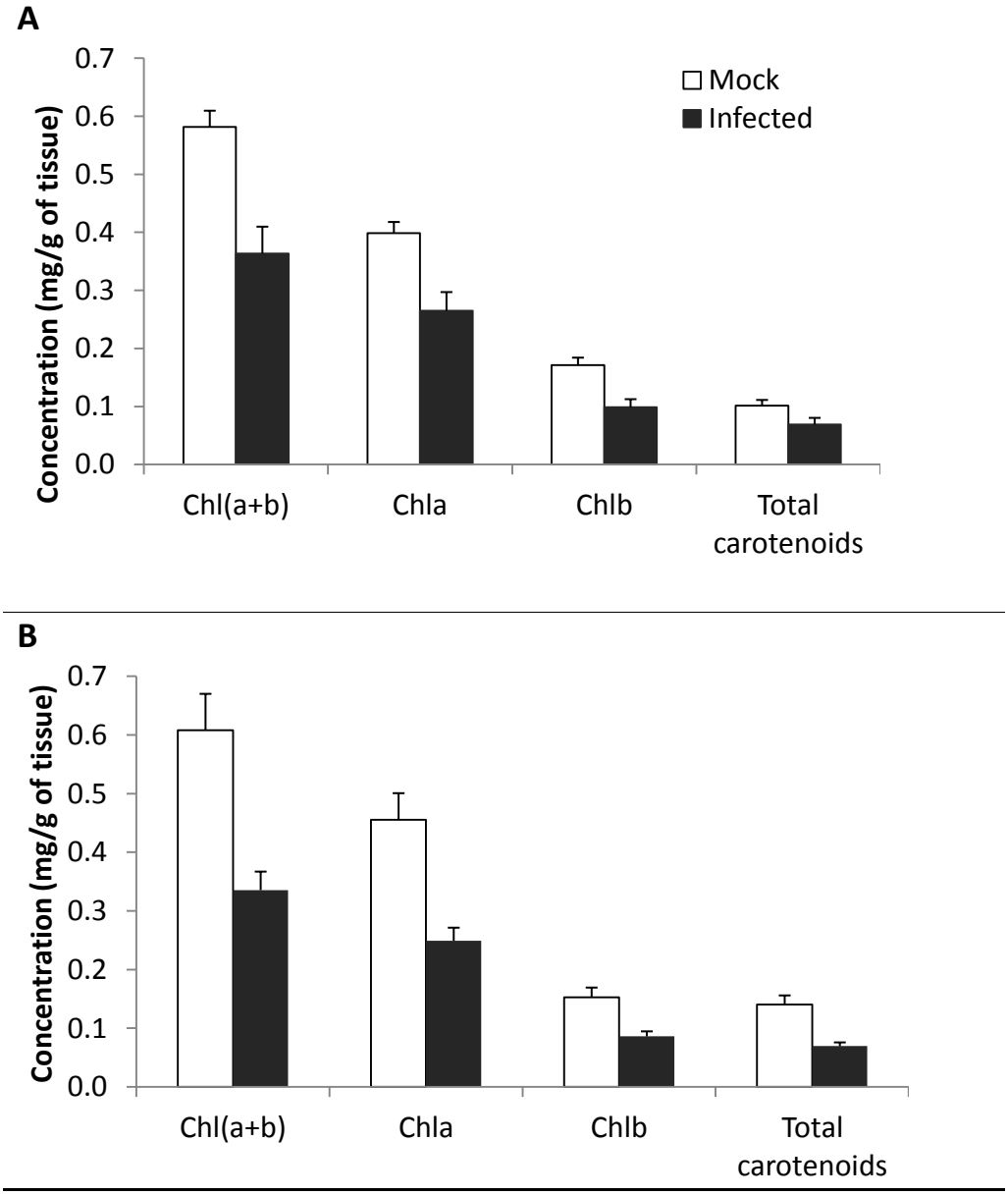

Figure 3-10: Quantification of Chla, Chlb and Total carotenoids.

Pigment abundance (mg/g of tissue) for *N. benthamiana* [A] and cassava [B] at 28

and 56 dpi respectively. Values represent the median of three independent replicates and bars indicate SEM. T-test was used for statistical analysis, *p* value≤ 0.05.

3.3.4 MeNOA1 abundance in plants is not directly related to NO accumulation

Since its identification in Arabidopsis, *NOA1* has recently been shown not to be associated with the production of NO as is the case for mammalian NOS (Moreau et al. 2008; Sudhamsu et al. 2008). The decrease in NO accumulation observed in *atnoa1* mutants is suggested to be indirect, however NOA1 is still regarded as an important tool in NO research (Moreau et al. 2008; Van Ree et al. 2011; Mandal et al. 2012). In an attempt to establish a link between the status of *NbNOA1* and *MeNOA1* expression and NO accumulation in response to SACMV infection.

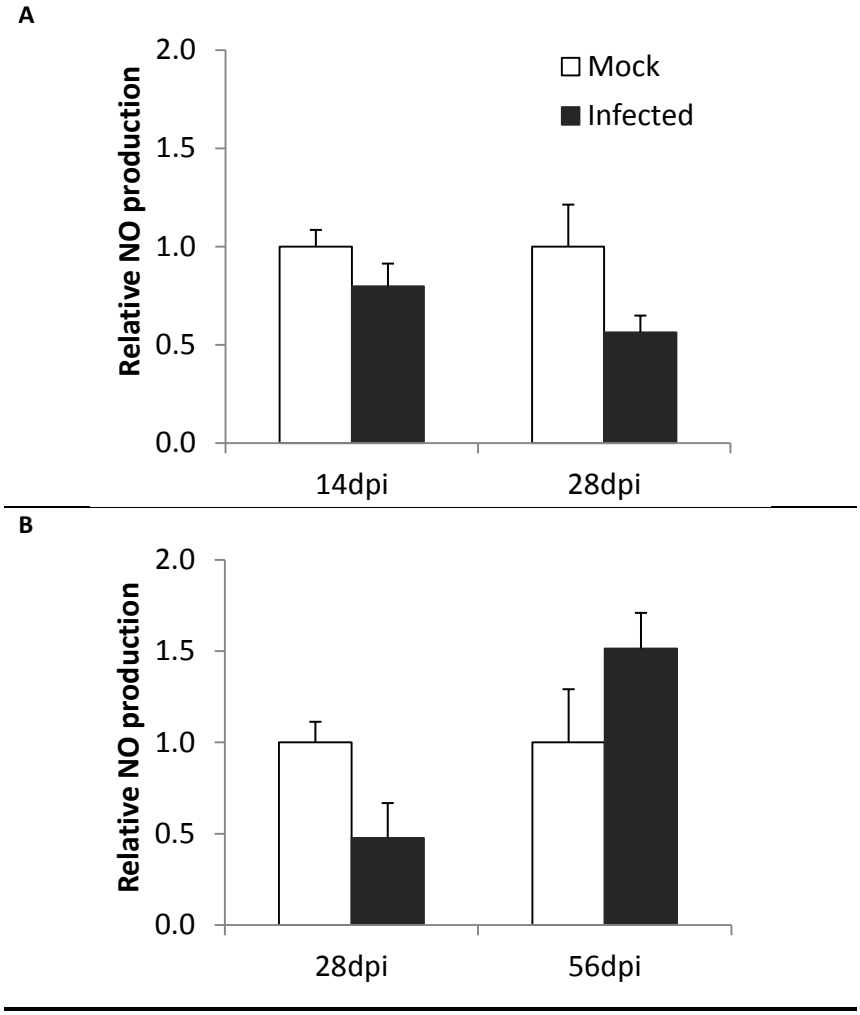

Figure 3-11: NO contents of infected vs control plants.
NO content was measured in leaves at 14 and 28 dpi for *N. benthamiana* [A] and 28 and 56 dpi for cassava [B] in SACMV-infected vs mock inoculated plants. Values represent the median of three independent replicates and bars indicate SEM. T-test was used for statistical analysis, *p* value≤ 0.05.

The abundance of NO in infected *N. benthamiana* and cassava T200 was measured at both early and late time points. In *N. benthamiana* at both 14 and 28 dpi, the measured downregulation of *NbNOA1* was matched with a decrease of NO accumulation in infected leaf tissue (10% at 14 dpi and 40% at 28 dpi) when compared to mock inoculated. In cassava T200, at 28 dpi when the expression of *MeNOA1* remained unchanged, there was a 40 % decrease in NO accumulation at

28 dpi and at 56 dpi, with a decrease in *MeNOA1* expression, the level of NO in infected leaf tissue was 37 % higher than that of mock inoculated leaf tissue (figure 3-11).

3.3.5 NO accumulation in infected N. benthamiana but not in cassava T200 is associated with alterations in organic acids

The discrepancy between NO accumulation and *NOA1* expression prompted an investigation into the levels of metabolites, particularly organic acids like fumaric acid, whose accumulation has been linked to NO abundance in NOA1 (Van Ree et al. 2011; Mandal et al. 2012). The ability of *noa1* to store carbon in the form of fumaric acid in Arabidopsis was assessed and *noa1* mutants were found defective in fumaric acid storage when grown on a sucrose-free medium (Van Ree et al. 2011). Fumaric acid is a major storage form of fixed carbon in Arabidopsis (Chia et al. 2000), and in *noa*1 mutants exhibiting defective chloroplasts, reduced stored carbon, reduced fumarate, and pale leaf phenotypes, sucrose restores NO accumulation.

A gas-chromatography experiment was carried out, to measure the level of organic acids in infected vs mock-inoculated leaves at the later time points (28 dpi for *N. benthamiana* and 56 dpi for cassava T200) corresponding with a downregulation in *NOA1* expression. A common trend in both *N. benthamiana* and cassava was a significant increase in levels of amino acids (table 3-4). However, in terms of organic acids, an increase in organic acids accumulation was detected in *N. benthamiana,* except for fumaric acid which was significantly downregulated (-7.35 $\log_2$ fold change). In contrast to *N. benthamiana,* there were no significant changes in organic acids namely γ-aminobutyric acid (GABA), glyceric acid, malic and oxalic acid. Moreover, no fumaric acid could be detected in cassava T200 leaf tissue. Of the sugars identified, the levels of structural sugars galactose and mannose were higher in infected samples of *N. benthamiana* but not of cassava T200, whilst glucose levels increased significantly in *N. benthamiana* but not in cassava T200 (table 3-4).

Table 3-4: GC-MS analysis comparisons of metabolites associated with between mock and SACMV-infected leaves at the later time points.

		Log2 Fold change	
	Name	*N. benthamiana*	Cassava T200
Amino acids	Asparagine	6.51	5.24
	L-Aspartic acid	3.51	2.58
	L-Glutamic acid	2.87	2.93
	L-Isoleucine	6.80	4.24
	L-Leucine	5.23	6.60
	L-Phenylalanine	4.12	4.16
	Glycine	2.55	5.02
	Serine	2.19	4.15
Organic acids	Fumaric acid	-7.37	ND[b]
	GABA	4.05	**3.11**
	Malic acid	2.48	**1.46**
	Succinic acid	1.98	-2.27
Sugars	Galactose	2.12	1.88
	Glucose	5.75	**2.75**
	Mannose	4.34	**1.04**

[a] Values reported in the table are significant, *p* value ≤ 0.05, except for those highlighted

[b] Fumaric acid was not detected in cassava T200 samples

3.4 Discussion

Although once believed to have NOS activity, it is now known that NOA1 is a circular permutated GTPase associated with chloroplast translation (Moreau et al. 2008; Sudhamsu et al. 2008). The expression of *NOA1* has been associated with plant responses in different host disease (Kato et al. 2007; Wünsche et al. 2011; Mandal et al. 2012; Kwan et al. 2015), and we sought to evaluate its role in SACMV response in the model plant *N. benthamiana* and the landrace cassava T200. The bioinformatics results from this study confirmed that cassava *MeNOA1* is closely related to other reported homologues in the genetic databases, and revealed the conserved domains (figure 3-3 and figure 3-4) supporting its identification, along with *NbNOA1*, as a cGTPase (table 3-2 and table 3-3). This is the first study identifying MeNOA1 in cassava and predicting its secondary structure (figure 3-5).

Results from this study show that SACMV infection causes the downregulation of *NOA1*, the more severe the infection, at 28 dpi for *N. benthamiana* and 56 dpi for cassava T200, the greater the suppression (figure 3-8). The link between suppression of *NOA1* expression and susceptibility in plants has been well established, although most of the research was not focused on its role in chloroplast ribosome assembly, but on its presumed ability to produce NO in response to plant pathogen (Zeidler et al. 2004; Kato et al. 2007; Kwan et al. 2015). Chloroplast ribosomes consist of small 30S and large 50S subunits, which assemble in a bacterial like 70S subunit. Associated with these chromosomes are tRNA synthetases, initiation factors, elongation factors, ribosome-recycling factor, peptide chain-release factor, plastid-specific ribosomal proteins and subunits of the 30S and 50S ribosome (Harris et al. 1994; Manuell et al. 2007; Tiller and Bock 2014). Although NOA1 is involved in ribosome assembly, it is not yet known how NOA1 contributes to ribosome assembly in chloroplast, however its bacterial homolog, YqeH, has been shown to bind to 30S ribosome of *Bacillus subtilis* (Anand et al. 2009). Knock out mutants of *noa1* in Arabidopsis were shown to have impaired chloroplast translation (Flores-Pérez et al. 2008). The decrease of *NOA1* expression observed in both SACMV-infected cassava T200 and *N. benthamiana* (figure 3-8) not only points toward a

decrease in the assembly of 30S and 50S ribosomes into a functional 70S unit but possibly indicates a decrease in chloroplast translation of infected cells.

Various members of the chloroplast translation machinery have previously been linked to development, abiotic and environmental stresses (Singh et al. 2004; Friso et al. 2010). In terms of pathogen response, upregulation of the elongation factor Tu1 was noted in response to herbivore attack in resistance rice lines (Sangha et al. 2013) and expression of AC2 derived from african cassava mosaic virus (ACMV) in transgenic tobacco plants resulted in decreased in chloroplast ribosomal proteins expression (Soitamo et al. 2012). Besides being the cellular energy producer, chloroplasts are the major source of resistance molecules production such as NO, ROS and phytohormones (Rodio et al. 2007; Caplan et al. 2015). Cellular disruptions that arise during plant infection can be detected by the chloroplast, affecting the delicate equilibrium at which these reactive molecules are produced. The outcome of these changes could be unfavourable to either the host or the invading pathogen, and this makes chloroplasts ideal targets of viruses during infection, as evident by the chlorosis, bleaching and yellowing of leaves observed in SACMV infection of cassava T200 and *N. benthamiana* (figure 3-7).

Although loss of function of NOA1 has been shown in numerous studies to affect NO levels (Guo et al. 2003; Zeidler et al. 2004; Guo and Crawford 2005; Bright et al. 2006; Zottini et al. 2007; Liao et al. 2013), the function of NOA1 in relation to NO accumulation in plants is believed to be indirect (Moreau et al. 2008). Downregulation of NOA1 in its role as a plastidial cGTPase has been previously shown to affect translation in the chloroplast, however this function is believed to be redundant as the phenotype of *noa1* knock-out mutants can be rescued by changing the growing conditions of plants (Flores-Pérez et al. 2008; Van Ree et al. 2011; Yang et al. 2011). To confirm whether downregulation in *NOA1* expression in both *N. benthamiana* and cassava T200 suggested a dysregulation of the chloroplast translation machinery, we measured the expression of other chloroplast translation factors involved in chloroplast ribosomal binding/assembly. Similarly to the expression of *NOA1* at 28 dpi and 56 dpi for *N. benthamiana* and cassava T200, the expression of *RRM, EF-G, EF-Tu, IF3-2, PSRP-6* and *RRF* is suppressed in SACMV-infected *N. benthamiana* as well as in cassava T200, apart

from *EF-Tu* and *RRF* for cassava (figure 3-9). All of the aforementioned translation factors are like NOA1, encoded in the nucleus, placing the nucleus at the center of chloroplast translation regulation in infected samples. Inter-organelle communication between chloroplasts and the nucleus in plant-pathogen responses, and in particular plant innate immunity, is well documented (Padmanabhan and Dinesh-Kumar 2010; Caplan et al. 2015; Zhao et al. 2016).

Recently in Arabidopsis, AtNOA1 was found to be essential for thylakoid protein assembly and *atnoa1* mutants had reduced photosynthesis and chloroplast protein accumulation (Qi et al. 2016). Examples of chloroplast encoded protein include component of the chloroplast transcription and translation machinery, structural proteins of the photosystem I, II, cytochrome b_6f and ATP synthase complex as well as the large subunit of RuBisCo (Marín-Navarro et al. 2007). Impairment in their translation impairs the functionality of the chloroplasts, the production of pro-defence molecules as well as photosynthesis, benefiting disease progression. The translation of RuBisCo in response to TYLCV infection is suppressed in susceptible tomato lines and promoted in resistant lines (Moshe et al. 2012). The βC1 betasatellite of the geminivirus Radish leaf curl virus (RaLCV) localises in the chloroplast and alters chlorophyll biosynthesis (Bhattacharyya et al. 2015). A decrease of photosynthesis as well as photosynthetic pigments is a factor known to occur in plants in response to different viruses (Funayama et al. 1997; Lehto et al. 2003; Wilhelmová et al. 2005; Liu et al. 2014; Alexander and Cilia 2016). In response to SACMV infection in this study, the concentration of chlorophyll a, b and carotenoids was reduced in infected cassava as well as in infected *N. benthamiana* at the later time point (Figure 3-10). A decrease in chlorophyll due to virus infection can be caused by downregulation of genes involved in chlorophyll biosynthesis (Bhattacharyya et al. 2015) or upregulation of genes involved in degradation (Liu et al. 2014), or a combination of both. The different genes involved in chlorophyll degradation/biosynthesis are encoded both in the nucleus and in the chloroplast (Beale 1999; Schelbert et al. 2009; Chatterjee and Kundu 2015), therefore the downregulation of chloroplast translation as shown in this study in response to SACMV infection, has the potential to directly affect the accumulation of photosynthetic pigments. It has been previously shown that suppression of translation of protein components

of PSII in the chloroplast causes the appearance of chlorotic symptoms observed in response to flavum TMV infection in *N. benthamiana* (Lehto et al. 2003).

To establish a link between NO accumulation and *NOA1* expression in response to SACMV infection in the susceptible *N. benthamiana* and cassava T200*,* NO was measured in infected leaf tissue at 14 dpi for *N. benthamiana* and 28 dpi for cassava T200 representing the early infection stage, and 28 dpi for *N. benthamiana* and 56 dpi for cassava T200 representing the full systemic infection stage. The accumulation of NO at 14 and 28 dpi was lower in infected leaf tissue when compared to mock at both time points coinciding with the downregulation of *NbNOA1* (figure 3-11). In cassava T200 however, NO accumulation in infected leaf tissue was lower at 28 dpi, with no change in *MeNOA1* expression whilst at 56 dpi, NO accumulation in infected samples was higher than in mock inoculated leaf tissue (figure 3-11). Given that NO is a pro-defence signalling molecule which when supplied in the form of NO donors promotes resistance to invading pathogens (Clarke et al. 2000; Grün et al. 2006; Kato et al. 2007; Ma et al. 2008; Kawakita 2014), it can be expected that in susceptible plant pathogen interactions, the production NO would decrease. Given however the ubiquitous nature of NO as a signalling molecule, it is unsurprising that alongside the various reports of a decrease in NO accumulation in infected susceptible hosts, there are reports the contrary. The production of NO in susceptible Kenaf plants in response to *Mesta yellow vein mosaic virus* (MeYVMV) is higher in infected leaf tissues in comparison to uninfected plants (Sarkar et al. 2010) and a time course analysis of fungal infection in palm tree revealed that NO production fluctuates during the course of infection (Kwan et al. 2015). In respect to SACMV infection in this study, the increase in NO that occurred concurrently to the downregulation of *MeNOA1* at 56 dpi, unlike in *N. benthamiana* where there was concurrent downregulation of *NbNOA1* expression and decrease in NO accumulation can be attributed to the difference in the nature of each plant with *N. benthamiana* being an annual plant and cassava T200 being a perennial natural host. The reach of NO involvement in cellular responses goes far beyond plant immunity, and therefore it is probable that differences in growth, storage, leaf turnover between *N. benthamiana* and cassava T200 could have an effect on the overall NO homeostasis. The opposite effects of NO in different plants genotypes has been previously shown, as in soybean, NO promotes the

upregulation of phenyl alanine lyase expression, a gene involved in the HR, but not in soybean and it has been suggested that NO effects in plants is genotype dependent (Desender et al. 2007).

In relation to NO accumulation and *NOA1* expression, research shows that the decrease in NO accumulation in *noa1* Arabidopsis mutants is believed to be influenced by metabolites related to carbon fixation, particularly fumaric acid, when grown on media lacking, or low in sucrose (Van Ree et al. 2011). We performed a GC-MS experiment looking at the metabolic profile of infected vs uninfected samples at the full systemic infection stage, as *NOA1* expression at this time point was downregulated in both *N. benthamiana* and cassava T200. The amino acid profiles in both *N. benthamiana* and cassava were similar, with amino acids identified in both cassava and *N. benthamiana* being upregulated in infected samples (table 3-4). An increase in amino acids is known to occur in response to viral infection, and most probably arising from the need to translate viral proteins, or to an increase in protein degradation as a result of infection (Moshe et al. 2012; Alexander and Cilia 2016). In Arabidopsis, fumaric acid is believed to be the link between NOA1 and NO, because fumaric acid and L-arginine are by-products of the breakdown of arginosuccinic acid by arginosuccinic acid lyase during the urea cycle. An increase in fumaric acid can mirror an increase in L-arginine, resulting in a potential increase in NO produced from the conversion of L-arginine to L-citrulline in a mammalian NOS-like pathway (Van Ree et al. 2011). There was a significant downregulation (-7.37 $\log_2$ fold change) of fumaric acid in SACMV-infected leaves compared with wild type. Fumaric acid could not be detected in infected cassava T200 even though fumaric acid is produced in cassava (Uarrota et al. 2016), it is possible that fumaric acids levels in cassava were below the detection levels for GC-MS.

The level of glucose increased in infected *N. benthamiana* in comparison to mock samples, but not in cassava T200 (table 3-4). The increase in plant hexoses in response to viral infection has previously been reported and is believed to be due to sucrose degradation or changes in sucrose localization (Berger et al. 2007; Sade et al. 2013). Sucrose is believed to be besides NO, a major signalling molecule involved in plant pathogen interactions (Bolouri-Moghaddam and Van den Ende 2012; Tauzin and Giardina 2014) and although we didn't measure sucrose, it is

believed to play a role as a signalling molecule in response to geminiviral infection and sucrose metabolism disturbance is a known occurrence during SACMV infection (Allie and Rey 2013; Allie et al. 2014). Whether it be sucrose degradation or changes in its localization, the disturbance in sucrose metabolism may indirectly play a role in NO reduction and reduction of NOA1 expression 28 dpi in SACMV-infected *N. benthamiana*. When it comes to cassava T200 however, the relationship between NO, NOA1 and sucrose metabolism is not clear, and further experiments will need to be performed.

The increase of glucose in *N. benthamiana* was paralleled generally to an increase in most organic acids detected including citric acid cycle intermediates malic and succinic acid. In cassava T200 however, there was a decrease in succinic acid and no change in the malic acid, suggesting that in cassava T200, the citric acid output could be affected differently to that in *N. benthamiana,* and perhaps the difference in the metabolites accumulation could contribute to the different results obtained in terms of NO availability in cassava T200 when compared to *N. benthamiana.* Succinic acid is a close relative of fumaric acid is part of the citric acid cycle, the GABA shunt, glyoxylate cycle and the electron transport chain, and each of these pathways can contribute to as well as decrease NO availability.

3.5 Conclusions

In this study we provide evidence to show that NO plays an indirect role in SACMV infection and symptoms in both cassava T200 and *N. benthamiana*. While in cassava T200 we could not provide evidence to conclusively link NO and *MeNOA1* to fumaric acid or other TCA organic acids or sugars, in *N. benthamiana* the link between reduced chlorophyll, fumaric acid, NO accumulation, *NbNOA1*, and increased TCA-associated GABA, succinic and malic acids, galactose, mannose and glucose, strongly suggests a role for these factors in SACMV symptoms and pathogenicity. Taken together, the decrease in *NOA1* expression, and inferred decrease in protein translation, chlorophyll and carotenoids accumulation as well as NO abundance observed in *N. benthamiana* is similar to the *noa*1 study in Arabidopsis where *atnoa*1 mutants accumulated less NO concurrently to low fumaric acid, had pale green leaves and reduced chlorophyll content (Van Ree et al. 2011).

Unlike in *N. benthamiana,* the relationship between *MeNOA1,* NO and fumaric acid is not as clear in cassava T200, and further investigation is required. Future studies would need to look at factors relating to respiratory pathways as well as its intermediates, and examine the role of NO and photosynthesis in SACMV-host pathogenicity. NO is also known to be an inducer or suppressor of salicylic acid (SA) biosynthesis which is also produced in the chloroplast (Mur et al. 2013), and it would be useful in future research to ascertain whether NO has an indirect effect on SA repression leading to impaired plant defence against SACMV. Since NOA1 is a member of the cGTPase family located in the chloroplast, more insights into translation, photosynthesis and other metabolic pathways, and their co-ordinated regulation between the chloroplast and the nucleus will prove interesting.

We provide a diagram (figure 3-12) for *N. benthamiana* which illustrates a proposed model for SACMV, NO and NbNOA1/cGTPase and pathogenicity. This study also for the first time has identified MeNOA1 homologues in cassava, and has made the first association of NO and MeNOA1/cGTPase involvement in a geminivirus infection.

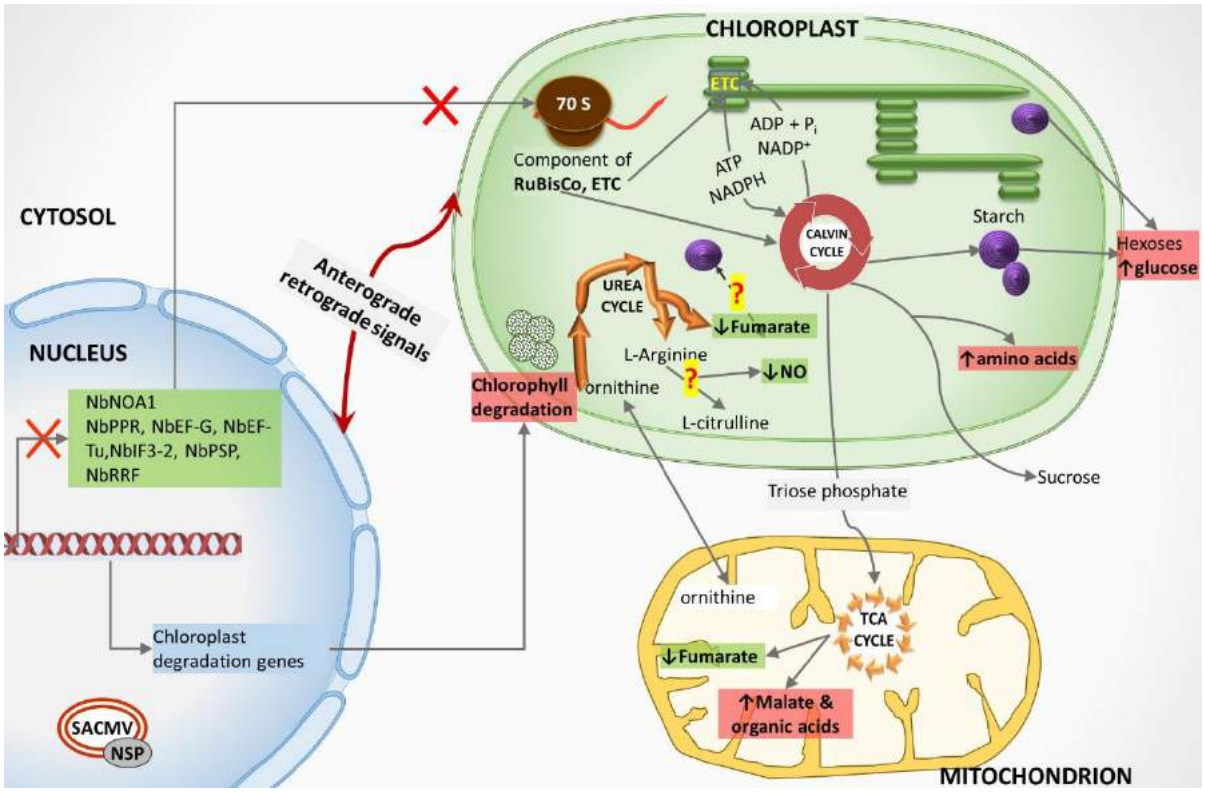

Figure 3-12: Proposed model of *NbNOA1* involvement in SACMV response at 28 dpi

Highlighted in red boxes are components that are increased, and in green, those that we show to be suppressed or decreased. The presence of SACMV in the cells triggers the downregulation of translation factors *NbNOA1*, *NbPPR*, *NbEF*-G, *NbEF*-Tu, *NbIF3*-2, *NbPSP* and *NbRRF*. It is proposed that this leads to the suppression of translation of components of the electron transport chain (ETC) in the chloroplast and RuBisCo, alongside a decrease in chlorophyll and carotenoids accumulation in SACMV-infected leaves. The downstream effect of the downregulation of translation in chloroplast could be amongst others, the dysregulation of Calvin cycle and the ETC in the chloroplast, as well as the dysregulation of the citric acid cycle (TCA) leading to an increase in some TCA related organic metabolites. Glucose, mannose and galactose levels were increased, indicating a possible reduction in carbon storage whilst the levels of fumarate and nitric oxide (NO) were lower in SACMV-infected leaves.

Chapter 4. Final discussions and conclusions

The question on how to prevent disease cannot be answered without knowledge and understanding of the mechanism of cassava mosaic virus-host interactions, both susceptible and resistant. The goal of the current study was the identification of genes directly or indirectly involved in virus-host interactions. The main concern was looking at south african cassava mosaic (SACMV) interactions with host factors involved in virus movement. The plant cytoskeleton was an ideal candidate because it is known that cytoskeletal proteins, particularly myosins are involved in cellular dynamics, rearranging organelles and moving vesicles from the endoplasmic reticulum, to Golgi sacks and back.

Most of the evidence of geminivirus movement available to date has established a link between the movement protein and the plant's endomembrane system (Lewis and Lazarowitz 2010; Lozano-Durán et al. 2011). Movement of plant viruses is said to follow a convergent evolution approach (Rojas et al. 2016) and to date, although no myosins has been directly connected to geminivirus movement, different RNA viruses have (Amari et al. 2014). A VIGS based approach was used to silence five different myosins and evaluate the effect that downregulation in myosin expression would have on SACMV infectivity. This was in order to select candidate myosins for further research, using either a microscopic approach, or a yeast to hybrid affinity approach. The VIGS approach was also used as a tool to compare the efficiency of myosin silencing between SACMV-VIGS constructs and TRV-VIGS constructs in *Nicotiana benthamiana* plants challenged with SACMV in order to establish whether or not, it would be appropriate to use SACMV VIGS vector for cassava mosaic geminiviruses responses in cassava, as TRV and other non-cassava geminiviruses VIGS vector presently available are unsuitable as they do not infect cassava.

Using a TRV-VIGS based approach we successfully reduced the expression of *NbXI-F* and *NbXI-K* and this is to our knowledge, the first study linking myosin expression and activity to cassava geminivirus infectivity. The reduction in *NbXI-K* resulted in decreased spread of SACMV, however the accumulation of SACMV was not different. NbXI-K is the main myosin in charge of

vesicular movement, and it works cooperatively with myosin XI-2 and XI-1 (Avisar et al. 2008b) and decrease in viral spread in plants with a reduction in *NbXI-K* suggests that SACMV moves using an endomembrane system that rides along myosin NbXI-K.

Results from our study also revealed an increase in *NbXI-F* expression at 28 dpi in *N. benthamiana* plants challenged with SACMV and silencing of *NbXI-F* using a TRV-VIGS approach affected both the spread and accumulation of SACMV, suggesting that *NbXI-F* may play a role in virus resistance in *N. benthamiana*. The significance of NbXI-F involvement in SACMV infectivity is not clear at this point because unlike NbXI-K, NbXI-F doesn't mediate vesicular transport (Avisar et al. 2008b; Harries et al. 2009). NbXI-F is found to be associated with stromules protruding from chloroplasts (Sattarzadeh et al. 2009) and induction of stromules formation has been noted in response to abutilon mosaic virus (AbMV) infection (Krenz et al. 2012). Upregulation of *NbXI-F* in response to SACMV-challenge suggests a possible induction in stromules production and the decrease in viral accumulation and spread observed in plants with a reduced *NbXI-F* expression suggests that unlike for N-mediated responses where the induction in stromules production is believed to boost resistance (Caplan et al. 2015; Ho and Theg 2016), in the case of SACMV, stromules formation benefits the virus.

Comparisons in the silencing efficiencies of SACMV-VIGS constructs and TRV-VIGS constructs revealed that silencing of myosin induced by TRV-VIGS was stronger than that of SACMV-VIGS in plants not challenged with SACMV. In SACMV-challenged plants the efficacy of both vectors was decreased, and silencing of myosin using TRV-VIGS constructs resulted in a reduction in expression of *NbXI-F* and *NbXI-K* at 28 dpi, whilst silencing of myosin by SACMV VIGS constructs reduced the expression of *NbXI-F* at 14 and 28 dpi. The presence of SACMV-VIGS vector and constructs resulted in lower viral load at 14 and 28 dpi, compared to untreated SACMV-challenged plants, and the decrease in viral load was unrelated to myosin expression. The presence of TRV-VIGS vector and constructs resulted in lower viral load than untreated SACMV-challenged plants load at 14 dpi and this decrease in viral load was also unrelated to decrease in myosin expression. At 28 dpi, there was no difference between viral load accumulated by TRV-

VIGS plants challenged with SACMV and untreated plants challenged with SACMV suggesting that TRV-VIGS vector plant had recovered.

From this study, we propose that the underlying mechanism of perceived resistance/tolerance is RNA silencing based and inoculation of plants using the SACMV-VIGS vector primes the plants against SACMV, resulting in lower viral accumulation. Inoculation of plants with TRV-VIGS vector also induces RNA-silencing responses which at the early time point affects the SACMV viral accumulation, however by 28 dpi, viral accumulation is no longer affected.

Although VIGS is a less laborious functional genomics method to use, in this study we show that there is more to silencing induced by VIGS as both SACMV and TRV-VIGS vector affected SACMV infectivity albeit differently. Although the effect of VIGS vector on infectivity of the challenging virus for has previously been described as insignificant (Luna et al. 2006), the effect of SACMV-VIGS vector on viral load accumulation is not and these results raise concerns on the suitability of using SACMV-VIGS vector for cassava geminiviruses studies in cassava.

In terms of myosin involvement in SACMV infectivity, protein interactions studies would prove useful in shedding light on the nature of an interaction if any between the two different myosins and SACMV viral molecules. Whilst the results from NbXI-K support a role for vesicles and the endomembrane system in SACMV trafficking, it would be interesting to know whether the chloroplast is central the relationship between myosin *NbXI-F* and SACMV. Future studies could consist of immunolocalization of myosins and SACMV, as well as a time course analysis of SACMV infectivity to visualise potential myosin mediated movement of SACMV viral particles. It would also be interesting to note whether silencing of the different myosins affects the expression of other cytoskeletal proteins, such as actin or tubulin.

The second part of this study assessed the role that the cGTPase nitric oxide associated protein 1 (NOA1) play in susceptibility responses to SACMV. Although our interest into NOA1 stemmed from its indirect link to nitric oxide (NO), results from this study implicates the chloroplast in disease development and progression in *N. benthamiana* and cassava T200.

The multitask nature of NO and the ubiquity of its functions has made its role in pathogenicity or defence in plants highly elusive. At best, most studies show an association between NOA1 and NO (Guo et al. 2003; Zeidler et al. 2004; Guo and Crawford 2005; Bright et al. 2006; Zhao et al. 2007; Chen et al. 2010), and NO and NOA1 and pathogen defence and susceptibility responses (Zeidler et al. 2004). Here in this study we provide further evidence to show that NO plays an indirect role in SACMV infection and symptoms in both cassava T200 and *N. benthamiana*.

While in cassava T200 we could not provide enough correlative evidence to conclusively link NO and *MeNOA1* to fumaric acid or other TCA organic acids or sugars, in *N. benthamiana* the correlation between reduced chlorophyll, fumaric acid, NO accumulation, *NbNOA1*, and increased TCA-associated GABA, succinic and malic acids, galactose, mannose and glucose, strongly suggests a role for these factors in SACMV symptoms and pathogenicity. Taken together, the decrease in *NOA1* expression, and inferred decrease in protein translation, chlorophyll and carotenoids accumulation as well as NO abundance observed in *N. benthamiana* is similar to the *noa*1 study in Arabidopsis where *atnoa*1 mutants accumulated less NO concurrently to low fumaric acid, had pale green leaves and reduced chlorophyll content (Van Ree et al. 2011).

Unlike in *N. benthamiana,* the relationship between *MeNOA1,* NO and fumaric acid is not as clear in cassava T200, and further investigation is required. Future studies would need to look at factors relating to respiratory pathways as well as its intermediates, and examine the role of NO and photosynthesis in SACMV-host pathogenicity. NO is also known to be an inducer or suppressor of salicylic acid (SA) biosynthesis which is also produced in the chloroplast (Mur et al. 2013), and it would be useful in future research to ascertain whether NO has an indirect effect on SA repression leading to impaired plant defence against SACMV. Since it is currently known that NOA1 is a member of the cGTPase family located in the chloroplast, now confirmed *in silico* in this study, more insights into translation, photosynthesis and other metabolic pathways, and their co-ordinated regulation between the chloroplast and the nucleus will prove interesting. Since most NOA1 studies have been performed in the experimental hosts

Arabidopsis and *N. benthamiana*, further studies comparing an experimental annual host with a natural perennial host will prove both exciting and invaluable. Both the chloroplast and the mitochondrion are known sources of NO production and scavenging, and in their mutual relationship possibly lies some answers to the indirect link between NOA1 and NO. Unravelling the networking and signalling between chloroplast, nucleus and mitochondrion organelles is crucial to understand the elusive NO response in both wild type and virus infected plant hosts.

Chapter 5. References

Agbeci M, Grangeon R, Nelson RS, et al (2013) Contribution of host intracellular transport machineries to intercellular movement of turnip mosaic virus. PLoS Pathogens 9:1–16.

Agurla S, Gayatri G, Raghavendra AS (2014) Nitric oxide as a secondary messenger during stomatal closure as a part of plant immunity response against pathogens. Nitric Oxide 43C:89–96.

Alderton WK, Cooper CE, Knowles RG (2001) Nitric oxide synthases: structure, function and inhibition. Biochemical Journal 615:593–615.

Alexander MM, Cilia M (2016) A molecular tug-of-war: Global plant proteome changes during viral infection. Current Plant Biology 5:13–24.

Allie F, Pierce EJ, Okoniewski MJ, et al (2014) Transcriptional analysis of south african cassava mosaic virus -infected susceptible and tolerant landraces of cassava highlights differences in resistance, basal defense and cell wall associated genes during infection. BMC Genomics. doi: 10.1186/1471-2164-15-1006

Allie F, Rey MEC (2013) Transcriptional alterations in model host, *Nicotiana benthamiana*, in response to infection by south african cassava mosaic virus. Eur J Plant Pathol. doi: 10.1007/s10658-013-0286-4

Amari K, Di Donato M, Dolja V V, Heinlein M (2014) Myosins VIII and XI play distinct roles in reproduction and transport of tobacco mosaic virus. PLoS pathogens 10:e1004448.

Amari K, Lerich A, Schmitt-Keichinger C, et al (2011) Tubule-guided cell-to-cell movement of a plant virus requires class XI myosin motors. PLoS pathogens 7:e1002327.

Anand B, Surana P, Bhogaraju S, et al (2009) Circularly permuted GTPase YqeH binds 30S ribosomal subunit: Implications for its role in ribosome assembly. Biochemical and Biophysical Research Communications 386:602–606.

Anand B, Surana P, Prakash B (2010) Deciphering the catalytic machinery in 30S ribosome assembly GTPase YqeH. PloS one 5:e9944.

Arasimowicz-Jelonek M, Floryszak-wieczorek J (2007) Nitric oxide as a bioactive signalling molecule in plant stress responses. Plant Science 172:876–887.

Aregger M, Borah BK, Seguin J, et al (2012) Primary and Secondary siRNAs in Geminivirus-induced Gene Silencing. PLoS Pathog. doi: 10.1371/journal.ppat.1002941

Avisar D, Abu-Abied M, Belausov E, Sadot E (2012) Myosin XIK is a major player in cytoplasm dynamics and is regulated by two amino acids in its tail. Journal of Experimental Botany 63:241–249.

Avisar D, Prokhnevsky AI, Dolja V V (2008a) Class VIII myosins are required for plasmodesmatal localization of a closterovirus Hsp70 homolog. Journal of virology 82:2836–2843.

Avisar D, Prokhnevsky AI, Makarova KS, et al (2008b) Myosin XI-K Is required for rapid trafficking of Golgi stacks, peroxisomes, and mitochondria in leaf cells of *Nicotiana benthamiana*. Plant Physiology 146:1098–1108.

Beale SI (1999) Enzymes of chlorophyll biosynthesis. Photosynthesis Research 60:43–73.

Bellin D, Asai S, Delledonne M, Yoshioka H (2013) Nitric oxide as a mediator for defense responses. Molecular Plant-Microbe Interactions 26:271–277.

Berger S, Sinha AK, Roitsch T (2007) Plant physiology meets phytopathology: Plant primary metabolism and plant-pathogen interactions. Journal of Experimental Botany 58:4019–4026.

Berrie LC, Rybicki EP, Rey M (2001) Complete nucleotide sequence and host range of South African cassava mosaic virus: further evidence for recombination amongst begomoviruses. Journal of General Virology 82:53–58.

Berry S, Rey MEC (2001) Molecular evidence for diverse populations of cassava-infecting begomoviruses in southern Africa. Archives of Virology 146:1795–1802.

Besson-Bard A, Astier J, Rasul S, et al (2009) Current view of nitric oxide-responsive genes in plants. Plant Science 177:302–309.

Beyene G, Chauhan RD, Taylor NJ (2017) A rapid virus-induced gene silencing (VIGS) method for assessing resistance and susceptibility to cassava mosaic disease. Virology Journal 14:47.

Bhat S, Folimonova SY, Cole A. B, et al (2012) Influence of host chloroplast proteins on Tobacco mosaic virus accumulation and intercellular movement. Plant Physiology 161:134–147.

Bhattacharyya D, Chakraborty S (2017) Chloroplast: The Trojan Horse in Plant-Virus Interaction. Molecular Plant Pathology 13:385–392.

Bhattacharyya D, Gnanasekaran P, Kumar RK, et al (2015) A geminivirus betasatellite damages the structural and functional integrity of chloroplasts leading to symptom formation and inhibition of photosynthesis. Journal of Experimental Botany 66:5881–5895.

Bieri S, Potrykus I, Fütterer J (2002) Geminivirus sequences as bidirectional transcription termination/polyadenylation signals for economic construction of stably expressed transgenes. Molecular Breeding 10:107–117.

Bisaro DM (2006) Silencing suppression by geminivirus proteins. Virology 344:158–168.

Bobik K, Burch-Smith TM (2015) Chloroplast signaling within, between and beyond cells. Frontiers in Plant Science 6:781.

Bolouri-Moghaddam MR, Van den Ende W (2012) Sugars and plant innate immunity. Journal of Experimental Botany 63:3989–3998.

Bombarely A, Menda N, Tecle IY, et al (2011) The sol genomics network (solgenomics.net): Growing tomatoes using Perl. Nucleic Acids Research 39:1149–1155.

Brandizzi F, Snapp EL, Roberts AG, et al (2002) Membrane protein transport between the endoplasmic reticulum and the Golgi in tobacco leaves is energy dependent but cytoskeleton independent: evidence from selective photobleaching. The Plant Cell 14:1293–1309.

Bredeson J V, Lyons JB, Prochnik SE, et al (2016) Sequencing wild and cultivated cassava and related species reveals extensive interspecific hybridization and genetic diversity. Nature Biotechnology 34:562–570.

Briddon RW, Robertson I, Markham PG, Stanley J (2004) Occurrence of South African cassava mosaic virus (SACMV) in Zimbabwe. Plant Pathology 53:233.

Bright J, Desikan R, Hancock JT, et al (2006) ABA-induced NO generation and stomatal closure in Arabidopsis are dependent on H2O2 synthesis. The Plant Journal 45:113–22.

Britton RA (2009) Role of GTPases in bacterial ribosome assembly. Annual review of microbiology 63:155–76.

Brown JK, Frohlich D., Rosell RC (1995) The sweet potato or silver leaf whiteflies: biotypes of *Bemisia tabaci* (Genn.), or a species complex? Annual Review of Entomology 40:511–534.

Brown JK, Zerbini FM, Navas-Castillo J, et al (2015) Revision of Begomovirus taxonomy based on pairwise sequence comparisons. Archives of Virology 160:1593–1619.

Brunkard JO, Runkel AM, Zambryski PC (2015) Chloroplasts extend stromules independently and in response to internal redox signals. Proceedings of the National Academy of Sciences 112:10044–10049.

Bull SE, Ndunguru J, Gruissem W, et al (2011) Cassava: constraints to production and the transfer of biotechnology to African laboratories. Plant cell reports 30:779–787.

Calcagno C, Novero M, Genre A, et al (2012) The exudate from an arbuscular mycorrhizal fungus induces nitric oxide accumulation in *Medicago truncatula* roots. Mycorrhiza 22:259–269.

Calvert LA, Cuervo M, Lozano I, et al (2008) Identification of three strains of a virus associated with cassava plants affected by frogskin disease. Journal of Phytopathology 156:647–653.

Calvert LA, Thresh JM (2002) The viruses and virus diseases of cassava. In: Hillocks RJ, Thresh JM, Bellotti AC (eds) Cassava: Biology, Production and Utilization. CAB International 2002, pp 237–260

Campbell T, Daigle D, Brown E (2005) Characterization of the *Bacillus subtilis* GTPase YloQ and its role in ribosome function. Biochemical Journal 852:843–852.

Caplan JL, Sampath Kumar A, Modla S, et al (2015) Chloroplast stromules function during innate immunity. Developmental Cell 34:45–57.

Carvajal-Yepes M, Olaya C, Lozano I, et al (2014) Unraveling complex viral infections in cassava (*Manihot esculenta* Crantz) from Colombia. Virus Research 186:76–86.

Carvalho CM, Fontenelle MR, Florentino LHLH, et al (2008a) A novel nucleocytoplasmic traffic GTPase identified as a functional target of the bipartite geminivirus nuclear shuttle protein. The Plant Journal 55:869–880.

Carvalho CM, Machado JPB, Zerbini FM, Fontes EPB (2008b) NSP-interacting GTPase. A cytosolic protein as cofactor for nuclear shuttle proteins. Plant Signaling & Behavior 3:752–754.

Carvalho CM, Santos AA, Pires SR, et al (2008c) Regulated nuclear trafficking of rpL10A mediated by NIK1 represents a defense strategy of plant cells against virus. PLoS Pathogens 4:e1000247.

Carvalho MF, Lazarowitz SG (2004) Interaction of the movement protein NSP and the Arabidopsis acetyltransferase AtNSI is necessary for cabbage leaf curl geminivirus infection and pathogenicity. Journal of virology 78:11161–11171.

Carvalho MF, Turgeon R, Lazarowitz SG (2006) The geminivirus nuclear shuttle protein NSP inhibits the activity of AtNSI, a vascular-expressed Arabidopsis acetyltransferase regulated with the sink-to-source transition. Plant Physiology 140:1317–1330.

Cecconi D, Orzetti S, Vandelle E, et al (2009) Protein nitration during defense response in *Arabidopsis thaliana*. Electrophoresis 30:2460–2468.

Chaki M, Valderrama R, Fernández-Ocaña AM, et al (2009) Protein targets of tyrosine nitration in sunflower (*Helianthus annuus* L.) hypocotyls. Journal of Experimental Botany 60:4221–4234.

Chandra-Shekara AC, Gupte M, Navarre D, et al (2006) Light-dependent hypersensitive response and resistance signaling against Turnip Crinkle Virus in Arabidopsis. Plant Journal 45:320–334.

Chandran SA, Levy Y, Mett A, et al (2012) Mapping of functional region conferring nuclear localization and karyopherin @-binding activity of the C2 protein of bhendi yellow vein mosaic virus. Journal of General Virology 93:1367–1374.

Chatterjee A, Kundu S (2015) Revisiting the chlorophyll biosynthesis pathway using genome scale metabolic model of *Oryza sativa* japonica. Scientific reports 5:14975.

Chen J, Deng F, Deng M, et al (2016) Identification and characterization of a chloroplast-targeted obg gtpase in dendrobium officinale. DNA and cell biology 35:1–10.

Chen M, Tian G, Gafni Y, Citovsky V (2005) Effects of Calreticulin on viral cell-to-cell movement. Plant Physiology 138:1866–1876.

Chen WW, Yang JL, Qin C, et al (2010) Nitric oxide acts downstream of auxin to trigger root ferric-chelate reductase activity in response to iron deficiency in Arabidopsis. Plant Physiology 154:810–819.

Chia DW, Yoder TJ, Reiter W-D, Gibson SI (2000) Fumaric acid: an overlooked form of fixed carbon in Arabidopsis and other plant species. Planta 211:743–751.

Chou K-C, Shen H-B (2010) Plant-mPloc: a top-down strategy to augment the power for predicting plant protein subcellular localization. PloS one 5:e11335.

Clarke A, Desikan R, Hurst RD, et al (2000) NO way back: nitric oxide and programmed cell death in *Arabidopsis thaliana* suspension cultures. The Plant Journal 24:667–677.

Corpas FJ, Barroso JB (2014) Peroxisomal plant nitric oxide synthase (NOS) protein is imported by peroxisomal targeting signal type 2 (PTS2) in a process that depends on the cytosolic receptor PEX7 and calmodulin. FEBS letters 588:2049–2054.

Corpas FJ, Palma JM, del Río LA, Barroso JB (2009) Evidence supporting the existence of L-arginine-dependent nitric oxide synthase activity in plants. The New phytologist 184:9–14.

Correa-aragunde N, Foresi N, Lamattina L (2013) Structure diversity of nitric oxide synthases (NOS): the emergence of new forms in photosynthetic organisms. Frontiers in Plant Science 4:1–3.

Costa A (1940) Observacoes sobre o mosaico comun e o mosaico das nervuras da mandioca (*Manihot ultissima* Pohl). Journal Agronomia (Piracicaba) 3:239–248.

Crawford NM, Guo F (2005) New insights into nitric oxide metabolism and regulatory functions. Trends in Plant Science 10:195–200.

Csorba T, Kontra L, Burgyán J (2015) Viral silencing suppressors: Tools forged to fine-tune host-pathogen coexistence. Virology 85–103.

Cui H, Tsuda K, Parker JE (2015) Effector-triggered immunity: from pathogen perception to robust defense. 1–25.

Czosnek H, Eybishtz A, Sade D, et al (2013) Discovering host genes involved in the infection by the tomato yellow leaf curl virus complex and in the establishment of resistance to the virus using tobacco rattle virus-based post transcriptional gene silencing. Viruses 5:998–1022.

Dean J V, Harper JE (1988) The conversion of nitrite to nitrogen oxide(s) by the constitutive NAD(P)H-nitrate reductase enzyme from soybean. Plant Physiology 88:389–395.

de Torres Zabala M, Littlejohn G, Jayaraman S, et al (2015) Chloroplasts play a central role in plant defence and are targeted by pathogen effectors. Nature Plants 1:15074.

del Río LA, Corpas FJ, Barroso JB (2004) Nitric oxide and nitric oxide synthase activity in plants. Phytochemistry 65:783–792.

Delledonne M, Xia Y, Dixon RA, Lamb C (1998) Nitric oxide functions as a signal in plant disease resistance. Nature 394:585–588.

Deng X, Kelloniemi J, Haikonen T, et al (2013) Modification of Tobacco rattle virus RNA1 to serve as a VIGS vector reveals that the 29K movement protein is an RNA silencing suppressor of the virus. Molecular Plant-Microbe Interactions 26:503–514.

Desender S, Andrivon D, Val F (2007) Activation of defence reactions in Solanaceae: where is the specificity? Cellular microbiology 9:21–30.

Desikan R, Griffiths R, Hancock JT, Neill S (2002) A new role for an old enzyme: nitrate reductase-mediated nitric oxide generation is required for abscisic acid-induced stomatal closure in *Arabidopsis thaliana*. Proceedings of the National Academy of Sciences 99:16314–16318.

Domingos P, Prado AM, Wong A, et al (2015) Nitric oxide: A multitasked signaling gas in plants. Molecular Plant 8:506–520.

Doyle J, Doyle J (1987) A rapid DNA isolation procedure for small quantities of fresh leaf tissue. Phytochemical Bulletin 19:11–15.

Durner J, Wendehenne D, Klessig DF (1998) Defense gene induction in tobacco by nitric oxide, cyclic GMP, and cyclic ADP-ribose. Proceedings of the National Academy of Sciences 95:10328–10333.

Emanuelsson O, Brunak S, Heijne G Von, Nielsen H (2007) Locating proteins in the cell using TargetP, SignalP and related tools. Nature Protocols 2:953–971.

Erb M, Meldau S, Howe G a. (2012) Role of phytohormones in insect-specific plant reactions. Trends in Plant Science 17:250–259.

Faigon-Soverna A, Harmon FG, Storani L, et al (2006) A constitutive shade-avoidance mutant implicates TIR-NBS-LRR Proteins in Arabidopsis photomorphogenic development. The Plant Cell 18:2919–2928.

Fauquet CM, Fargette D (1990) African cassava mosaic virus: etiology, epidemiology, and control. Plant Disease 74:404–411.

Felsenstein J (1985) Confidence-limits on phylogenies - an approach using the bootstrap. Evolution 39:783–791.

Fernandez-Pozo N, Rosli HG, Martin GB, Mueller LA (2015) The SGN VIGS tool: User-friendly software to design virus-induced gene silencing (VIGS) Constructs for functional genomics. Molecular Plant 8:486–488.

Flores-Pérez U, Sauret-Güeto S, Gas E, et al (2008) A mutant impaired in the production of plastome-encoded proteins uncovers a mechanism for the homeostasis of isoprenoid biosynthetic enzymes in Arabidopsis plastids. The Plant Cell 20:1303–1315.

Flores T, Todd CD, Tovar-Mendez A, et al (2008) Arginase-negative mutants of Arabidopsis exhibit increased nitric oxide signaling in root development. Plant Physiology 147:1936–1946.

Fofana IBF, Sangaré A, Collier R, et al (2004) A geminivirus-induced gene silencing system for gene function validation in cassava. Plant Molecular Biology 56:613–624.

Foissner I, Wendehenne D, Langebartels C, Durner J (2000) In vivo imaging of an elicitor-induced nitric oxide burst in tobacco. The Plant Journal 23:817–824.

Fondong VN (2013) Geminivirus protein structure and function. Molecular plant pathology 1–15.

Fontes EPB, Santos AA, Luz DF, et al (2004) The geminivirus nuclear shuttle protein is a virulence factor that suppresses transmembrane receptor kinase activity. Genes & development 18:2545–2556.

Foresi N, Correa-Aragunde N, Parisi G, et al (2010) Characterization of a nitric oxide synthase from the plant kingdom: NO generation from the green alga Ostreococcus tauri is light irradiance and growth phase dependent. The Plant Cell 22:3816–3830.

Foth BJ, Goedecke MC, Soldati D (2006) New insights into myosin evolution and classification. Proceedings of the National Academy of Sciences 103:3681–3686.

Frischmuth S, Wege C, Hülser D, Jeske H (2007) The movement protein BC1 promotes redirection of the nuclear shuttle protein BV1 of Abutilon mosaic geminivirus to the plasma membrane in fission yeast. Protoplasma 230:117–123.

Friso G, Majeran W, Huang M, et al (2010) Reconstruction of metabolic pathways, protein expression, and homeostasis machineries across maize bundle sheath and mesophyll chloroplasts: large-scale quantitative proteomics using the first maize genome assembly. Plant Physiology 152:1219–1250.

Fröhlich A, Durner J (2011) The hunt for plant nitric oxide synthase (NOS): is one really needed? Plant science : an international journal of experimental plant biology 181:401–4.

Fu L-J, Shi K, Gu M, et al (2010) Systemic induction and role of mitochondrial alternative oxidase and nitric oxide in a compatible tomato-tobacco mosaic virus interaction. Molecular Plant-Microbe Interactions 23:39–48.

Fu ZQ, Dong X (2013) Systemic acquired resistance: turning local infection into global defense. Annual review of plant biology 64:839–863.

Funayama S, Sonoike K, Terashima I (1997) Photosynthetic properties of leaves of *Eupatorium makinoi* infected by a geminivirus. Photosynthesis Research 53:253–261.

Gafni Y, Epel BL (2002) The role of host and viral proteins in intra- and inter-cellular trafficking of geminiviruses. Physiological and Molecular Plant Pathology 60:231–241.

Garrido-Ramirez ER, Sudarshana MR, Lucas WJ, Gilbertson RL (2000) Bean dwarf mosaic virus BV1 Protein Is a Determinant of the Hypersensitive Response and Avirulence in *Phaseolus vulgaris*. Molecular Plant-Microbe Interactions 13:1184–1194.

Gas E, Flores-Pérez U, Sauret-Güeto S, Rodríguez-Concepción M (2009) Hunting for plant nitric oxide synthase provides new evidence of a central role for plastids in nitric oxide metabolism. The Plant Cell 21:18–23.

Golenberg EM, Sather DN, Hancock LC, et al (2009) Development of a gene silencing DNA vector derived from a broad host range geminivirus. Plant Methods 5:9.

Golomb L, Abu-Abied M, Belausov E, Sadot E (2008) Different subcellular localizations and functions of Arabidopsis myosin VIII. BMC plant biology 8:3.

Gorovits R, Moshe A, Ghanim M, Czosnek H (2013) Recruitment of the host plant heat shock protein 70 by tomato yellow leaf curl virus coat protein is required for virus infection. PloS one 8:e70280.

Gosselé V, Faché I, Meulewaeter F, et al (2002) SVISS - a novel transient gene silencing system for gene function discovery and validation in tobacco plants. The Plant Journal 32:859–866.

Gotte G, Amelio E, Russo S, et al (2002) Short-time non-enzymatic nitric oxide synthesis from L - arginine and hydrogen peroxide induced by shock waves treatment. FEBS Letters 520:153–155.

Graziosi I, Minato N, Alvarez E, et al (2016) Emerging pests and diseases of South-east Asian cassava: A comprehensive evaluation of geographic priorities, management options and research needs. Pest Management Science 72:1071–1089.

Gröning BR, Abouzid A, Jeske H (1987) Single-stranded DNA from abutilon mosaic virus is present in the plastids of infected *Abutilon sellovianum*. Proceedings of the National Academy of Sciences 84:8996–9000.

Grün S, Lindermayr C, Sell S, Durner J (2006) Nitric oxide and gene regulation in plants. Journal of Experimental Botany 57:507–516.

Guerra-Peraza O, Kirk D, Seltzer V, et al (2005) Coat proteins of Rice tungro bacilliform virus and mungbean yellow mosaic virus contain multiple nuclear-localization signals and interact with importin α. Journal of General Virology 86:1815–1826.

Guo F, Crawford NM (2005) Arabidopsis nitric oxide synthase1 is targeted to mitochondria and protects against oxidative damage and dark-induced senescence. The Plant Cell 17:3436–3450.

Guo F, Okamoto M, Crawford NM (2003) Identification of a plant nitric oxide synthase gene involved in hormonal signaling. Science (New York, NY) 302:100–103.

Gupta KJ, Fernie AR, Kaiser WM, van Dongen JT (2011a) On the origins of nitric oxide. Trends in Plant Science 16:16016–16018.

Gupta KJ, Igamberdiev AU, Manjunatha G, et al (2011b) The emerging roles of nitric oxide (NO) in plant mitochondria. Plant science : an international journal of experimental plant biology 181:520–6.

Gururani MA, Venkatesh J, Upadhyaya CP, et al (2012) Plant disease resistance genes: Current status and future directions. Physiol. Mol. Plant Pathol. 78:51–65.

Hanley-Bowdoin LK, Bejarano ER, Robertson D, Mansoor S (2013) Geminiviruses: masters at redirecting and reprogramming plant processes. Nature reviews Microbiology 11:777–788.

Haraguchi T, Tominaga M, Matsumoto R, et al (2014) Molecular characterization and subcellular localization of Arabidopsis class viii myosin, ATM1. Journal of Biological Chemistry 289:12343–12355.

Haraguchi T, Tominaga M, Nakano A, et al (2016) Myosin XI-I is mechanically and enzymatically unique among class-XI myosins in Arabidopsis. Plant and Cell Physiology 57:1732–1743.

Harimalala M, Lefeuvre P, De Bruyn A, et al (2012) A novel cassava-infecting begomovirus from Madagascar: cassava mosaic Madagascar virus. Archives of Virology 157:2027–2030.

Harries PA, Ding B (2011) Cellular factors in plant virus movement: at the leading edge of macromolecular trafficking in plants. Virology 411:237–243.

Harries PA, Park J-W, Sasaki N, et al (2009) Differing requirements for actin and myosin by plant viruses for sustained intercellular movement. Proceedings of the National Academy of Sciences 106:17594–17599.

Harries PA, Schoelz JE, Nelson RS (2010) Intracellular transport of viruses and their components: utilizing the cytoskeleton and membrane highways. Molecular Plant-Microbe Interactions 23:1381–1393.

Harris EH, Boynton JE, Gillham NW (1994) Chloroplast ribosomes and protein synthesis. Microbiological reviews 58:700–754.

Harrison BD (2002) Begomovirus coat protein: serology, variation and functions. Physiological and Molecular Plant Pathology 60:257–271.

Hehnle S, Wege C, Jeske H (2004) Interaction of DNA with the movement proteins of geminiviruses revisited. Journal of Virology 78:7698–7706.

Heinlein M (2016) Viral Transport and Interaction with the Host Cytoskeleton. In: Plant-Virus Interactions. Springer International Publishing, Cham, pp 39–66

Himeno H, Hanawa-Suetsugu K, Kimura T, et al (2004) A novel GTPase activated by the small subunit of ribosome. Nucleic Acids Research 32:5303–5309.

Hipp K, Schäfer B, Kepp G, Jeske H (2016) Properties of African cassava mosaic virus capsid protein expressed in fission yeast. Viruses. doi: 10.3390/v8070190

Hiriart J-B, Aro E-M, Lehto K (2003) Dynamics of the VIGS-mediated chimeric silencing of the *Nicotiana benthamiana* ChlH gene and of the tobacco mosaic virus vector. Molecular Plant-Microbe Interactions 16:99–106.

Ho J, Theg SM (2016) The formation of stromules in vitro from chloroplasts isolated from *Nicotiana benthamiana*. PLOS ONE 11:e0146489.

Hong JK, Yun B-W, Kang J-G, et al (2008) Nitric oxide function and signalling in plant disease resistance. Journal of Experimental Botany 59:147–154.

Huang C, Xie Y, Zhou X (2009) Efficient virus-induced gene silencing in plants using a modified geminivirus DNA1 component. Plant biotechnology journal 7:254–65.

Huang X, Von Rad U, Durner J (2002) Nitric oxide induces transcriptional activation of the nitric oxide-tolerant alternative oxidase in Arabidopsis suspension cells. Planta 215:914–923.

Hussain M, Mansoor S, Iram S, et al (2005) The nuclear shuttle protein of Tomato leaf curl New Delhi virus is a pathogenicity determinant. Journal of Virology 79:4434–4439.

Igamberdiev AU, Ratcliffe RG, Gupta KJ (2014) Plant mitochondria: Source and target for nitric oxide. Mitochondrion 19:329–333.

Im CH, Hwang SM, Son YS, et al (2011) Nuclear/nucleolar GTPase 2 proteins as a subfamily of YlqF/YawG GTPases function in pre-60S ribosomal subunit maturation of mono- and dicotyledonous plants. The Journal of biological chemistry 286:8620–32.

Ingram GC, Simon R, Carpenter R, Coen ES (1998) The Antirrhinum ERG gene encodes a protein related to bacterial small GTPases and is required for embryonic viability. Current Biology 8:1079–1082.

Janda M, Ruelland E (2014) Magical mystery tour: Salicylic acid signalling. Environmental and Experimental Botany 114:117–128.

Jasid S, Simontacchi M, Bartoli CG, Puntarulo S (2006) Chloroplasts as a nitric oxide cellular source. Effect of reactive nitrogen species on chloroplastic lipids and proteins. Plant Physiology 142:1246–55.

Jeandroz S, Lamotte O, Astier J, et al (2013) There's more to the picture than meets the eye: nitric oxide cross talk with Ca2+ signaling. Plant Physiology 163:459–470.

Jeske H, Lütgemeier M, Preiss W (2001) DNA forms indicate rolling circle and recombination-dependent replication of Abutilon mosaic virus. The EMBO journal 20:6158–6167.

Jian W, Zhang D wei, Zhu F, et al (2016) Alternative oxidase pathway is involved in the exogenous SNP-elevated tolerance of *Medicago truncatula* to salt stress. Journal of Plant Physiology 193:79–87.

Jian W, Zhang D, Zhu F, et al (2015) Nitrate reductase-dependent nitric oxide production is required for regulation alternative oxidase pathway involved in the resistance to Cucumber mosaic virus infection in Arabidopsis. Plant Growth Regulation 77:99–107.

Jones DT, Taylor WR, Thornton JM (1992) The rapid generation of mutation data matrices from protein sequences. Computer applications in the biosciences : CABIOS 8:275–82.

Jones JDG, Dangl JL (2006) The plant immune system. Nature 444:323–329.

Jones L, Keining T, Eamens A, Vaistij FE (2006) Virus-induced gene silencing of argonaute genes in *Nicotiana benthamiana* demonstrates that extensive systemic silencing requires Argonaute1-like and Argonaute4-like genes. Plant Physiology 141:598–606.

Ju Z, Wang L, Cao D, et al (2016) A viral satellite DNA vector-induced transcriptional gene silencing via DNA methylation of gene promoter in *Nicotiana benthamiana*. Virus Research 223:99–107.

Kato H, Asai S, Yamamoto-Katou A, et al (2007) Involvement of NbNOA1 in NO production and defense responses in INF1-treated *Nicotiana benthamiana*. Journal of General Plant Pathology 74:15–23.

Kawakami S, Watanabe Y, Beachy RN (2004) Tobacco mosaic virus infection spreads cell to cell as intact replication complexes. Proceedings of the National Academy of Sciences 101:6291–6296.

Kawakita K (2014) Studies on NO functions in plant defense responses. Journal of General Plant Pathology 80:510–513.

Kelkar V, Kushawaha AK, Dasgupta I (2016) Identification of amino acid residues of the coat protein of Sri Lankan cassava mosaic virus affecting symptom production and viral titer in *Nicotiana benthamiana*. Virus Research 217:38–46.

Kelley LA, Mezulis S, Yates CM, et al (2015) The Phyre2 web portal for protein modeling, prediction and analysis. Nature Protocols 10:845–858.

Kim BH, Malec P, Waloszek A, von Arnim AG (2012) Arabidopsis BPG2: A phytochrome-regulated gene whose protein product binds to plastid ribosomal RNAs. Planta 236:677–690.

Kitajima JP, Costa AS (1979) Rhabdovirus-like particles in tissues of five different plant species. Fitopatologia Brasilera 4:55–62.

Kjemtrup S, Sampson KS, Peele CG, et al (1998) Gene silencing from plant DNA carried by a geminivirus. The Plant Journal 14:91–100.

Kleinow T, Holeiter G, Nischang M, et al (2008) Post-translational modifications of Abutilon mosaic virus movement protein (BC1) in fission yeast. Virus research 131:86–94.

Kleinow T, Nischang M, Beck A, et al (2009) Three C-terminal phosphorylation sites in the Abutilon mosaic virus movement protein affect symptom development and viral DNA accumulation. Virology 390:89–101.

Kolanczyk M, Pech M, Zemojtel T, et al (2011) NOA1 is an essential GTPase required for mitochondrial protein synthesis. Molecular biology of the cell 22:1–11.

Kolbert Z, Ortega L, Erdei L (2010) Involvement of nitrate reductase (NR) in osmotic stress-induced NO generation of *Arabidopsis thaliana* L. roots. Journal of Plant Physiology 167:77–80.

Komatsu T, Kawaide H, Saito C, et al (2010) The chloroplast protein BPG2 functions in brassinosteroid-mediated post-transcriptional accumulation of chloroplast rRNA. The Plant Journal 61:409–422.

Kovacs I, Durner J, Lindermayr C (2015) Crosstalk between nitric oxide and glutathione is required for NONEXPRESSOR OF PATHOGENESIS-RELATED GENES 1 (NPR1)-dependent defense signaling in *Arabidopsis thaliana*. New Phytologist 208:860–872.

Krenz B, Jeske H, Kleinow T, et al (2012) The induction of stromule formation by a plant DNA-virus in epidermal leaf tissues suggests a novel intra- and intercellular macromolecular trafficking route. Frontiers in Plant Science 3:1–12.

Krenz B, Windeisen V, Wege C, et al (2010) A plastid-targeted heat shock cognate 70kDa protein interacts with the Abutilon mosaic virus movement protein. Virology 401:6–17.

Kumagai MH, Donson J, Della-Cioppa G, et al (1995) Cytoplasmic inhibition of carotenoid biosynthesis with virus-derived RNA. Proceedings of the National Academy of Sciences 92:1679–1683.

Kumar D, Kumar R, Hyun TK, Kim JY (2014) Cell-to-cell movement of viruses via plasmodesmata. Journal of Plant Research 128:37–47.

Kumar S, Stecher G, Tamura K (2016) MEGA7: Molecular Evolutionary Genetics Analysis Version 7.0 for bigger datasets. Molecular biology and evolution 33:1870–1874.

Kunik T, Mizrachy L, Citovsky V, Gafni Y (1999) Characterization of a tomato karyopherin alpha that interacts with the tomato yellow leaf curl virus (TYLCV) capsid protein. Journal of Experimental Botany 50:731–732.

Kwan Y-M, Meon S, Ho C-L, Wong M-Y (2015) Cloning of nitric oxide associated 1 (NOA1) transcript from oil palm (*Elaeis guineensis*) and its expression during Ganoderma infection. Journal of Plant Physiology 174:131–136.

Lacatus G, Sunter G (2009) The Arabidopsis PEAPOD2 transcription factor interacts with geminivirus AL2 protein and the coat protein promoter. Virology 392:196–202.

Lange M, Yellina AL, Orashakova S, Becker A (2013) Virus-Induced Gene Silencing (VIGS) in plants: an overview of target species and the virus-derived vector systems. in: Becker A (ed) virus-induced gene silencing. In: Becker A (ed) Virus-Induced Gene Silencing. Humana Press, Totowa, NJ, pp 1–14

Laxalt AM, Raho N, Ten Have A, Lamattina L (2007) Nitric oxide is critical for inducing phosphatidic acid accumulation in xylanase-elicited tomato cells. Journal of Biological Chemistry 282:21160–21168.

Lazarowitz SG, Wu LC, Rogers SG, Elmer JS (1992) Sequence-specific interaction with the vira1 ALI protein identifies a geminivirus DNA replication origin. The Plant Cell 4:799–809.

Lee YJ, Liu B (2004) Cytoskeletal motors in Arabidopsis. Sixty-one kinesins and seventeen myosins. Plant Physiology 136:3877–3883.

Legg JP, Thresh JM (2000) Cassava mosaic virus disease in East Africa: a dynamic disease in a changing environment. Virus Research 71:135–149.

Lehto K, Tikkanen M, Hiriart J-B, et al (2003) Depletion of the photosystem II core complex in mature tobacco leaves infected by the flavum strain of tobacco mosaic virus. Molecular Plant-Microbe Interactions 16:1135–1144.

Leipe DD, Wolf YI, Koonin E V, Aravind L (2002) Classification and evolution of P-loop GTPases and related ATPases. Journal of molecular biology 317:41–72.

Leitner M, Vandelle E, Gaupels F, et al (2009) NO signals in the haze. Nitric oxide signalling in plant defence. Curr. Opin. Plant Biol. 12:451–458.

Lennon A, Aiton M, Harrison BD (1986) Cassava viruses from South america. In: Annual Report 1985. Scottish crop research institute. p 167

Lennon AM, Aiton MM, Harrison BD (1987) Purification and properties of cassava green mottle, a previously undescribed virus from the Solomon Islands. Annals of Applied Biology 110:545–555.

Levy A, Tzfira T (2010) Bean dwarf mosaic virus: a model system for the study of viral movement. Molecular Plant Pathology 11:451–461.

Lewis JD, Lazarowitz SG (2010) Arabidopsis synaptotagmin SYTA regulates endocytosis and virus movement protein cell-to-cell transport. Proceedings of the National Academy of Sciences 107:2491–2496.

Li F, Xu X, Huang C, et al (2015) The AC5 protein encoded by Mungbean yellow mosaic India virus is a pathogenicity determinant that suppresses RNA silencing-based antiviral defenses. New Phytologist 208:555–569.

Li Z, Liang W-S, Carr JP (2014) Effects of modifying alternative respiration on nitric oxide-induced virus resistance and PR1 protein accumulation. Journal of General Virology 95:2075–2081.

Liao YWK, Sun ZH, Zhou YH, et al (2013) The role of hydrogen peroxide and nitric oxide in the induction of plant-encoded RNA-dependent RNA polymerase 1 in the basal defense against tobacco mosaic virus. Plos ONE 8:1–10.

Lichtenthaler HK, Buschmann C (2001) Chlorophylls and carotenoids: measurement and characterization by UV-VIS spectroscopy. Current Protocols in Food Analytical Chemistry F4.3.1-F4.:1–8.

Lindermayr C (2006) Differential inhibition of Arabidopsis methionine adenosyltransferases by protein s-nitrosylation. Journal of Biological Chemistry 281:4285–4291.

Lisec J, Schauer N, Kopka J, et al (2006) Gas chromatography mass spectrometry-based metabolite profiling in plants. Nature Protocols 1:387–396.

Liu E, Page JE (2008) Optimized cDNA libraries for virus-induced gene silencing (VIGS) using tobacco rattle virus. Plant Methods 4:5.

Liu J, Yang J, Bi H, Zhang P (2014) Why mosaic? Gene expression profiling of African cassava mosaic virus-infected cassava reveals the effect of chlorophyll degradation on symptom development. Journal of integrative plant biology 56:122–132.

Liu Y, Schiff M, Dinesh-Kumar SP (2002a) Virus-induced gene silencing in tomato. The Plant Journal 31:777–86.

Liu Y, Schiff M, Marathe R, Dinesh-Kumar SP (2002b) Tobacco Rar1, EDS1 and NPR1/NIM1 like genes are required for N-mediated resistance to tobacco mosaic virus. Plant Journal 30:415–429.

Locato V, Paradiso A, Sabetta W, et al (2016) Nitric oxide and reactive oxygen species in PCD signaling. Advances in Botanical Research 77:165–192.

Louis B, Rey MEC (2015) Resistance gene analogs involved in tolerant cassava-geminivirus interaction that shows a recovery phenotype. Virus Genes 51:393–407.

Lozano-Durán R, Rosas-Díaz T, Luna AP, Bejarano ER (2011) Identification of host genes involved in geminivirus infection using a reverse genetics approach. PloS one 6:e22383.

Lozano-Juste J, Colom-Moreno R, León J (2011) In vivo protein tyrosine nitration in *Arabidopsis thaliana*. Journal of Experimental Botany 62:3501–3517.

Lucas WJ (2006) Plant viral movement proteins: Agents for cell-to-cell trafficking of viral genomes. Virology 344:169–184.

Luna AP, Morilla G, Voinnet O, Bejarano ER (2006) Functional analysis of gene-silencing suppressors from tomato yellow leaf curl disease viruses. Molecular Plant-Microbe Interactions 25:1294–1306.

Ma W, Smigel A, Tsai Y-C, et al (2008) Innate immunity signaling: cytosolic Ca2+ elevation is linked to downstream nitric oxide generation through the action of calmodulin or a calmodulin-like protein. Plant Physiology 148:818–828.

Maia LB, Moura JJG (2011) Nitrite reduction by xanthine oxidase family enzymes: A new class of nitrite reductases. Journal of Biological Inorganic Chemistry 16:443–460.

Mandadi KK, Scholthof K-BG (2013) Plant immune responses against viruses: how does a virus cause disease? The Plant Cell 25:1489–1505.

Mandal MK, Chandra-Shekara AC, Jeong R-D, et al (2012) Oleic acid-dependent modulation of nitric oxide associated1 protein levels regulates nitric oxide-mediated defense signaling in Arabidopsis. The Plant Cell 24:1654–1674.

Manuell AL, Quispe J, Mayfield SP (2007) Structure of the chloroplast ribosome: novel domains for translation regulation. PLoS biology 5:e209.

Mariano AC, Andrade MO, Santos AA, et al (2004) Identification of a novel receptor-like protein kinase that interacts with a geminivirus nuclear shuttle protein. Virology 318:24–31.

Marín-Navarro J, Manuell AL, Wu J, P Mayfield S (2007) Chloroplast translation regulation. Photosynthesis research 94:359–374.

Mata-pérez C, Begara-morales JC, Luque F, et al (2016) Transcriptomic Analyses on the Role of Nitric Oxide in Plant Disease Resistance. Current Issues in Molecular Biology 19:121–128.

Matsuo Y, Morimoto T, Kuwano M, et al (2006) The GTP-binding protein YlqF participates in the late step of 50 S ribosomal subunit assembly in *Bacillus subtilis*. The Journal of biological chemistry 281:8110–8117.

Maule AJ (2008) Plasmodesmata: structure, function and biogenesis. Current opinion in plant biology 11:680–686.

Mayer B, Hemmens B (1997) Biosynthesis and action of nitric oxide in mammalian cells. Trends in biochemical sciences 22:477–481.

McGarry RC, Barron YD, Carvalho MF, et al (2003) A novel Arabidopsis acetyltransferase interacts with the geminivirus movement protein NSP. The Plant Cell 15:1605–1618.

Misra AN, Vladkova R, Singh R, et al (2014) Action and target sites of nitric oxide in chloroplasts. Nitric Oxide 39:35–45.

Moche M, Stremlau S, Hecht L, et al (2010) Effect of nitrate supply and mycorrhizal inoculation on characteristics of tobacco root plasma membrane vesicles. Planta 231:425–436.

Modolo L V., Augusto O, Almeida IMG, et al (2006) Decreased arginine and nitrite levels in nitrate reductase-deficient *Arabidopsis thaliana* plants impair nitric oxide synthesis and the hypersensitive response to Pseudomonas syringae. Plant Science 171:34–40.

Moncada S, Palmer RMJ, Higgs EA (1989) Biosynthesis a pathway for nitric oxide from l-arginine the regulation of cell function and communication. Biochemical Pharmacology 38:1709–1715.

Moreau M, Lee GI, Wang Y, et al (2008) AtNOS/AtNOA1 is a functional *Arabidopsis thaliana* cGTPase and not a nitric-oxide synthase. The Journal of Biological Chemistry 283:32957–32967.

Moreau M, Lindermayr C, Durner J, Klessig DF (2010) NO synthesis and signaling in plants, where do we stand? Physiologia Plantarum 138:372–383.

Moreau P, Brandizzi F, Hanton S, et al (2007) The plant ER-Golgi interface: a highly structured and dynamic membrane complex. Journal of Experimental Botany 58:49–64.

Morilla G, Jeske H, Bejarano ER (2006) A versatile transreplication-based system to identify cellular proteins involved in Geminivirus replication. Journal of Virology 80:3624–3633.

Morimoto T, Loh PC, Hirai T, et al (2002) Six GTP-binding proteins of the Era / Obg family are essential for cell growth in *Bacillus subtilis*. Microbiology 148:3539–3552.

Moshe A, Belausov E, Niehl A, et al (2015) The Tomato yellow leaf curl virus V2 protein forms aggregates depending on the cytoskeleton integrity and binds viral genomic DNA. Scientific reports 5:9967.

Moshe A, Jens P, Brotman Y, et al (2012) Stress responses to tomato yellow leaf curl virus (TYLCV) infection of resistant and susceptible tomato plants are different. Metabolomics: Open Access s1:1–13.

Muangsan N, Beclin C, Vaucheret H, Robertson D (2004) Geminivirus VIGS of endogenous genes requires SGS2/SDE1 and SGS3 and defines a new branch in the genetic pathway for silencing in plants. The Plant Journal 38:1004–1014.

Mühlhausen S, Kollmar M (2013) Whole genome duplication events in plant evolution reconstructed and predicted using myosin motor proteins. BMC evolutionary biology 13:202.

Mur LAJ, Carver TLW, Prats E (2006) NO way to live; the various roles of nitric oxide in plant-pathogen interactions. Journal of Experimental Botany 57:489–505.

Mur LAJ, Kenton P, Lloyd AJ, et al (2008) The hypersensitive response; the centenary is upon us but how much do we know? Journal of Experimental Botany 59:501–520.

Mur LAJ, Prats E, Pierre S, et al (2013) Integrating nitric oxide into salicylic acid and jasmonic acid/ ethylene plant defense pathways. Frontiers in Plant Science 4:215.

Murashige T, Skoog F (1962) A revised medium for rapid growth and bio assays with tobacco tissue cultures. Physiologia Plantarum 15:473–497.

Mwaba II (2010) Development of a VIGS vector based on SACMV for genomic studies in tobacco and cassava.

Nagar S, Pedersen TJ, Carrick KM, et al (1995) A geminivirus induces expression of a host DNA synthesis protein in terminally differentiated plant cells. The Plant Cell 7:705–719.

Nagase S, Takemura K, Ueda A, et al (1997) A novel nonenzymatic pathway for the generation of nitric oxide by the reaction of hydrogen peroxide and D- or L-arginine. Biochemical and biophysical research communications 233:150–153.

Natesan SKA, Sullivan JA, Gray JC (2009) Myosin XI is required for actin-associated movement of plastid stromules. Molecular Plant 2:1262–1272.

Nawaz-ul-rehman MS, Fauquet CM (2009) Evolution of geminiviruses and their satellites. FEBS Letters 583:1825–1832.

Nebenführ A (2002) Vesicle traffic in the endomembrane system: a tale of COPs, Rabs and SNAREs. Current Opinion in Plant Biology 5:507–512.

Neill SJ, Bright J, Desikan R, et al (2008) Nitric oxide evolution and perception. Journal of Experimental Botany 59:25–35.

Neill SJ, Desikan R, Clarke A, et al (2002) Hydrogen peroxide and nitric oxide as signalling molecules in plants. Journal of Experimental Botany 53:1237–1247.

Newman M-A, Sundelin T, Nielsen JT, Erbs G (2013) MAMP (microbe-associated molecular pattern) triggered immunity in plants. Frontiers in Plant Science 4:139.

Nicaise V (2014) Crop immunity against viruses: outcomes and future challenges. Frontiers in Plant Science 5:1–18.

Niehl A, Heinlein M (2011) Cellular pathways for viral transport through plasmodesmata. Protoplasma 248:75–99.

Niehl A, Wyrsch I, Boller T, Heinlein M (2016) Double-stranded RNAs induce a pattern-triggered immune signaling pathway in plants. New Phytologist 211:1008–1019.

Noueiry AO, Lucas WJ, Gilbertson RL (1994) Two proteins of a plant DNA virus coordinate nuclear and plasmodesmal transport. Cell 76:925–932.

Nuwamanya E, Chiwona-Karltun L, Kawuki RS, Baguma Y (2012) Bio-ethanol production from non-food parts of cassava (*Manihot esculenta* Crantz). AMBIO 41:262–270.

Odronitz F, Kollmar M (2007) Drawing the tree of eukaryotic life based on the analysis of 2,269 manually annotated myosins from 328 species. Genome Biology 8:R196.

Ojangu E-L, Järve K, Paves H, Truve E (2007) *Arabidopsis thaliana* myosin XIK is involved in root hair as well as trichome morphogenesis on stems and leaves. Protoplasma 230:193–202.

Okigbo BN (1980) Nutritional implications of projects giving high priority to the production of staples of low nutritive quality: The Case for Cassava (*Manihot esculenta*, Crantz) in the Humid Tropics of West Africa. Africa 4:Accessed 08.09.09.

Oláh E, Pesti R, Taller D, et al (2016) Non-targeted effects of virus-induced gene silencing vectors on host endogenous gene expression. Archives of Virology 161:2387–2393.

Oliveira HC, Saviani EE, Oliveira JFP, Salgado I (2010) Nitrate reductase-dependent nitric oxide synthesis in the defense response of *Arabidopsis thaliana* against Pseudomonas syringae. Tropical plant pathology 35:104–107.

Onaga G, Wydra K (2016) Advances in plant tolerance to biotic stresses. In: Plant Genomics. InTech, pp 229–272

Oparka KJ (2004) Getting the message across: how do plant cells exchange macromolecular complexes? Trends in Plant Science 9:33–41.

Padmanabhan MS, Dinesh-Kumar SP (2010) All hands on deck—The role of chloroplasts, endoplasmic reticulum, and the nucleus in driving plant innate immunity. Molecular Plant-Microbe Interactions 23:1368–1380.

Pallas V, Garcia JA (2011) How do plant viruses induce disease? Interactions and interference with host components. The Journal of General Virology 92:2691–2705.

Palmieri MC, Sell S, Huang X, et al (2008) Nitric oxide-responsive genes and promoters in *Arabidopsis thaliana*: a bioinformatics approach. Journal of Experimental Botany 59:177–186.

Palukaitis P, Groen SC, Carr JP (2013) The Rumsfeld paradox: some of the things we know that we don’t know about plant virus infection. Current opinion in plant biology 16:513–519.

Pandey P, Choudhury NR, Mukherjee SK (2009) A geminiviral amplicon (VA) derived from Tomato leaf curl virus (ToLCV) can replicate in a wide variety of plant species and also acts as a VIGS vector. Virology Journal 6:152.

Parani M, Rudrabhatla S, Myers R, et al (2004) Microarray analysis of nitric oxide responsive transcripts in Arabidopsis. Plant Biotechnology Journal 2:359–366.

Parihar A, Parihar MS, Chen Z, Ghafourifar P (2008) mAtNOS1 induces apoptosis of human mammary adenocarcinoma cells. Life sciences 82:1077–1082.

Park E, Nebenführ A (2013) Myosin XIK of *Arabidopsis thaliana* accumulates at the root hair tip and is required for fast root hair growth. PloS one 8:e76745.

Pascal E, Sanderfoot AA, Ward BM, et al (1994) The geminivirus BR1 movement protein binds single-stranded DNA and localizes to the cell nucleus. The Plant Cell 6:995–1006.

Peele CG, Jordan C V, Muangsan N, et al (2001) Silencing of a meristematic gene using geminivirus-derived vectors. The Plant Journal 27:357–366.

Perchepied L, Balagué C, Riou C, et al (2010) Nitric oxide participates in the complex interplay of defense-related signaling pathways controlling disease resistance to *Sclerotinia sclerotiorum* in *Arabidopsis thaliana*. Molecular plant-microbe interactions 23:846–860.

Peremyslov V V., Klocko AL, Fowler JE, Dolja V V. (2012) Arabidopsis Myosin XI-K Localizes to the Motile Endomembrane Vesicles Associated with F-actin. Frontiers in Plant Science 3:1–10.

Peremyslov V V, Mockler TC, Filichkin SA, et al (2011) Expression, splicing, and evolution of the myosin gene family in plants. Plant Physiology 155:1191–1204.

Peremyslov V V, Prokhnevsky AI, Avisar D, Dolja V V (2008) Two class XI myosins function in organelle trafficking and root hair development in Arabidopsis. Plant Physiology 146:1109–1116.

Peremyslov V V, Prokhnevsky AI, Dolja V V (2010) Class XI myosins are required for development, cell expansion, and F-Actin organization in Arabidopsis. The Plant Cell 22:1883–1897.

Petersen BO, Albrechtsen M (2005) Evidence implying only unprimed RdRP activity during transitive gene silencing in plants. Plant Molecular Biology 58:575–583.

Planchet E, Kaiser WM (2006) Nitric oxide production in plants: facts and fictions. Plant signaling & behavior 1:46–51.

Polverari A, Molesini B, Pezzotti M, et al (2003) Nitric Oxide-mediated transcriptional changes in *Arabidopsis thaliana*. Molecular Plant-Microbe Interactions 16:1094–1105.

Pooma W, Gillette WK, Jeffrey JL, Petty ITD (1996) Host and viral factors determine the dispensability of coat protein for bipartite geminivirus systemic movement. Virology 218:264–268.

Porebski S, Bailey LG, Baum BR (1997) Modification of a CTAB DNA extraction protocol for plants containing high polysaccharide and polyphenol components. Plant Molecular Biology Reporter 15:8–15.

Prats E, Mur LAJ, Sanderson R, Carver TLW (2005) Nitric oxide contributes both to papilla-based resistance and the hypersensitive response in barley attacked by *Blumeria graminis* f. sp. hordei. Molecular Plant Pathology 6:65–78.

Prokhnevsky AI, Peremyslov V V, Dolja V V (2005) Actin cytoskeleton is involved in targeting of a viral hsp70 homolog to the cell periphery. Journal of Virology 79:14421–14428.

Prokhnevsky AI, Peremyslov V V, Dolja V V (2008) Overlapping functions of the four class XI myosins in Arabidopsis growth, root hair elongation, and organelle motility. Proceedings of the National Academy of Sciences 105:19744–19749.

Qi Y, Zhao J, An R, et al (2016) Mutations in circularly permuted GTPase family genes AtNOA1/RIF1/SVR10 and BPG2 suppress var2-mediated leaf variegation in *Arabidopsis thaliana*. Photosynthesis Research 127:355–367.

Qiao W, Fan L (2008) Nitric oxide signaling in plant responses to abiotic stresses. Journal of Integrative Plant Biology 50:1238–1246.

Qiao W, Xiao S, Yu L, Fan L (2009) Expression of a rice gene OsNOA1 re-establishes nitric oxide synthesis and stress-related gene expression for salt tolerance in Arabidopsis nitric oxide-associated 1 mutant Atnoa1. Environmental and Experimental Botany 65:90–98.

Qin S, Ward B, Lazarowitz SG (1998) The bipartite geminivirus coat protein aids BR1 function in viral movement by affecting the accumulation of viral single-stranded DNA. Journal of Virology 72:9247–9256.

Rasul S, Dubreuil-Maurizi C, Lamotte O, et al (2012) Nitric oxide production mediates oligogalacturonide-triggered immunity and resistance to Botrytis cinerea in *Arabidopsis thaliana*. Plant, Cell and Environment 35:1483–1499.

Ratcliff FG, Martin-hernandez AM, Baulcombe DC (2001) Tobacco rattle virus as a vector for analysis of gene function by silencing. The Plant Journal 25:237–245.

Reddy AS, Day IS (2001) Analysis of the myosins encoded in the recently completed *Arabidopsis thaliana* genome sequence. Genome biology 2: research0021.1-research0024.7.

Reddy RVC, Dong W, Njock T, et al (2011) Molecular interaction between two cassava geminiviruses exhibiting cross-protection. Virus research 163:169–177.

Reichelt S, Knight AE, Hodge TP, et al (1999) Characterization and localization of the unconventional myosin VIII in plant cells. Plant Journal 19:555–567.

Reinero A, Beachy RN (1989) Reduced photosystem 11 activity and accumulation of viral coat protein in chloroplasts of leaves infected with tobacco mosaic virus. Plant Physiology 89:111–116.

Roberts IM, Robinson DJ, Harrison BD (1984) Serological elationships and genome homologies among geminiviruses. Journal of General Virology 65:1723–1730.

Robertson D (2004) VIGS vectors for gene silencing: many targets, many tools. Annual review of plant biology 55:495–519.

Rockel P, Strube F, Rockel A, et al (2002) Regulation of nitric oxide (NO) production by plant nitrate reductase in vivo and in vitro. Journal of Experimental Botany 53:103–110.

Rodio M-E, Delgado S, De Stradis A, et al (2007) A viroid RNA with a specific structural motif inhibits chloroplast development. The Plant Cell 19:3610–3626.

Rojas MR, Hagen C, Lucas WJ, Gilbertson RL (2005) Exploiting chinks in the plant's armor: evolution and emergence of geminiviruses. Annual review of phytopathology 43:361–394.

Rojas MR, Jiang H, Salati R, et al (2001) Functional analysis of proteins involved in movement of the monopartite begomovirus, Tomato yellow leaf curl virus. Virology 291:110–125.

Rojas MR, Maliano MR, de Souza JO, et al (2016) Cell-to-cell movement of plant viruses: A diversity of mechanisms and strategies. In: Wang A, Zhou X (eds) Current Research Topics in Plant Virology. Springer International Publishing, Cham, pp 113–152

Rojas MR, Noueiry AO, Lucas WJ, Gilbertson RL (1998) Bean dwarf mosaic geminivirus movement proteins recognize DNA in a form- and size-specific manner. Cell 95:105–13.

Romero-Puertas MC, Delledonne M (2004) Nitric oxide signaling in plant-pathogen interactions. IUBMB Life 55:579–583.

Romero-Puertas MC, Laxa M, Matte A, et al (2007) S-Nitrosylation of peroxiredoxin II E promotes peroxynitrite-mediated tyrosine nitration. The Plant Cell 19:4120–4130.

Rothenstein D, Krenz B, Selchow O, Jeske H (2007) Tissue and cell tropism of Indian cassava mosaic virus (ICMV) and its AV2 (precoat) gene product. Virology 359:137–145.

Ruiz MT, Voinnet O, Baulcombe DC (1998) Initiation and maintenance of virus-induced gene silencing gene silencing. The Plant Cell 10:937–946.

Rutherford S, Moore I (2002) The Arabidopsis Rab GTPase family: another enigma variation. Current Opinion in Plant Biology 5:518–528.

Sade D, Brotman Y, Eybishtz A, et al (2013) Involvement of the hexose transporter gene LEHT1 and of sugars in resistance of tomato to tomato yellow leaf curl virus. Molecular Plant 6:1707–1710.

Sanderfoot AA, Ingham DJ, Lazarowitz SG (1996) A viral movement protein as a nuclear shuttle (the geminivirus BR1 movement protein contains domains essential for interaction with BL1 and nuclear localization). Plant Physiology 110:23–33.

Sang J, Jiang M, Lin F, et al (2008) Nitric oxide reduces hydrogen peroxide accumulation involved in water stress-induced subcellular anti-oxidant defense in maize plants. Journal of Integrative Plant Biology 50:231–243.

Sangha JS, Yolanda HC, Kaur J, et al (2013) Proteome analysis of rice (*Oryza sativa* L.) mutants reveals differentially induced proteins during brown planthopper (*Nilaparvata lugens*) infestation. Int J Mol Sci. doi: 10.3390/ijms14023921

Sanz L, Albertos P, Mateos I, et al (2015) Nitric oxide (NO) and phytohormones crosstalk during early plant development. Journal of Experimental Botany 66:2857–2868.

Sarkar TS, Majumdar U, Roy A, et al (2010) Production of Nitric Oxide in host-virus interaction. Plant Signaling & Behavior 5:668–676.

Sattarzadeh A, Franzen R, Schmelzer E (2008) The Arabidopsis class VIII myosin ATM2 is involved in endocytosis. Cell motility and the cytoskeleton 65:457–68.

Sattarzadeh A, Krahmer J, Germain AD, Hanson MR (2009) A myosin XI tail domain homologous to the yeast myosin vacuole-binding domain interacts with plastids and stromules in *Nicotiana benthamiana*. Molecular plant 2:1351–8.

Sattarzadeh A, Schmelzer E, Hanson MR (2011) Analysis of Organelle Targeting by DIL Domains of the Arabidopsis Myosin XI Family. Frontiers in Plant Science 2:1–11.

Savatin D V., Gramegna G, Modesti V, Cervone F (2014) Wounding in the plant tissue: the defense of a dangerous passage. Frontiers in Plant Science 5:1–11.

Schattat MH, Klösgen RB (2011) Induction of stromule formation by extracellular sucrose and glucose in epidermal leaf tissue of *Arabidopsis thaliana*. BMC plant biology 11:115.

Schelbert S, Aubry S, Burla B, et al (2009) Pheophytin pheophorbide hydrolase (pheophytinase) is involved in chlorophyll breakdown during leaf senescence in Arabidopsis. The Plant Cell 21:767–785.

Schmittgen TD (2001) Real-time quantitative PCR. Methods (San Diego, Calif) 25:383–385.

Scholthof KG, Adkins S, Czosnek H, et al (2011) Top 10 plant viruses in molecular plant pathology. Molecular plant pathology 12:938–954.

Schrödinger L (2015) The PyMOL molecular graphics system, version 1.8.

Scott SW, MacFarlane SA, McGavin WJ, Fargette D (2014) Cassava Ivorian bacilliform virus is a member of the genus Anulavirus. Archives of Virology 159:2791–2793.

Sebe-Pedros A, Grau-Bove X, Richards TA, Ruiz-Trillo I (2014) Evolution and classification of myosins, a paneukaryotic whole-genome approach. Genome Biology and Evolution 6:290–305.

Selth LA, Dogra SC, Rasheed MS, et al (2005) A NAC domain protein interacts with tomato leaf curl virus replication accessory protein and enhances viral replication. The Plant Cell 17:311–325.

Senthil-Kumar M, Mysore KS (2014) Tobacco rattle virus-based virus-induced gene silencing in *Nicotiana benthamiana*. Nature Protocols 9:1549–1562.

Senthil-Kumar M, Mysore KS (2011a) New dimensions for VIGS in plant functional genomics. Trends in Plant Science 16:656–665.

Senthil-Kumar M, Mysore KS (2011b) Virus-induced gene silencing can persist for more than 2years and also be transmitted to progeny seedlings in *Nicotiana benthamiana* and tomato. Plant Biotechnology Journal 9:797–806.

Serrano I, Audran C, Rivas S (2016) Chloroplasts at work during plant innate immunity. Journal of Experimental Botany 67:3845–3854.

Sharma K, Misra RS (2011) Molecular approaches towards analyzing the viruses infecting maize (Zea mays L .). Virology 3:1–17.

Sharma P, Ikegami M (2008) RNA-silencing suppressors of geminiviruses. Journal of General Plant Pathology 74:189–202.

Sharma P, Ikegami M (2010) Tomato leaf curl Java virus V2 protein is a determinant of virulence, hypersensitive response and suppression of posttranscriptional gene silencing. Virology 396:85–93.

Shivaprasad P V, Akbergenov R, Trinks D, et al (2005) Promoters, transcripts, and regulatory proteins of Mungbean yellow mosaic geminivirus. Journal of Virology 79:8149–8163.

Silaghi-Dumitrescu R, Mich M, Matyas C, Cooper CE (2012) Nitrite and nitrate reduction by molybdenum centers of the nitrate reductase type: Computational predictions on the catalytic mechanism. Nitric Oxide 26:27–31.

Singh BN, Mishra RN, Agarwal PK, et al (2004) A pea chloroplast translation elongation factor that is regulated by abiotic factors. Biochemical and Biophysical Research Communications 320:523–530.

Soitamo AJ, Jada B, Lehto K (2012) Expression of geminiviral AC2 RNA silencing suppressor changes sugar and jasmonate responsive gene expression in transgenic tobacco plants. BMC plant biology 12:204.

Song F, Goodman RM (2001) Activity of nitric oxide is dependent on, but is partially required for function of, salicylic acid in the signaling pathway in tobacco systemic acquired resistance. Molecular Plant-Microbe Interactions 14:1458–1462.

Soosaar JLM, Burch-smith TM, Dinesh-kumar SP (2005) Mechanisms of plant resistance to viruses. Nature reviews Microbiology 3:789–798.

Sparkes I A, Teanby NA, Hawes C (2008) Truncated myosin XI tail fusions inhibit peroxisome, Golgi, and mitochondrial movement in tobacco leaf epidermal cells: a genetic tool for the next generation. Journal of Experimental Botany 59:2499–2512.

Stöhr C, Strube F, Marx G, et al (2001) A plasma membrane-bound enzyme of tobacco roots catalyses the formation of nitric oxide from nitrite. Planta 212:835–841.

Stöhr C, Ullrich WR (2002) Generation and possible roles of NO in plant roots and their apoplastic space. Journal of Experimental Botany 53:2293–2303.

Stuehr DJ (2004) Enzymes of the L-arginine to nitric oxide pathway. The Journal of Nutrition 2748–2751.

Sudhamsu J, Lee GI, Klessig DF, Crane BR (2008) The structure of YqeH. An AtNOS1/AtNOA1 ortholog that couples GTP hydrolysis to molecular recognition. The Journal of Biological Chemistry 283:32968–32976.

Sun A, Li Z (2013) Regulatory role of nitric oxide in lipopolysaccharides-triggered plant innate immunity. Plant Signaling & Behavior 8:134–136.

Sun A, Nie S, Xing D (2012) Nitric oxide-mediated maintenance of redox homeostasis contributes to NPR1-dependent plant innate immunity triggered by lipopolysaccharides. Plant Physiology 160:1081–1096.

Suwastika IN, Denawa M, Yomogihara S, et al (2014) Evidence for lateral gene transfer (LGT) in the evolution of Eubacteria-derived small GTPases in plant organelles. Front Plant Sci. doi: 10.3389/fpls.2014.00678

Tada Y, Spoel SH, Pajerowska-Mukhtar K, et al (2008) Plant immunity requires conformational charges of NPR1 via s-nitrosylation and thioredoxins. Science 321:952–956.

Takemoto D, Hardham AR (2004) The cytoskeleton as a regulator and target of biotic interactions in plants. Plant Physiology 136:3864–3876.

Talts K, Ilau B, Ojangu E, et al (2016) Arabidopsis myosins XI1, XI2, and XIK are crucial for gravity-induced bending of inflorescence stems. Frontiers in Plant Science 7:1–12.

Tamura K, Iwabuchi K, Fukao Y, et al (2013a) Myosin XI-i links the nuclear membrane to the cytoskeleton to control nuclear movement and shape in Arabidopsis. Current Biology 23:1776–1781.

Tamura K, Stecher G, Peterson D, et al (2013b) MEGA6: Molecular Evolutionary Genetics Analysis Version 6.0. Molecular Biology and Evolution 30:2725–2729.

Tao X, Zhou X (2004) A modified viral satellite DNA that suppresses gene expression in plants. The Plant Journal 38:850–860.

Tauzin AS, Giardina T (2014) Sucrose and invertases, a part of the plant defense response to the biotic stresses. Frontiers in Plant Science 5:293.

Tewari RK, Prommer J, Watanabe M (2013) Endogenous nitric oxide generation in protoplast chloroplasts. Plant cell reports 32:31–44.

Tiller N, Bock R (2014) The translational apparatus of plastids and its role in plant development. Molecular Plant 7:1105–1120.

Trapet P, Kulik A, Lamotte O, et al (2015) NO signaling in plant immunity: A tale of messengers. Phytochemistry 112:72–79.

Turnage MA, Muangsan N, Peele CG, Robertson D (2002) Geminivirus-based vectors for gene silencing in Arabidopsis. The Plant Journal 30:107–114.

Uarrota VG, Nunes E da C, Peruch LAM, et al (2016) Toward better understanding of postharvest deterioration: biochemical changes in stored cassava (*Manihot esculenta* Crantz) roots: Food Science & Nutrition 4:409–422.

Ueda H, Tamura K, Hara-Nishimura I (2015) Functions of plant-specific myosin XI: From intracellular motility to plant postures. Current Opinion in Plant Biology 28:30–38.

Ueda H, Yokota E, Kutsuna N, et al (2010) Myosin-dependent endoplasmic reticulum motility and F-actin organization in plant cells. Proceedings of the National Academy of Sciences 107:6894–6899.

Uicker WC, Schaefer L, Koenigsknecht M, Britton RA (2007) The essential GTPase YqeH is required for proper ribosome assembly in *Bacillus subtilis*. Journal of bacteriology 189:2926–9.

Unseld S, Hohnle M, Ringel M, Frischmuth T (2001) Subcellular Targeting of the Coat Protein of African Cassava Mosaic Geminivirus. Virology 383:373–383.

Van Ree K, Gehl B, Wassim Chehab E, et al (2011) Nitric oxide accumulation in Arabidopsis is independent of NOA1 in the presence of sucrose. The Plant Journal 68:225–233.

Vanderschuren H, Stupak M, Fütterer J, et al (2007) Engineering resistance to geminiviruses--review and perspectives. Plant Biotechnology Journal 5:207–220.

Vanitharani R, Chellappan P, Pita JS, Fauquet CM (2004) Differential roles of AC2 and AC4 of cassava geminiviruses in mediating synergism and suppression of posttranscriptional gene silencing. Journal of Virology 78:9487–9498.

Varsani A, Roumagnac P, Fuchs M, et al (2017) Capulavirus and Grablovirus: two new genera in the family Geminiviridae. Archives of Virology 162:1819–1831.

Velasquez AC, Chakravarthy S, Martin GB (2009) Virus-induced Gene Silencing (VIGS) in *Nicotiana benthamiana* and Tomato. J Vis Exp. doi: 10.3791/1292

Vlot AC, Dempsey DA, Klessig DF (2009) Salicylic Acid, a multifaceted hormone to combat disease. Annual Review of Phytopathology 47:177–206.

Voinnet O (2001) RNA silencing as a plant immune system against viruses. Trends in Genetics 17:449–459.

Von Arnim A, Frischmuth T, Stanley J (1993) Detection and possible functions of African cassava mosaic virus DNA B gene products. Virology 192:264–272.

Walter B, Ladeveze I, Etienne L, Fuchs M (1989) Some properties of a previously undescribed virus from cassava: Cassava American Latent Virus. Annals of Applied Biology 115:279–289.

Wang G, Zhong M, Wang J, et al (2014) Genome-wide identification, splicing, and expression analysis of the myosin gene family in maize (Zea mays). Journal of Experimental Botany 65:923–938.

Wang Y, Loake GJ, Chu C (2013) Cross-talk of nitric oxide and reactive oxygen species in plant programed cell death. Frontiers in Plant Science 4:314.

Waterhouse PM, Wang M, Lough T (2001) Gene silencing as an adaptive defence against viruses. Nature 411:834–842.

Wilhelmová N, Procházková D, Sindelarova M, Sindelar L (2005) Photosynthesis in leaves of *Nicotiana tabacum* L. infected with tobacco mosaic virus. Photosynthetica 43:597–602.

Winter S, Koerbler M, Stein B, et al (2010) Analysis of cassava brown streak viruses reveals the presence of distinct virus species causing cassava brown streak disease in East Africa. Journal of General Virology 91:1365–1372.

Wojtaszek P (2000) Nitric oxide in plants: To NO or not to NO. Phytochemistry 54:1–4.

Wu C, Lai Y, Lin N-S, et al (2008) A simplified method of constructing infectious clones of begomovirus employing limited restriction enzyme digestion of products of rolling circle amplification. Journal of virological methods 147:355–9.

Wu J, Baldwin IT (2009) Herbivory-induced signalling in plants: Perception and action. Plant, Cell and Environment 32:1161–1174.

Wu SZ, Bezanilla M (2014) Myosin VIII associates with microtubule ends and together with actin plays a role in guiding plant cell division. eLife 3:1–20.

Wünsche H, Baldwin IT, Wu J (2011) Silencing NOA1 elevates herbivory-induced jasmonic acid accumulation and compromises most of the carbon-based defense metabolites in *Nicotiana attenuate* (F). Journal of Integrative Plant Biology 53:619–631.

Xia J, Sinelnikov I V., Han B, Wishart DS (2015) MetaboAnalyst 3.0--making metabolomics more meaningful. Nucleic Acids Research 43:W251-257.

Xu J, Aileni M, Abbagani S, Zhang P (2010) A reliable and efficient method for total RNA isolation from various members of spurge family (Euphorbiaceae). Phytochemical analysis 21:395–398.

Yang Q, He H, Li H, et al (2011) NOA1 functions in a temperature-dependent manner to regulate chlorophyll biosynthesis and RUBISCO formation in rice. Plos ONE 6:e20015.

Yang X, Wang B, Li F, et al (2016) Research advances in geminiviruses. In: Current Research Topics in Plant Virology. Springer International Publishing, Cham, pp 251–269

Yemets AI, Krasylenko Y, Lytvyn DI, et al (2011) Nitric oxide signalling via cytoskeleton in plants. Plant science: an international journal of experimental plant biology 181:545–554.

Yesbergenova Z, Yang G, Oron E, et al (2005) The plant Mo-hydroxylases aldehyde oxidase and xanthine dehydrogenase have distinct reactive oxygen species signatures and are induced by drought and abscisic acid. Plant Journal 42:862–876.

Yokota E, Shimmen T (2011) Plant myosins. In: Liu B (ed) The Plant Cytoskeleton. Springer New York, New York, NY, pp 229–243

Yoon MY, Kim MY, Shim S, et al (2016) Transcriptomic Profiling of Soybean in Response to High-Intensity UV-B Irradiation Reveals Stress Defense Signaling. Front Plant Sci. doi: 10.3389/fpls.2016.01917

Zeidler D, Zähringer U, Gerber I, et al (2004) Innate immunity in *Arabidopsis thaliana*: lipopolysaccharides activate nitric oxide synthase (NOS) and induce defense genes. Proceedings of the National Academy of Sciences 101:15811–15816.

Zeier J, Delledonne M, Mishina T, et al (2004) Genetic elucidation of nitric oxide signaling in incompatible plant-pathogen interactions. Plant Physiology 136:2875–2886.

Zemojtel T, Kolanczyk M, Kossler N, et al (2007) Corrigendum to “Mammalian mitochondrial nitric oxide synthase: Characterization of a novel candidate” [FEBS Lett. 580 (2006) 455–462]. FEBS Letters 581:2072–2073.

Zhang SC, Wege C, Jeske H (2001) Movement proteins (BC1 and BV1) of Abutilon mosaic geminivirus are cotransported in and between cells of sink but not of source leaves as detected by green fluorescent protein tagging. Virology 290:249–260.

Zhang X-F, Qu F (2016) Cross protection of plant viruses: Recent developments and mechanistic implications. In: Wang A, Zhou X (eds) Current Research Topics in Plant Virology. Springer International Publishing, Cham, pp 241–250

Zhao J, Zhang X, Hong Y, Liu Y (2016) Chloroplast in plant-virus interaction. Frontiers in Microbiology 7:1–20.

Zhao M-G, Tian Q-Y, Zhang W-H (2007) Nitric oxide synthase-dependent nitric oxide production is associated with salt tolerance in Arabidopsis. Plant Physiology 144:206–217.

Zhao M, Chen L, Zhang L-L, Zhang W (2009) Nitric reductase-dependent nitric oxide production is involved in cold acclimation and freezing tolerance in Arabidopsis. Plant Physiology 151:755–67.

Zhou B, Guo Z, Xing J, Huang B (2005) Nitric oxide is involved in abscisic acid-induced antioxidant activities in Stylosanthes guianensis. Journal of Experimental Botany 56:3223–3228.

Zhou Y-C, Garrido-Ramirez ER, Sudarshana MR, et al (2007) The N-terminus of the Begomovirus nuclear shuttle protein (BV1) determines virulence or avirulence in *Phaseolus vulgaris*. Molecular Plant-Microbe Interactions 20:1523–1534.

Zhou Y, Rojas MR, Park M-R, et al (2011) Histone H3 interacts and colocalizes with the nuclear shuttle protein and the movement protein of a Geminivirus. Journal of Virology 85:11821–11832.

Ziebell H, Carr JP (2010) Cross-Protection. In: Natural and engineered resistance to plant viruses, Part B, 1st edn. Elsevier Inc., pp 211–264

Zottini M, Costa A, De Michele R, et al (2007) Salicylic acid activates nitric oxide synthesis in Arabidopsis. Journal of Experimental Botany 58:1397–1405.

Zrachya A, Glick E, Levy Y, et al (2007) Suppressor of RNA silencing encoded by tomato yellow leaf curl virus-israel. Virology 358:159–165.

Zurbriggen MD, Carrillo N, Hajirezaei MR (2010) ROS signaling in the hypersensitive response: when, where and what for? Plant Signaling & Behavior 5:393–396.

APPENDIX

1. Appendices to Chapter 2

A1.1 Summary of the results of the study

		SACMV-VIGS						TRV-VIGS					
		RELATIVE TO VECTOR ONLY	RELATIVE TO SACMV-CHALLENGED/VIGS-VECTOR					RELATIVE TO VECTOR ONLY	RELATIVE TO SACMV-CHALLENGED/VIGS-VECTOR				
		Myosin expression	Myosin expression	Viral load	DNA-A/ DNA-B	SSS	Plant height	Myosin expression	Myosin expression	Viral load	DNA-A/ DNA-B	SSS	Plant height
14 DPI	VIGS::15.1	↓ -	-	↑	-	↑	-	↓ ↓	-	-	-	-	↑
	VIGS::8.B	↓ -	-	-	-	-	↓	↓ -	-	-	-	↑	-
	VIGS::11.F	↓ ↓	↓	↑	-	↓	-	- -	-	-	-	↑	-
	VIGS::11.2	↓ ↓	-	-	↓	-	-	↓ -	-	-	-	↑	-
	VIGS::11.K	↓ -	-	-	-	-	-	↓ -	-	-	-	-	-
	NO-VIGS			↑	-	-	-			↑	↓	↑	↑
28 DPI	VIGS::15.1	-	-	↑	-	-	↑	- ↓	-	-	↓	-	↑
	VIGS::8.B	- -	-	↑	-	↓	-	↓ -	-	-	↓	-	↑
	VIGS::11.F	- ↑	↓	↑	-	-	↑	↓ ↓	↓	↓	↓	-	↑
	VIGS::11.2	↓ -	↑	↑	-	-	↑	↓ ↑	-	↓	↓	-	↑
	VIGS::11.K	↓ ↓	-	↓	-	↓	↑	↓	↓	-	↓	-	↑
	NO-VIGS			↑	↓	↑	↓			-	↓	↑	-

In green is the expression of myosin in SACMV-challenged/VIGS-myosin

- denotes no change

RELATIVE TO SACMV-CHALLENGED/VIGS-VECTOR are data collected from the SACMV-challenge/VIGS study

A1.2 Student's t-test

A1.2.1 Student's t-test assessing the expression of myosins in silencing experiment relative to vector-only at 14 and 28 dpi

		SACMV VIGS					TRV VIGS				
		SACMV::M15.1	**SACMV::M8.B**	**SACMV::M11.F**	**SACMV::M11.2**	**SACMV::M11.K**	**TRV::M15.1**	**TRV::M8.B**	**TRV::M11.F**	**TRV::M11.2**	**TRV::M11.K**
14 DPI	**FC**	4.10	2.38	1.73	2.65	2.38	7.64	27.08	0.18	15.11	5.37
	***p* value**	**0.00**	**0.00**	**0.01**	**0.00**	**0.00**	**0.00**	**0.00**	0.20	**0.00**	**0.00**
28 DPI	**FC**	1.86	0.43	0.37	1.50	1.88	1.43	1.85	1.50	1.49	0.94
	***p* value**	0.10	0.19	0.11	**0.03**	**0.00**	0.14	**0.02**	**0.03**	**0.00**	0.42

A1.2.2 Student's t-test assessing the expression of myosins in SACMV-challenged/VIGS::myosin experiment relative to vector-only at 14 and 28 dpi

		SACMV VIGS					TRV VIGS				
		SACMV::M15.1	**SACMV::M8.B**	**SACMV::M11.F**	**SACMV::M11.2**	**SACMV::M11.K**	**TRV::M15.1**	**TRV::M8.B**	**TRV::M11.F**	**TRV::M11.2**	**TRV::M11.K**
14 DPI	**FC**	0.50	1.39	1.5	1.72	1.41	10.41	1.37	0.11	1.78	2.01
	***p* value**	0.08	0.24	**0.01**	**0.02**	0.12	**0.00**	0.32	0.17	0.16	0.06
28 DPI	**FC**	0.66	0.05	0.26	0.45	2.10	3.11	1.58	1.83	*0.55*	3.44
	***p* value**	0.15	0.06	**0.05**	0.17	**0.00**	**0.01**	0.06	**0.00**	**0.00**	**0.00**

A1.2.3 Student's t-test assessing the expression of myosins in SACMV-challenged/VIGS::myosin experiment relative to SACMV-challenged/VIGS vector at 14 and 28 dpi

		SACMV VIGS					TRV VIGS				
		SACMV::M15.1	**SACMV::M8.B**	**SACMV::M11.F**	**SACMV::M11.2**	**SACMV::M11.K**	**TRV::M15.1**	**TRV::M8.B**	**TRV::M11.F**	**TRV::M11.2**	**TRV::M11.K**
14 DPI	**FC**	0.93	1.96	1.67	1.67	0.75	1.46	1.17	0.66	0.69	0.42
	***p* value**	0.43	0.15	**0.00**	0.33	0.12	0.26	0.26	0.28	0.10	0.18
28 DPI	**FC**	0.06	0.17	2.14	0.16	1.19	0.69	1.29	2.39	0.10	3.73
	***p* value**	0.20	0.10	**0.00**	**0.01**	0.27	0.35	0.35	**0.00**	0.14	**0.00**

A1.2.4 Student's t-test assessing the expression of myosins in SACMV-challenged/VIGS vector experiment relative to vector-only at 14 and 28 dpi

		SACMV VIGS					TRV VIGS				
		M15.1	**M8.B**	**M11.F**	**M11.2**	**M11.K**	**M15.1**	**M8.B**	**M11.F**	**M11.2**	**M11.K**
14 DPI	**FC**	0.30	0.38	*-0.44*	1.53	1.62	3.20	1.12	0.24	2.99	2.78
	***p* value**	0.17	0.14	**0.03**	**0.00**	0.11	**0.00**	0.43	0.07	**0.01**	**0.02**
28 DPI	**FC**	0.44	0.20	*-0.13*	2.31	2.00	0.90	0.49	0.68	2.47	0.81
	***p* value**	0.20	0.14	**0.02**	**0.03**	**0.04**	0.45	0.24	0.19	**0.01**	0.26

A1.2.5 Student's t-test assessing the expression the expression of myosins in SACMV-challenged/NO VIGS, relative to mock

		M15.1	M8.B	M11.F	M11.2	M11.K
14 DPI	**FC**	0.3663	0.27	0.6211	1.052632	0.346021
	***p* value**	0.25	0.32	0.31	0.28	0.44
28 DPI	**FC**	2.7	3.7	1.61	0.95	2.85
	***p* value**	0.08	0.12	0.02	0.14	0.31

A1.2.6 Student's t-test assessing the expression of myosins in SACMV-challenged/NO VIGS, relative to vector only

		Relative to SACMV-VIGS vector					Relative to TRV VIGS vector				
		M15.1	**M8.B**	**M11.F**	**M11.2**	**M11.K**	**M15.1**	**M8.B**	**M11.F**	**M11.2**	**M11.K**
14 DPI	**FC**	1.54	2.23	1.92	1.36	1.62	4.21	5.31	0.29	2.75	1.69
	***p* value**	**0.02**	**0.00**	**0.03**	0.33	0.17	**0.00**	**0.00**	0.08	**0.00**	**0.04**
28 DPI	**FC**	1.74	0.40	0.29	18.21	1.95	1.53	1.29	*0.62*	0.77	0.76
	***p* value**	0.20	0.08	0.07	**0.02**	**0.00**	0.43	0.30	**0.05**	0.22	0.20

A1.2.7 Student's t-test assessing the viral load accumulation (DNA-A) in SACMV-challenged/VIGS construct relative to SACMV-challenged/VIGS vector

		SACMV VIGS						TRV VIGS					
		SACMV::M15.1	**SACMV::M8.B**	**SACMV::M11.F**	**SACMV::M11.2**	**SACMV::M11.K**	**SACMV NO VIGS**	**TRV::M15.1**	**TRV::M8.B**	**TRV::M11.F**	**TRV::M11.2**	**TRV::M11.K**	**SACMV NO VIGS**
14 DPI	**FC**	47.43	0.21	12.94	6.14	9.79	191.36	4.66	8.69	2.23	5.06	2.53	228.77
	***p* value**	**0.01**	0.26	**0.00**	0.08	0.16	**0.00**	0.09	0.17	0.46	0.23	0.09	**0.00**
28 DPI	**FC**	5.86	0.17	2.63	5.02	1.02	16.69	0.27	0.54	0.07	0.18	0.16	3.74
	***p* value**	**0.01**	**0.02**	**0.03**	**0.05**	0.34	**0.00**	0.48	0.09	**0.05**	**0.05**	0.09	0.37

A1.2.8 Student's t-test assessing the difference in viral load measured in SACMV-challenged/SACMV-VIGS vector and construct to that in SACMV-challenged/TRV-VIGS vector and construct

		SACMV-challenged/VIGS vector	**SACMV-challenged/VIGS::M15.1**	**SACMV-challenged/VIGS::M8.B**	**SACMV-challenged/VIGS::M11.F**	**SACMV-challenged/VIGS::M11.2**	**SACMV-challenged/VIGS::M11.K**
SACMV-VIGS	**FC**	1.20	12.21	*0.03*	6.94	1.45	4.63
	***p* value**	0.08	**0.02**	**0.03**	0.18	0.17	0.17
TRV-VIGS	**FC**	*0.22*	4.86	*0.07*	9.06	6.41	1.40
	***p* value**	0.06	0.38	**0.04**	**0.03**	**0.03**	0.30

A1.2.9 Student's t-test assessing the fold increase in viral load at 28 dpi, over 14 dpi

		SACMV-challenged/VIGS vector	SACMV-challenged/VIGS ::M15.1	SACMV-challenged/VIGS ::M8.B	SACMV-challenged/VIGS ::M11.F	SACMV-challenged/VIGS ::M11.2	SACMV-challenged/VIGS ::M11.K	SACMV-challenged/NO-VIGS
SACMV-VIGS	**FC**	16.22	2.00	12.55	3.31	13.27	1.69	1.41
	***p* value**	**0.01**	0.27	**0.05**	**0.03**	0.07	0.17	0.14
TRV-VIGS	**FC**	86.64	5.03	5.35	2.53	3.01	5.58	1.41
	***p* value**	**0.05**	0.08	0.07	0.08	0.23	0.30	0.14

A1.2.10 Student's t-test assessing the DNA-A/DNA-B ratio

			SACMV-challenged/ VIGS vector	SACMV-challenged/VIGS: :M15.1	SACMV-challenged/VIGS ::M8.B	SACMV-challenged/VIGS: :M11.F	SACMV-challenged/VIGS: :M11.2	SACMV-challenged/VIGS: :M11.K
SACMV VIGS	**14 DPI**	**FC**	1.00	0.71	0.86	0.82	0.64	0.66
		***p* value**		0.22	0.32	0.44	**0.03**	0.13
	28 DPI	**FC**	1.00	1.03	0.73	2.77	1.01	1.17
		***p* value**		0.49	0.17	0.14	0.31	0.10
TRV VIGS	**14 DPI**	**FC**	1.00	0.81	0.77	0.81	0.72	0.86
		***p* value**		0.13	0.09	0.19	0.11	0.12
	28 DPI	**FC**	1.00	0.75	0.71	0.75	0.82	0.87
		***p* value**		0.00	0.00	0.00	0.02	0.04

A1.2.11 Student's t-test assessing SSS

			SACMV-challenged/VIGS vector	SACMV-challenged/VIGS::M15.1	SACMV-challenged/VIGS::M8.B	SACMV-challenged/VIGS::M11.F	SACMV-challenged/VIGS::M11.2	SACMV-challenged/VIGS::M11.K	SACMV-challenged/NO-VIGS
SACMV VIGS	**14 DPI**	**Median**	2.00	3.00	2.00	1.50	2.00	2.00	3.00
		***p* value**		0.00	0.14	0.00	0.27	0.09	0.27
	28 DPI	**Median**	5.00 (4.33)*	4.00	3.00	4.00	4.00	3.00	5.00 (4.89)*
		***p* value**		0.30	0.04	0.21	0.37	0.00	0.05
TRV VIGS	**14 DPI**	**Median**	2.00	3.00	3.00	3.00	2.00	2.00	3.00
		***p* value**		0.00	0.00	0.03	0.17	0.17	0.03
	28 DPI	**Median**	4.00	5.00	4.00	4.00	5.00	4.00	4
		***p* value**		0.50	0.16	0.13	0.37	0.19	0.03
*average value in brackets									

A1.2.12 Student's t-test assessing SSS increase over the 2 time points (*p* values shown)

EXPERIMENT	SACMV-challenged/VIGS vector	SACMV-challenged/VIGS::M15.1	SACMV-challenged/VIGS::M8.B	SACMV-challenged/VIGS::M11.F	SACMV-challenged/VIGS::M11.2	SACMV-challenged/VIGS::M11.K	SACMV-challenged/NO-VIGS
SACMV-VIGS	**0.00**	**0.02**	**0.00**	**0.00**	**0.00**	0.06	**0.00**
TRV-VIGS	**0.00**	**0.00**	**0.01**	**0.00**	**0.00**	**0.00**	**0.00**

A1.2.13 Student's t-test assessing plant height in SACMV-challenged plants

			SACMV-challenged/ VIGS vector	SACMV-challenged/VIGS::M15.1	SACMV-challenged/VIGS::M8.B	SACMV-challenged/VIGS::M11.F	SACMV-challenged/VIGS::M11.2	SACMV-challenged/VIGS::M11.K	SACMV-challenged/NO-VIGS
SACMV VIGS	**14 DPI**	**FC**	**5.03**	**5.17**	**4.67**	**5.00**	**4.67**	**5.00**	**4.67**
		***p* value**		**0.08**	**0.01**	**0.31**	**0.28**	**0.46**	**0.07**
	28 DPI	**FC**	**6.42**	**15.03**	**6.93**	**15.03**	**17.82**	**19.80**	**5.00**
		***p* value**		**0.00**	**0.07**	**0.00**	**0.01**	**0.00**	**0.00**
TRV-VIGS	**14 DPI**	**FC**	**4.33**	**4.67**	**4.33**	**4.33**	**4.33**	**4.33**	**4.67**
		***p* value**	**0.50**	**0.02**	**0.11**	**0.07**	**0.15**	**0.15**	**0.03**
	28 DPI	**FC**	**5.00**	**16.13**	**11.35**	**7.07**	**8.67**	**10.30**	**5.00**
		***p* value**	**0.50**	**0.00**	**0.00**	**0.00**	**0.00**	**0.00**	0.07

A1.2.14 Student's t-test assessing plant growth in SACMV-challenged plants

		SACMV-challenged/VIGS vector	SACMV-challenged/VIGS::M15.1	SACMV-challenged/VIGS::M8.B	SACMV-challenged/VIGS::M11.F	SACMV-challenged/VIGS::M11.2	SACMV-challenged/VIGS::M11.K	SACMV-challenged/NO-VIGS
SACMV-VIGS	**FC**	1.27	2.91	1.49	3.01	3.82	3.96	1.07
	***p* value**	**0.00**	**0.00**	**0.00**	**0.00**	**0.00**	**0.00**	**0.04**
TRV-VIGS	**FC**	1.15	3.46	2.62	1.63	2.00	2.38	1.07
	***p* value**	0.48	**0.00**	**0.00**	**0.01**	**0.00**	**0.00**	**0.04**

A1.3 ANOVA

A1.3.1 1-way ANOVA assessing the significance of myosin expression in VIGS::myosin at 14 dpi vs 28 dpi

Anova: Single Factor SACMV VIGS

SUMMARY

Groups	*Count*	*Sum*	*Average*	*Variance*
Column 1	6.00	2.39	0.40	0.03
Column 2	6.00	3.89	0.65	0.03

ANOVA

Source of Variation	*SS*	*df*	*MS*	*F*	*P value*	*F crit*
Between Groups	0.19	1.00	0.19	6.03	**0.03**	4.96
Within Groups	0.31	10.00	0.03			
Total	0.49	11.00				

Anova: Single Factor: TRV-VIGS

SUMMARY

Groups	*Count*	*Sum*	*Average*	*Variance*
Column 1	6.00	0.31	0.05	0.00
Column 2	6.00	3.64	0.61	0.03

ANOVA

Source of Variation	*SS*	*df*	*MS*	*F*	*P value*	*F crit*
Between Groups	0.92	1.00	0.92	51.26	0.00	4.96
Within Groups	0.18	10.00	0.02			
Total	1.10	11.00				

A1.3.2 1-way ANOVA assessing the significant in expression values between SACMV-VIGS construct and TRV-VIGS constructs

Anova: Single Factor

SUMMARY

Groups	*Count*	*Sum*	*Average*	*Variance*
SACMV-VIGS	15.00	6.68	**0.45**	0.05
TRV-VIGS	15.00	3.27	**0.22**	0.06

ANOVA

Source of Variation	*SS*	*df*	*MS*	*F*	*P value*	*F crit*
Between Groups	0.39	1.00	0.39	7.13	**0.01**	4.20
Within Groups	1.52	28.00	0.05			
Total	1.90	29.00				

A1.3.3 2-way ANOVA assessing the statistical difference of DNA-A viral load between TRV VIGS and SACMV VIGS

ANOVA	14 DPI					
Source of Variation	*SS*	*df*	*MS*	*F*	*p* value	*F crit*
Sample	6948130842.24	1.00	6.95E+09	1.11	0.29	3.94
Columns	30227422893.22	5.00	6.05E+09	0.97	0.44	2.31
Interaction	31240320425.65	5.00	6.25E+09	1.00	0.42	2.31
Within	601161342241.66	96.00	6.26E+09			
Total	669577216402.77	107.00				

ANOVA	28 DPI					
Source of Variation	*SS*	*df*	*MS*	*F*	*p* value	*F crit*
Sample	15764702576.38	1.00	1.58E+10	3.57	0.06	3.94
Columns	76554226255.54	5.00	1.53E+10	3.46	**0.01**	2.31
Interaction	85328358465.81	5.00	1.71E+10	3.86	**0.00**	2.31
Within	424286746979.66	96.00	4.42E+09			
Total	601934034277.39	107.00				

A1.3.4 2-way ANOVA assessing the statistical difference of SSS in SACMV-challenged TRV VIGS and SACMV VIGS in SACMV-challenged plants

ANOVA at 14 dpi

Source of Variation	*SS*	*df*	*MS*	*F*	*P*value	*F crit*
Sample	1.69	1.00	1.69	6.48	**0.01**	3.94
Columns	17.12	5.00	3.42	13.15	**0.00**	2.31
Interaction	7.66	5.00	1.53	5.88	**0.00**	2.31
Within	25.00	96.00	0.26			
Total	51.47	107.00				

ANOVA at 28 dpi

SS	*df*	*MS*	*F*	*P*value	*F crit*
3.34	1.00	3.34	4.81	**0.03**	3.94
17.82	5.00	3.56	5.13	**0.00**	2.31
7.16	5.00	1.43	2.06	0.08	2.31
66.67	96.00	0.69			

A1.3.5 2-way ANOVA assessing the statistical difference of plant height between TRV VIGS and SACMV VIGS in SACMV-challenged plants

ANOVA At 14 dpi

Source of Variation	*SS*	*df*	*MS*	*F*	*P*value	*F crit*
Sample	3.39	1.00	3.39	23.30	**0.00**	3.94
Columns	1.64	5.00	0.33	2.26	**0.05**	2.31
Interaction	0.79	5.00	0.16	1.08	0.37	2.31
Within	13.97	96.00	0.15			
Total	19.79	107.00				

ANOVA at 28 dpi

Source of Variation	*SS*	*df*	*MS*	*F*	*P*value	*F crit*
Sample	405.49	1.00	405.49	13.79	0.00	3.94
Columns	1,277.70	5.00	255.54	8.69	0.00	2.31
Interaction	533.31	5.00	106.66	3.63	0.00	2.31
Within	2,822.88	96.00	29.40			
Total	5,039.36	107.00				

A1.4 Pearson's correlation

A1.4.1 Pearson's correlation analysis between DNA-A viral load and SSS

			SACMV-challenged/VIGS vector	SACMV-challenged/VIGS::M15.1	SACMV-challenged/VIGS::M8.B	SACMV-challenged/VIGS::M11.F	SACMV-challenged/VIGS::M11.2	SACMV-challenged/VIGS::M11.K	SACMV-challenged/VIGS::SACMV
SACMV-VIGS	**14 DPI**	**r-value**	0.33	-0.43	0.64	-0.68	-0.35	-0.44	-0.09
		***p* value**	0.38	0.24	**0.05**	**0.03**	0.35	0.23	0.82
	28 DPI	**r-value**	0.54	-0.73	0.16	0.85	-0.02	-0.33	#DIV/0!
		***p* value**	0.13	**0.02**	0.67	**0.00**	0.95	0.38	#DIV/0!
TRV-VIGS	**14 DPI**	**r-value**	-0.20	0.13	0.09	0.53	0.28	-0.14	-0.27
		***p* value**	0.60	0.75	0.83	0.14	0.46	0.72	0.48
	28 DPI	**r-value**	-0.38	-0.62	-0.46	0.12	-0.33	0.32	#DIV/0!
		***p* value**	0.31	0.07	0.20	0.77	0.37	0.39	#DIV/0!

A1.4.2 Pearson's correlation analysis between DNA-A viral load and plant height

			SACMV-challenged/VIGS vector	SACMV-challenged/VIGS::M15.1	SACMV-challenged/VIGS::M8.B	SACMV-challenged/VIGS::M11.F	SACMV-challenged/VIGS::M11.2	SACMV-challenged/VIGS::M11.K	SACMV-challenged/VIGS::SACMV
SACMV-VIGS	**14 DPI**	**r-value**	0.29	-0.63	-1.00	-0.83	-0.61	0.10	0.21
		***p* value**	0.23	**0.03**	**0.00**	**0.00**	**0.04**	0.40	0.29
	28 DPI	**r-value**	-0.79	0.83	-0.24	-0.41	0.34	-0.05	0.36
		***p* value**	**0.00**	**0.00**	0.26	0.13	0.18	0.44	0.17
TRV-VIGS	**14 DPI**	**r-value**	0.51	-0.54	0.53	0.18	0.11	0.05	0.21
		***p* value**	0.08	0.06	0.07	0.32	0.38	0.44	0.29

	28 DPI	**r-value**	0.35	0.30	-0.60	-0.40	-0.33	0.10	0.36
		***p* value**	0.18	0.22	**0.04**	0.14	0.19	0.40	0.17